BIOCHEMICAL METHANE POTENTIAL TESTING AND MODELLING FOR INSIGHT INTO ANAEROBIC DIGESTER PERFORMANCE

by

Sarah Elizabeth Daly

A Dissertation

Submitted to the Faculty of Purdue University

In Partial Fulfillment of the Requirements for the degree of

Doctor of Philosophy

Department of Agricultural and Biological Engineering

West Lafayette, Indiana

August 2020

THE PURDUE UNIVERSITY GRADUATE SCHOOL
STATEMENT OF COMMITTEE APPROVAL

Dr. Jiqin Ni, Chair

Department of Agricultural and Biological Engineering

Dr. Nathan Mosier

Department of Agricultural and Biological Engineering

Dr. Kevin Solomon

Department of Agricultural and Biological Engineering

Dr. George (Zhi) Zhou

Lyle School of Civil Engineering

Approved by:

Dr. Nathan Mosier

To a healthy world.

ACKNOWLEDGMENTS

I would like to thank Purdue University for their support of my Ph.D. study in the form of two fellowships. The Ross fellowship and the Henry Ford II fellowship. I would like to thank the Agricultural and Biological Engineering Department at Purdue University for their support by providing me with a research assistantship for two years of my Ph.D. study.

I would like to thank the anaerobic digester operators and Indiana farm owners who graciously allowed me to tour their facilities, answered my numerous questions, and assisted me in the collection of samples. Materials for my research projects were also supported by Lafayette Renew.

I would like to thank my major advisor Dr. Jiqin Ni for his support during my Ph.D. studies. He has provided me with numerous opportunities to gain hands-on experience in the field of anaerobic digestion, scientific research, the writing and reviewing of academic papers, and dissertation writing. He has also encouraged my own professional development in academia and encouraged me to take leadership positions in the department. His research group has provided me with friendship and support during my Ph.D. studies. I have met many remarkable individuals who have hailed from all around the world.

I would also like to thank the members of my committee including Dr. Nathan Mosier, Dr. Kevin Solomon, and Dr. George Zhou who have provided insightful feedback on my work and have also collaborated on different funding opportunities.

I would like to thank the wonderful community which is the Purdue Agricultural and Biological Engineering Department. The staff, including Scott Brand, Barbara Davies, Stan Harlow, Pamela Hancock, Rebecca Peer, Dan Taylor, Carol Weaver, Vanessa Williams, Nikki Zimmerman, and many others have kindly assisted me in both my academic studies and extracurriculars. I have had the pleasure of interacting with many faculty members in the department and have received nothing but support and encouragement from them. I have met so many remarkable students in the department who have helped me socially, academically, and professionally. The Agricultural and Biological Engineering Graduate Student Association is an amazing organization and has been a huge source of support for me. I would especially like to thank fellow grad students, Dr. Yang Yang and Jennifer Rackliffe who assisted me with sample

collection and have collaborated with me on the discussion of anaerobic digestion topics and manuscript preparation.

I would like to thank several organizations at Purdue which have assisted me with my professional development including the Susan Bulkeley Butler Center for Leadership Excellence, Mentoring at Purdue, the Office of Professional Development, the Purdue Graduate Student Government, the Engineering Academic Career Club, Center for Instructional Excellence, and the Graduate Women in Engineering Network. These organizations are real assets for graduate student support, both professionally and socially. I would also like to thank Dr. Joanne Lax and Dr. Jacqueline McDermott in the College of Engineering at Purdue, who have provided not only me, but all graduate students in the College with excellent professional development opportunities, opportunities for community building, and provided a source of genuine support. Additionally, I would like to thank Dr. Alice Pawley, for her insight in Engineering Education.

Finally, I would like to thank my close friends and family for their support during my educational endeavors.

TABLE OF CONTENTS

LIST OF TABLES

LIST OF FIGURES

LIST OF ABBREVIATIONS, SYMBOLS, AND CHEMICAL FORMULAS

Abbreviations

AD, anaerobic digestion;

ADM1, anaerobic digestion model number 1;

ANN, artificial neural network;

AnSBR, anaerobic sequencing batch reactor;

ARIMA, autoregressive integrated moving average;

ARIMAX, auto-regressive integrated moving average with explanatory variable;

BMP, biochemical methane potential;

CART, classification and regression trees;

CHP, combined heat and power;

COD, chemical oxygen demand;

COG, center of gravity;

CSTR, continuously stirred tank reactor;

DL-E, digester liquid from the east digester;

DL-W, digester liquid from the west digester;

df, degree of freedom;

DM, dairy manure;

E, effect;

EF-E, effluent from the east digester;

EF-R, effluent after phosphorus recovered and solids separation;

EF-L, liquid fraction of effluent after solid separation;

EF-W, effluent from the west digester;

ELM, Extreme Learning Machine;

Eq., equation;

F, F-distribution;

FID, flame ionization detector;

FD-T-LD = Field digester - Test number – Lab digester group number;

FPE, final prediction-error criterion;

FS, fixed solids (g L^{-1});

FSMY, final specific methane yield at the end of the BMP test (mL g VS^{-1});

FW, food waste;

g, gaseous phase;

gam, generalized additive model;

GC, gas chromatograph;

GHG, greenhouse gas;

Glmnet, generalized linear model via penalized maximum likelihood;

GWP, global warming potential;

HRT, hydraulic retention time (days);

HYFIS, hybrid neural fuzzy inference system;

ID, inner diameter (mm);

INF, influent;

InorgN, inorganic nitrogen (g L^{-1});

ISR, inoculum to substrate ratio;

IW, industry waste;

KNN, *k*-nearest neighbor;

LASSO, Least Absolute Shrinkage and Selection Operator;

Loess, local polynomial regression fitting;

LS, least squares;

LW, live weight (Mg);

M, model;

MLP, multi-layer perceptron;

mS, milli Siemens;

MSD, mean square of the deviations;

MSW, municipal solid wastes;

MULTINOM, multinomial logistic regression;

NA, not applicable;

ND, no data;

NMVFR, non-mixed vertical flow reactor;

NN, neural network;

nnetar, neural network forecasting algorithm;

No., number;

OD, outer diameter;

OLR, organic load rate;

OLS, ordinary least squares regression;

OP, orthophosphate (g L^{-1});

P, pressure (atm);

PCA, principle component analysis;

PCR, principle component regression;

PLS, partial least squares regression;

PS, primary sludge;

PVC, polyvinyl chloride;

rAE, relative absolute error;

RF, random forest;

RMSE, root mean square error;

RO, reverse osmosis;

rRMSE, relative root mean squared error;

RSS, residual sum of squares;

S:I, substrate to inoculum ratio;

SL, sludge, a mixture of primary sludge and waste active sludge;

SMAPE, symmetric mean absolute percentage error;

SMY, specific methane yield (mL g VS^{-1});

SRB, sulfate reducing bacteria;

SRT, solids retention time (days);

STP, standard temperature and pressure;

SVM, support vector machines;

T, temperature (°C);

t, time (days);

TALK, total alkalinity (g L^{-1});

TAN, total ammonia nitrogen (g L^{-1});

TCD, thermal conductivity detection;

TCOD, total chemical oxygen demand (g L^{-1});

TDS, total dissolved sulfide (g L^{-1});

TKN, total kjeldahl nitrogen (g L^{-1});

TOC, total organic carbon (g L^{-1});

TP, total phosphorus (g L^{-1}),

TS, total solids (g L^{-1});

TVFA, total volatile fatty acids (g L^{-1});

UAF, up-flow anaerobic filter;

UASB, up-flow anaerobic sludge blanket;

V, volume of biogas (mL);

VFA, volatile fatty acid (g L^{-1});

VS, volatile solids (g L^{-1});

WAS, waste activated sludge;

WWTP, wastewater treatment plant

Symbols

B, methane yield (mL g VS^{-1});

$B_{H,}$ hydrolytic (acidogenic) biomass concentration (g L^{-1});

$B_{o,}$ ultimate (measured) methane yield (mL g^{-1});

$B_{u,}$ theoretical methane yield (mL g^{-1});

$C_{CH4cor,}$ the corrected concentration of dry methane gas (%);

$C_{CH4,}$ the measured concentration of methane gas (%);

$C_{CO2,}$ is the measured concentration of carbon dioxide gas (%);

C_{H2S}, concentration of H_2S in biogas (ppm);

C_n, number of carbon atoms;

c, regularization parameter for support vector machine models;

d, degrees of differencing;

f, fraction of free H_2S gas to total dissolved sulfide;

f_d, biodegradable fraction of substrate;

f_m, gam smoothing function;

$f_{VS,}$ biodegradable fraction of VS;

g, gaseous phase;

H, Gompertz methane production potential (mL g^{-1} VS);

H_a, number of hydrogen atoms;

i, i^{th} value;

J, objective function;

k, rate coefficient (day^{-1});

k_1, rate coefficient for the first order equation (day^{-1});

k_{M1}, rate coefficient for the quadratic Monod equation (day^{-1});

k_{1mod}, rate coefficients for first order modified equation (day^{-1});

k_2, rate coefficient for the second order equation (day^{-1});

k_{M2}, rate coefficient for the quadratic Monod equation (day^{-1});

k_{2mod}, rate coefficients for first order modified equation (day^{-1});

K_{CH}, Chen and Hashimoto kinetic constant (dimensionless),

K_d, equilibrium constant for H_2S dissociation;

k_h, hydrolysis coefficient (day^{-1});

$\hat{K}_{VS,}$ half-saturation coefficient (dimensionless);

l, liquid phase;

n, number of data points;

N_c, number of nitrogen atoms;

$O_{b,}$ number of oxygen atoms;

p, autoregressive parameter;

p_n, number of parameters;

q, moving average component;

R^2, coefficient of determination;

s, gam link function;

S1, S2, S3, and SM, corn-starch based industrial wastes;

$R_{m,}$ maximum specific methane production (mL day^{-1});

T_{80}, time to reach 80% of biogas production (days);

T_{90}, time to reach 90% of biogas production (days);

$V_{Biogas,}$ volume of biogas (L);

V_m, measured biogas volume;

W_{VS}, initial weight of VS fed into digester (g);

$\bar{y}$, the mean of values;

$Y_{H,}$ hydrolytic (acidogenic) biomass yield coefficient;

y_i, the measured value;

$\hat{y}_i$, the predicted value;

y_t`, differenced time series;

α, absorption coefficient, Henry's Law;

$\beta_{0,}$ gam intercept;

γ, time dependency;

Δ, difference;

ε, previous error terms;

θ, moving average parameter;

λ, lag phase (days);

$\mu_{m,}$ maximum specific growth rate (day^{-1});

$\rho_{mH,}$ maximum specific hydrolytic rate (day^{-1});

σ, set of parameter values;

ϕ, slope coefficient;

ω, conversion coefficient of waste into methane (mL CH_4 g^{-1} VS)

Chemical Formulas

$AlCl_3$, aluminum chloride;

C, carbon;

$CaCl_2 \cdot 2H_2O$, calcium chloride dihydrate;

$CaCO_3$, calcium carbonate;

CH_4, methane;

$C_6H_{10}O_5$, carbohydrate;

$C_5H_7O_2N$, protein;

$C_{57}H_{104}O_6$, lipid;

CO_2, carbon dioxide;

CO_3^{2-}, carbonate ion;

$CoCl_2 \cdot 6\ H_2O$, Cobalt(II) Chloride Hexahydrate;

Cu, copper (g L^{-1});

$CuCl_2 \cdot 2\ H_2O$, Copper(II) Chloride Dihydrate;

Fe, iron ($g\ L^{-1}$);

$FeCl_2 \cdot 4\ H_2O$, iron dichloride tetrahydrate;

$FeOH_3$, ferric hydroxide;

FeS, iron(II) sulfide;

$Fe_3(PO_4)_2$, iron (II) phosphate;

H_2, hydrogen gas;

H_2O, water;

HS^{-1}, bisulfide;

H_2S, hydrogen sulfide;

H_3BO_3, boric acid;

HCl, hydrochloric acid;

HCO_3^-, bicarbonate;

He, helium;

$K_2HPO_4 \cdot 3H_2O$, potassium hydrogen phosphate trihydrate;

KOH, potassium hydroxide;

$MgCl_2 \cdot 6H_2O$, magnesium chloride hexahydrate;

$MnCl_2 \cdot 4\ H_2O$, manganese(II) chloride tetrahydrate;

N, nitrogen;

Na^+, sodium;

N_2, nitrogen gas;

$Na_2S \cdot 9H_2O$, sodium sulfide nonahydrate;

$Na_2SeO_3 \cdot 5\ H_2O$, sodium selenite pentahydrate;

NaCl, sodium chloride;

$NaHCO_3$, sodium bicarbonate;

NaOH, sodium hydroxide;

NH_3, ammonia;

NH_3-N, nitrogen-ammonia;

NH_4^+, ammonium;

NH_4Cl, ammonium chloride;

$(NH_4)_6Mo_7O_{24} \cdot 4H_2O$, ammonium heptamolybdate tetrahydrate;

Ni, nickel (g L^{-1});

$NiCl_2 \cdot 6\ H_2O$, nickel(II) chloride hexahydrate;

O, oxygen;

PO_4, phosphate;

PO_4^{3-}, phosphate;

S, sulfur;

S^{2-}, sulfide;

SO_4^{-2}, sulfate;

$ZnCl_2$, zinc chloride

GLOSSARY

Acetogenesis: The conversion of acidogenesis products to simpler compounds.

Acidogenesis: The conversion of solubilized materials to simpler compounds.

Anaerobic: An environment in which bacteria do not use free molecular oxygen.

Artificial Intelligence: Machines simulate human knowledge through learning and problem solving.

Batch: Samples collected on the same date.

Biodegradability: The ultimate rate and extent to which organic material is metabolized by microorganisms.

Biogas: A gas mixture, usually containing 50–75% methane, produced *via* anaerobic fermentation.

Biogas curve: The collected times series data of biogas volume which is connected and denotes trends in the data.

Black-box model: Describes a relationship between the input and output variables without prior knowledge about the physical and chemical relationships between the variables.

Biochemical methane potential (BMP test): A laboratory experimental process to determine the biogas/methane production from a specific substrate under controlled anaerobic digestion.

BMP data: Methane yield (mL g VS added^{-1}) from a lab-digester collected over time.

Co-digestion: Anaerobic digestion using a mixture of more than one types of feedstock.

Continuously stirred tank reactor: Provides continuous or intermittent mixing so materials are suspended uniformly in the tank.

Cross validation: A resampling procedure to evaluate the skill of machine learning models on unseen data with limited datasets (based on https://machinelearningmastery.com/k-fold-cross-validation/).

Decay: A regularization parameter which reduces overfitting in the machine learning model (based on https://towardsdatascience.com/this-thing-called-weight-decay-a7cd4bcfccab).

Digestate: *see* Effluent.

Digester: A container whose contents are undergoing anaerobic fermentation.

Digestion liquid (DL): Liquid inside the digester body under anaerobic digestion (based on http://digester.com/learning/introduction-to-anaerobic-digestion/).

Digester materials: The substance which the anaerobic digestion container is composed of (e.g., glass).

Digester type: The design of the system used for anaerobic digestion which affects how the anaerobic digestion process is executed (based on https://www.epa.gov/anaerobic-digestion/types-anaerobic-digesters).

Effluent: The material from anaerobic digesters after anaerobic fermentation. Also called digestate.

Feedstock: Any raw, renewable, biological material that can be used for anaerobic digestion to produce methane.

Field digester: An industrial-scale digester for treating livestock manure, agro-industrial wastes, or municipal wastewater.

Foam: A mass of tiny bubbles generated in a liquid and accumulated above the liquid.

Fuzzy logic: A technique which maps data between 0 and 1 and uses linguistic rules to classify elements.

Greenhouse gas (GHG): A gas which can trap heat in the atmosphere, including carbon dioxide (CO_2), methane (CH_4), nitrous oxide (N_2O), and fluorinated gases (based on https://www.epa.gov/ghgemissions/overview-greenhouse-gases).

Headspace: The internal space between the digester liquid contents and the top of the digester.

Hybrid knowledge-based systems: Systems where artificial intelligence techniques are applied to knowledge-based systems.

Hydrolysis: The solubilization process of an organic material.

Influent: Prepared liquid materials to feed into digesters, usually a mixture of feedstock, inoculum, and water.

Inoculum: Liquid material containing an anaerobic microbial community and obtained from anaerobic digesters for inoculation of feedstock to prepare digester influent.

Kappa value: Measurement of agreement within a model which corrects for category imbalances (based on https://www.statisticshowto.com/cohens-kappa-statistic/, https://remiller1450.github.io/s230f19/caret3.html).

Kinetic model: The mathematical description of the course of the reaction for each reaction step as a function of components in the system (based on https://www.crt.tf.fau.eu/forschung/arbeitsgruppen/katalytische-reaktoren-und-prozesstechnik/kinetische-modellierung/).

Knowledge-based approach: A method which involves knowledge acquisition, representation, and management.

Lab-digester: A laboratory-scale anaerobic digester (0.5 L or 1 L in this study).

Machine learning: An area of artificial intelligence in which model building is automated (based on https://expertsystem.com/machine-learning-definition/).

Metabolism: The use of the material as both an energy and carbon source for the microorganisms.

Methane production: In this dissertation, a general term for the generation of methane gas through a fermentation process.

Methane production curve: The collected times series data of methane production which has been connected to depict trends in the data.

Methane yield: The production of methane from a lab-digester test divided by a unit of mass (mL g VS^{-1}).

Methanogenesis: The production of methane *via* anaerobic fermentation.

Methanogenic inoculum: Inoculum which contains viable methanogens.

mtry: The number of randomly sampled variables as candidates at each split in the random forest model (based on https://www.rdocumentation.org/packages/randomForest/versions/4.6-14/topics/randomForest).

Neural network: A system of interconnected elements which can send and receive signals.

Non-parametric test: A statistical test which does not assume that the data fits a normal distribution (based on http://www.biostathandbook.com/normality.html).

Nutrient media: A mixture of micronutrients and growth factors for an anaerobic microbial community.

Organic waste: Waste which is biodegradable and comes from a plant or animal source.

Oxidation: A process in which a compound loses one or more electrons.

Parameter: A numerical constant that is used to describe a model.

Particulate: A macroparticle which is not easily dissolved or taken up by microorganisms.

Plug flow digester: A digester in which material enters one end and moves to the other end where it is removed (based on http://digester.com/learning/introduction-to-anaerobic-digestion/).

Precipitation reaction: A reaction in which ionic liquids combine to form a solid product.

Predictive accuracy: A measurement of reliability for a model which measures the proportion of observations that the model classifies correctly (based on https://remiller1450.github.io/s230f19/caret3.html, https://pubmed.ncbi.nlm.nih.gov/12854094/#:~:text=Measures%20of%20the%20predictive%20accuracy,on%20covariates%20replaces%20unconditional%20prediction).

Raw: Untreated material.

Reduction: A chemical process in which a compound gains one or more electrons.

Sample: A grab sample from the same source at a given time point.

Soluble: Material which can be dissolved by water, particularly material which is easily taken up by microorganisms.

Specific methane yield (SMY): The final day cumulative methane yield per unit of volatile solids (mL g VS^{-1}) from a biomethane potential test.

Substrate: In this dissertation, materials collected at industrial anaerobic digester systems and used in lab-scale digesters for bacteria to obtain carbon and energy.

Supervised machine learning: A machine learning process that is trained with a labelled data set of known values (based on http://digester.com/learning/introduction-to-anaerobic-digestion/).

Surface active agent: A substance which lowers the surface tension of a liquid.

Times series forecasting analysis: An area of machine learning in which future values are predicted based on historical data (based on https://machinelearningmastery.com/time-series-forecasting/).

Tuning Parameter: A model parameter which is not directly estimated from the data and is used to determine optimal model structure (based on https://www.datacamp.com/community/tutorials/parameter-optimization-machine-learning-models).

ABSTRACT

Anaerobic digestion uses a mixed, microbial community to convert organic wastes to biogas, thereby generating a clean renewable energy and reducing greenhouse gas emissions. However, few studies have quantified the relationship between waste composition and the subsequent physical and chemical changes in the digester. This Ph.D. dissertation aimed to gain new knowledge about how these differences in waste composition ultimately affect digester function. This dissertation examined three areas of digester function: (1) hydrogen sulfide production, (2) digester foaming, and (3) methane yield.

To accomplish these aims, a variety of materials from four different large-scale field digesters were collected at different time points and from different locations within the digester systems, including influent, liquid in the middle of the digesters, effluent, and effluent after solids separation. The materials were used for biochemical methane potential (BMP) tests in 43 lab-scale lab-digester groups, each containing triplicate or duplicate digesters. The materials from field digesters and the effluents from the lab-digesters were analyzed for an extensive set of chemical and physical characteristics. The three areas of digester function were examined with the physical and chemical characteristics of the digester materials and effluents, and the BMP performances.

Hydrogen sulfide productions in the lab-digesters ranged from non-detectable to 1.29 mL g VS^{-1}. Higher H_2S concentrations in the biogas were observed within the first ten days of testing. The initial Fe(II) : S ratio and OP concentrations had important influences on H_2S productions. Important parameters of digester influents related to digester foaming were the ratios of Fe(II) : S, Fe(II) : TP, and TVFA : TALK; and the concentrations of Cu. Digesters receiving mixed waste streams could be more vulnerable to foaming. The characteristics of each waste type varied significantly based on substrate and inoculum type, and digester functioning. The influent chemical characteristics of the waste significantly impacted all aspects of digester function. Using multivariate statistics and machine learning, models were developed and the prediction of digester outcomes were simulated based on the initial characteristics of the waste types.

CHAPTER 1. GENERAL INTRODUCTION

Global energy demand is projected to increase in the next decade (IEA, 2019). Therefore, the development of sustainable, affordable, and reliable energy technologies is a global concern (UN, 2019). Specifically, renewable energy technologies are projected to play an increasingly important role in meeting global energy demand (IEA, 2019). Climate change, sustainable development, and resource scarcity and availability are the main motivators for renewable energy development (Vanek, Francis M.l, Albright, & Angenent, 2012).

Organic waste management has received attention in recent years. Increases in livestock production in the United States have resulted in concern about manure management. Traditionally, the manure can be spread on crop fields as fertilizer due to its high nutrient content (Wilkie, 2005). However, field application of manure can become a significant source of odor, water pollution, antibiotic resistant bacteria, pathogens, greenhouse gas (GHG) emissions, and ammonia (NH_3) emissions due to the incomplete anaerobic decomposition of manure during storage (Aguirre-Villegas & Larson, 2017; Amon, Kryvoruchko, Amon, & Zechmeister-Boltenstern, 2006; Armstrong et al., 2010; Udikovic-Kolic, Wichmann, Broderick, & Handelsman, 2014; Wilkie, 2005). These problems are exacerbated by the fact that the number of farms with more than 2000 cows are increasing while the number of smaller farms (fewer than 200 cows) is decreasing (Macdonald et al., 2007). Larger dairy farms rarely have enough land to apply the manure in order to meet zero excess nitrogen and phosphorus goals (Macdonald et al., 2007). Therefore, there is interest in on-site treatment of livestock manure. Specifically, incorporating anaerobic digesters into these treatment systems is of particular interest.

Other types of organic wastes include food waste, yard waste, pet waste, and paper waste. Food waste is a particular issue, with a reported 36 million tons of food waste generated in the United States in 2012 (EPA, 2014). The majority of organic wastes in the United States is landfilled (CEC, 2017). Regulations on state and local disposal of waste have gone into effect and have increased interest in anaerobic digestion (AD) and composting. It is estimated that there could be an over 50% reduction in greenhouse gas emissions (GHG) from organic wastes through 100% diversion to AD and composting (CEC, 2017).

Consequently, better insight into the effect of different types of waste streams in AD systems will help to improve understanding of the AD process in order to contribute to environmental sustainability.

1.1 Overview of anaerobic digestion

Anaerobic digestion is an established technology which is used to treat organic waste streams while simultaneously generating energy. During AD, a mixed microbial community converts complex organic solids to biogas without the presence of oxygen (De Baere, 2000; Mata-Alvarez, Mac, & Llabr, 2000). The recovered solids after digestion are stabilized, thereby having reduced odor, solids concentration, weed-seed concentration, GHG emissions, and pathogen concentration for land application (Amon et al., 2006; Jeyanayagam & Collins Jr., 1984; ten Brummeler, 2000). Other benefits of AD include energy production, fertilizer production, nutrient conservation and mineralization, co-product production, compliance with environmental regulations, and tipping fees (Betts & Ling, 2009; Wilkie, 2005).

Anaerobic digestion systems have been installed throughout the United States. Increases in energy prices in the 1970s initially sparked interest in AD. However, from 1970-1990, agricultural AD systems in the United States had a reported 60% failure rate and faced numerous technical and economic difficulties (Betts & Ling, 2009; Bishop & Shumway, 2009). Today, concerns about increasing GHG emissions and air and water pollution from organic wastes have increased local, state, and federal interest in AD in the United States (Betts & Ling, 2009). Additionally, new technology, governmental funding, and innovative partnerships have encouraged AD installations throughout the United States (Betts & Ling, 2009; Bishop & Shumway, 2009; Innovation Center for U.S. Dairy, 2016). In 2019, AD systems on livestock farms in the United States generated 1.28 million megawatt hour equivalents of energy and avoided 4.64 million metric tons of CO_2 equivalents (U.S. EPA, 2020). Anaerobic digestion installations are also commonly found at wastewater treatment plants (WWTPs). Despite technological advances and research, AD systems can still face process imbalance, resulting in decreased biogas production and economic loss.

Anaerobic digestion relies on a series of interconnected biological processes. The stages of AD are hydrolysis, acidogenesis, acetogenesis, and methanogenesis (Figure 1-1). Because the entire process operates near thermodynamic equilibrium, the rate of reaction in each stage must remain in balance with the other stages in order for the digester to function efficiently. The stability

in the digester is determined by the unique consortia of microorganisms in the digester (Venkiteshwaran, Bocher, Maki, & Zitomer, 2016). The microorganisms in the digester are specific to the environmental conditions at each stage of digestion. The microorganisms require simple substrates such as H_2, CO_2, formate, ethanol, and acetate.

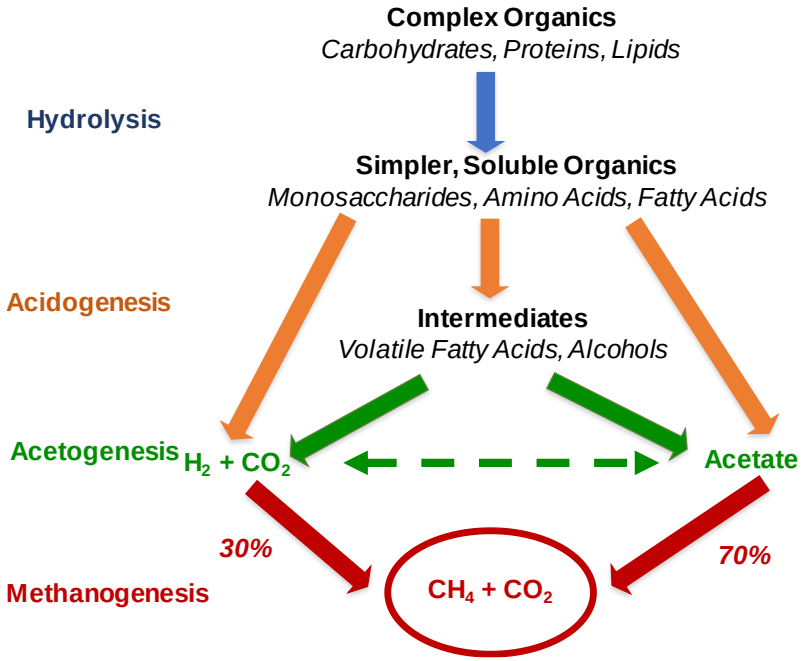

Figure 1-1. Overview of anaerobic digestion, consisting of hydrolysis, acidogenesis acetogenesis , and methanogenesis stages.

1.1.1 Hydrolysis

The first stage of AD is hydrolysis (Figure 1-1). Organic matter is composed of a biodegradable and non-biodegradable fraction (Parkin & Owen, 1987). The biodegradable fraction can then be divided into a particulate and soluble fraction (Pavlostathis & Gossett, 1986). Hydrolysis is the breakdown of complex, organic molecules, such as polysaccharides, lipids, and proteins, by hydrolytic extracellular enzymes released by hydrolytic microorganisms. These molecules are thus converted to smaller, soluble molecules which can be taken up by the cell membrane of microorganisms. Hydrolysis is often the rate-limiting step in AD when recalcitrant molecules are present (Parkin & Owen, 1987; Pavlostathis & Gossett, 1986; Venkiteshwaran et al., 2016).

1.1.2 Acidogenesis

Crucial intermediate compounds are generated during acidogenesis. Specifically, the solubilized molecules from hydrolysis undergo conversion to volatile fatty acids (VFAs), alcohols, carbon dioxide (CO_2), hydrogen (H_2), and ammonia (Figure 1-1). The acidogenesis stage is a common point of digester failure. If the digester experiences a disturbance, such as overloading, a rapid temperature change, or toxicity, the VFAs can accumulate and cause a drop in digester pH which can ultimately inhibit methanogenesis (Venkiteshwaran et al., 2016).

1.1.3 Acetogenesis

More intermediate compounds are generated during the acetogenesis stage. Some compounds from the acidogenesis stage, such as propionate, butyrate, isobutyrate, valerate, isovalerate, and ethanol are further degraded to acetic acid, formate, H_2 and CO_2 (Figure 1-1). Medium and long-chain fatty acids are degraded to acetate, H_2, and CO_2 during this stage (Venkiteshwaran et al., 2016). The accumulation of VFAs, especially propionate, during this stage can inhibit methanogenesis (Venkiteshwaran et al., 2016).

1.1.4 Methanogenesis

There are two primary pathways for methane (CH_4) production (Figure 1-1). These are acetoclastic methanogenesis and hydrogenotrophic methanogenesis. Acetoclastic methanogenesis is when CH_4 is produced from the cleaving of the acetate molecule. Hydrogenotrophic methanogenesis is when CH_4 is produced by the reduction of CO_2 by H_2. About 30% of CH_4 comes from hydrogenotrophic methanogenesis and 70% from acetoclastic methanogenesis (Parkin & Owen, 1987; Venkiteshwaran et al., 2016).

1.2 Field digester systems

A field AD system consists of infrastructure for feedstock collection, anaerobic digestion, effluent storage, gas handling, and gas use (United States Environmental Protection Agency, 2004). A great amount of variability can exist within each segment of a field digester system. A simplified field AD system in the United States is shown in Figure 1-2.

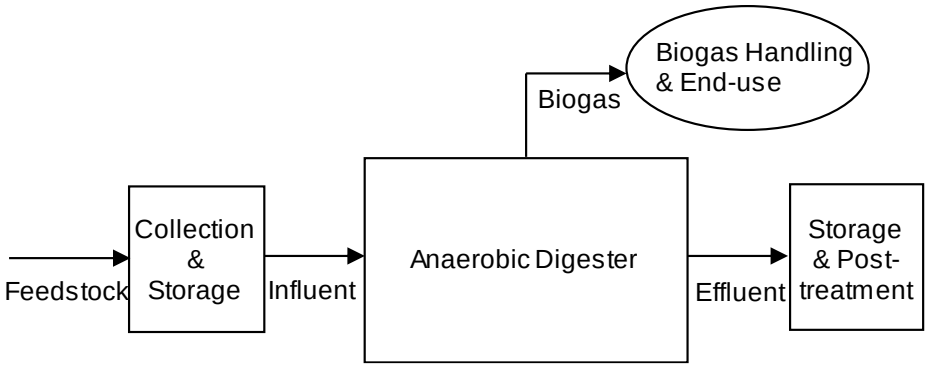

Figure 1-2. A simplified field digester system.

1.2.1 Feedstock collection

Feedstock collection methods are dependent on the location of the digester. Manure for on-farm digesters can be collected through scraping and flushing. Scraped manure is collected from the pen floor using a mechanical scraper and thus typically has a solids content of 10-20% (Martin & Roos, 2007; Safley Jr., Barker, & Westerman, 1984; Safley, Westerman, & Barker, 1986; United States Environmental Protection Agency, 2004). In a flush manure system, the manure from the barn is flushed with water and passed through a solid-liquid separation system with a resulting solids concentration of less than 5% (Chastain, Vanotti, & Wingfield, 2001; Frear, Wang, Li, & Chen, 2011; United States Environmental Protection Agency, 2004). Digesters at WWTPs receive waste activated sludge (WAS) or primary sludge (PS) from the on-site wastewater treatment system (Mao, Feng, Wang, & Ren, 2015). Other types of wastes include food waste, lignocellulose wastes, and other industrial wastes. These materials may be collected and trucked to an off-site AD system. The feedstock may then be stored or subjected to a pre-treatment process to enhance its performance in the AD system.

1.2.2 Influent

The collected and stored feedstock can then be used to prepare the influent which is fed to the anaerobic digester. The influent may be a mixture of several different types of wastes for "co-digestion". The influent usually contains inoculum, which may be taken from the digester effluent. Sometimes water or wastewater, e.g., lagoon water, may also be added to dilute the feedstock.

In fact, co-digestion is implemented at many AD locations. Co-digestion treats a mixture of different feedstocks, or waste streams, to make better use of available feedstock and improve

digester performance. Agricultural wastes, animal wastes, sewage sludge, and food wastes are among the many waste streams which have been co-digested (Beneragama, Iwasaki, & Umetsu, 2017; Bouallagui, Lahdheb, Ben Romdan, Rachdi, & Hamdi, 2009; Hills, 1979; Hills & Roberts, 1981; Kafle & Kim, 2013; Toumi et al., 2015; Usack & Angenent, 2015). Co-digestion can improve digester performance by creating a more balanced nutrient load, introducing suitable microorganisms into the microbial community, increasing the load of biodegradable matter, and improving buffering capacity (Bouallagui et al., 2009). The exact mixing ratio of co-digested substrates depends on the individual substrate characteristics (Kafle & Kim, 2013). The drawbacks of co-digestion include transportation costs for the wastes and local policy on waste generation (Mata-Alvarez et al., 2000).

1.2.3 Anaerobic digester

The anaerobic digester is the closed tank where the materials undergo fermentation to produce the biogas. The digester type is the design of the AD system. Different digester types include different temperatures, sizes, mixing strategies, feedstock types, loading rates, and total solids (TS) concentrations. These considerations are important factors in determining pre-treatment requirements during digestion as well as the optimal digester performance parameters (Betts & Ling, 2009). The suitability of each type of anaerobic digester will depend on the facility, feedstock management system, the solids content of the feedstock, and climate. Most anaerobic digesters operate at mesophilic (25-37°C) or thermophilic (55-65°C) conditions (Vanek, Albright, & Angenent, 2012).

Two common field digesters include the continuous stirred tank reactor (CSTR) and the plug flow digester. The CSTR is commonly used at WWTPs (Mao et al., 2015). The CSTR digesters are ideal for treating high-strength industrial wastes (Mao et al., 2015). A CSTR has a hydraulic retention time (HRT) of 15-20 days and works best with waste streams of 3-10% TS (Betts & Ling, 2009; Wilkie, 2005). In a plug flow digester, the new material is added on one end and moves as a “plug” to the other end. Plug flow digesters perform optimally with waste streams of 11-14% TS and have a longer HRT of 15-30 days (Betts & Ling, 2009; Wilkie, 2005). The plug flow reactor is relatively low maintenance and inexpensive to operate (Lazarus & Rudstrom, 2007).

Other types of digesters include covered lagoons, fixed film digesters, and up-flow anaerobic sludge blanket (UASB) digesters. Covered lagoons have minimal control and are suited for TS concentrations of less than 3% and are operated at psychrophilic (-20°C-10°C) temperatures (Betts & Ling, 2009). Fixed film digesters contain a biofilm of mesophilic or thermophilic microorganisms. The HRT is usually less than 6 days, and this digester type is suited for feedstocks with less than 5% TS (Betts & Ling, 2009). The UASB digesters have smaller volumes, faster flow velocities, higher biogas productions, and can handle higher TS concentrations (Mao et al., 2015).

1.2.4 Effluent

The effluent, also known as the digestate, has several potential uses. The effluent from the digester typically has a reduced solids content and is more uniform than the raw feedstock (Betts & Ling, 2009). It is, therefore, easier to process. The effluent can undergo a post-treatment process to extract valuable by-products (Bishop & Shumway, 2009; Lazarus & Rudstrom, 2007; United States Environmental Protection Agency, 2004). In many facilities, the digestate undergoes solid-liquid separation in which the solids are recovered and sold as bedding, soil amendments, potting soil, or organic fertilizer while the liquids are land applied (Betts & Ling, 2009). This can also improve the economics of the AD system.

1.2.5 Biogas handling and use

The gas handling system contains the equipment for gas storage, treatment, and transport to its end-use. This equipment may include in-digester and/or separated biogas storages, a scrubber to remove hydrogen sulfide (H_2S), piping, pumps, meters, pressure regulators, and condensate drains (United States Environmental Protection Agency, 2004). The biogas from an AD system typically contains about 50-70% CH_4, 30-50% CO_2, and trace gases including H_2S (NREL, 2013). During digestion, the gas is collected under the digester cover and then is pushed out through the collection pipe under the positive pressure inside the digester. The biogas then can undergo scrubbing and the removal of water vapor. The biogas may be used for heating, electricity, refrigeration, trigeneration, or as natural gas (Mao et al., 2015; United States Environmental

Protection Agency, 2004). The generated electricity can be sold to the local utility or be used to meet the energy needs of the site.

1.3 Benefits of anaerobic digestion

1.3.1 Renewable energy production

The main benefit of AD is renewable energy production. Specifically, the biogas can be combusted for usage in boilers or combined heat and power systems (CHP). Additionally, the biogas can be upgraded to CH_4 gas which can be used as a natural gas (NREL, 2013). In the United States, the CH_4 potential from organic wastes could displace 5% and 56% of natural gas consumption in the electric power and transportation sectors, respectively (NREL, 2013). Globally, the adoption of biogas technologies has the potential to increase substantially by 2040 (IEA, 2019).

1.3.2 Environmental

AD systems provide several environmental benefits. The installation of AD systems reduces GHG emissions by treating organic waste and replacing conventional fossil fuels for energy (Amon et al., 2006; Mao et al., 2015; Weiske et al., 2006). Organic wastes from landfills as well as from livestock manure are significant sources of CH_4 emissions (17.4%, and 9.7% respectively) (U.S. EPA, 2020). Fossil fuels account for 92.7% of CO_2 emissions in the U.S. (U.S. EPA, 2020). It is estimated that the biogas from AD could reduce GHG emissions from electricity by almost 4% (Cuéllar & Webber, 2008). At WWTPs, AD systems can generate enough energy so that the plant can be carbon neutral (Vanek, Albright, & Angenent, 2012). Additional environmental benefits include the replacement of inorganic fertilizers, the conservation of forest vegetation, reduction of acidification and eutrophication, and air and water pollution reduction (Mao et al., 2015). Installations with co-digested material typically receive more environmental benefits (Clemens, Trimborn, Weiland, & Amon, 2006; Ebner et al., 2015).

1.3.3 Economic

AD systems can provide several economic benefits. Often manure is co-digested with other feedstocks. Therefore, the digester owners can receive the tipping fees from accepting these additional waste streams (Bishop & Shumway, 2009; Vanek, Albright, & Angenent, 2012). The

removal of valuable co-products from the digestate is another source of income. Methane gas, electricity, and other separated nutrients and fiber from the digestate are additional sources of revenue (Bishop & Shumway, 2009; Lazarus & Rudstrom, 2007). It has been reported that AD plants can produce 165-245 kWh per ton of energy in excess of the 15 kWh per ton required for operation which could be sold (De Baere, 2000). However, the relatively low natural gas and electricity prices in the United States can result in low returns (Vanek, Albright, & Angenent, 2012). Credits for GHG reductions are also another future source of revenue (Lazarus & Rudstrom, 2007). However, the economic benefits can vary due to the different circumstances of the individual farms, with larger farms benefiting more. The price of electricity and availability of subsidies may determine profitability in the United States (Lazarus & Rudstrom, 2007).

1.4 BMP testing

A biochemical methane potential (BMP) test determines the suitability of specific feedstock for CH_4 production in AD. The BMP test is a controlled batch test to determine the CH_4 production of a substrate under ideal conditions for methanogenesis. Other characteristics of the substrate such as the biodegradability, and the rate of degradation are also determined (Angelidaki et al., 2009). The information obtained from a BMP test can then be used to determine the substrate's suitability for a field digester system (Lesteur et al., 2010; Strömberg, Nistor, & Liu, 2014). Chapters 2 and 3 provide more background information about different BMP methodologies and modeling processes.

1.5 Knowledge gaps

There is a lack of comprehensive knowledge about the chemical and physical properties of the influent in AD systems. The substrates tested in BMP systems rarely receive in-depth characterization of their chemical attributes even though different substrates in BMP testing can substantially affect the digester behavior. Additionally, the digester liquid from BMP testing is rarely given in-depth characterization beyond pH, solids content, total alkalinity (TALK), total volatile fatty acids (TVFA), and nitrogen concentrations. Further insight into substrate and digester liquid characterization in BMP testing can improve the following areas.

There is a lack of knowledge about the complex relationships between digester function and the physical and chemical characteristics of the digester liquid. This extends to the phenomenon of foaming, which has received little attention as to its causes in AD systems. Prediction of anaerobic digester phenomena such as foaming is required to better understand the introduction of co-digested substrates into field AD systems. Obtaining more data about AD characterization can illuminate these relationships.

Little comprehensive modeling of the biogas curves from AD systems has been conducted. There are a variety of models that have been identified for different CH_4 production curves, but few for H_2S production. Hydrogen sulfide production is a toxic, corrosive gas which often must be removed from the biogas. A greater understanding of H_2S production can aide in the development of solutions for its removal and treatment. Additionally, understanding and identifying these models is crucial for determining feasibility of substrates for AD.

1.6 Research objectives

The objective of this Ph.D. dissertation was to gain new knowledge about the function of AD systems in the areas of CH_4 production, H_2S production, and digester foaming. These are areas in which digesters can experience technical difficulty. Low CH_4 yields, the presence of H_2S in the biogas, and digester foaming can be detrimental economically to the AD systems. Digester foaming is the rapid production of bubbles in the digester system and can lead to digester overspill, low CH_4 yield, and foaming of the pipework. Foaming has also been observed in manure pits (Boe, Kougias, Pacheco, O-Thong, & Angelidaki, 2012) and WAS systems (Blackall, Harbers, Hayward, & Greenfield, 1991), so insight into AD foaming can be applicable in other areas of research. Insight into H_2S production in AD could be useful to H_2S production in manure pits.

Specifically, this dissertation seeks to gain information on (1) the influence of the physical and chemical properties of substrate on these AD processes and (2) different modeling strategies for characterizing and predicting these AD processes.

1.7 Hypothesis

The hypothesis of this dissertation is that there are unique and measurable differences in mesophilic anaerobic digestion under different operational conditions.

1.8 Dissertation outline

This dissertation is composed of seven chapters. In addition to the general introduction of the dissertation in Chapter 1, Chapter 2 is a literature review of BMP testing methodology. It synthesizes information about BMP test design, operation, and data processing based on 139 literature publications. Chapter 3 is a literature review of BMP test modeling. It provides details about the various models used in this dissertation. Chapter 3 is structured as a separate review from Chapter 2 because of the amount of literature (~150 cited publications) about BMP modeling, which is generally at a different level of BMP research.

Chapters 4-6 are original research papers based on eight different experimental BMP studies. The BMP studies were conducted using substrate and inoculum collected from four different field digesters. The data includes CH_4 production data, H_2S production data, physical and chemical characteristic data from both the field digesters and BMP digesters, and qualitative data about the field and BMP digester conditions. The data was analyzed using a mix of linear and non-linear modeling techniques, basic and multivariate statistical calculations, and machine learning. The results were used to explain and simulate predictions of AD function in the areas of H_2S production, foaming, and CH_4 production. An overview of data collection and analyses for Chapters 3-5 is presented in Figure 1-3.

Specifically, Chapter 4 studies the production of H_2S during BMP testing and models this process. Chapter 5 investigates foaming in a field digester and lab-digesters and uses machine learning to simulate predictions of foaming status. Chapter 6 develops BMP models using machine learning for specific methane yield simulation. An overview of data collection and analysis for Chapters 4-6 is presented in Figure 1-3. Finally, the general conclusions from this dissertation are presented in Chapter 7.

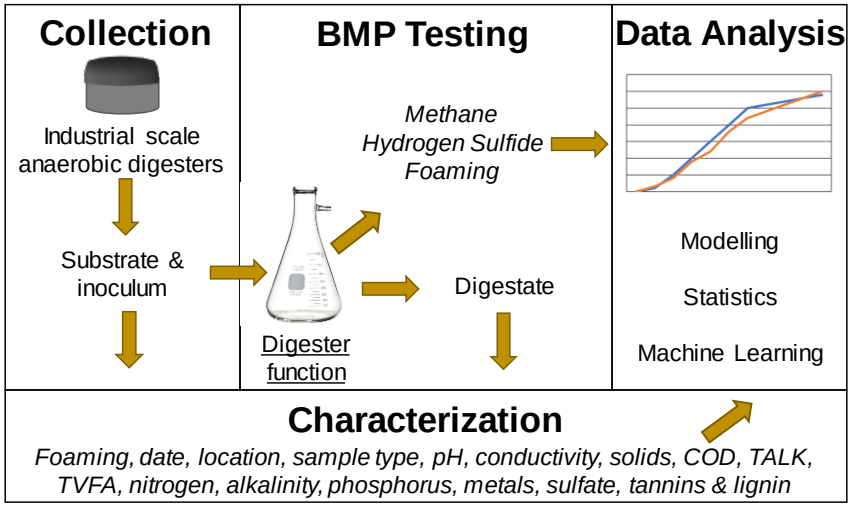

Figure 1-3. Overview of data collection and analysis in Chapters 3-5 of this dissertation.

1.9 References

Aguirre-Villegas, H. A., & Larson, R. A. (2017). Evaluating greenhouse gas emissions from dairy manure management practices using survey data and lifecycle tools. *Journal of Cleaner Production*, *143*, 169–179. https://doi.org/10.1016/j.jclepro.2016.12.133

Amon, B., Kryvoruchko, V., Amon, T., & Zechmeister-Boltenstern, S. (2006). Methane, nitrous oxide and ammonia emissions during storage and after application of dairy cattle slurry and influence of slurry treatment. *Agriculture, Ecosystems and Environment*, *112*(2–3), 153–162. https://doi.org/10.1016/j.agee.2005.08.030

Angelidaki, I., Alves, M., Bolzonella, D., Borzacconi, L., Campos, J. L., Guwy, A. J., … van Lier, J. B. (2009). Defining the biomethane potential (BMP) of solid organic wastes and energy crops: A proposed protocol for batch assays. *Water Science and Technology*, *59*(5), 927–934. https://doi.org/10.2166/wst.2009.040

Armstrong, S. D., Smith, D. R., Joern, B. C., Owens, P. R., Leytem, A. B., Huang, C., & Adeola, L. (2010). Transport and fate of phosphorus during and after manure spill simulations. *Journal of Environmental Quality*, *39*(1), 345–352. https://doi.org/10.2134/jeq2009.0234

Barber, E. M., & Mcquitty, J. B. (1977). Chemical Control of Hydrogen Sulfide From Anaerobic Swine Manure I . Oxidizing Agents. *Canadian Agricultural Engineering*, *19*(1), 15–19.

Beneragama, N., Iwasaki, M., & Umetsu, K. (2017). Methane production from thermophilic co-digestion of dairy manure and waste milk obtained from therapeutically treated cows. *Animal Science Journal*, *88*(2), 401–409. https://doi.org/10.1111/asj.12624

Betts, C., & Ling, C. (2009). *Cooperative Approaches for Implementation of Dairy Manure Digesters*. *USDA Research Report 217*. Washington D.C.

Bishop, C. P., & Shumway, C. R. (2009). The economics of dairy anaerobic digestion with coproduct marketing. *Review of Agricultural Economics*, *31*(3), 394–410.

Blackall, L. L., Harbers, A. E., Hayward, A. C., & Greenfield, P. F. (1991). Activated sludge foams: Effects of environmental variables on organism growth and foam formation. *Environmental Technology (United Kingdom)*, *12*(3), 241–248. https://doi.org/10.1080/09593339109385001

Boe, K., Kougias, P. G., Pacheco, F., O-Thong, S., & Angelidaki, I. (2012). Effect of substrates and intermediate compounds on foaming in manure digestion systems. *Water Science and Technology*, *66*(10), 2146–2154. https://doi.org/10.2166/wst.2012.438

Bouallagui, H., Lahdheb, H., Ben Romdan, E., Rachdi, B., & Hamdi, M. (2009). Improvement of fruit and vegetable waste anaerobic digestion performance and stability with co-substrates addition. *Journal of Environmental Management*, *90*(5), 1844–1849. https://doi.org/10.1016/j.jenvman.2008.12.002

CEC. (2017). *Characterization and Mangement of Organic Waste in North America*. Montreal.

Chastain, J. P., Vanotti, M. B., & Wingfield, M. M. (2001). Effectiveness of Liquid-Solid Seperation for Treatment of Flushed Dairy Manure: A Case Study. *Applied Engineering in Agriculture*, *17*(3), 343–354.

Clemens, J., Trimborn, M., Weiland, P., & Amon, B. (2006). Mitigation of greenhouse gas emissions by anaerobic digestion of cattle slurry. *Agriculture, Ecosystems and Environment*, *112*(2–3), 171–177. https://doi.org/10.1016/j.agee.2005.08.016

Cuéllar, A. D., & Webber, M. E. (2008). Cow power: The energy and emissions benefits of converting manure to biogas. *Environmental Research Letters*, *3*(3). https://doi.org/10.1088/1748-9326/3/3/034002

De Baere, L. (2000). Anaerobic digestion of solid waste: state-of-the-art. *Water Science and Technology : A Journal of the International Association on Water Pollution Research*, *41*(3), 283–290.

Ebner, J. H., Labatut, R. A., Rankin, M. J., Pronto, J. L., Gooch, C. A., Williamson, A. A., & Trabold, T. A. (2015). Lifecycle Greenhouse Gas Analysis of an Anaerobic Codigestion Facility Processing Dairy Manure and Industrial Food Waste. *Environmental Science and Technology*, *49*(18), 11199–11208. https://doi.org/10.1021/acs.est.5b01331

EPA. (2014). *Municipal Solid Waste Generation , Recycling, and Disposal in the United States : Facts and Figures for 2012*. Washington, DC.

Frear, C., Wang, Z. W., Li, C., & Chen, S. (2011). Biogas potential and microbial population distributions in flushed dairy manure and implications on anaerobic digestion technology. *Journal of Chemical Technology and Biotechnology*, *86*(1), 145–152. https://doi.org/10.1002/jctb.2484

Hills, D. J. (1979). Effects of carbon: nitrogen ratio on anaerobic digestion of dairy manure. *Agricultural Wastes*, *1*(4), 267–278.

Hills, D. J., & Roberts, D. W. (1981). Anaerobic digestion of dairy manure and field crop residues. *Agricultural Wastes*, *3*(3), 179–189. https://doi.org/10.1016/0141-4607(81)90026-3

IEA. (2019). *World Energy Outlook 2019*. Paris.

Innovation Center for U.S. Dairy. (2016). *2016 US Dairy Sustainability Report*.

Jeyanayagam, S. S., & Collins Jr., E. R. (1984). Weed Seed Survival in a Dairy Manure Anaerobic Digester. *Trans ASAE*, *27*(5), 1518–1523.

Kafle, G. K., & Kim, S. H. (2013). Anaerobic treatment of apple waste with swine manure for biogas production: Batch and continuous operation. *Applied Energy*, *103*, 61–72. https://doi.org/10.1016/j.apenergy.2012.10.018

Lazarus, W. F., & Rudstrom, M. (2007). The economics of anaerobic digester operation on a Minnesota dairy farm. *Review of Agricultural Economics*, *29*(2), 349–364. https://doi.org/10.1111/j.1467-9353.2007.00347.x

Lesteur, M., Bellon-Maurel, V., Gonzalez, C., Latrille, E., Roger, J. M., Junqua, G., & Steyer, J. P. (2010). Alternative methods for determining anaerobic biodegradability: A review. *Process Biochemistry*, *45*(4), 431–440. https://doi.org/10.1016/j.procbio.2009.11.018

Macdonald, J. M., Donoghue, E. J. O., Mcbride, W. D., Nehring, R. F., Sandretto, C. L., & Mosheim, R. (2007). *Profits, Costs, and the Changing Structure of Dairy Farming*. *United States Department of Agriculture*. Washington D.C. https://doi.org/10.2139/ssrn.1084458

Mao, C., Feng, Y., Wang, X., & Ren, G. (2015). Review on research achievements of biogas from anaerobic digestion. *Renewable and Sustainable Energy Reviews*, *45*, 540–555. https://doi.org/10.1016/j.rser.2015.02.032

Martin, J. H., & Roos, K. F. (2007). *Comparison of the Performance of a Conventional and a Modified Plug-Flow Digester for Scraped Dairy Manure* (No. 701P0907). *International Symposium on Air Quality and Waste Management in Agriculture*. Broomfield, Colorado.

Mata-Alvarez, J., Mac, S., & Llabr, P. (2000). Anaerobic digestion of organic solid wastes. An overview of research achievements and perspectives. *Bioresource Technology*, *74*(1), 3–16. https://doi.org/10.1016/S0960-8524(00)00023-7

NREL. (2013). *Biogas Potential in the United States (Fact Sheet)*. *Related Information: Energy Analysis, NREL (National Renewable Energy Laboratory)*. Golden, CO. https://doi.org/10.2172/1097303

Parkin, B. G. F., & Owen, W. F. (1987). Fundamentals of anaerobic digestion of wastewater sludges. *Journal of Environmental Engineering*, *112*(5), 867–920.

Pavlostathis, S. G., & Gossett, J. M. (1986). A kinetic model for anaerobic digestion of biological sludge. *Biotechnology and Bioengineering*, *28*(10), 1519–1530. https://doi.org/10.1002/bit.260281010

Safley Jr., L. M., Barker, J. C., & Westerman, P. W. (1984). Characteristics of Fresh Dairy Manure. *Transactions of the ASAE*, *27*(4), 1150–1153. https://doi.org/10.13031/2013.32937

Safley, L. M., Westerman, P. W., & Barker, J. C. (1986). Fresh dairy manure characteristics and barnlot nutrient losses. *Agricultural Wastes*, *17*(3), 203–215. https://doi.org/10.1016/0141-4607(86)90094-6

Strömberg, S., Nistor, M., & Liu, J. (2014). Towards eliminating systematic errors caused by the experimental conditions in Biochemical Methane Potential (BMP) tests. *Waste Management*, *34*(11), 1939–1948. https://doi.org/10.1016/j.wasman.2014.07.018

ten Brummeler, E. (2000). Full scale experience with the BIOCEL process. *Water Science and Technology*, *41*(3), 299–304.

Toumi, J., Miladi, B., Farhat, A., Nouira, S., Hamdi, M., Gtari, M., & Bouallagui, H. (2015). Microbial ecology overview during anaerobic codigestion of dairy wastewater and cattle manure and use in agriculture of obtained bio-fertilisers. *Bioresource Technology*, *198*, 141–149. https://doi.org/10.1016/j.biortech.2015.09.004

U.S. EPA. (2020). Potential for Anaerobic Digestion on Livestock Farms in the United States. Retrieved April 15, 2020, from https://www.epa.gov/agstar/agstar-data-and-trends#adpotential

Udikovic-Kolic, N., Wichmann, F., Broderick, N. A., & Handelsman, J. (2014). Bloom of resident antibiotic-resistant bacteria in soil following manure fertilization. *Proceedings of the National Academy of Sciences*, *111*(42), 15202–15207. https://doi.org/10.1073/pnas.1409836111

UN. (2019). Energy-United Nations Sustainable Development. Retrieved September 29, 2019, from https://www.un.org/sustainabledevelopment/sustainable-development-goals/

United States Environmental Protection Agency. (2004). *A Manual For Developing Biogas Systems at Commercial Farms in the United States*. (K. F. Roos, J. B. Martin Jr., & M. A. Moser, Eds.), *AgSTAR Handbook* (2nd ed.).

Usack, J. G., & Angenent, L. T. (2015). Comparing the inhibitory thresholds of dairy manure co-digesters after prolonged acclimation periods: Part 1 – Performance and operating limits. *Water Research*, *87*, 1–12. https://doi.org/10.1016/j.watres.2015.05.055

Vanek, Francis M.l, Albright, L. D., & Angenent, L. T. (2012). Introduction. In *Energy Systems Engineering: Evaluation and Implementation* (Second, pp. 1–28). New York: McGraw Hill.

Vanek, F. M. ., Albright, L. D., & Angenent, L. T. (2012). Bioenergy Resources and Systems. In *Energy Systems Engineering: Evaluation and Implementation* (Second, pp. 449–476). New York: McGraw Hill.

Venkiteshwaran, K., Bocher, B., Maki, J., & Zitomer, D. (2016). Relating anaerobic digestion microbial community and process function. *Microbiology Insights*, *8*, 37–44. https://doi.org/10.4137/MBI.S33593

Weiske, A., Vabitsch, A., Olesen, J. E., Schelde, K., Michel, J., Friedrich, R., & Kaltschmitt, M. (2006). Mitigation of greenhouse gas emissions in European conventional and organic dairy farming. *Agriculture, Ecosystems and Environment*, *112*(2–3), 221–232. https://doi.org/10.1016/j.agee.2005.08.023

Wilkie, A. C. (2005). Anaerobic Digestion of Dairy Manure : Design and Process Considerations. In *Dairy Manure Management: Treatment, Handling, and Community Relations* (pp. 301–312). Ithaca, NY: Natural Resource, Agriculture, and Engineering Service.

CHAPTER 2. REVIEW OF BIOCHEMICAL METHANE POTENTIALS IN ANAEROBIC DIGESTION—PART I: TESTING METHODOLOGIES

2.1 Abstract

Biochemical methane potential (BMP) tests are a frequently used method to determine the feasibility of a substrate for anaerobic digestion (AD). However, there is significant variability in reported BMP methodologies. This chapter synthesized 88 peer-reviewed studies in which batch BMP testing was reported. From these studies, the major sources of variability in the BMP test methodologies were identified and test conditions for reliable comparisons of BMP test results to large-scale AD systems were determined. Biogas measurements were the greatest source of variability. State-of-the-art improvements in biogas measurements through the use of automated BMP tests were identified. Additionally, the use of controls and the consistent standardization of biogas volumes improved the reliability of reported biogas measurements.

2.2 Introduction

Anaerobic digestion (AD) is a mature technology, which is used for the treatment of waste and the simultaneous generation of energy. Anaerobic digestion uses a mixed microbial community to convert complex organic materials to biogas, a renewable energy containing about 55–70% methane (CH_4), without the presence of molecular oxygen (De Baere, 2000; Mao, Feng, Wang, & Ren, 2015; Q. Zhang, Hu, & Lee, 2016). Organic materials, such as land-applied livestock manure, can decompose and release significant quantities of CH_4 into the atmosphere. Therefore, AD technology is a solution to capture this CH_4, which has a high Global Warming Potential (GWP) of 28–36 over 100 years (USEPA, 2017). A desire to generate renewable energy as well as concern about increasing global greenhouse gas (GHG) emissions from organic wastes has sparked interest in AD in recent years (Abbasi, Tauseef, & Abbasi, 2012).

Anaerobic digestion is a series of biochemical and microbiological processes. The four main stages of AD are hydrolysis, acidogenesis, acetogenesis, and methanogenesis (Gavala, Angelidaki, & Ahring, 2003). Because the entire process operates near thermodynamic equilibrium, AD relies on syntrophic relationships among a unique guild of microorganisms in order to function efficiently (Leng et al., 2018; Venkiteshwaran, Bocher, Maki, & Zitomer, 2016). Additionally, the

type of substrate being tested can cause process imbalance (V.A. Vavilin, Lokshina, Jokela, & Rintala, 2004; V.A. Vavilin, Rytov, & Lokshina, 1996; Vedrenne, Béline, Dabert, & Bernet, 2008). Therefore, before designing a full-scale AD system with a specific substrate or introducing a new type of substrate into an existing AD system, it is necessary to know the substrate's characteristics and feasibility for digestion.

A common method for substrate characterization is the biochemical methane potential (BMP) test. During the BMP test, the substrate undergoes controlled batch AD under laboratory conditions to determine the specific CH_4 yield, also known as the SMY (mL CH_4 g $mass^{-1}$), the biodegradability, and the rate of degradation (I. Angelidaki et al., 2009). These values can be used to approximate the substrate's suitability of digestion or co-digestion with other substrates, retention time, organic loading rate (OLR), and the microbial behavior in a full scale digester (Lesteur et al., 2010; Strömberg, Nistor, & Liu, 2014).

Various methodologies have been reported in BMP tests. As a result of the complexity of the AD process and the lack of a standardized method, BMP tests may provide inaccurate predictions for the performance of the same feedstock in large-scale digesters. Some major drawbacks of the BMP test have been identified as the investment of time, and the limited understanding of the complex microbiological, physical, and chemical processes that occur during AD (I. Angelidaki et al., 2009; Lesteur et al., 2010). However, much information concerning the BMP test methodologies in literature still remains to be synthesized.

This chapter reviews the past and current methodologies for BMP tests in combination with the author's own BMP test practices. It also summarizes the challenges of obtaining high quality data for modeling large-scale digester performance. Additionally, this paper also identifies the major sources of variability in BMP testing. Eighty-eight peer-reviewed BMP studies were synthesized to identify and report these sources of variability. Finally, this chapter provides recommendations for more reliable, consistent, and accurate results from BMP testing.

2.3 Overview of the BMP test

In this dissertation, a BMP test is defined as a laboratory experimental process to determine the biogas/methane production from a specific substrate under controlled AD. The general process of the BMP test includes analysis of the substrate to the digester, anaerobic digestion of the substrate for a selected number of days, measurement and analysis of biogas produced during the

test, and analysis of effluent, also called digestate, at the end of digestion (Figure 2-1). The BMP test generates data that can be used for BMP modeling, which is reviewed in Chapter 3.

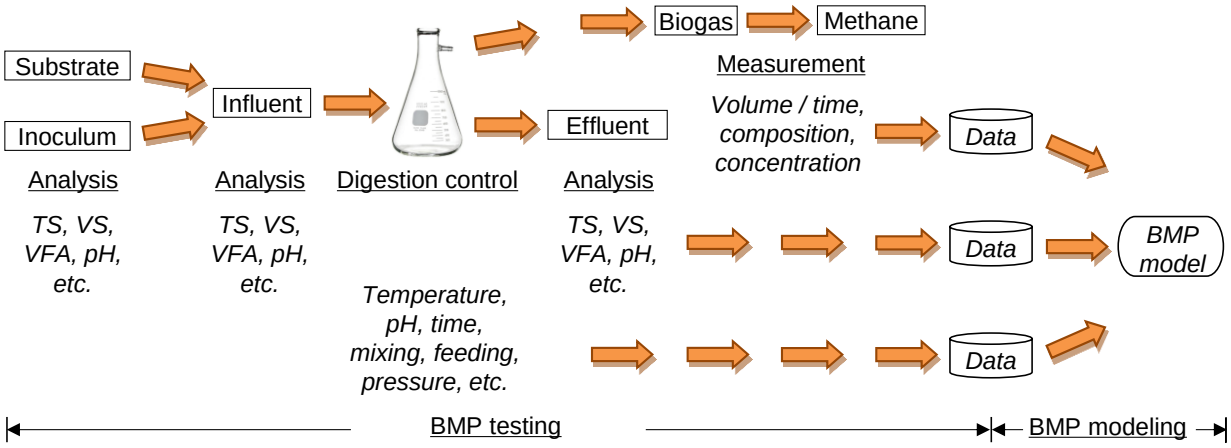

Figure 2-1. Overview of the general process of BMP testing and modeling.

The BMP test methodology has been reported and scrutinized in many studies. One of the first BMP bioassay protocols to give comparatively rapid and reliable results, when compared with a semi-continuously fed bench-scale study, was developed by Owen et al. (1979). This method has been modified in subsequent years but the basic principles and methods have been retained. Generally, the BMP test adds known volumes of a well-defined substrate, methanogenic inoculum, and nutrient media to lab-scale, batch digesters under favorable conditions for CH_4 production (I. Angelidaki et al., 2009; Irini Angelidaki & Sanders, 2004; Chynoweth, Turick, Owens, Jerger, & Peck, 1993; Filer, Ding, & Chang, 2019; Owen et al., 1979; Pearse, Hettiaratchi, & Kumar, 2018). These favorable conditions include sufficient nutrients, a neutral pH (6.8–7.2), strictly anaerobic conditions, a diverse and abundant population of active methanogens, a constant and uniform temperature, and a substrate concentration below inhibition (Gerardi, 2003). However, many factors in the BMP tests, including physical setup and control, substrate and inoculum preparation, biogas collection and quantification, and BMP calculation, may influence BMP test quality and deserve close attention (Table 2-1). Often, the choice of these key operational parameters depends on the type of substrate being tested, equipment, laboratory space, and financial limitations.

Table 2-1. Factors that can influence the outcomes of the BMP test.

BMP Test Set-up	BMP Test Operation	Biogas Quantification	BMP Calculation

• Digester
  • Material
  • Configuration
  • Working volume
  • Headspace volume
• Measurement and control method
  • Temperature
  • Mixing
  • Data acquisition
  • Sampling
• Statistical design
  • Replicates
  • Number of controls
  • Test duration
	• Mode of operation
	• Temperature
	• Mixing
	• Test duration
	• Statistical design
	• Substrate
	  • Uniformity
	  • Storage
	• Inoculum
	  • Inoculum-to-substrate ratio
	  • Source
	  • Storage
	• Nutrient media
	• pH measurement
	• Liquid sampling
		• Headspace treatment
		• Collection and measurement
		  • Biogas volume
		  • Biogas composition
			• STP normalization
			• Mass unit for normalization

2.4 BMP test set-up

2.4.1 Digester material

Anaerobic digesters are the major hardware in the BMP test setup. They are essentially sealed containers that provide an anaerobic condition for a substrate to go through the biogas production process. These containers have been called different names, such as flasks, bottles, or vessels. The most common shapes of BMP test digesters were cylindrical or conical.

The digesters in the reviewed BMP studies were made of several different materials. Glass was the most commonly used material for the digesters (Browne & Murphy, 2013; Hashimoto, 1989; Kafle & Chen, 2016; Kafle & Kim, 2013; Kafle, Kim, & Sung, 2013; Luste, Heinonen-Tanski, & Luostarinen, 2012; Nizami, Orozco, Groom, Dieterich, & Murphy, 2012; V.A. Vavilin et al., 2004; Vedrenne et al., 2008). Plastic (Oslaj, Mursec, & Vindis, 2010; Y. Wang, Odle, Eleazer, & Barlaz, 1997), polyvinyl chloride (PVC) (Rico, García, Rico, & Tejero, 2007), and aluminum (Martín-González, Colturato, Font, & Vicent, 2010) were less frequently used as digester material (Figure 2-2). Over 50% of the digesters examined in the reviewed BMP studies were made of glass (Figure 2-2). However, there is little information concerning the effect of different materials on digester function.

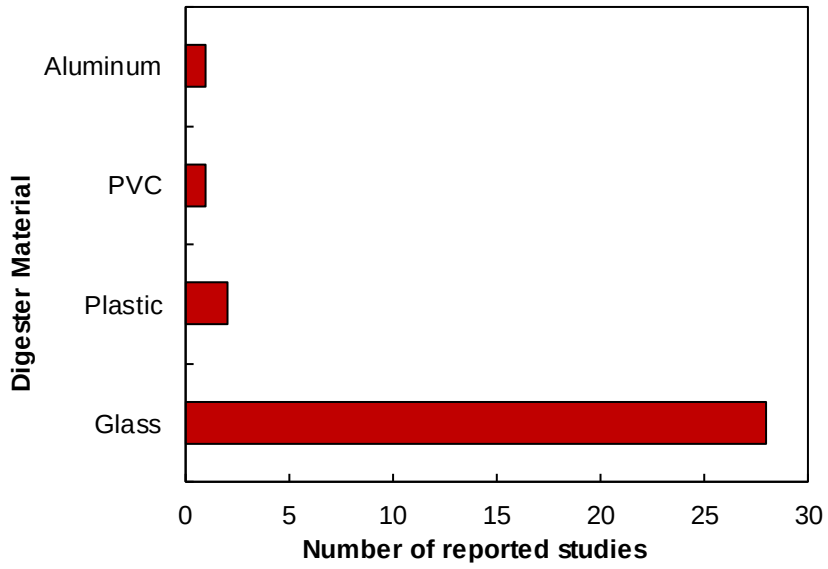

Figure 2-2. Digester materials and their distribution in 88 reported BMP studies.

2.4.2 Digester configurations

The digester configuration is how the digesters are set-up relative to their heating source, gas collection, and other data acquisition methods. Various configurations were reported in the BMP studies. The configurations were generally dictated by the method of gas measurement and desired size and headspace. Serum bottles were commonly used, usually with the bottle capped by a butyl rubber septum and sealed with an aluminum crimp (Alzate, Muñoz, Rogalla, Fdz-Polanco, & Pérez-Elvira, 2012; Luste et al., 2012; Nizami et al., 2012). Incubators or shaking incubators were also frequently used to maintain appropriate temperatures. Other studies used large vessels with internal stirring systems and heating blankets (Browne & Murphy, 2013).

Automation of the BMP test is an emerging area of digester configurations. Automated BMP systems have increased in popularity (I Angelidaki, Schmidt, Ellegaard, & Ahring, 1998; Badshah, Lam, Liu, & Mattiasson, 2012; Browne & Murphy, 2013; Koch, Hafner, Weinrich, & Astals, 2019; Koch, Lippert, & Drewes, 2017; Koch, Plabst, Schmidt, Helmreich, & Drewes, 2016; Kolbl, Paloczi, Panjan, & Stres, 2014; Ma, Gu, & Liu, 2018; McEniry, Allen, Murphy, & O'Kiely, 2014; Meng et al., 2018; Strömberg, Nistor, & Liu, 2015; J. Zhang et al., 2016), since they were first demonstrated by Angelidaki et al. (1998). Automated BMP systems can test different combinations of digesters in parallel with reproducible and reliable results (Badshah et al., 2012). They allow for online data acquisition and can reduce the labor required for the BMP tests as well

as the possibility of operator error. However, they can be prohibitively expensive for many research spaces.

2.4.3 Digester working volumes

Reported working volumes varied considerably in the reviewed BMP studies. The reported working volumes ranged from 20 to 5000 mL (Figure 2-3). Over 50% of the reported studies had working volumes of 250 mL or less (Figure 2-3). However, several studies have used digester sizes greater than 500 mL for the BMP test (Browne & Murphy, 2013; Buffiere, Loisel, Bernet, & Delgenes, 2006; Kafle & Kim, 2013; Kafle et al., 2013; Neves, Gonçalo, Oliveira, & Alves, 2008; Rao, Singh, Singh, & Sodha, 2000; Rincón, Banks, & Heaven, 2010).

Comparisons among BMP tests conducted with digesters of differing volumes have yielded inconsistent results. Browne and Murphy (2013) compared a large volume continuously stirred tank reactor (CSTR) BMP setup (5 L) to a small volume BMP setup (0.5 L) treating food. They found that the smaller BMP setup gave higher SMYs than the large volume BMP setup. This outcome was most likely due to better mixing and more precise gas measurements in the smaller bottles. Conversely, another study found that the SMY in a larger digester (1500 mL working volume) was higher than in a smaller digester (70 mL working volume) for grass silage under similar conditions with continuous mixing (Nizami et al., 2012). It has been suggested that non-homogenous samples may need a larger working volume to obtain consistent results (Raposo et al., 2011).

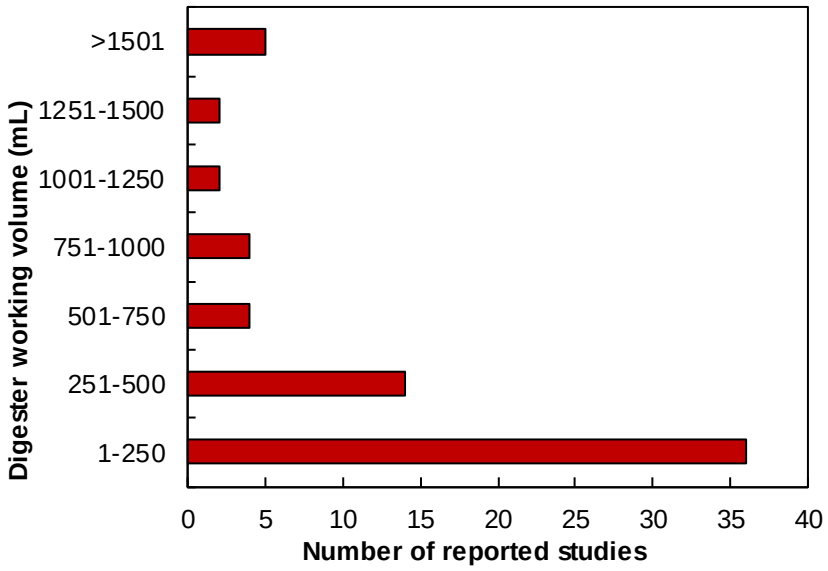

Figure 2-3. Digester working volumes and their distribution in 88 reported BMP studies.

2.4.4 Digester headspace volumes

Headspace volume may also affect the selection of digesters. The recommended headspace volume is 10–30% of the total digester volume (OECD, 2006). In the reported BMP studies, the headspace volume was frequently over 25% (Figure 2-4). Owen et al. (1979) suggested that the sample size and liquid-to-headspace ratio should be selected so that the measurable cumulative CH_4 volume over the course of the experiment is between 20–120 mL. In that study, this resulted in a 100 mL working volume in a 264 mL serum bottle. The selection of headspace volume may also depend on how frequently gas is released from the digester. If the headspace is vented regularly, only 10% of the total digester volume could also be necessary as headspace (OECD, 2006). However, there is little experimental comparison about the effect of headspace volume on digester performance. One recent study recommends a headspace of 75% of the total digester volume to minimize BMP measurement errors when using manometric measurements (Hafner & Astals, 2019). The reasoning for this is that a greater headspace may reduce errors from the volatilization of CH_4 during measurements. Overall, consideration of the biogas volume and production rate as well as the sampling frequency would influence digester headspace selection.

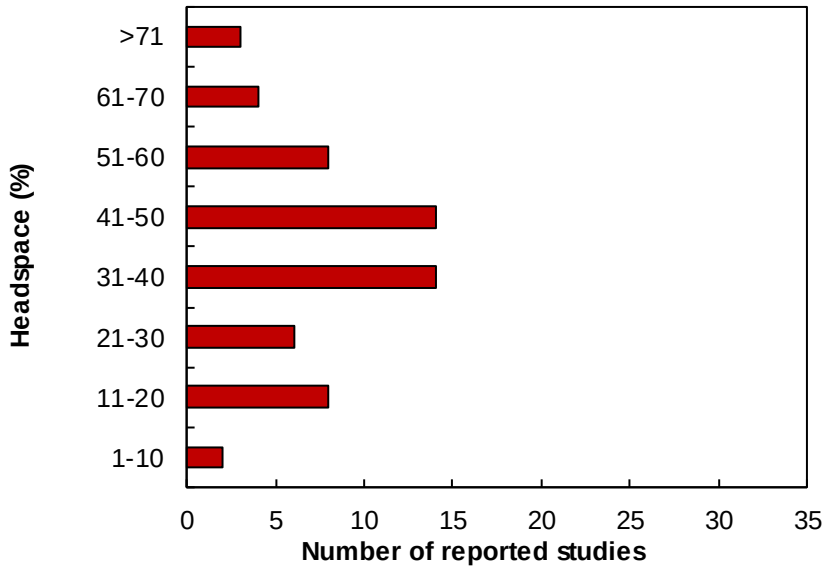

Figure 2-4. Headspace volume in digesters and their distribution in 88 reported BMP studies.

2.5 BMP operation and physical control

2.5.1 Mode of operation

The digesters can be set up to be continuous, semi-continuous, or batch, although batch is most common due to its simplicity. Typically, the digesters are fed at the beginning of the experiment, sparged to maintain an anaerobic environment, and then sealed. Semi-continuous or continuous fed batch tests are typically time-intensive and are therefore used less frequently than batch tests. Semi-continuous fed batch studies are typically used to compare the reliability of BMP batch testing (Chynoweth et al., 1993; Labatut, 2012; Usack & Angenent, 2015). The focus of this chapter is on batch tests.

2.5.2 Temperature measurement and control

The temperature of the BMP test affects several aspects of the digester function. This includes the degradation rates of the substrate, the survival and growth of microorganisms, and the microbial metabolism (Irini Angelidaki & Sanders, 2004; Mata-Alvarez et al., 2014). Typically, the BMP tests are conducted at mesophilic (25 – 40°C) temperatures (Irini Angelidaki & Sanders, 2004) The digesters are commonly placed in a temperature-controlled chamber or in a thermostatic water bath. BMP tests have also been conducted at thermophilic (45 – 60°C) and psychrophilic (<

20°C) temperatures (Irini Angelidaki & Sanders, 2004). Thermophilic temperatures have greater solids destruction and may be used with difficult to degrade substrates or high OLRs (Mata-Alvarez, Mac, & Llabr, 2000; Wandera et al., 2018). However, thermophilic digesters typically experience issues with process instability related to propionate accumulation (Moonil Kim, Ahn, & Speece, 2002). The temperature selection will depend on the conditions which are reflected in the real-life digester which is being tested. Theoretically, temperature should not affect the ultimate biodegradability, but it can influence the rate of degradation.

2.5.3 Digester liquid mixing

Mixing has several effects on the BMP test. Mixing can prevent the stratification of the liquid in the bottle and allow for uniform samples during collection (Labatut, Angenent, & Scott, 2011). Mixing can also prevent the saturation of carbon dioxide (CO_2) in the liquid phase of the experiment (I Angelidaki et al., 1998). However, the mixing intensity during AD may negatively affect the formation of the methanogenic community (Vasily A. Vavilin & Angelidaki, 2005). High-intensity mixing may disturb the formation of methanogenic communities within the digester and limit methanogenesis (Vasily A. Vavilin & Angelidaki, 2005).

Reported mixing intensity can vary from intermittent to continuous. At minimum, the BMP digester is mixed at least once before gas sampling. In many cases, mixing is continuous using a stir bar or mechanical shaker. Intermittent mixing consists of mixing the bottle once every 1 – 2 days, typically before gas sampling. Thorough mixing may be needed to maximize CH_4 production (Browne & Murphy, 2013). For example, high mixing intensity in batch digestion has been linked to the prevention of the formation of methanogenic communities and lower CH_4 yields (Moonil Kim et al., 2002; Vasily A. Vavilin & Angelidaki, 2005; Vedrenne et al., 2008). Continuous mixing may also prevent the syntrophic oxidation of volatile fatty acids (VFAs) which is crucial for methanogenesis (McMahon, Stroot, Mackie, & Raskin, 2001). Low-intensity mixing appears to be better than intense mixing (Stroot, McMahon, Mackie, & Raskin, 2001). Overall, low intensity or minimal mixing may be the best method to maximize CH_4 production.

2.5.4 Test duration

The digestion time is also a critical parameter in the BMP test. However, there is disagreement about the necessary time needed to ensure that the substrate has reached its maximum SMY. Additionally, the length of the BMP test can prolong the acquisition of desired information. Typically, the test continues until there is nearly no detectable CH_4 production. In some studies, this is when the CH_4 production is less than 1% of the cumulative CH_4 volume (Strömberg et al., 2015). In other studies, this is when biogas production is less than 1% of the biogas volume (Belle, Lansing, Mulbry, & Weil, 2015).

The length of the BMP test is highly variable (Figure 2-5). Of the reviewed BMP studies, over 60% of reported digestion lengths were between 21-60 days (Figure 2-5). Lignocellulosic materials such as grasses had longer test lengths over of 60 days. Manure collection methods can affect degradability and length of the BMP test. Dairy manure ranged from 30-100 days in the papers reviewed (Figure 2-5). Lignocellulosic materials such as woody biomass or paper products have required test lengths of 60 days or longer (Amon et al., 2007; Tong, Smith, & McCarty, 1990). For example, using the 1% rule as an indicator of digestion time may be deceptive for lignocellulosic substrates because they have been shown to have biphasic CH_4 production (Turick et al., 1991). A longer digestion time may ensure that all CH_4 is accounted for during the test.

Therefore, recommendations of BMP test lengths are inconsistent. Some studies have suggested that BMP analyses should have a minimum operation time of at least 50 days to ensure that the maximum SMY has been reached (Hansen et al., 2004; Turick et al., 1991). Others suggest a longer period of 80 or 100 days (Ponsá, Gea, & Sánchez, 2011; Vedrenne et al., 2008). Ultimately, the composition of the substrate may be a determining factor on digestion time. Overall, close monitoring of the BMP test is required to ensure that the maximum CH_4 potential is reached before ending the experiment.

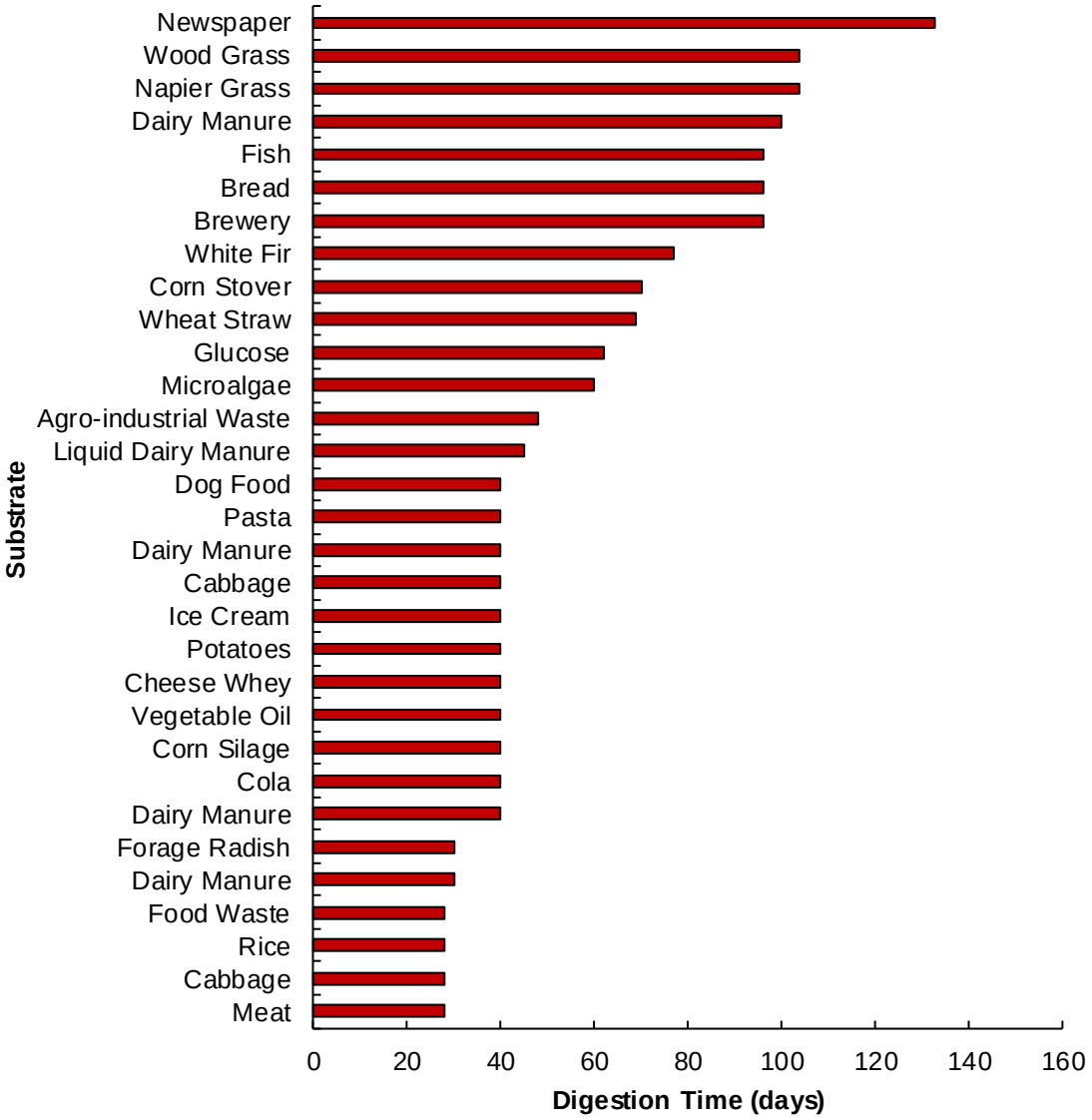

References: Alzate et al. (2012); Belle, Lansing, Mulbry, & Weil (2015); Cho, Park, & Chang (1995); Daly & Ni, (n.d.); Kafle et al. (2013); Labatut et al. (2011); Møller, Sommer, & Ahring (2004); Rico et al. (2007); Tong et al., (1990); R. Zhang et al. (2007).

Figure 2-5. The durations of the BMP test to complete with the type of substrate in cited BMP studies.

2.5.5 BMP test statistical design

There are certain measures that can be taken to improve the accuracy of the BMP test. BMP tests are typically performed in triplicate in order to determine the precision and accuracy of the results. A positive control using a well-characterized substrate should also be included.

Cellulose is one of the most common positive controls. A negative control, also known as a blank, should also be used to test the activity of the experiment. The comparisons performed depend on the objective of the test. One of the benefits of the BMP tests is its flexibility in testing different combinations of independent variables.

2.6 BMP operation and biochemical and microbiological control

The operation of the BMP test contains many different aspects. Variables related to the substrate (e.g., inoculum to substrate (ISR) ratio, nutrient media, buffering capacity) and digestion conditions (e.g., temperature, mixing intensity) can influence the test results. Consideration of these variables may affect the predictive applicability of the BMP tests for large-scale digestion. Additionally, a lack of reporting is difficult for the comparison of BMP results among inter-laboratory studies.

2.6.1 Substrate

The substrate is one of the most crucial influences on the BMP test. The substrate is typically characterized for, at minimum, pH and solids concentration on the first and final days of the test. The solids concentration is required for the normalization of the biogas measurements and to determine loading rates. The pH is required to determine sufficient buffering capacity. Solids concentration is most often reported as Volatile Solids (VS) or Chemical Oxygen Demand (COD). Measurements of VFAs, individual fatty acids, or total ammonia nitrogen (TAN), can also provide insight into possible inhibition of the system. Continuous monitoring of these parameters can provide further insight but would require a more advanced technical setup. The digesters are typically operated with a uniform working volume and solids concentration during the experiment. Typically, the solids concentration (VS or COD) is calculated to be uniform among all of the digesters at the beginning of the test. Often, water is added to the digester to adjust the solids concentration to the uniform volume (Astals, Batstone, Mata-Alvarez, & Jensen, 2014; De Vrieze et al., 2015; Feng et al., 2013; Luostarinen, Luste, & Sillanpää, 2009; Nizami et al., 2012; Wandera et al., 2018). Owen et al. (1979) recommended that less than 2 g L^{-1} of readily degradable COD be present in the BMP digester.

The substrate can affect the microbial community in the digester. Specifically, microbial abundance and diversity in AD systems is strongly influenced by the substrate composition (Mata-Alvarez et al., 2014). Therefore, microbial community analysis of the materials can provide further insight into the behavior of the system (Amha, Sinha, Lagman, Gregori, & Smith, 2017; De Vrieze et al., 2015; Meng et al., 2018; Palatsi, Viñas, Guivernau, Fernandez, & Flotats, 2011; Petropoulos, Dolfing, Davenport, Bowen, & Curtis, 2017). Overall, pretreatment and characterization of the substrate is essential for SMY reporting.

Uniformity

The uniformity of the substrate can affect the BMP test results. The substrate after collection may contain particulates which are not uniform in size. Substrate particle size can affect the rate of hydrolysis and rate of AD, with smaller particle sizes increasing the rate of AD (Barlaz, Ham, Schaefer, Isaacson, & Carolina, 1990; Pearse et al., 2018; V.A. Vavilin et al., 1996). Therefore, homogenizing particle sizes can improve reproducibility of the BMP test (I. Angelidaki et al., 2009; Chynoweth et al., 1993; Davidsson, Gruvberger, Christensen, Hansen, & Jansen, 2007). It is recommended that particle size should be at least 1 mm (Chynoweth et al., 1993). Error in characterizing the substrates may be a source of error in determining the volume or concentration of substrate to add to the digester (Raposo et al., 2011). Overall, the concentration and particle size of the substrate should be considered in the BMP test.

Storage

In many studies, the substrate is stored frozen and then thawed before testing. Freezing is used to prevent degradation of the substrate between collection time and the start of the test. However, freezing and then thawing a substrate may affect the microbial and chemical composition of the substrate. Additionally, the rate and temperature of freezing may affect the extent of change (Qunhui Wang, Fujisaki, Ohsumi, & Ogawa, 2001). The effect of substrate storage and freezing on BMP performance has not been extensively examined in the literature. One study found that freezing waste activated sludge (WAS) at -10°C resulted in a higher rate and volume of CH_4 production in lab-scale digesters through increasing VFA concentrations (Qunhui Wang, Kuninobu, Ogawa, & Kato, 1999). Another study found an average 1.5 increase in biogas

yield in sludge which had been frozen at -25°C for 24 hours and then thawed at room temperature compared to raw sludge in a mesophilic CSTR (Montusiewicz, Lebiocka, Rozej, Zacharska, & Pawłowski, 2010). In this study, the freezing and thawing process increased the solubility of the sludge. Additionally, they suggested that the presence of fat and protein in the substrate may prevent microorganism death during freezing. Overall, freezing and thawing of the substrate may provide a small increase in CH_4 production.

2.6.2 Inoculum

The concentration, source, and storage of inoculum plays a crucial role in the BMP test results. Typically, inoculum is taken from a stable, healthy AD system to provide the necessary microorganisms for all stages of AD. The contribution of methanogenic inoculum is determined from several "blank" digesters, which are prepared according to the same procedure but without substrate addition. The contribution of inoculum to total CH_4 volume in the digester should not be more than 20% in order to avoid overestimating the SMY (Owen et al., 1979; Vedrenne et al., 2008). However, some procedures use "pre-incubated" inoculum in which the inoculum has been previously degassed and, therefore, there is no need for a blank assay (Edward, Edwards, Egwu, & Sallis, 2015; Elbeshbishy, Nakhla, & Hafez, 2012).

Positive controls are often included in BMP tests. The inoculum activity can be tested using a positive control. There has been a call for greater inclusion of positive controls in BMP testing as they can be used to determine the reliability of the BMP results (Juliet Ohemeng-Ntiamoah & Datta, 2019; Reilly, Dinsdale, & Guwy, 2016). Positive controls contain a "standard" substrate, such as starch, gelatin, or cellulose (I. Angelidaki et al., 2009; Raposo, De La Rubia, Fernández-Cegrí, & Borja, 2012). The selection of a positive control will depend on the type of substrate being tested. Of the 88 reviewed BMP studies, over 52% of reported positive controls were cellulose (Figure 2-6). Cellulose can represent the CH_4 production of a recalcitrant substrate undergoing degradation. Since cellulose is so commonly used, there are multiple references to compare the results to, and therefore this may explain why it is so commonly used (Figure 2-6).

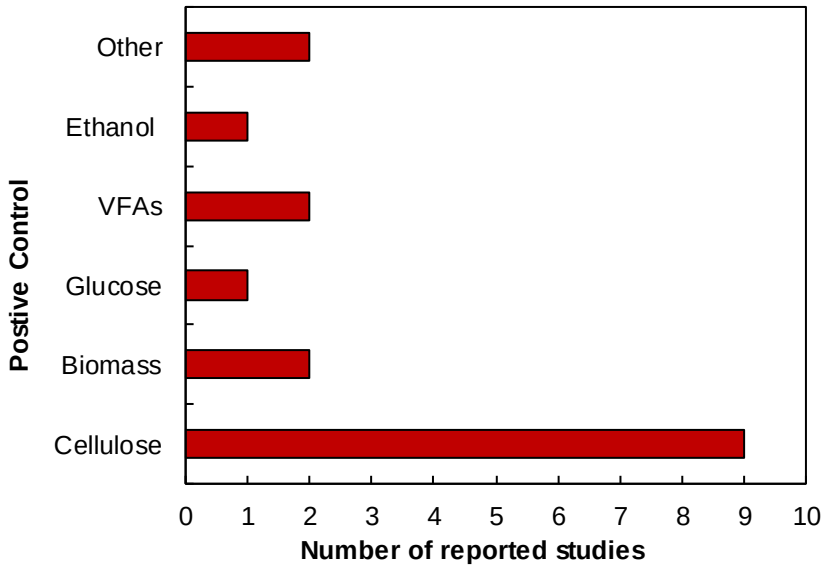

Figure 2-6. Positive controls and their distribution in 88 reported BMP studies.

Inoculum-to-substrate ratio

The selection of the inoculum-to-substrate (ISR) ratio is an important criteria of the BMP test. Different ISR ratios can significantly affect the SMY and rate of CH_4 production (Costa, Oliveira, & Alves, 2016; Dechrugsa, Kantachote, & Chaiprapat, 2013; Kawai et al., 2014; G. Liu, Zhang, El-Mashad, & Dong, 2009). The ISR ratio is a critical operational parameter because it is related to the food to microorganism ratio. However, reporting of the ISR ratio in BMP literature is not always consistent and there has been a call for more ISR reporting in literature (Juliet Ohemeng-Ntiamoah & Datta, 2019). The inoculum to substrate ratio is typically 2 or less on a g g^{-1} VS basis (Figure 2-7). The selection of the best ISR ratio is highly dependent on the substrate type. Several studies have suggested that a 2:1 ISR ratio on a VS basis is ideal for CH_4 production (Chynoweth et al., 1993; Hashimoto, 1989). A minimum ratio of 0.5 may be needed to ensure productivity. However, low ISR values such as 0.05-0.1 may cause overloading of the microorganisms in the digester and reduce the time to reach the final SMY (Koch et al., 2019). Low ISR values may also lead to acidification of the digester liquid (Irini Angelidaki & Sanders, 2004). If ISR volumes are too high, the inoculum may add too much CH_4 volume and skew the results (Irini Angelidaki & Sanders, 2004). Often, multiple combinations of ISRs can be tested to determine the best for the particular substrate.

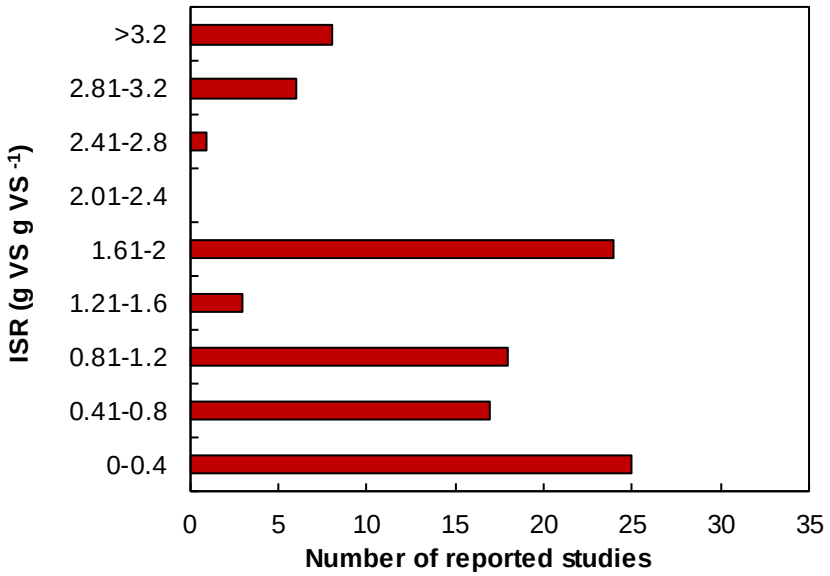

Figure 2-7. Inoculum to substrate ratios and their distribution in 88 reported BMP studies.

Source

Inoculum sources can vary, but the selection of the inoculum source can be critical. The inoculum source can influence substrate degradation (Raposo et al., 2011; Shelton & Tiedje, 1984). Additionally, different sources of inocula will contain different microorganism phyla and abundance (T. Liu, Sun, Müller, & Schnürer, 2017). It has been recommended that inoculum with a high abundance of methanogens is favorable for the BMP test (De Vrieze et al., 2015). One of the most common sources of inoculum is from the effluent from digesters treating sewage sludge (Table 2-2). However, this effluent may contain heavy metals which could be toxic (Álvarez, Mochón, Sánchez, & Rodríguez, 2002; Y. Chen, Cheng, & Creamer, 2008). Other studies use effluent from operating digesters treating a similar type of substrate, thereby assuming that the necessary microbial consortia is present.

Table 2-2. Most frequently used inoculum sources and their pros and cons.

Inoculum Source	Pros	Cons	Ref.
Industrial scale anaerobic digester treating sewage sludge	Compatible with a variety of substrates; commonly used	May contain heavy metals	1
Full scale anaerobic digester treating waste similar to substrate	May contain relevant organisms for methanogenesis	May contain inhibitory concentrations of chemical parameters	2

Table 2-2 continued.

Inoculum Source	Pros	Cons	Ref.
Cultured/Acclimated for substrate in lab	Shown to have the highest BMP when acclimated to substrate-type	Time consuming, labor intensive	3

1. Achinas, Li, Achinas, & Euverink (2019); Astals et al. (2014); Batstone, Tait, & Starrenburg (2009); Cho et al. (1995); Chynoweth et al. (1993); Elbeshbishy & Nakhla (2012); Erguder, Guven, & Demirer (2000); Eskicioglu & Ghorbani (2011); Isci & Demirer (2007); Jensen, Ge, & Batstone (2011); Koch et al. (2016); Ma et al. (2018); J. Ohemeng-Ntiamoah & Datta (2018); Rincón et al. (2010); Souza, Carvajal, Donoso-Bravo, Peña, & Fdz-Polanco (2013); Strömberg et al. (2015); R. Zhang et al. (2007); Zhu et al. (2009)
2. Belle et al. (2015); De Vrieze et al. (2015); Kafle & Chen (2016); Labatut et al. (2011); Meng et al. (2018); Neves et al. (2008); Posmanik et al. (2017); Yan, Zhang, Feng, Sun, & Dang (2018)
3. T. H. Chen & Hashimoto (1996); Gunaseelan (1995); Heo, Park, Lee, & Kang (2003); Martín-González et al. (2010); Mottet et al. (2010); Owens, J.M. and Chynoweth (1993); Y. Wang et al. (1997)

Storage

The storage conditions of inoculum can vary based on the purpose of the BMP test. Inoculum can be acclimated to specific environmental conditions or the substrate type before use (Irini Angelidaki & Sanders, 2004). It has been suggested that inoculum which has been acclimated to the specific substrate gives the best BMP results (Browne & Murphy, 2013; Koch et al., 2017). Vedrenne et al. (2008) recommended that the inoculum should be a mix of anaerobic sludge from several different digesters and that CH_4 production from inoculum should not exceed 20% of the total biogas production. Inoculum sourced from a digester treating wastewater sludge is often recommended (Filer et al., 2019).

Careful consideration of the storage temperature for inoculum should be made. Inoculum which was stored at 38°C for two weeks had decreased CH_4 production compared to fresh inoculum or inoculum that had been stored for the same about of time at 4°C (Koch et al., 2019). However, degassing the inoculum for 1-5 days at 35°C has been recommended to remove the contribution of CH_4 from the inoculum (Filer et al., 2019). Therefore, storage length and temperature of inoculum can play a critical role in BMP test results.

Ultimately, while the extent of degradation may be the same, the inoculum storage conditions can significantly affect the degradation rate (Costa et al., 2016; Koch et al., 2017; Vedrenne et al., 2008).

2.6.3 Nutrient media

The nutrients added to the BMP test can vary. Typically, the BMP test is supplemented with a nutrient media to prevent inhibition due to nutrient deficiency (Irini Angelidaki & Sanders, 2004). The bioavailability of inorganic nutrients may significantly affect AD performance (Moonil Kim et al., 2002). The nutrient media typically contains supplements for nitrogen, phosphorus, sulfur, potassium, magnesium, sodium, calcium, iron, micronutrients and growth factors (Irini Angelidaki & Sanders, 2004; Owen et al., 1979) (Table 2-3). The concentrations in nutrient media are carefully determined to meet bacterial growth requirements. Additionally, a pH buffer (NaOH) can be added to adjust the pH to neutral. The optimum range for methanogenesis is between 7–8 (Irini Angelidaki & Sanders, 2004).

However, not all BMP tests require supplemental nutrients for microbial growth. Some substrates already contain the required micronutrients for growth and the addition of nutrient media could cause toxicity to microorganisms. Dairy manure, for example, is high in required micronutrients (Belle et al., 2015). Wastewater effluents additionally contains trace nutrients (Y. Chen et al., 2008). Therefore, nutrient media would be more beneficial for pure substrates such as acetate or glucose.

Table 2-3. Concentrations and purposes of the different chemicals added to BMP testing.

Chemical	**Concentration (g L^{-1} in distilled water)**	**Purpose**
Stock Solution		
NH_4Cl	100	Nitrogen source (element in proteins and amino acids)
NaCl	10	Sodium source (used by enzymes)
$MgCl_2 \cdot 6H_2O$	10	Magnesium Source (stabilizer for ribosomes, cell membranes, nucleic acids)
$CaCl_2 \cdot 2H_2O$	5	Calcium source (stabilizer for bacterial cell wall and endospores)
$K_2HPO_4 \cdot 3H_2O$	200	Phosphorus source (nucleic acids and phospholipids)
Trace metal and selenite solution		
$FeCl_2 \cdot 4H_2O$	2	Iron source
H_3BO_3	0.05	Boron source
$ZnCl_2$	0.05	Micronutrients for enzymes
$CuCl_2 \cdot 2H_2O$	0.038	Micronutrients for enzymes
$MnCl_2 \cdot 4H_2O$	0.05	Micronutrients for enzymes
$(NH_4)_6Mo_7O_{24} \cdot 4H_2O$	0.05	Micronutrients for enzymes

Table 2-3 continued.

Chemical	Concentration (g L^{-1} in distilled water)	Purpose
Trace metal and selenite solution		
$AlCl_3$	0.05	Micronutrients for enzymes
$CoCl_2 \cdot 6H_2O$	0.05	Micronutrients for enzymes
$NiCl_2 \cdot 6H_2O$	0.092	Micronutrients for enzymes
ethylenediaminetetraacetate	0.5	
Concentrated HCl	1 mL	
$Na_2SeO_3 \cdot 5H_2O$	0.1	Micronutrients for enzymes
Vitamin Mixture		
biotin	2	Growth factor
folic Acid	2	Growth factor
pyridoxine acid	10	Growth factor
ridoflavin	5	Growth factor
thiamine hydrochloride	5	Growth factor
cyanocobalamine	0.1	Growth factor
nicotinic acid	5	Growth factor
P-aminobenzoic acid	5	Growth factor
lipoic acid	5	Growth factor
DL-pantothenic acid	5	Growth factor
Other		
Resazurin	0.5	Indicates presence of oxygen
Cysteine hydrochloride	0.5 g	Sulfur source
$NaHCO_3$	2.6 g	pH buffer
$Na_2S \cdot 9H_2O$	Add until 0.025%	Creates a reducing environment

Sources: Irini Angelidaki & Sanders (2004); Labatut (2012); Owen et al. (1979). Note, that based on the individual substrate being tested, modifications to the media used may change.

The addition of micronutrients have purposes other than for aiding microbial growth. The introduction of metal nutrients have helped to reduce VFA concentrations in mesophilic and thermophilic continuously fed AD systems (Moonil Kim et al., 2002). The addition of inorganic nutrients can also increase the hydrolysis and acidogenesis of particulates in mesophilic and thermophilic CSTR digesters receiving synthetic primary sludge (M Kim, Gomec, Ahn, & Speece, 2003). However, toxicity from the nutrient media can also occur. Metals can be involved in complex interactions during the digestion process and can affect enzyme structure and function (Y. Chen et al., 2008). Sulfate can be reduced to sulfide which can be toxic at a range from 100–800mg L^{-1} (Y. Chen et al., 2008). Inoculum used from a wastewater treatment plant (WWTP) may also contain metals which can result in toxicity (Abdel-Shafy & Mansour, 2014). Therefore, the addition of nutrients should be carefully monitored based on the type of substrate and inoculum used.

2.6.4 pH measurement and control

The pH of the digester plays a crucial role in determining methanogenic activity. In most instances, the pH is not controlled during the digestion time. More commonly, the initial pH of the digester is adjusted to 7.0 using a solution of sodium bicarbonate ($NaHCO_3$), sodium hydroxide (NaOH), or hydrochloric acid (HCL). A pH meter is typically used to measure the pH throughout the digestion period, or at minimum, on the first and final days of digestion. Sparging the digester headspace with a mixture of nitrogen gas (N_2) and CO_2 is also a method for maintaining a neutral pH in the digester. When pH is controlled throughout the digestion period in the reviewed BMP studies, it was with an automatic titration of 4-molar HCl or 4-molar NaOH (Qilin Wang et al., 2016).

2.6.5 Digester liquid sampling and sampling analyses

Typically, pH and solid concentrations are the crucial characteristics of the digestate. Solids concentrations (*i.e.*, COD, VS) are used to calculate the specific methane yields. However, measurement of other characteristics can provide insight into the influence of various properties of the substrate on CH_4 yield. For example, many studies conduct an elemental analysis of the material. Commonly measured elements are carbon (C), nitrogen (N), hydrogen (H), sulfur (S), and oxygen (O) (Cho et al., 1995; Feng et al., 2013; Posmanik et al., 2017; Romagnoli, Pastare, Sabūnas, Bāliņa, & Blumberga, 2017; Yan et al., 2018). The lignin, cellulose, and the hemi-cellulose concentrations of the substrates are also measured, particularly for feedstock crops (Achinas et al., 2019; Amon et al., 2007; Buffiere et al., 2006; Chynoweth et al., 1993; Kafle & Chen, 2016; Labatut et al., 2011; Oslaj et al., 2010; Rico et al., 2007; Triolo, Pedersen, Qu, & Sommer, 2012). Individual or total VFAs, alkalinity, TAN, total kjeldahl nitrogen (TKN), are also commonly measured. Sampling is sometimes done during the digestion period, but often times is at the beginning and end only. However, in the reviewed studies, it was rare to find a substrate which has been characterized for a comprehensive range of all these characteristics or others including conductivity, metal, phosphorus, and sulfate concentrations.

2.7 Biogas collection and quantification

2.7.1 Digester headspace air treatment

Treatment of the headspace pressure and gas composition may affect the operation of the digester. Many studies sparged the reactor with inert gases before sealing in order to remove oxygen from the headspace or liquid. In the BMP studies reviewed, nitrogen (N_2) gas was one of the most commonly used gases for sparging. In many studies, the headspace is flushed with nitrogen or a N_2/CO_2 gas mixture before sealing to remove any residual oxygen. Oxygen free N_2 gas, 70/30 or 75/25 N_2/CO_2 gas, and helium (He) were also used to flush out the headspace. However, a pressure greater than 0.5 atm in the headspace can negatively affect gas production or cause gas leakage (Owen et al., 1979).

There have been few investigations regarding sparging gas and its effect on the BMP test. Sparging with N_2 and CO_2 gas has been used to increase hydrogen (H_2) production rate by reducing the H_2 partial pressure and inhibiting acetogens and lactic acid bacteria (D. H. Kim, Han, Kim, & Shin, 2006). Additionally, a mix of N_2 and CO_2 may help maintain pH at an appropriate level for AD (Erguder et al., 2000). One inter-laboratory study found that there were no significant differences in BMP results from purging with different headspace gases (N_2, N_2-CO_2, Helium (He)) (Raposo et al., 2011). Ultimately, very few studies have examined the effect of different gases for purging the headspace on BMP results.

2.7.2 Biogas collection and measurement

The biogas produced from the individual digesters is collected periodically. In most of the BMP studies reviewed, there was less than a 5-day interval between biogas sampling dates. Frequent sampling was attributed to the prevention of pressure build-up in the digester headspace. In BMP testing, the CH_4 content of the gas is typically measured until there is a negligible amount of CH_4 production, usually a daily production of < 1% of the accumulated production from a digester (Strömberg et al., 2015). In some protocols, the experiment continues until the daily biogas volume is below < 1% of the cumulative biogas volume from the digester (Belle et al., 2015; Koch & Drewes, 2014).

Measurement of biogas volume

Several different biogas collection methods were reported in the reviewed BMP studies (Table 2-4). Biogas measurement methods were either volumetric, in which the volume was measured while the pressure was constant, or manometric, in which pressure was measured at a constant volume. The device used for determining biogas volume depended on the volume of gas produced and the digester setup.

Biogas collection and measurement is critical to prevent error in BMP testing. Volumetric methods typically operate on the principle of displacement. The syringe method uses a syringe lubricated with deionized water which has been flushed with a CO_2-N_2 mixture to evacuate the gas in the headspace. This method was popularized by Owen et al. (1979) as a standard method for the BMP test due to its easy and inexpensive setup. It can be a laborious method with precision lost depending on the demarcations of the syringe as well as friction between the piston and barrel (Guwy, 2004).

The use of water gasometers, in which the displacement of water in the device determines the volume, was also commonly used. The main issue with this method was that gas, particularly CO_2, could easily diffuse into the water resulting in inaccurate gas composition measurements (Walker, Zhang, Heaven, & Banks, 2009). Other barrier solutions, such as acidified sodium chloride, have been used and have shown decrease in CO_2 losses (Walker et al., 2009).

Continuous gas meters also operate on the principles of displacement. In on-line continuous gas flow meters, a counter will be activated when the liquid is displaced at a certain biogas pressure. They have been shown to be within 5% of the correct volume, but care must be taken to calibrate them correctly (Browne & Murphy, 2013; McEniry et al., 2014; Walker et al., 2009). Other issues with continuous gas flow meters involve corrosion, algal growth, and CO_2 solubility in water (Guwy, 2004).

Pressure transducers have been used to measure gas pressure and are fast, accurate, precise, and cost effective (Shelton & Tiedje, 1984). Online data acquisition systems allow for continuous monitoring of gas pressure and concentrations and continuous data acquisition. Continuous on-line pressure measurements from pressure transducers have been used (I Angelidaki et al., 1998; Labatut et al., 2011). Ultimately, there are several different methods for data acquisition and gas collection.

Table 2-4. Most frequently used biogas measurement methods in 88 reported BMP studies.

Method	Pros	Cons	Ref.
Manometric Methods			
Pressure transducers	Fast, accurate, precise and cost effective; data can be continuously acquired	Laborious to set up	1
Volumetric Methods			
Syringe	Easy to use, inexpensive	Limited by graduations of syringe, laborious process, friction between the piston and barrel can affect measurement	2
Water displacement gasometer	Commonly used	Gas can diffuse into water easily resulting in inaccurate volumes and gas composition measurements; labor intensive and inaccurate	3
Continuous gas flow meter	Accurate within 5%	Needs to be calibrated correctly; difficult to control CO_2 solubility, corrosive, algal growth	4

1. *I Angelidaki et al. (1998); Labatut et al. (2011); Luna-delRisco, Normak, & Orupõld (2011); Montañés, Solera, & Pérez (2015); Neves et al. (2008); Shelton & Tiedje (1984); Wagner, Lins, Malin, Reitschuler, & Illmer (2013)*
2. *Belle et al. (2015;) T. H. Chen & Hashimoto (1996); Elbeshbishy & Nakhla (2012); Elbeshbishy et al. (2012); Erguder et al. (2000); Guwy (2004); Hashimoto (1989); Lim & Fox (2013); Owens, J.M. and Chynoweth (1993); Posmanik et al. (2017); Tong et al. (1990); Turick et al. (1991); Usack & Angenent (2015); Qilin Wang et al. (2016)*
3. *Guwy (2004); Jokela (2002); Rao et al. (2000); Strömberg et al. (2015); R. Zhang et al. (2007)*
4. *Browne & Murphy (2013); Buffiere et al. (2006); Forster-Carneiro, Pérez, Romero, & Sales (2007); McEniry et al. (2014); Reilly et al. (2016)*

Measurement of biogas composition and concentration

Methane and CO_2 concentrations are most often measured with a gas chromatograph (GC). The two main GC methods are thermal conductivity detection (TCD) where both CH_4 and CO_2 are measured using N_2 as a reference gas, and flame ionization detection (FID) where only CH_4 is measured based on a standard (Irini Angelidaki & Sanders, 2004). The FID method requires a short amount of time (less than 1 minute typically) to measure the CH_4 concentration (Irini Angelidaki & Sanders, 2004). One of the benefits of a GC is that a small volume (less than 5 mL) of biogas is needed to determine a measurement. Additionally, a GC can provide highly precise readings. The drawbacks of a GC include expense, effort for calibration and operation, and variability between machines.

Another method for determining CH_4 concentration is through reacting the biogas with an alkaline solution. In this method, a known volume of biogas is injected into a serum bottle

containing a known concentration of the alkaline solution, such as potassium hydroxide (KOH) or NaOH. The serum bottle is shaken and the CO_2 and hydrogen sulfide (H_2S) gases are absorbed by the liquid for 3–4 minutes. The remaining gas in the headspace is 99.9% CH_4 and can be measured by withdrawing the gas with a syringe (Ahmadi-Pirlou, Ebrahimi-Nik, Khojastehpour, & Ebrahimi, 2017; Erguder et al., 2000; Isci & Demirer, 2007; J. Ohemeng-Ntiamoah & Datta, 2018; Pham, Triolo, Cu, Pedersen, & Sommer, 2013; Romagnoli et al., 2017; Veluchamy & Kalamdhad, 2017; Wickham, Galway, Bustamante, & Nghiem, 2016). This method has been found to produce slightly higher CH_4 concentrations than a GC, most likely due to trace gases which are not absorbed in the base liquid, but it is an inexpensive option for laboratories without access to a GC (Pham et al., 2013).

Methane measurements are preferable over CO_2 measurements as an indicator of digester activity. The CO_2 concentrations in the digester headspace may be affected by flux between the solid and liquid phases as well as ionization to bicarbonate (HCO_3^-) and carbonate (CO_3^{2-}) thereby not providing a true representation of CO_2 concentration (I Angelidaki et al., 1998; Irini Angelidaki & Sanders, 2004; Shelton & Tiedje, 1984). Methane has been found to be present in insignificant amounts in the liquid phase (I Angelidaki et al., 1998). Therefore, CH_4 production potential may be a more reliable indicator of digester activity.

2.8 BMP calculations and expressions

The general procedure for gas collection and calculations is as follows. First, the dry CH_4 gas concentration (C_{CH4}) is measured from each bottle and then corrected for the concentration of carbon dioxide (C_{CO2}) assuming insignificant fractions of a H_2S and ammonia (Kafle & Kim, 2013; Kafle et al., 2013; Triolo et al., 2012; Triolo, Sommer, Møller, Weisbjerg, & Jiang, 2011) as shown in Eq. 2-1:

$$C_{CH_4Cor} = C_{CH_4} \cdot \frac{100}{\left(C_{CH_4} + C_{CO_2}\right)} \qquad (2\text{-}1)$$

where C_{CH4cor} is the corrected concentration of dry CH_4 gas (%), C_{CH4} is the measured concentration of CH_4 gas (%) and C_{CO2} is the measured concentration of CO_2 gas (%).

Next, the measured biogas volume (V_m) of each digester is converted to Standard Temperature Pressure (STP) (Hansen et al., 2004; Kafle & Kim, 2013; Kafle et al., 2013) (Eq. 2-

2). Due to the variability of room temperatures and pressures across laboratories, the instantaneous temperature and pressure for each gas should be measured to correctly calculate gas volumes (Walker et al., 2009):

$$V_{STP} = V_m \cdot \frac{(T_{\text{standard}} \cdot P_m)}{(T_m \cdot P_{\text{standard}})} \quad (2\text{-}2)$$

where V_{STP} is the biogas volume at STP, V_m is the measured biogas volume, T_m is the measured temperature, and P_m is the measured pressure.

Then, the corrected substrate biogas volume ($V_{STP,\ substrate}$) is determined by subtracting the mean corrected blank biogas volume ($V_{STP,\ blank}$) from the corrected sample biogas volume ($V_{STP,sample}$) (Owen et al., 1979). Finally, the corrected substrate biogas volume is multiplied by the corrected CH_4 fraction to obtain the corrected volume of CH_4 gas from the substrate (Triolo et al., 2011) as shown in Eq (2-3):

$$B = C_{CH_4 Cor} \cdot V_{STP,Substrate} \quad (2\text{-}3)$$

where B is the volume of CH_4 (mL).

Finally, the CH_4 yield is determined. Methane yield is the volume of methane produced per unit of mass (Hill, 1984). Ultimate CH_4 yield (B_o) is the SMY (Møller et al., 2004). Ultimate CH_4 yield is a fraction of the theoretical CH_4 yield (B_u) due to energy requirements for cell synthesis, washout, or the presence of recalcitrant or inhibitory compounds (Møller et al., 2004). For animal manure, the animal species, breed, growth stage, feed, amount and type of bedding, manure collection method, and manure degradation extent during storage can affect SMY (Møller et al., 2004).

There are several ways to express CH_4 yield. The mass variable can be VS destroyed, VS loaded, total solids (TS) loaded, animal live weight (LW), sample mass, TCOD loaded, or sample volume (Table 2-5). Each variable has different degrees of usefulness. The VS loaded (mL CH_4 g VS^{-1}) is the most common unit for CH_4 yield. However, VS destroyed corresponds to the theoretical CH_4 yield if there were 100% biodegradability of the organic fraction (Møller et al., 2004). This metric is expected to be relatively constant between all wastes types (Hill, 1984). The VS loaded is less consistent between waste types because it corresponds to the SMY, which will vary because biodegradability can be highly variable between different waste types (Hill, 1984;

Møller et al., 2004). Additionally, using VS as opposed to COD for the mass variable does not account for the volatile fatty acids (VFAs) that are present in the feedstock and are evaporated during the VS test; these VFAs also contribute to CH_4 production (Rico et al., 2007). Because TS is a characteristic of the raw waste, dividing by TS loaded can cause variability in the reported CH_4 yields (Hill, 1984). A LW basis (m^3 CH_4 Mg LW-day^{-1}) is the most useful for economic comparisons and provides the amount of CH_4 per animal (Hill, 1984). Comparisons using sample volume (L CH_4 m^{-3}) can also be useful for economic comparisons but can be skewed by the water content of the substrate (Møller et al., 2004). Overall, the expression of CH_4 yield can be chosen based on the intended application of the data (Table 2-5).

Table 2-5. Seven most frequently used SMY expression methods.

Method	Unit	Remarks	Ref.
VS destroyed	mL CH_4 g VS^{-1}	Corresponds to the theoretical CH_4 yield	1
VS loaded	mL CH_4 g VS^{-1}	Less constant between waste types; corresponds to ultimate CH_4 yield	2
TS loaded	mL CH_4 g TS^{-1}	Greater variance between samples	3
Animal LW	m^3 CH_4 Mg LW-day^{-1}	Useful for economic comparisons	1
Sample volume	L CH_4 m^{-3}	Can be skewed by water content	3
TCOD loaded	mL CH_4 g TCOD $added^{-1}$	Includes soluble VFAs which may be lost in VS process	4
Mass loaded	mL CH_4 g $waste^{-1}$	Useful for economic comparisons	5

1. Gaur & Suthar (2017); Hill (1984); Møller et al. (2004);
2.(Alzate et al. (2012); Badshah et al. (2012); Belle et al. (2015); Browne & Murphy (2013); Cho et al. (1995); Chynoweth et al. (1993); Labatut et al. (2011); Luostarinen et al. (2009); Luste et al. (2012); Møller et al. (2004); Neves et al. (2008); Owens, J.M. and Chynoweth (1993); Rico et al. (2007); Rincón et al. (2010); Turick et al. (1991); Usack & Angenent (2015); Vedrenne et al. (2008)
3. Hill (1984);
4. Elbeshbishy & Nakhla (2012); Kafle & Kim (2012, 2013); Palatsi et al. (2011);
5. Isci & Demirer (2007); Wickham et al. (2016).

2.9 Reliability and applicability of the BMP test data

There was considerable variability within each BMP testing methodology for the reviewed BMP studies. Whereas the BMP test can be a useful metric, there has been a call for increased standardization of the BMP test (I. Angelidaki et al., 2009; Strömberg et al., 2014; Walker et al., 2009). Notably, the collection, storage, measurement, and calculations of CH_4 volumes are often poorly reported and variable among studies (Walker et al., 2009).

The BMP test results have been compared with CH_4 production from lab-scale or full-scale continuous or semi-continuous digesters (Chynoweth et al., 1993; Jerger, Chynoweth, & Isaacson,

1987; M. Kim, Chowdhury, Nakhla, & Keleman, 2016; Koch et al., 2016; Usack & Angenent, 2015). There has been agreement between SMYs obtained from the BMP test to those obtained from semi-continuously fed lab-scale digesters (Chynoweth et al., 1993). Semi-continuously fed or continuously fed digesters, if the hydraulic retention time (HRT) is long enough, can approach similar degradation kinetics as batch systems for similar substrates, despite their operational differences (Labatut, 2012). However, Jerger et al. (1987) found that SMYs of sorghum were higher than in a lab-scale continuously stirred tank reactor (CSTR) and non-mixed vertical flow reactor (NMVFR) at the same temperature and HRT, but different solids retention time (SRT); but the NMVFR digester had a higher SMY than the CSTR, indicating that the type of large scale digester may affect BMP results.

Additionally, the BMP test is less ideal for co-digested mixtures. Mixtures of substrates can have synergistic effects that may be obscured by the favorable conditions of the BMP test (Koch, Hafner, Weinrich, Astals, & Holliger, 2020; Koch et al., 2016; Nielfa, Cano, Pérez, & Fdez-Polanco, 2015). Koch et al. (2016) found that the CH_4 yield from a mesophilic semi-continuous full scale (1350 m^3) digester co-digesting food waste and raw sludge was generally higher than in batch tests, though they hypothesized this was because of a slight increase in the percentage of sludge during the large-scale operation. Conversely, Labatut (2012) found that the CH_4 yields for co-digested substrates (manure, dog food) were higher in the BMP test than in semi-continuously fed mesophilic and thermophilic lab-scale digesters. The results of BMP tests using co-digested materials should thus be carefully examined.

The data from a BMP tests typically has a limited range of application. Inter-laboratory differences, such as laboratory setup, operation, substrate and inoculum treatment, and SMY calculations can affect the BMP results more than within an individual test. Within individual tests, results can often be reproduced with less than 10% error among replicates (Shelton & Tiedje, 1984). Therefore, BMP results may be reliable for an individual test, but may not be applicable to a broader scope. Overall, consideration of the large-scale substrate type, digester configuration, operational parameters, and application are essential for predictive applicability of the BMP test to large-scale digesters.

2.10 Conclusions

The following conclusions were drawn from this chapter:

1. Automated BMP tests are a state-of-the-art-method that can improve precision and accuracy of the results through reducing operator error.
2. Glass serum bottles of a volume of 250 mL or less are commonly used as digesters in BMP tests.
3. Close monitoring of the BMP test in regards to temperature, mixing, and duration is required to ensure that the maximum CH_4 potential is reached before ending the experiment.
4. Collection, storage, and pretreatment of the substrate and inoculum can significantly affect BMP results.
5. The reliability of BMP test results can be improved through the use of a positive control, correcting gas volumes at STP, and consistent BMP calculations.
6. Factors such as co-digestion, digester type, and volume should be considered when comparing BMP test results to large-scale AD systems.

2.11 References

Abbasi, T., Tauseef, S. M., & Abbasi, S. A. (2012). Anaerobic digestion for global warming control and energy generation - An overview. *Renewable and Sustainable Energy Reviews*, *16*(5), 3228–3242. https://doi.org/10.1016/j.rser.2012.02.046

Abdel-Shafy, H. I., & Mansour, M. S. M. (2014). Biogas production as affected by heavy metals in the anaerobic digestion of sludge. *Egyptian Journal of Petroleum*, *23*(4), 409–417. https://doi.org/10.1016/j.ejpe.2014.09.009

Achinas, S., Li, Y., Achinas, V., & Euverink, G. J. W. (2019). Biogas Potential from the Anaerobic Digestion of Potato Peels: Process Performance and Kinetics Evaluation. *Energies*, *12*(12), 2311. https://doi.org/10.3390/en12122311

Ahmadi-Pirlou, M., Ebrahimi-Nik, M., Khojastehpour, M., & Ebrahimi, S. H. (2017). Mesophilic co-digestion of municipal solid waste and sewage sludge: Effect of mixing ratio, total solids, and alkaline pretreatment. *International Biodeterioration and Biodegradation*, *125*, 97–104. https://doi.org/10.1016/j.ibiod.2017.09.004

Álvarez, E. A., Mochón, M. C., Sánchez, J. C. J., & Rodríguez, M. T. (2002). Heavy metal extractable forms in sludge from wastewater treatment plants. *Chemosphere*, *47*(7), 765–775. https://doi.org/10.1016/S0045-6535(02)00021-8

Alzate, M. E., Muñoz, R., Rogalla, F., Fdz-Polanco, F., & Pérez-Elvira, S. I. (2012). Biochemical methane potential of microalgae: Influence of substrate to inoculum ratio, biomass concentration and pretreatment. *Bioresource Technology*, *123*, 488–494. https://doi.org/10.1016/j.biortech.2012.06.113

Amha, Y. M., Sinha, P., Lagman, J., Gregori, M., & Smith, A. L. (2017). Elucidating microbial community adaptation to anaerobic co-digestion of fats, oils, and grease and food waste. *Water Research*, *123*, 277–289. https://doi.org/10.1016/j.watres.2017.06.065

Amon, T., Amon, B., Kryvoruchko, V., Zollitsch, W., Mayer, K., & Gruber, L. (2007). Biogas production from maize and dairy cattle manure-Influence of biomass composition on the methane yield. *Agriculture, Ecosystems and Environment*, *118*(1–4), 173–182. https://doi.org/10.1016/j.agee.2006.05.007

Angelidaki, I., Alves, M., Bolzonella, D., Borzacconi, L., Campos, J. L., Guwy, A. J., … van Lier, J. B. (2009). Defining the biomethane potential (BMP) of solid organic wastes and energy crops: A proposed protocol for batch assays. *Water Science and Technology*, *59*(5), 927–934. https://doi.org/10.2166/wst.2009.040

Angelidaki, I., Schmidt, J. E., Ellegaard, L., & Ahring, B. K. (1998). An automatic system for simultaneous monitoring of gas evolution in multiple closed vessels. *Journal of Microbiological Methods*, *33*(1), 93–100. https://doi.org/10.1016/S0167-7012(98)00044-X

Angelidaki, Irini, & Sanders, W. (2004). Assessment of the anaerobic biodegradability of macropollutants. *Reviews in Environmental Science and Biotechnology*, *3*(2), 117–129. https://doi.org/10.1007/s11157-004-2502-3

Astals, S., Batstone, D. J., Mata-Alvarez, J., & Jensen, P. D. (2014). Identification of synergistic impacts during anaerobic co-digestion of organic wastes. *Bioresource Technology*, *169*, 421–427. https://doi.org/10.1016/j.biortech.2014.07.024

Badshah, M., Lam, D. M., Liu, J., & Mattiasson, B. (2012). Use of an Automatic Methane Potential Test System for evaluating the biomethane potential of sugarcane bagasse after different treatments. *Bioresource Technology*, *114*, 262–269. https://doi.org/10.1016/j.biortech.2012.02.022

Barlaz, M. A., Ham, R. K., Schaefer, D. M., Isaacson, R., & Carolina, N. (1990). Methane production from municipal refuse : A review of enhancement techniques and microbial dynamics. *Critical Reviews in Environmental Control*, *19*(6), 557–584. https://doi.org/10.1080/10643389009388384

Barrera, E. L., Spanjers, H., Dewulf, J., Romero, O., & Rosa, E. (2013). The sulfur chain in biogas production from sulfate-rich liquid substrates: A review on dynamic modeling with vinasse as model substrate. *Journal of Chemical Technology and Biotechnology*, *88*(8), 1405–1420. https://doi.org/10.1002/jctb.4071

Batstone, D. J., Tait, S., & Starrenburg, D. (2009). Estimation of hydrolysis parameters in full-scale anerobic digesters. *Biotechnology and Bioengineering*, *102*(5), 1513–1520. https://doi.org/10.1002/bit.22163

Belle, A. J., Lansing, S., Mulbry, W., & Weil, R. R. (2015). Methane and hydrogen sulfide production during co-digestion of forage radish and dairy manure. *Biomass and Bioenergy*, *80*, 44–51. https://doi.org/10.1016/j.biombioe.2015.04.029

Browne, J. D., & Murphy, J. D. (2013). Assessment of the resource associated with biomethane from food waste. *Applied Energy*, *104*, 170–177. https://doi.org/10.1016/j.apenergy.2012.11.017

Buffiere, P., Loisel, D., Bernet, N., & Delgenes, J.-P. (2006). Towards new indicators for the prediction of solid waste anaerobic digestion properties. *Water Science and Technology*, *53*(8), 233–241. https://doi.org/10.2166/wst.2006.254

Chen, T. H., & Hashimoto, A. G. (1996). Effects of pH and substrate:inoculum ratio on batch methane fermentation. *Bioresource Technology*, *56*(2–3), 179–186. https://doi.org/10.1016/0960-8524(96)00016-8

Chen, Y., Cheng, J. J., & Creamer, K. S. (2008). Inhibition of anaerobic digestion process: A review. *Bioresource Technology*, *99*(10), 4044–4064. https://doi.org/10.1016/j.biortech.2007.01.057

Cho, J. K., Park, S. C., & Chang, H. N. (1995). Biochemical methane potential and solid state anaerobic digestion of Korean food wastes. *Bioresource Technology*, *52*(3), 245–253. https://doi.org/10.1016/0960-8524(95)00031-9

Chynoweth, D. P., Turick, C. E., Owens, J. M., Jerger, D. E., & Peck, M. W. (1993). Biochemical methane potential of biomass and waste feedstocks. *Biomass and Bioenergy*, *5*(1), 95–111. https://doi.org/10.1016/0961-9534(93)90010-2

Costa, J. C., Oliveira, J. V., & Alves, M. M. (2016). Response surface design to study the influence of inoculum, particle size and inoculum to substrate ratio on the methane production from Ulex sp. *Renewable Energy*, *96*, 1071–1077. https://doi.org/10.1016/j.renene.2015.10.028

Daly, S. E., & Ni, J. (n.d.). No Title.

Davidsson, Å., Gruvberger, C., Christensen, T. H., Hansen, T. L., & Jansen, J. la C. (2007). Methane yield in source-sorted organic fraction of municipal solid waste. *Waste Management*, *27*(3), 406–414. https://doi.org/10.1016/j.wasman.2006.02.013

De Baere, L. (2000). Anaerobic digestion of solid waste: state-of-the-art. *Water Science and Technology : A Journal of the International Association on Water Pollution Research*, *41*(3), 283–290.

De Vrieze, J., Raport, L., Willems, B., Verbrugge, S., Volcke, E., Meers, E., … Boon, N. (2015). Inoculum selection influences the biochemical methane potential of agro-industrial substrates. *Microbial Biotechnology*, *8*(5), 776–786. https://doi.org/10.1111/1751-7915.12268

Dechrugsa, S., Kantachote, D., & Chaiprapat, S. (2013). Effects of inoculum to substrate ratio, substrate mix ratio and inoculum source on batch co-digestion of grass and pig manure. *Bioresource Technology*, *146*, 101–108. https://doi.org/10.1016/j.biortech.2013.07.051

Edward, M., Edwards, S., Egwu, U., & Sallis, P. (2015). Bio-methane potential test (BMP) using inert gas sampling bags with macroalgae feedstock. *Biomass and Bioenergy*, *83*, 516–524. https://doi.org/10.1016/j.biombioe.2015.10.026

Elbeshbishy, E., & Nakhla, G. (2012). Batch anaerobic co-digestion of proteins and carbohydrates. *Bioresource Technology*, *116*, 170–178. https://doi.org/10.1016/j.biortech.2012.04.052

Elbeshbishy, E., Nakhla, G., & Hafez, H. (2012). Biochemical methane potential (BMP) of food waste and primary sludge: Influence of inoculum pre-incubation and inoculum source. *Bioresource Technology*, *110*, 18–25. https://doi.org/10.1016/j.biortech.2012.01.025

Erguder, T. H., Guven, E., & Demirer, G. N. (2000). Anaerobic treatment of olive mill wastewaters in batch reactors. *Process Biochemistry*, *36*(3), 243–248. https://doi.org/10.1016/S0032-9592(00)00205-3

Eskicioglu, C., & Ghorbani, M. (2011). Effect of inoculum/substrate ratio on mesophilic anaerobic digestion of bioethanol plant whole stillage in batch mode. *Process Biochemistry*, *46*(8), 1682–1687. https://doi.org/10.1016/j.procbio.2011.04.013

Feng, L., Li, Y., Chen, C., Liu, X., Xiao, X., Ma, X., … Liu, G. (2013). Biochemical methane potential (BMP) of vinegar residue and the influence of feed to inoculum ratios on biogas production. *BioResources*, *8*(2), 2487–2498. https://doi.org/10.15376/biores.8.2.2487-2498

Filer, J., Ding, H. H., & Chang, S. (2019). Biochemical Methane Potential (BMP) Assay Method for Anaerobic Digestion Research. *Water*, *11*(921). https://doi.org/10.3390/w11050921

Forster-Carneiro, T., Pérez, M., Romero, L. I., & Sales, D. (2007). Dry-thermophilic anaerobic digestion of organic fraction of the municipal solid waste: Focusing on the inoculum sources. *Bioresource Technology*, *98*(17), 3195–3203. https://doi.org/10.1016/j.biortech.2006.07.008

Gaur, R. Z., & Suthar, S. (2017). Anaerobic digestion of activated sludge, anaerobic granular sludge and cow dung with food waste for enhanced methane production. *Journal of Cleaner Production*, *164*, 557–566. https://doi.org/10.1016/j.jclepro.2017.06.201

Gavala, H. N., Angelidaki, I., & Ahring, B. K. (2003). Kinetics and Modeling of Anaerobic Digestion Process. In B. K. Ahring (Ed.), *Biomethanation I* (pp. 57–93). Berlin: Springer.

Gerardi, M. H. (2003). *The Microbiology of Anaerobic Digesters*. Hoboken, NJ: John Wiley & Sons, Inc. https://doi.org/10.1002/0471468967

Gunaseelan, N. V. (1995). Effect of inoculum/substrate ratio and pretreatments on methane yield from Parthenium. *Biomass and Bioenergy*, *8*(1), 39–44. https://doi.org/10.1016/0961-9534(94)00086-9

Guwy, A. J. (2004). Equipment used for testing anaerobic biodegradability and activity. *Reviews in Environmental Science and Biotechnology*, *3*(2), 131–139. https://doi.org/10.1007/s11157-004-1290-0

Hafner, S. D., & Astals, S. (2019). Systematic error in manometric measurement of biochemical methane potential: Sources and solutions. *Waste Management*, *91*, 147–155. https://doi.org/10.1016/j.wasman.2019.05.001

Hansen, T. L., Schmidt, J. E., Angelidaki, I., Marca, E., Jansen, J. L. C., Mosbæk, H., & Christensen, T. H. (2004). Method for determination of methane potentials of solid organic waste. *Waste Management*, *24*(4), 393–400. https://doi.org/10.1016/j.wasman.2003.09.009

Hashimoto, A. G. (1989). Effect of inoculum/substrate ratio on methane yield and production rate from straw. *Biological Wastes*, *28*, 247–255. https://doi.org/10.1016/0269-7483(89)90108-0

Heo, N. H., Park, S. C., Lee, J. S., & Kang, H. (2003). Solubilization of waste activated sludge by alkaline pretreatment and biochemical methane potential (BMP) tests for anaerobic co-digestion of municipal organic waste. *Water Science and Technology*, *48*(8), 211–219.

Hill, D. T. (1984). Methane productivity of the major animal waste types. *Transactions of the ASAE*, *27*(2), 530–534. https://doi.org/10.13031/2013.32822

Isci, A., & Demirer, G. N. (2007). Biogas production potential from cotton wastes. *Renewable Energy*, *32*(5), 750–757. https://doi.org/10.1016/j.renene.2006.03.018

Jensen, P. D., Ge, H., & Batstone, D. J. (2011). Assessing the role of biochemical methane potential tests in determining anaerobic degradability rate and extent. *Water Science and Technology*, *64*(4), 880–886. https://doi.org/10.2166/wst.2011.662

Jerger, D. E., Chynoweth, D. P., & Isaacson, H. R. (1987). Anaerobic digestion of sorghum biomass. *Biomass*, *14*(2), 99–113. https://doi.org/10.1016/0144-4565(87)90013-8

Jokela, J. (2002). *Landfill operation and waste management procedures in the reduction of methane and leachate pollutant emissions from municipal solid waste landfills*. University of JYVÄSKYLÄ, Finland.

Kafle, G. K., & Chen, L. (2016). Comparison on batch anaerobic digestion of five different livestock manures and prediction of biochemical methane potential (BMP) using different statistical models. *Waste Management*, *48*, 492–502. https://doi.org/10.1016/j.wasman.2015.10.021

Kafle, G. K., & Kim, S. H. (2012). Kinetic Study of the Anaerobic Digestion of Swine Manure at Mesophilic Temperature : A Lab Scale Batch Operation. *Journal of Biosystems Engineering*, *37*(4), 233–244. https://doi.org/http://dx.doi.org/10.5307/JBE.2012.37.4.233

Kafle, G. K., & Kim, S. H. (2013). Anaerobic treatment of apple waste with swine manure for biogas production: Batch and continuous operation. *Applied Energy*, *103*, 61–72. https://doi.org/10.1016/j.apenergy.2012.10.018

Kafle, G. K., Kim, S. H., & Sung, K. I. (2013). Ensiling of fish industry waste for biogas production: A lab scale evaluation of biochemical methane potential (BMP) and kinetics. *Bioresource Technology*, *127*, 326–336. https://doi.org/10.1016/j.biortech.2012.09.032

Kawai, M., Nagao, N., Tajima, N., Niwa, C., Matsuyama, T., & Toda, T. (2014). The effect of the labile organic fraction in food waste and the substrate/inoculum ratio on anaerobic digestion for a reliable methane yield. *Bioresource Technology*, *157*, 174–180. https://doi.org/10.1016/j.biortech.2014.01.018

Kim, D. H., Han, S. K., Kim, S. H., & Shin, H. S. (2006). Effect of gas sparging on continuous fermentative hydrogen production. *International Journal of Hydrogen Energy*, *31*(15), 2158–2169. https://doi.org/10.1016/j.ijhydene.2006.02.012

Kim, M., Ahn, Y.-H., & Speece, R. E. (2002). Comparative process stability and efficiency of anaerobic digestion; mesophilic vs. thermophilic. *Water Research*, *36*(17), 4369–4385. https://doi.org/10.1016/S0043-1354(02)00147-1

Kim, M., Chowdhury, M. M. I., Nakhla, G., & Keleman, M. (2016). Synergism of co-digestion of food wastes with municipal wastewater treatment biosolids. *Waste Management*, 1–11. https://doi.org/10.1016/j.wasman.2016.10.010

Kim, M., Gomec, C. Y., Ahn, Y., & Speece, R. E. (2003). Hydrolysis and acidogenesis of particulate organic material in mesophilic and thermophilic anaerobic digestion. *Environmental Technology*, *24*(9), 1183–1190. https://doi.org/10.1080/09593330309385659

Koch, K., & Drewes, J. E. (2014). Alternative approach to estimate the hydrolysis rate constant of particulate material from batch data. *Applied Energy*, *120*, 11–15. https://doi.org/10.1016/j.apenergy.2014.01.050

Koch, K., Hafner, S. D., Weinrich, S., & Astals, S. (2019). Identification of Critical Problems in Biochemical Methane Potential (BMP) Tests From Methane Production Curves. *Frontiers in Environmental Science*, *7*(November), 1–8. https://doi.org/10.3389/fenvs.2019.00178

Koch, K., Hafner, S. D., Weinrich, S., Astals, S., & Holliger, C. (2020). Power and Limitations of Biochemical Methane Potential (BMP) Tests. *Frontiers in Energy Research*, *8*(April), 1–4. https://doi.org/10.3389/fenrg.2020.00063

Koch, K., Lippert, T., & Drewes, J. E. (2017). The role of inoculum's origin on the methane yield of different substrates in biochemical methane potential (BMP) tests. *Bioresource Technology*, *243*, 457–463. https://doi.org/10.1016/j.biortech.2017.06.142

Koch, K., Plabst, M., Schmidt, A., Helmreich, B., & Drewes, J. E. (2016). Co-digestion of food waste in a municipal wastewater treatment plant: Comparison of batch tests and full-scale experiences. *Waste Management*, *47*, 28–33. https://doi.org/10.1016/j.wasman.2015.04.022

Kolbl, S., Paloczi, A., Panjan, J., & Stres, B. (2014). Addressing case specific biogas plant tasks: Industry oriented methane yields derived from 5L Automatic Methane Potential Test Systems in batch or semi-continuous tests using realistic inocula, substrate particle sizes and organic loading. *Bioresource Technology*, *153*, 180–188. https://doi.org/10.1016/j.biortech.2013.12.010

Labatut, R. A. (2012). *Anaerobic Biodegradability of Complex Substrates: Performance and Stability At Mesophilic And Thermophilic Conditions*. Cornell University.

Labatut, R. A., Angenent, L. T., & Scott, N. R. (2011). Biochemical methane potential and biodegradability of complex organic substrates. *Bioresource Technology*, *102*(3), 2255–2264. https://doi.org/10.1016/j.biortech.2010.10.035

Leng, L., Yang, P., Singh, S., Zhuang, H., Xu, L., Chen, W. H., … Lee, P. H. (2018). A review on the bioenergetics of anaerobic microbial metabolism close to the thermodynamic limits and its implications for digestion applications. *Bioresource Technology*, *247*, 1095–1106. https://doi.org/10.1016/j.biortech.2017.09.103

Lesteur, M., Bellon-Maurel, V., Gonzalez, C., Latrille, E., Roger, J. M., Junqua, G., & Steyer, J. P. (2010). Alternative methods for determining anaerobic biodegradability: A review. *Process Biochemistry*, *45*(4), 431–440. https://doi.org/10.1016/j.procbio.2009.11.018

Lim, S. J., & Fox, P. (2013). Biochemical methane potential (BMP) test for thickened sludge using anaerobic granular sludge at different inoculum/substrate ratios. *Biotechnology and Bioprocess Engineering*, *18*(2), 306–312. https://doi.org/10.1007/s12257-012-0465-8

Liu, G., Zhang, R., El-Mashad, H. M., & Dong, R. (2009). Effect of feed to inoculum ratios on biogas yields of food and green wastes. *Bioresource Technology*, *100*(21), 5103–5108. https://doi.org/10.1016/j.biortech.2009.03.081

Liu, T., Sun, L., Müller, B., & Schnürer, A. (2017). Importance of inoculum source and initial community structure for biogas production from agricultural substrates. *Bioresource Technology*, *245*(July), 768–777. https://doi.org/10.1016/j.biortech.2017.08.213

Luna-delRisco, M., Normak, A., & Orupõld, K. (2011). Biochemical methane potential of different organic wastes and energy crops from Estonia. *Agronomy Research*, *9*(1–2), 331–342.

Luostarinen, S., Luste, S., & Sillanpää, M. (2009). Increased biogas production at wastewater treatment plants through co-digestion of sewage sludge with grease trap sludge from a meat processing plant. *Bioresource Technology*, *100*(1), 79–85. https://doi.org/10.1016/j.biortech.2008.06.029

Luste, S., Heinonen-Tanski, H., & Luostarinen, S. (2012). Co-digestion of dairy cattle slurry and industrial meat-processing by-products - Effect of ultrasound and hygienization pre-treatments. *Bioresource Technology*, *104*, 195–201. https://doi.org/10.1016/j.biortech.2011.11.003

Ma, Y., Gu, J., & Liu, Y. (2018). Evaluation of anaerobic digestion of food waste and waste activated sludge: Soluble COD versus its chemical composition. *Science of the Total Environment*, *643*, 21–27. https://doi.org/10.1016/j.scitotenv.2018.06.187

Mao, C., Feng, Y., Wang, X., & Ren, G. (2015). Review on research achievements of biogas from anaerobic digestion. *Renewable and Sustainable Energy Reviews*, *45*, 540–555. https://doi.org/10.1016/j.rser.2015.02.032

Martín-González, L., Colturato, L. F., Font, X., & Vicent, T. (2010). Anaerobic co-digestion of the organic fraction of municipal solid waste with FOG waste from a sewage treatment plant: Recovering a wasted methane potential and enhancing the biogas yield. *Waste Management*, *30*(10), 1854–1859. https://doi.org/10.1016/j.wasman.2010.03.029

Mata-Alvarez, J., Dosta, J., Romero-Güiza, M. S., Fonoll, X., Peces, M., & Astals, S. (2014). A critical review on anaerobic co-digestion achievements between 2010 and 2013. *Renewable and Sustainable Energy Reviews*, *36*, 412–427. https://doi.org/10.1016/j.rser.2014.04.039

Mata-Alvarez, J., Mac, S., & Llabr, P. (2000). Anaerobic digestion of organic solid wastes. An overview of research achievements and perspectives. *Bioresource Technology*, *74*(1), 3–16. https://doi.org/10.1016/S0960-8524(00)00023-7

McEniry, J., Allen, E., Murphy, J. D., & O'Kiely, P. (2014). Grass for biogas production: The impact of silage fermentation characteristics on methane yield in two contrasting biomethane potential test systems. *Renewable Energy*, *63*, 524–530. https://doi.org/10.1016/j.renene.2013.09.052

McMahon, K. D., Stroot, P. G., Mackie, R. I., & Raskin, L. (2001). Anaerobic codigestion of municipal solid waste and biosolids under various mixing conditions-II: Microbial population dynamics. *Water Research*, *35*(7), 1817–1827. https://doi.org/10.1016/S0043-1354(00)00438-3

Meng, L., Xie, L., Kinh, C. T., Suenaga, T., Hori, T., Riya, S., … Hosomi, M. (2018). Influence of feedstock-to-inoculum ratio on performance and microbial community succession during solid-state thermophilic anaerobic co-digestion of pig urine and rice straw. *Bioresource Technology*, *252*(October 2017), 127–133. https://doi.org/10.1016/j.biortech.2017.12.099

Møller, H. B., Sommer, S. G., & Ahring, B. K. (2004). Methane productivity of manure, straw and solid fractions of manure. *Biomass and Bioenergy*, *26*(5), 485–495. https://doi.org/10.1016/j.biombioe.2003.08.008

Montañés, R., Solera, R., & Pérez, M. (2015). Anaerobic co-digestion of sewage sludge and sugar beet pulp lixiviation in batch reactors: Effect of temperature. *Bioresource Technology*, *180*, 177–184. https://doi.org/10.1016/j.biortech.2014.12.056

Montusiewicz, A., Lebiocka, M., Rozej, A., Zacharska, E., & Pawłowski, L. (2010). Freezing/thawing effects on anaerobic digestion of mixed sewage sludge. *Bioresource Technology*, *101*(10), 3466–3473. https://doi.org/10.1016/j.biortech.2009.12.125

Mottet, A., François, E., Latrille, E., Steyer, J. P., Déléris, S., Vedrenne, F., & Carrère, H. (2010). Estimating anaerobic biodegradability indicators for waste activated sludge. *Chemical Engineering Journal*, *160*(2), 488–496. https://doi.org/10.1016/j.cej.2010.03.059

Neves, L., Gonçalo, E., Oliveira, R., & Alves, M. M. (2008). Influence of composition on the biomethanation potential of restaurant waste at mesophilic temperatures. *Waste Management*, *28*(6), 965–972. https://doi.org/10.1016/j.wasman.2007.03.031

Nielfa, A., Cano, R., Pérez, A., & Fdez-Polanco, M. (2015). Co-digestion of municipal sewage sludge and solid waste: Modelling of carbohydrate, lipid and protein content influence. *Waste Management & Research : The Journal of the International Solid Wastes and Public Cleansing Association, ISWA*, *33*(3), 241–249. https://doi.org/10.1177/0734242X15572181

Nizami, A. S., Orozco, A., Groom, E., Dieterich, B., & Murphy, J. D. (2012). How much gas can we get from grass? *Applied Energy*, *92*, 783–790. https://doi.org/10.1016/j.apenergy.2011.08.033

OECD. (2006). *Test No. 311: Anaerobic Biodegradability of Organic Compounds in Digested Sludge: by Measurement of Gas Production*. *OECD Guidelines for the Testing of Chemicals*. Paris: OECD Publishing. https://doi.org/10.1787/9789264016842-en

Ohemeng-Ntiamoah, J., & Datta, T. (2018). Evaluating analytical methods for the characterization of lipids, proteins and carbohydrates in organic substrates for anaerobic co-digestion. *Bioresource Technology*, *247*(September 2017), 697–704. https://doi.org/10.1016/j.biortech.2017.09.154

Ohemeng-Ntiamoah, Juliet, & Datta, T. (2019). Perspectives on variabilities in biomethane potential test parameters and outcomes: A review of studies published between 2007 and 2018. *Science of the Total Environment*, *664*, 1052–1062. https://doi.org/10.1016/j.scitotenv.2019.02.088

Oslaj, M., Mursec, B., & Vindis, P. (2010). Biogas production from maize hybrids. *Biomass and Bioenergy*, *34*(11), 1538–1545. https://doi.org/10.1016/j.biombioe.2010.04.016

Owen, W. F., Stuckev, D. C., Healy, J. B., Young, L. Y., & Mccarty, P. L. (1979). Bioassay for monitering biochemical methane potential and anaerobic toxicity. *Water Research*, *13*(6), 485–492. https://doi.org/10.1016/0043-1354(79)90043-5

Owens, J.M. and Chynoweth, D. P. (1993). Biochemical methane potential of municipal solid waste (MSW) components. *Water Science & Technology*, *27*(2), 1–14. https://doi.org/10.2166/wst.1993.0065

Palatsi, J., Viñas, M., Guivernau, M., Fernandez, B., & Flotats, X. (2011). Anaerobic digestion of slaughterhouse waste: Main process limitations and microbial community interactions. *Bioresource Technology*, *102*(3), 2219–2227. https://doi.org/10.1016/j.biortech.2010.09.121

Pearse, L. F., Hettiaratchi, J. P., & Kumar, S. (2018). Towards developing a representative biochemical methane potential (BMP) assay for landfilled municipal solid waste – A review. *Bioresource Technology*, *254*(January), 312–324. https://doi.org/10.1016/j.biortech.2018.01.069

Petropoulos, E., Dolfing, J., Davenport, R. J., Bowen, E. J., & Curtis, T. P. (2017). Developing cold-adapted biomass for the anaerobic treatment of domestic wastewater at low temperatures (4, 8 and 15 °C) with inocula from cold environments. *Water Research*, *112*, 100–109. https://doi.org/10.1016/j.watres.2016.12.009

Pham, C. H., Triolo, J. M., Cu, T. T. T., Pedersen, L., & Sommer, S. G. (2013). Validation and recommendation of methods to measure biogas production potential of animal manure. *Asian-Australasian Journal of Animal Sciences*, *26*(6), 864–873. https://doi.org/10.5713/ajas.2012.12623

Ponsá, S., Gea, T., & Sánchez, A. (2011). Short-time estimation of biogas and methane potentials from municipal solid wastes. *Journal of Chemical Technology and Biotechnology*, *86*(8), 1121–1124. https://doi.org/10.1002/jctb.2615

Posmanik, R., Labatut, R. A., Kim, A. H., Usack, J. G., Tester, J. W., & Angenent, L. T. (2017). Coupling hydrothermal liquefaction and anaerobic digestion for energy valorization from model biomass feedstocks. *Bioresource Technology*, *233*, 134–143. https://doi.org/10.1016/j.biortech.2017.02.095

Rao, M. S., Singh, S. P., Singh, A. K., & Sodha, M. S. (2000). Bioenergy conversion studies of the organic fraction of MSW: assessment of ultimate bioenergy production potential of municipal garbage. *Applied Energy*, *66*(1), 75–87. https://doi.org/10.1016/S0306-2619(99)00056-2

Raposo, F., De La Rubia, M. A., Fernández-Cegrí, V., & Borja, R. (2012). Anaerobic digestion of solid organic substrates in batch mode: An overview relating to methane yields and experimental procedures. *Renewable and Sustainable Energy Reviews*, *16*(1), 861–877. https://doi.org/10.1016/j.rser.2011.09.008

Raposo, F., Fernández-Cegrí, V., de la Rubia, M. A., Borja, R., Béline, F., Cavinato, C., … de Wilde, V. (2011). Biochemical methane potential (BMP) of solid organic substrates: Evaluation of anaerobic biodegradability using data from an international interlaboratory study. *Journal of Chemical Technology and Biotechnology*, *86*(8), 1088–1098. https://doi.org/10.1002/jctb.2622

Reilly, M., Dinsdale, R., & Guwy, A. (2016). The impact of inocula carryover and inoculum dilution on the methane yields in batch methane potential tests. *Bioresource Technology*, *208*, 134–139. https://doi.org/10.1016/j.biortech.2016.02.060

Rico, J. L., García, H., Rico, C., & Tejero, I. (2007). Characterisation of solid and liquid fractions of dairy manure with regard to their component distribution and methane production. *Bioresource Technology*, *98*(5), 971–979. https://doi.org/10.1016/j.biortech.2006.04.032

Rincón, B., Banks, C. J., & Heaven, S. (2010). Biochemical methane potential of winter wheat (Triticum aestivum L.): Influence of growth stage and storage practice. *Bioresource Technology*, *101*(21), 8179–8184. https://doi.org/10.1016/j.biortech.2010.06.039

Romagnoli, F., Pastare, L., Sabūnas, A., Bāliņa, K., & Blumberga, D. (2017). Effects of pre-treatment on Biochemical Methane Potential (BMP) testing using Baltic Sea Fucus vesiculosus feedstock. *Biomass and Bioenergy*, *105*, 23–31. https://doi.org/10.1016/j.biombioe.2017.06.013

Shelton, D., & Tiedje, J. (1984). General method for determining anaerobic biodegradation potential. *Applied and Environmental Microbiology*, *47*(4), 850–857.

Souza, T. S. O., Carvajal, A., Donoso-Bravo, A., Peña, M., & Fdz-Polanco, F. (2013). ADM1 calibration using BMP tests for modeling the effect ofautohydrolysis pretreatment on the performance ofcontinuous sludge digesters. *Water Research*, *47*(9), 3244–3254. https://doi.org/10.1016/j.watres.2013.03.041

Strömberg, S., Nistor, M., & Liu, J. (2014). Towards eliminating systematic errors caused by the experimental conditions in Biochemical Methane Potential (BMP) tests. *Waste Management*, *34*(11), 1939–1948. https://doi.org/10.1016/j.wasman.2014.07.018

Strömberg, S., Nistor, M., & Liu, J. (2015). Early prediction of Biochemical Methane Potential through statistical and kinetic modelling of initial gas production. *Bioresource Technology*, *176*, 233–241. https://doi.org/10.1016/j.biortech.2014.11.033

Stroot, P. G., McMahon, K. D., Mackie, R. I., & Raskin, L. (2001). Anaerobic codigestion of municipal solid waste and biosolids under various mixing conditions - II: Microbial population dynamics. *Water Research*, *35*(7), 1804–1816. https://doi.org/10.1016/S0043-1354(00)00439-5

Tong, X., Smith, L. H., & McCarty, P. L. (1990). Methane fermentation of selected lignocellulosic materials. *Biomass*, *21*(4), 239–255. https://doi.org/10.1016/0144-4565(90)90075-U

Triolo, J. M., Pedersen, L., Qu, H., & Sommer, S. G. (2012). Biochemical methane potential and anaerobic biodegradability of non-herbaceous and herbaceous phytomass in biogas production. *Bioresource Technology*, *125*, 226–232. https://doi.org/10.1016/j.biortech.2012.08.079

Triolo, J. M., Sommer, S. G., Møller, H. B., Weisbjerg, M. R., & Jiang, X. Y. (2011). A new algorithm to characterize biodegradability of biomass during anaerobic digestion: Influence of lignin concentration on methane production potential. *Bioresource Technology*, *102*(20), 9395–9402. https://doi.org/10.1016/j.biortech.2011.07.026

Turick, C. E., Peck, M. W., Chynoweth, D. P., Jerger, D. E., White, E. H., Zsuffa, L., & Andy Kenney, W. (1991). Methane fermentation of woody biomass. *Bioresource Technology*, *37*(2), 141–147. https://doi.org/10.1016/0960-8524(91)90202-U

Usack, J. G., & Angenent, L. T. (2015). Comparing the inhibitory thresholds of dairy manure co-digesters after prolonged acclimation periods: Part 1 – Performance and operating limits. *Water Research*, *87*, 1–12. https://doi.org/10.1016/j.watres.2015.05.055

USEPA. (2017). Understanding global warming potentials. Retrieved June 30, 2018, from https://www.epa.gov/ghgemissions/understanding-global-warming-potentials

Vavilin, V.A., Lokshina, L. Y., Jokela, J. P. Y., & Rintala, J. A. (2004). Modeling solid waste decomposition. *Bioresource Technology*, *94*(1), 69–81. https://doi.org/10.1016/j.biortech.2003.10.034

Vavilin, V.A., Rytov, S. V., & Lokshina, L. Y. (1996). A description of hydrolysis kinetics in anaerobic degradation of particulate organic matter. *Bioresource Technology*, *56*, 229–237. https://doi.org/10.1016/0960-8524(96)00034-X

Vavilin, Vasily A., & Angelidaki, I. (2005). Anaerobic degradation of solid material: Importance of initiation centers for methanogenesis, mixing intensity, and 2D distributed model. *Biotechnology and Bioengineering*, *89*(1), 113–122. https://doi.org/10.1002/bit.20323

Vedrenne, F., Béline, F., Dabert, P., & Bernet, N. (2008). The effect of incubation conditions on the laboratory measurement of the methane producing capacity of livestock wastes. *Bioresource Technology*, *99*(1), 146–155. https://doi.org/10.1016/j.biortech.2006.11.043

Veluchamy, C., & Kalamdhad, A. S. (2017). Biochemical methane potential test for pulp and paper mill sludge with different food / microorganisms ratios and its kinetics. *International Biodeterioration and Biodegradation*, *117*, 197–204. https://doi.org/10.1016/j.ibiod.2017.01.005

Venkiteshwaran, K., Bocher, B., Maki, J., & Zitomer, D. (2016). Relating anaerobic digestion microbial community and process function. *Microbiology Insights*, *8*, 37–44. https://doi.org/10.4137/MBI.S33593

Wagner, A. O., Lins, P., Malin, C., Reitschuler, C., & Illmer, P. (2013). Impact of protein-, lipid- and cellulose-containing complex substrates on biogas production and microbial communities in batch experiments. *The Science of the Total Environment*, *458–460*, 256–266. https://doi.org/10.1016/j.scitotenv.2013.04.034

Walker, M., Zhang, Y., Heaven, S., & Banks, C. (2009). Potential errors in the quantitative evaluation of biogas production in anaerobic digestion processes. *Bioresource Technology*, *100*(24), 6339–6346. https://doi.org/10.1016/j.biortech.2009.07.018

Wandera, S. M., Qiao, W., Algapani, D. E., Bi, S., Yin, D., Qi, X., … Dong, R. (2018). Searching for possibilities to improve the performance of full scale agricultural biogas plants. *Renewable Energy*, *116*, 720–727. https://doi.org/10.1016/j.renene.2017.09.087

Wang, Qilin, Sun, J., Zhang, C., Xie, G. J., Zhou, X., Qian, J., … Wang, D. (2016). Polyhydroxyalkanoates in waste activated sludge enhances anaerobic methane production through improving biochemical methane potential instead of hydrolysis rate. *Scientific Reports*, *6*(November 2015), 1–9. https://doi.org/10.1038/srep19713

Wang, Qunhui, Fujisaki, K., Ohsumi, Y., & Ogawa, H. I. (2001). Enhancement of dewaterability of thickened waste activated sludge by freezing and thawing treatment. *Journal of Environmental Science and Health - Part A Toxic/Hazardous Substances and Environmental Engineering*, *36*(7), 1361–1371. https://doi.org/10.1081/ESE-100104884

Wang, Qunhui, Kuninobu, M., Ogawa, H. I., & Kato, Y. (1999). Degradation of volatile fatty acids in highly efficient anaerobic digestion. *Biomass and Bioenergy*, *16*(6), 407–416. https://doi.org/10.1016/S0961-9534(99)00016-1

Wang, Y., Odle, W. S. I., Eleazer, W. E., & Barlaz, M. A. (1997). Methane potential of food waste and anaerobic toxicity of leachate produced during food wase decomposition. *Waste Management and Research*, *15*, 149–167. https://doi.org/10.1006/wmre.1996.0073

Wickham, R., Galway, B., Bustamante, H., & Nghiem, L. D. (2016). Biomethane potential evaluation of co-digestion of sewage sludge and organic wastes. *International Biodeterioration and Biodegradation*, *113*, 3–8. https://doi.org/10.1016/j.ibiod.2016.03.018

Yan, Y., Zhang, L., Feng, L., Sun, D., & Dang, Y. (2018). Comparison of varying operating parameters on heavy metals ecological risk during anaerobic co-digestion of chicken manure and corn stover. *Bioresource Technology*, *247*(July 2017), 660–668. https://doi.org/10.1016/j.biortech.2017.09.146

Zhang, J., Lv, C., Tong, J., Liu, J., Liu, J., Yu, D., … Wei, Y. (2016). Optimization and microbial community analysis of anaerobic co-digestion of food waste and sewage sludge based on microwave pretreatment. *Bioresource Technology*, *200*, 253–261. https://doi.org/10.1016/j.biortech.2015.10.037

Zhang, Q., Hu, J., & Lee, D. J. (2016). Biogas from anaerobic digestion processes: Research updates. *Renewable Energy*, *98*, 108–119. https://doi.org/10.1016/j.renene.2016.02.029

Zhang, R., El-Mashad, H. M., Hartman, K., Wang, F., Liu, G., Choate, C., & Gamble, P. (2007). Characterization of food waste as feedstock for anaerobic digestion. *Bioresource Technology*, *98*(4), 929–935. https://doi.org/10.1016/j.biortech.2006.02.039

Zhu, B., Gikas, P., Zhang, R., Lord, J., Jenkins, B., & Li, X. (2009). Characteristics and biogas production potential of municipal solid wastes pretreated with a rotary drum reactor. *Bioresource Technology*, *100*(3), 1122–1129. https://doi.org/10.1016/j.biortech.2008.08.024

CHAPTER 3. REVIEW OF BIOCHEMICAL METHANE POTENTIALS IN ANAEROBIC DIGESTION—PART II: RESULT MODELING

3.1 Abstract

Biochemical methane potential (BMP) tests are commonly used to predict the methane yield of a feedstock for large-scale anaerobic digestion (AD) systems. Kinetic modeling is often applied to the BMP results to improve their predictive applicability to these large-scale systems. However, recent literature has revealed that kinetic modeling in the BMP test is often overly simplistic and fails to capture the complexity of the system. In this chapter, 88 peer-reviewed BMP studies were examined. From these studies, the most frequent approaches for calculating, modeling, and predicting methane yield and substrate biodegradability were identified and compared for their reliability in predicting methane yield. Specifically, non-linear models or models which accounted for the initial characteristics of the substrate were more reliable in their predictions. The development of more comprehensive models, which account for the various dynamics in the AD process, could reduce test time via early parameter estimation.

3.2 Introduction

Anaerobic digestion (AD) is becoming increasingly widespread. Anaerobic digestion is a potential solution for mitigating greenhouse gas (GHG) emissions and odor from organic wastes while generating energy (Abbasi, Tauseef, & Abbasi, 2012). Anaerobic digestion uses a mixed microbial community to convert complex organic materials to biogas in the absence of molecular oxygen (De Baere, 2000; Mao, Feng, Wang, & Ren, 2015; Q. Zhang, Hu, & Lee, 2016). A variety of organic materials have been used for AD including food waste, manure, slaughterhouse waste, industry waste, and agricultural residue.

The biochemical methane potential (BMP) test is a commonly used method to determine substrate feasibility for AD. During the BMP test, the substrate undergoes batch digestion to determine its ultimate CH_4 yield (B_o) per unit of volatile solids (VS), also known as the specific methane yield (SMY). Besides providing the SMY, the BMP test is most commonly used to determine the biodegradability and the rate of degradation of a given substrate (Strömberg, Nistor, & Liu, 2015). These values can be used to approximate the most suitable substrate, retention time,

or organic loading rate (OLR) in a full scale digester (Lesteur et al., 2010; Strömberg, Nistor, & Liu, 2014).

The AD process is a complex series of syntrophic relationships among a consortium of microorganisms which operates near thermodynamic equilibrium (Leng et al., 2018; Venkiteshwaran, Bocher, Maki, & Zitomer, 2016). The four main stages of AD are hydrolysis, acidogenesis, acetogenesis, and methanogenesis (Gavala, Angelidaki, & Ahring, 2003). The rate of each stage is dependent on the previous stages. Generally, organic matter is reduced to smaller, soluble monomers (*i.e.*, hydrolysis) which are converted to volatile fatty acids (VFAs), hydrogen gas (H_2), carbon dioxide (CO_2), and other byproducts (*i.e.*, acidogenesis, acetogenesis) which are then converted to methane (CH_4) (*i.e.*, methanogenesis). The biogas production and composition can be significantly affected by an imbalance at one of the four stages.

Several modeling processes have been developed and applied in conjunction with BMP test data. Several of these models are kinetic models which describe the rate and extent of CH_4 production during the BMP test. Many of the kinetic models are developed from common models for microbial growth. The parameters are estimated using linear or nonlinear regression techniques. However, many of the models used to calculate the process rates during the BMP test are overly simplistic and have failed to capture the complexities of the system. Therefore, some researchers have applied more nuanced kinetic models that account for the complexities of the batch fermentation process and can improve predictive applicability of the BMP test.

This chapter reviews the modeling techniques for BMP studies. This chapter synthesized 88 peer-reviewed articles in which batch BMP tests were reported. Then, the most frequently used methods for predicting the SMY, calculating substrate biodegradability, and modeling CH_4 yield profiles were examined. After an overview of the BMP test and modeling methodologies, this chapter examined the main ways that BMP test modeling has been applied in the literature. These ways were: 1.) prediction of the theoretical SMY for a given substrate; 2.) calculating substrate degradation; 3.) dynamic modeling prediction of BMP performance for a given substrate over time; and 4.) parameter estimation from BMP test data.

This chapter compared the advantages and disadvantages of various existing models and whether they could reduce the time needed for the BMP test and whether they would be applicable for predicting large-scale digester performance. Improvements for BMP modeling were also proposed.

3.3 Overview of modeling

A model structure consists of a set of equations containing variables, constants, and parameters. Determining a model structure (*i.e.*, structural identifiability) in which all the parameters can be solved for a unique value is one of the challenges in mathematical modeling (Dochain, Vanrolleghem, & Van Daele, 1995). A model structure should: 1.) be directly associated with the physical process under consideration; 2.) have a structure whose methodology can be well characterized; 3.) be able to estimate a unique value for all parameters; 4.) have a good fit with experimental data (*i.e.*, practical identifiability); 5.) be simple with the least number of parameters; and 6.) maintain a balance between parameter precision and model accuracy (Spriet, 1985).

The basic steps for mathematical model development are: 1.) definition of the problem and goal; 2.) collection of preliminary data and developing an experimental design; 3.) identification of the framework model structure; 4.) creation of an experimental design; 5.) performance of parameter estimation and precision; and 6.) testing the model with new data and revising it if necessary (Carstensen, Vanrolleghem, Rauch, & Reichert, 1997; Flotats, Ahring, & Angelidaki, 2003; Lauwers et al., 2013).

3.3.1 Modeling anaerobic digestion

There is interest in modeling the entire AD process. Multi-step dynamic modeling of the AD process can improve understanding of its mechanisms and optimize operation and design (I. Angelidaki, Ellegraard, & Aharing, 1993; Irini Angelidaki, Ellegaard, & Ahring, 1999; Andres Donoso-Bravo et al., 2011; Flotats et al., 2003; Kovalovszki, Alvarado-Morales, Fotidis, & Angelidaki, 2017). The Anaerobic Digestion Model No. 1 (ADM1) is one of the more prevalent, comprehensive AD models in recent years (Batstone et al., 2002). The ADM1 model accounts for multiple biochemical and physiochemical processes in AD. The ADM1 model has been successfully calibrated using BMP test data (Astals, Batstone, Mata-Alvarez, & Jensen, 2014; Souza, Carvajal, Donoso-Bravo, Peña, & Fdz-Polanco, 2013). Furthermore, the ADM1 model has been expanded to include sulfate reduction processes (Fedorovich, Lens, & Kalyuzhnyi, 2003) and microbial diversity (Ramirez, Volcke, Rajinikanth, & Steyer, 2009). However, the application of ADM1 models to industrial-scale co-digested plants is rare (Nordlander, Thorin, & Yan, 2017).

In fact, modeling of co-digested systems has received limited attention (Mata-Alvarez et al., 2014). Additionally, a lack of substrate characterization limits the applicability of the ADM1 model (Lauwers et al., 2013; Nordlander et al., 2017),

Other types of modeling techniques can avoid the need for exhaustive characterization of the substrate or in-depth knowledge of the microbial or physical chemical processes in the digester. Black-box models are typically used when a specific parameter is desired but little is known about the processes within the digester. Examples of black-box models commonly used in AD include principle component regression (PCR), artificial neural networks (ANN), partial least squares regression (PLS), neuro-fuzzy systems, and support vector machines (SVM) (Lauwers et al., 2013). The drawbacks of black-box modeling include over-fitting, ambiguity in the results, and interpretability (Lauwers et al., 2013).

Generally, there are few systematic procedures for modeling AD processes as well as a lack of validation for the model and parameter accuracy (Andres Donoso-Bravo et al., 2011). Due to the complexity of the physical, chemical, and microbiological processes of AD, the kinetic models involve complex, high order nonlinear systems with a large number of state variables and parameters and require high quality and a large number of data points (Batstone et al., 2002; Bernard, Hadj-Sadok, Dochain, Genovesi, & Steyer, 2001; Dochain et al., 1995; Souza et al., 2013). The inclusion of controls for inoculum and substrate activity can increase the reliability of the data results (Juliet Ohemeng-Ntiamoah & Datta, 2019; Reilly, Dinsdale, & Guwy, 2016). Advances in automated BMP tests and continuous data acquisition may provide a solution for generating a larger number of reliable and reproducible data points to improve modeling (I Angelidaki, Schmidt, Ellegaard, & Ahring, 1998; Badshah, Lam, Liu, & Mattiasson, 2012; Kolbl, Paloczi, Panjan, & Stres, 2014). Including parameters for specific microbial species in the model or for changes in microbial fluxes or populations could also advance BMP modeling.

3.3.2 Parameter estimation techniques

There is a need for a universal method of parameter estimation for AD processes (Andres Donoso-Bravo et al., 2011). The typical parameter estimation techniques for mathematical modeling include linearization and subsequent algebraic calculations and recursive algorithms (Spriet, 1985). Parameter estimation is challenging for nonlinear models or models with a high number of parameters (López & Borzacconi, 2010). Any parameter estimation method must

include a statistically valid objective function (J) as well as an appropriate statistical test for determining model uncertainty (Jensen, Ge, & Batstone, 2011; Vanrolleghem, Van Daele, & Dochain, 1995). For AD processes, the objective function is typically solved through the minimization of the sum of least squares using a software program for nonlinear curve fitting (Andrés Donoso-Bravo, García, Pérez-Elvira, & Fdz-Polanco, 2011; Andres Donoso-Bravo et al., 2011). Various methods have been used to determine model uncertainty for BMP tests.

Parameter certainty should meet the requirements of goodness of fit, discriminating power, efficiency, computational robustness, statistical robustness, computation requirements, consistency, and small sample behavior (Spriet, 1985). Common optimality criteria include relative root mean squared error of prediction (rRMSE), mean square of the deviations (MSD), relative absolute error (rAE), residual sum of squares (RSS), final prediction error criteria (FPE), least squares, and coefficient of determination (R^2) (Lobry, Rosso, & Flandrois, 1991; Lokshina et al., 2001; Rao, Singh, Singh, & Sodha, 2000; Strömberg et al., 2014; Vavilin, Lokshina, Jokela, & Rintala, 2004). These methods are based on the sum of differences between observed and theoretical data points. Theoretically a minimal difference between the measured and calculated data points indicates a better fit. Modified least squares methods have been suggested, especially for batch AD tests which have low CH_4 production in the first few days (Koch & Drewes, 2014). Because the least squares method for regression analysis will have high sensitivity for the early days of a BMP test, it is suggested to minimize the sum of the relative error instead of the sum of the squared differences as seen in Eq. 3-1:

$$LS = \sum_{i=1}^{n} \frac{\left| y_{i,measured} - y_{i,calculated} \right|}{y_{i,measured}} \qquad (3\text{-}1)$$

where LS is the sum of errors between the measured and calculated values; $y_{i,measured}$ is the measured value at point *i*; $y_{i,calculated}$ is the calculated value at point *i*.

If there is more than one parameter in a model, parameter correlation should be determined (Jensen et al., 2011). Noisy and limited experimental data can result in parameters which are highly correlated (Vanrolleghem et al., 1995). Parameter correlation indicates the change in one parameter when another parameter is changed. Parameter correlation has been estimated for AD using the secant method (Batstone, Pind, & Angelidaki, 2003). Parameter uncertainty and

correlation can be more effective than goodness of fit values for representing model uncertainty (Jensen et al., 2011).

For nonlinear models specifically, parameter surface searching can also be used to determine model uncertainty (Batstone et al., 2003; Batstone, Tait, & Starrenburg, 2009; Jensen et al., 2011; Lobry et al., 1991). First, there is a set of parameters that minimizes J. The desired parameters will lie on J_{crit} as seen in Eq. (3-2):

$$J_{crit} = J_{opt}\left(1 + \frac{p_n}{n - p_n}\right) F_{\alpha,p,n-p_n} \tag{3-2}$$

where J_{crit} is the critical value, n is the number of measured data points, p_n is the number of parameters, and J_{opt} is the value when RSS is minimized. Assuming the residuals are normally distributed, the critical value of the surface of the parameter uncertainty region can be determined from J_{min} using the F distribution and the input values α, p, $n\text{-}p_n$ (Batstone et al., 2003). The confidence region for the set of parameters can then be visualized as a hypervolume surrounded by a hypersurface (Lobry et al., 1991). The confidence limits for the parameter values is visualized as the extent of this hypersurface (Lobry et al., 1991). A 1-α confidence region for parameters is defined as the set of parameter values (σ) such that RSS is less than the confidence region threshold as seen in Eq. (3-3) (Lobry et al., 1991):

$$\left\{\sigma: RSS(\sigma) \leq \left(1 + \frac{p_n}{n - p_n} F^{\alpha}_{p,n-p_n}\right)\right\} \tag{3-3}$$

where n is the number of points, p_n is the number of parameters, and F is the F-distribution with the input values α, p, $n\text{-}p_n$. One method for determining this confidence region is computing a homogenous distribution of points on the hypersurface (10,000 – 30,000). The first step is to start with a "hypersphere" of radius 1 and randomly generate points within the range of [-1,1] until one point falls within the hypersphere. Its coordinates are then divided by its distance from the origin so it is projected onto the surface of the hypersphere. The hypersphere is then *translated* so its origin is placed where RSS is minimized. The hypersphere is then *scaled* along each axis by adjusting the radius to acceptable limits for each parameter so the confidence region is then enclosed. An iterative method based on linear interpolation is then used to determine the point enclosing the confidence region. The difference between the threshold and RSS must be less than

a user defined small value (10^{-3}) (Eq. 3-4). The smaller the difference (Δ), the more accurate the location of the point.

$$\frac{Threshold - RSS}{Threshold} < \Delta \quad (3\text{-}4)$$

The user may also define a maximum number of iterations (10^3) (Lobry et al., 1991). The hypersurface can be projected onto $(p_n^2\text{-}p_n)/2$ planes to determine the parameter values and their correlation

Jensen et al. (2011) determined the rate (k) and extent of biodegradability (f_d) from BMP tests of cellulose. They used CH_4 production to calculate the parameters using both a linearized first order model and a nonlinear parameter model and an uncertainty estimation procedure (surface searching method). The parameter estimations from both models were similar, but the nonlinear model provided metrics for parameter correlation and uncertainty and was less sensitive to the end point of the test.

3.4 Theoretical methane potential models

In the reviewed BMP studies, many parameters were calculated from both the observed CH_4 yield data and the theoretical CH_4 yield of the substrate. Additionally, an estimate of the theoretical SMY was useful for experimental design. For theoretical BMP calculations, consideration of individual substrate biodegradability was important for generating accurate predictions. There were several methods for calculating the theoretical SMY.

3.4.1 Buswell equation

The theoretical SMY can be calculated using the stoichiometric coefficients of the substrate in a redox reaction known as the Buswell Equation (Symons & Buswell, 1933). The Buswell equation was originally developed from carbohydrate fermentation and has since been modified based on empirical observation (M. Buswell & Muellepi, 1952; Richards, Cummings, White, & Jewell, 1991) to a general fermentation equation as shown in Eq. (3-5):

$$C_nH_aO_bN_c + (n - 0.25a - 0.5b + 1.75c)H_2O \rightarrow (0.5n - 0.125a + 0.25b - 0.625c)CO_2 + (0.5n + 0.125a - 0.25b - 0.375c)CH_4 + cNH_4^+ + cHCO_3^- \quad (3\text{-}5)$$

where C, H, O, and N represent the elements of carbon, hydrogen, oxygen, and nitrogen, and n, a, b, and c represent the number of atoms of the respective element. Symons and Buswell (1933) reported that a very small amount of substrate was converted for bacterial cell synthesis; therefore, the electrons used for cell synthesis are ignored in the equation. Additionally, the Buswell equation assumes that the substrate is 100% biodegradable. Eq. (3-5) assumes that one mole of CO_2 is produced in the solution per mole ammonia (NH_3) and that the ammonium (NH_4^+) and bicarbonate (HCO_3^-) are in their aqueous forms. Specifically, NH_4^+ can react with CO_2 to form HCO_3^-, which can act as a pH buffer (Kayhanian, 1999; B. Zhang, Zhang, Zhang, Shi, & Cai, 2005). The general fermentation equation can therefore be used to determine the theoretical SMY of a substrate, assuming that the atomic fraction composition is known (Edward, Edwards, Egwu, & Sallis, 2015; Raposo et al., 2011). Many studies have used Buswell's equation to estimate theoretical CH_4 yield (Browne & Murphy, 2013; Curry & Pillay, 2012; Davidsson, Gruvberger, Christensen, Hansen, & Jansen, 2007; Edward et al., 2015; Labatut, Angenent, & Scott, 2011; Triolo, Pedersen, Qu, & Sommer, 2012; Yoon, Kim, Shin, & Kim, 2014).

However, Buswell's equation is limited in its application. Many experimental factors including solubility, temperature, volume, media composition, and substrate biodegradability can affect the accuracy of the calculated theoretical SMY from Buswell's equation (Shelton & Tiedje, 1984). Symons and Buswell (1933) tested pure compounds including starch, lactic acid, acetic acid, and sucrose, thereby oversimplifying its biodegradability assumption. Additionally, Buswell's equation fails to account for the substrate which is used for both energy and cell synthesis.

3.4.2 McCarty's Bioenergetics method

McCarty's Bioenergetics method accounts for both energy and cell synthesis in CH_4 production. Energy and cell synthesis are determined separately, then added together (McCarty, 1971). The energy equation accounts for the flow of electrons from donors to acceptors. Ultimately, three half reactions (electron donor, electron accepter, oxidation of cells) can be combined to yield

the appropriate oxidation-reduction reaction for methane fermentation. The stoichiometric coefficients for synthesis and energy must equal the coefficients of the overall equation. However, the Bioenergetics Method does not account for biodegradability.

Both the Buswell and McCarthy's Bioenergetics methods have been shown to overestimate CH_4 yield (Labatut et al., 2011; Lesteur et al., 2010). Labatut et al. (2011) compared the experimentally obtained SMYs to the theoretical SMYs calculated by Buswell and McCarty's Bioenergetics method for seventeen unique substrates. They found that the theoretical SMYs overestimated the experimental SMYs (mL CH_4 g VS^{-1}), with the Buswell equation giving the worst estimate; they suggested this was because it did not account for cell synthesis. The largest differences between experimental SMYs (mL CH_4 g VS^{-1}) and the theoretical calculations were for substrates with the lowest biodegradability. When they accounted for biodegradability in the theoretical SMY calculations, there was an over 90% agreement. They concluded that the Buswell estimation was the closest to the experimentally observed value when including biodegradability because cell synthesis is accounted for in the biodegradability calculations.

Closer examination of substrate composition can improve these theoretical CH_4 potential calculations. Performing a theoretical CH_4 potential calculation on the component composition (*i.e.,* fats, proteins, lipids) instead of the elemental composition may provide a closer approximation since there are inherent differences in component degradability (A. M. Buswell & Neave, 1930; Lesteur et al., 2010; Neves, Gonçalo, Oliveira, & Alves, 2008; J. Ohemeng-Ntiamoah & Datta, 2018; Raposo et al., 2011; Wagner, Lins, Malin, Reitschuler, & Illmer, 2013). Testing for the component composition rather than the elemental composition may also be less time consuming. For substrates with known lipid, protein, and carbohydrate organic fraction compositions, the theoretical SMY (B_u) can be estimated using an equation derived from the average stoichiometric formulae for carbohydrates ($C_6H_{10}O_5$), proteins ($C_5H_7O_2N$), and lipids ($C_{57}H_{104}O_6$) (Raposo et al., 2011) as seen in Eq. (3-6).

$$B_u = 415 \cdot \%Carbohydrates + 496 \cdot \%Proteins + 1014 \cdot \%Lipids \qquad (3\text{-}6)$$

Davidsson et al. (2007) calculated B_u using both the elemental composition (C, H, O, N) and the component composition (fats, proteins, lipids) of the organic fraction of municipal solid wastes (MSW). They found that the component composition was 87% of the observed yield versus 74% for elemental composition. Formulas only relying on composition, however, can over-predict

SMY because they do not account for biodegradability; only the biodegradable fraction can be converted to methane (Kafle & Chen, 2016). To account for biodegradability, Triolo et al. (2011) and Møller et al. (2004) proposed including lignin and VFA concentrations in the theoretical BMP calculation as seen in Eq. (3-7).

$$B_u = 415 \cdot \%Carbohydrates + 496 \cdot \%Proteins + 1014 \cdot \%Lipids + 373 \cdot \%VFA + 727 \cdot \%Lignin \quad (3\text{-}7)$$

3.4.3 Additional theoretical BMP models

Additional theoretical BMP models have been developed. These models include multiple linear regression models which use substrate composition to predict SMY (Amon et al., 2007; Gunaseelan, 2007; Triolo et al., 2011). Triolo et al. (2011) regressed the SMY against several different fiber fractions of the substrate to develop a combined statistical model for manure and energy crops. They found that the lignin fraction was the only significant predictor of B_u when testing cellulose, acid detergent fiber, and acid detergent lignin. Results showed that lignin was the strongest predictor of B_u for animal manure ($R^2 = 0.91$) and energy crops ($R^2 = 0.76$), though the model could still be improved. Other models for predicting B_u include the ADM1 Model (Souza et al., 2013), and the General Integrated Solid Waste Co-Digestion Model (Zaher, Li, Jeppsson, Steyer, & Chen, 2009).

The theoretical SMY can also be estimated based on the chemical oxygen demand (COD) concentration of the substrate. In theory, 1 g of COD can produce 0.35 L of CH_4 at STP (0 °C, 1 atm) (Buffiere et al., 2006; McCarty, 1964). Therefore, the maximum theoretical SMY can be determined from multiplying the amount of total COD in a substrate by 0.35 and dividing by the unit mass (Morris, Jewell, & Loehr, 1977; Tong, Smith, & McCarty, 1990; Wandera et al., 2018).

Theoretical SMY calculations can thus be modified in several ways. Overall, the elemental composition of a substrate does not account for the unique interactions and degradation of various bio-molecules in the substrate, and therefore will likely overestimate SMY unless there is a correction factor. Developing statistical models which are unique to the characteristics of the substrate tested show promise. Potentially, the BMP test can be circumvented through the use of a reliable theoretical methane potential model.

3.5 Modeling biodegradability

Biodegradable material is the portion of organic material that can be metabolized by microorganisms. *Metabolism* refers to the use of the material as both an energy and carbon source for the microorganisms (Irini Angelidaki & Sanders, 2004). Organic material is composed of a soluble fraction and a particulate fraction. By definition, *particulates* are colloids or macro particles that are taken up by bacteria less easily than *solubles*.

Biodegradability refers to the ultimate rate and extent of substrate utilization. Biodegradability can be influenced by nutrient availability, substrate type, co-digestion, inoculum source, inoculum to substrate (ISR) ratio, electron donor and acceptor availability, oxygen concentration, temperature, pH, moisture, salinity, sorption of chemicals to particulate material, and the chemical concentration (Irini Angelidaki & Sanders, 2004; Costa, Oliveira, & Alves, 2016; Hafner et al., 2018; Isci & Demirer, 2007; Kawai et al., 2014; Koch, Hafner, Weinrich, & Astals, 2019; Koch, Lippert, & Drewes, 2017; Ma, Gu, & Liu, 2018; McEniry, Allen, Murphy, & O'Kiely, 2014; Meng et al., 2018; Nizami, Orozco, Groom, Dieterich, & Murphy, 2012; Usack & Angenent, 2015; Vedrenne, Béline, Dabert, & Bernet, 2008; Y. Wang, Odle, Eleazer, & Barlaz, 1997; Yan, Zhang, Feng, Sun, & Dang, 2018).

The BMP test is often used to determine the rate and extent of biodegradability of a substrate. Biodegradability is calculated from either measured product formation (*i.e.*, biogas, methane, intermediates), or substrate depletion (*i.e.*, volatile solids (VS), total organic carbon (TOC), COD, or another specific compound) in the BMP test (Irini Angelidaki & Sanders, 2004; Guwy, 2004). The biodegradability of organic wastes can range from 5% to 90% without a dependence on temperature (Mata-Alvarez, Mac, & Llabr, 2000; Veeken & Hamelers, 1999). The batch BMP test has been shown to give a comparable estimate of the extent of degradability when compared to continuous systems (Batstone et al., 2009). Generally, the more biodegradable the substrate is, the higher the SMY (Figure 3-1).

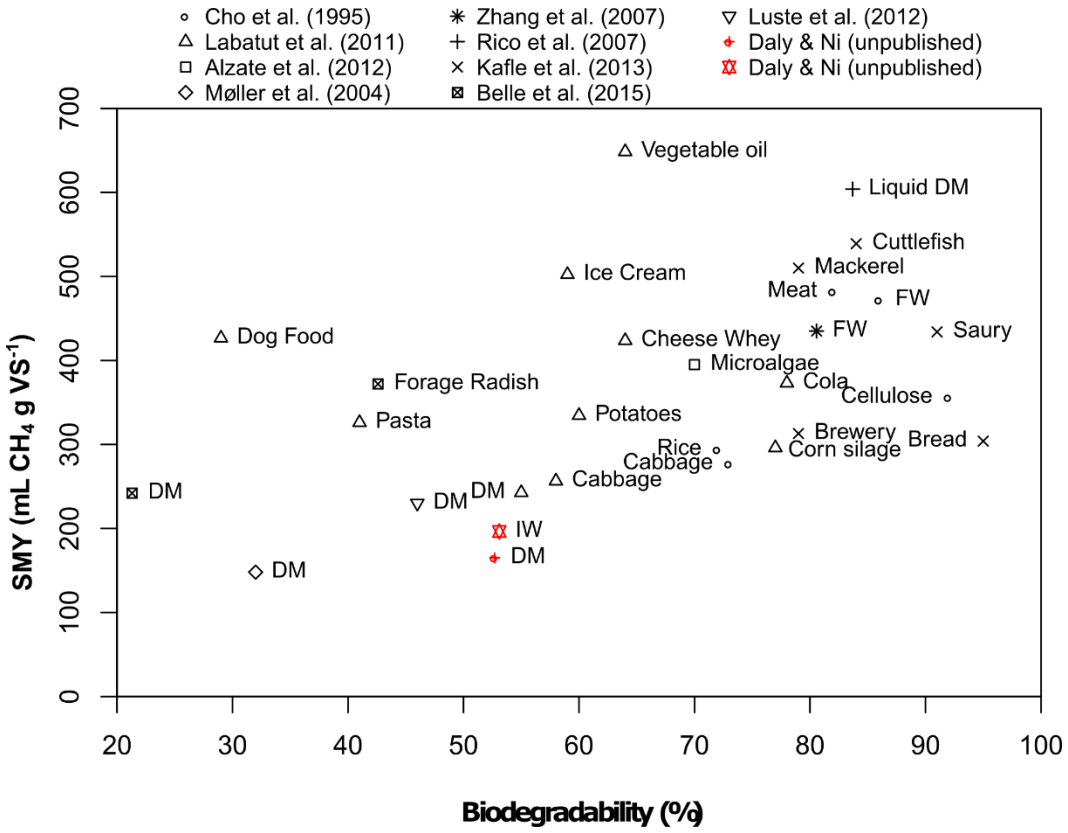

DM = dairy manure, FW = food waste, IW = Industry Waste.

Figure 3-1. Biodegradability versus SMY (mL CH_4 g VS^{-1}) from cited BMP studies.

3.5.1 Biodegradability calculated from measured product formation

The CH_4 yield from the BMP test is one of the most commonly measured products used to calculate biodegradability. Generally, the biodegradable fraction (f_d) of the substrate is calculated by dividing the observed SMY (B_o) by B_u as seen in Eq. (3-8) (Buffiere et al., 2006; Cavaleiro, Ferreira, Pereira, Tommaso, & Alves, 2013; Cho, Park, & Chang, 1995; Elbeshbishy, Nakhla, & Hafez, 2012; Møller et al., 2004; Mottet et al., 2010; Posmanik et al., 2017; Souza et al., 2013; Tong et al., 1990; Q. L. Wang, Li, Gao, & Li, 2016):

$$f_d = \frac{B_o}{B_u} \tag{3-8}$$

where f_d is the biodegradable fraction (decimal), B_o is the observed SMY at Standard Temperature and Pressure (STP), and B_u is the theoretical CH_4 yield. Theoretically, the B_o value will always be a fraction of B_u due to inhibition of CH_4 production by certain compounds, uptake by cells for

cell synthesis, biomass washout, and the presence of recalcitrant compounds (Irini Angelidaki & Sanders, 2004; Møller et al., 2004). However, there are several different methods for calculating B_u as described in section (3.4). Accounting for the minor losses in CH_4 yield due to cell synthesis, cell death, biomass washout, and inhibition is of particular concern in these calculations. Because biodegradability calculations reflect the extent to which the substrate can be metabolized by the microorganisms, the accounting of these losses can influence the biodegradability measurement.

3.5.2 Biodegradability calculated from substrate depletion

Biodegradability is commonly determined through the measurement of substrate depletion. The content of the substrate can strongly influence degradation kinetics and CH_4 production (Amha, Sinha, Lagman, Gregori, & Smith, 2017; Christ, Wilderer, Angerhöfer, & Faulstich, 2000; Oslaj, Mursec, & Vindis, 2010). Either "lumped parameters" (*i.e.*, VS, COD, TOC) or specific components (*i.e.*, acetate, glucose, lignin, proteins) are used as indicators of substrate depletion (Irini Angelidaki & Sanders, 2004; Guwy, 2004). However, COD and VS are the most frequently used metrics for determining biodegradability (Achinas, Li, Achinas, & Euverink, 2019; Ahmadi-Pirlou, Ebrahimi-Nik, Khojastehpour, & Ebrahimi, 2017; Alzate, Muñoz, Rogalla, Fdz-Polanco, & Pérez-Elvira, 2012; Belle, Lansing, Mulbry, & Weil, 2015; Elbeshbishy & Nakhla, 2012; Erguder, Guven, & Demirer, 2000; Eskicioglu & Ghorbani, 2011; Forster-Carneiro, Pérez, Romero, & Sales, 2007; Heo, Park, Lee, & Kang, 2003; Jerger, Chynoweth, & Isaacson, 1987; Kafle & Chen, 2016; Kafle & Kim, 2012, 2013; Kafle, Kim, & Sung, 2013; Labatut et al., 2011; Liu, Zhang, El-Mashad, & Dong, 2009; Luostarinen, Luste, & Sillanpää, 2009; Luste, Heinonen-Tanski, & Luostarinen, 2012; Martín-González, Colturato, Font, & Vicent, 2010; Montañés, Solera, & Pérez, 2015; Palatsi, Viñas, Guivernau, Fernandez, & Flotats, 2011; Petropoulos, Dolfing, Davenport, Bowen, & Curtis, 2017; Rico, García, Rico, & Tejero, 2007; Vidal, Carvalho, Méndez, & Lema, 2000; Wandera et al., 2018; Wickham, Galway, Bustamante, & Nghiem, 2016; R. Zhang et al., 2007). Basically, COD and VS measurements lump together several components of the substrate including solids and intermediate compounds. Specifically, COD is determined experimentally from the amount of an oxidizing agent required to fully oxidize an organic substrate (APHA, 1999). VS is determined experimentally by calculating the loss of material after drying at 550°C (APHA, 1999). The relationship between VS and COD can be determined if the atomic fraction composition is known (Irini Angelidaki & Sanders, 2004). Substrate depletion methods

are suitable for processes where there is likely to be inhibition or for early estimation of biodegradability (Irini Angelidaki & Sanders, 2004).

Models to predict anaerobic biodegradability have been developed. Biodegradability has been predicted from the initial characteristics of the substrate (Lesteur et al., 2010; Mottet et al., 2010). Regression techniques can be applied to the initial chemical characteristics of the substrate and experimental BMP test results to determine the strongest predictor variables for biodegradability.

There is particular interest in the initial concentration of lignin since it is a known inhibitor of biodegradability. One statistical model (R^2 = 0.94) developed from a variety of substrates (manure, newspaper, straw leaves, agricultural material) shows that one percent of lignin can decrease VS digestion by almost 3% (Lesteur et al., 2010) (Eq. 3-9):

$$f_{VS} = 0.83 - (0.028) \cdot \%Lignin \quad (3\text{-}9)$$

where f_{VS} is the biodegradable fraction of VS ($0 < B < 1$), and the initial lignin concentration ($0 < \%Lignin < 20\%$) in (%VS). They reported that about 83% of VS can be degraded, while 17% is used for cell synthesis and metabolic products.

Other chemical characteristics of the substrate have also been considered for biodegradability prediction. Mottet et al. (2010) developed a partial least squares regression model from twelve different parameters to predict anaerobic sludge biodegradability. The key predictors of biodegradability were component composition (protein, carbohydrate, lipid) and soluble organic carbon concentration, and the COD to TOC ratio. In many cases, there is a relationship between the initial chemical characteristics of a substrate and its biodegradability. One of the drawbacks of early predictive chemical analysis is the investment of time and materials. However, this time may be less than a BMP test, which needs a minimum of 30 days for complete digestion.

3.6 Kinetic modeling BMP test performance

3.6.1 First order models

The first order kinetic model (Eq. 3-10) is one of the most commonly used kinetic models for the BMP test (Table 3-1). This first order equation assumes that only one reaction is rate limiting, typically hydrolysis, which is a suitable assumption for complex substrates (Strömberg

et al., 2015; Vavilin et al., 1996). The parameters are the rate coefficient (k) and observed SMY (B_o). For AD processes, CH_4 is the input variable when hydrolysis is the limiting step (Vavilin, Fernandez, Palatsi, & Flotats, 2008). Several studies have fitted batch CH_4 yield data to the first order model (T. H. Chen & Hashimoto, 1996; Elbeshbishy & Nakhla, 2012; Gaur & Suthar, 2017; Hashimoto, 1989; Koch & Drewes, 2014; Koch et al., 2019; Lim & Fox, 2013; Luna-delRisco, Normak, & Orupõld, 2011; Owens, J.M. and Chynoweth, 1993; Posmanik et al., 2017; Turick et al., 1991; Veeken & Hamelers, 1999; Q. L. Wang et al., 2016; Zeng, Yuan, Shi, & Qiu, 2010) as shown in Eq. (3-10):

$$B = B_o[1 - exp(-k_1 t)] \quad (3\text{-}10)$$

where B is the cumulative specific CH_4 production (mL CH_4 g mass^{-1}), B_o is the ultimate methane yield (mL CH_4 g mass^{-1}), k_1 is the CH_4 production rate (day^{-1}), and t is time in days. The k can also be defined as the reciprocal when half of the ultimate CH_4 production is reached (Koch & Drewes, 2014). It represents the rates of degradation and biogas production (Koch & Drewes, 2014). The parameter k can be determined through linearization (I. Angelidaki et al., 2009; Koch & Drewes, 2014), the Secant method (Posmanik et al., 2017), nonlinear least squares regression (Luna-delRisco et al., 2011; Owens, J.M. and Chynoweth, 1993; Turick et al., 1991), and surface searching (Jensen et al., 2011; Q. L. Wang et al., 2016) (Table 3-1).

Table 3-1. Kinetic models, their parameter estimates, B_O values, and calculation techniques for BMP tests in literature.

Model name [(1)]	**Substrate**	**Model input** [(2)]	**Parameter estimate**	**Parameter estimation method**	**Statistical measurement**	**Reference**
First order	Wet food waste	CH_4 yield	k=0.15	Regression curve fitting	R^2	Browne and Murphy (2013)
First order	Cellulose	CH_4 yield	k=0.14-0.37	Newton Search Along Vectors	Confidence region	Jensen et al. (2011)
First order	Livestock manure	CH_4 yield	B_o=142-321 k=0.07-0.12	Nonlinear regression	R^2, rRMSE	Kafle and Chen (2016)
First Order	Raw Sewage Sludge	CH_4 yield	B_o =315 k_1=0.320	Nonlinear regression	Model Efficiency	Koch et al. (2019)
First order	Yard waste	CH_4 yield	B_o=23-371 k=0.04-0.08	Nonlinear regression	Standard deviation	Owens, J.M. and Chynoweth (1993)

Table 3-1 continued.

Model name [1]	Substrate	Model input [2]	Parameter estimate	Parameter estimation method	Statistical measurement	Reference
First order	Carbohydrate and proteins	CH_4 yield	k=0.10-0.34	Secant method	ND	Posmanik et al. (2017)
First order	Corn stover	CH_4 yield	k=0.14	Linearization	R^2	Tong et al. (1990)
First order	Wood species	CH_4 yield	B_o=140-310 k=0.01-0.12	Least squares fit	Standard Deviation	Turick et al. (1991)
First order	Grey waste	CH_4 volume	B_o=159-169 k=0.03-0.03	Nonlinear regression	Standard Deviation, FPE	Vavilin et al. (2004)
Modified first order	MSW	Biogas volume	k_1=0.003 k_2=0.023 f_d=0.341	Exponential regression	R^2, MSD	(Rao et al., 2000)
Modified first order	Wheat	CH_4 yield	k_1=0.67-0.83 k_2=0.07-0.08 f_d=0.63-0.67	ND	R^2	Rincón et al. (2010)
Modified first order	Wood species	CH_4 yield	B_o=160-320 k_1=0.07-0.25 k_2=0.01-0.31	Least squares fit	Standard Deviation	Turick et al. (1991)
Second order	Organic wastes	CH_4 yield	ND	Constrained nonlinear minimization	rRMSE, rAE, R^2	Strömberg et al. (2015)
Modified Gompertz	Swine manure	CH_4 yield	Bo=273 g TCOD added, λ=1.1 day, R_m=8 mL gTCOD-day^{-1}	Nonlinear least square regression	R^2, rRMSE	Kafle and Kim (2012)
Modified Gompertz	Fish waste, bread waste, silage	CH_4 yield	Bo=396 λ=0.5 R_m=19.3	Nonlinear least squares regression	R^2, Standard Deviation	Kafle et al. (2013)
Modified Gompertz	Livestock manures	CH_4 yield	Bo=148-511 λ=0-4 R_m=2.8-12.6	Nonlinear fit	R^2	Wandera et al. (2018)
Modified Gompertz	Livestock manures	CH_4 yield	Bo=138-312 λ=0 R_m=5.5-25.2	Nonlinear regression	R^2, rRMSE	Kafle and Chen (2016)
Modified Gompertz	Raw Sewage Sludge	CH_4 yield	B_o = 315 R_m = 56.67 λ = -0.50	Nonlinear regression	Model Efficiency	Koch et al. (2019)
Integrated Contois	Grey waste	CH_4 volume	$\alpha B_{0H} Y_H^{-1}$ =3-21 $\rho_{mH} Y_H^{-1}$ =0.30-0.55,$\hat{K}_{VS} \rho_{mH}^{-1}$ =4.20-7.66 α=145-154	Weighted nonlinear regression	Standard Deviation, FPE	Vavilin et al. (2004)
Chen & Hashimoto	Swine manure	CH_4 yield	K_{CH} =0.54 μ_m=0.11 HRT_{crit}=19	Linearization	ND	Kafle and Kim (2012)
Chen & Hashimoto	Fish, bread waste, silage	CH_4 yield	HRT_{crit}=23.8 K_{ch}=0.13 μ_m =0.04	Linearization	R^2	Kafle et al. (2013)

Table 3-1 continued.

Model name [1]	Substrate	Model input [2]	Parameter estimate	Parameter estimation method	Statistical measurement	Reference
Chen & Hashimoto	Livestock manure	CH_4 yield	B_o=129-301 K_{ch}=2.5-5.1 μ_m =0.51-0.85	Nonlinear regression	R^2, rRMSE	Kafle and Chen (2016)

Note: [1] First order: Eq. (3-10); Modified first order: Eq. (3-11); Second order: Eq. (3-16); Modified Gompertz: Eq. (3-14); Integrated Contois: Eq. (3-15); Chen & Hashimoto: Eq (3-18); [2] Typical model inputs are: methane yield, mL g^{-1}; methane volume, mL CH_4.

However, Eq. (3-10) does not account for variance in substrate characteristics and essentially lumps together all the kinetic processes. Specifically, first order kinetics are not appropriate when the biodegradability of the substrate is low. Therefore, there is interest in incorporating a term for substrate biodegradability into the first order model (Chynoweth, Turick, Owens, Jerger, & Peck, 1993; Tong et al., 1990). Specifically, there is interest in correlating the rate of CH_4 fermentation to the lignin concentration of the substrate (Chynoweth et al., 1993; Tong et al., 1990). Tong et al. (1990) attempted to relate the biodegradability and rate of CH_4 fermentation to lignin concentration. The principle behind this is that lignin is particularly recalcitrant to degradation during anaerobic fermentation and could determine the limiting rate of substrate degradation (Boruff & Buswell, 1934; Masoud, 1995; Robbins, Armold, & Lacher, 1979).

Lignocellulosic substrates can pose a challenge in BMP testing. Tong et al. (1990) performed BMP tests on several lignin-rich substrates using inoculum from an anaerobic fermenter treating WWTP sludge. They modelled CH_4 fermentation of lignocellulosic materials using the first order model. When comparing the first order rate constant and CH_4 conversion efficiencies to lignin concentration, they found a negative correlation (R^2 = 0.82). However, they were not able to relate the rate of CH_4 fermentation or biodegradability with only lignin concentration. They hypothesized that this was due to structural bonds that the lignin formed with cellulose which are resistant to hydrolytic enzymes. Chynoweth et al. (1993) has noted a correlation between the rate of conversion for the first order model of several biomass feedstocks and their lignin concentrations.

Modified first order equations have been developed by combining two first order equations. The CH_4 yield profile may be better assessed using two rate constants to account for the rapid degradation of readily degradable components followed by the slower degradation of fibrous material (Eq. 3-11) (Owens, J.M. and Chynoweth, 1993; Rao et al., 2000; Rincón et al., 2010; Strömberg et al., 2015):

$$B(t) = B_o(1 - f_d \cdot exp(-k_{1mod} \cdot t) - (1 - f_d) \cdot exp(-k_{2mod} \cdot t)) \quad (3\text{-}11)$$

where f_d is the fraction of the readily degradable part of the substrate, k_{1mod} is the rate constant of the more readily degradable substrate, and k_{2mod} is the rate constant of the less readily degradable substrate. When compared to the first order model for the BMP of wheat, the pseudo first order model was a better fit (Rincón et al., 2010) (Table 3-1).

The typical first order model has been modified to include a time dependency as seen in Eq. (3-12) (Strömberg et al., 2015):

$$B(t) = B_o \cdot \left(1 - exp(-k \cdot t^{\gamma})\right) \quad (3\text{-}12)$$

where γ is the time dependency. The k_h for hydrolysis can also be calculated assuming first order degradation using the time once the CH_4 production is less than 1% of total gas production as seen in Eq (3-13) (Koch & Drewes, 2014):

$$k_h = \frac{t - 100}{t - t^2} \quad (3\text{-}13)$$

where t is a real number and does not equal 0 or 1.

The time-dependent first order model (Eq 3-13) has been used for early prediction of the SMY. The time-dependent first order model had better predictions of the final SMY than the first order or modified first order in a BMP test of sludge and other types of organic wastes (Strömberg et al., 2015).

Overall, there are several ways to improve the first order equation. Substrate-specific modifications of the first order equation can provide better parameter estimates and generate a more precise BMP profile. Improvements in parameter estimation techniques can also increase the accuracy of the first order model. Nonlinear parameter estimation methods can provide more precise parameter estimates and uncertainty than typical linearization methods.

3.6.2 Gompertz equation

The modified Gompertz equation is another frequently cited BMP model. The Gompertz equation is a sigmoidal growth curve which was developed to model bacterial population growth without including substrate uptake (Zwietering, Jongenburger, Rombouts, & Van, 1990). A

modified form of the Gompertz equation Eq. (3-14) can be used to calculate the CH_4 production potential and maximum specific CH_4 production rate (Beneragama, Iwasaki, & Umetsu, 2017; Dechrugsa, Kantachote, & Chaiprapat, 2013; Feng et al., 2013; Gaur & Suthar, 2017; Kafle & Kim, 2013; Kafle et al., 2013; Koch et al., 2019; Romagnoli, Pastare, Sabūnas, Bāliņa, & Blumberga, 2017; Strömberg et al., 2015; Veluchamy & Kalamdhad, 2017; Wandera et al., 2018; Zhu et al., 2009; Zwietering et al., 1990):

$$B_{(t)} = B_o \cdot exp\left\{-exp\left[\frac{R_m \cdot e}{H}(\lambda - t) + 1\right]\right\} \quad (3\text{-}14)$$

where B(t) is the cumulative specific CH_4 production (mL g mass^{-1}) at time t, exp(1) is 2.71828, R_m is the maximum specific CH_4 production rate (mL g mass day^{-1}), H is the specific CH_4 production potential (mL g mass^{-1}), λ is the lag phase time in days. The parameters can be estimated using non-linear least square regression methods.

The modified Gompertz model has performed well when compared to other models. The modified Gompertz model provided a better fit and closer prediction of SMYs when compared to the first order kinetic model for several substrates including fish waste, bread waste, brewery grain waste, and swine manure (Kafle & Kim, 2012; Kafle et al., 2013) (Table 3-1). In one case, the modified Gompertz model had worst predictions for SMYs for several different types of livestock manures in batch mesophilic digestion when compared to the first order model but was still a good fit ($R^2 > 0.99$) (Kafle & Chen, 2016) (Table 3-1). They attributed this result to the fact that there was no lag phase in CH_4 production due to the use of an active inoculum and the presence of readily degradable material in the substrate. In Kafle and Kim (2012) and Kafle et al. (2013), the modified Gompertz model may have been a better fit due to the initial lag time in CH_4 production. Overall, the modified Gompertz model is suitable when there is a lag in CH_4 production during the initial days of the test.

3.6.3 Contois nonlinear regression

Integrated Contois model

Contois kinetics can be applied to AD. Contois kinetics were derived from the microbial growth kinetics of continuous and batch cultures of aqueous solutions (Contois, 1959). Contois kinetics have been adapted for hydrolysis kinetics of anaerobic degradation. For a particulate

substrate, there are two separate phases for hydrolysis: colonization and degradation (Vavilin et al., 1996). During colonization, hydrolytic microorganisms surround the individual particle and release enzymes to produce smaller particles, called monomers. The hydrolytic microorganisms can then degrade the surface of the monomers at a constant depth per unit time. Vavilin et al. (1996) showed that the Contois model is a good fit for the surface-related hydrolysis kinetics model. Vavilin et al. (1996) developed a surface-related hydrolysis kinetics model to account for colonization that combines both the saturation of the substrate and biomass into a single parameter. Vavilin et al. (2004) developed the integrated Contois model by combining Contois hydrolysis kinetics with the conversion of organic waste to CH_4, as seen in Eq. (3-15):

$$t = \frac{1}{Y_H \rho_{mH}} ln\left(1 + \frac{V_{CH_4} - V_{(CH_4,0)}}{\omega \frac{B_{0H}}{Y_H}}\right) - \frac{\widehat{K}_{VS}}{\rho_{mH}} ln\left(1 - \frac{V_{CH_4} - V_{(CH_4,0)}}{\omega VS_0}\right) \quad (3\text{-}15)$$

where the coefficients are $\omega B_{0H}/Y_H$ (mL CH_4 L^{-1}), ρ_{mH}/Y_H (day^{-1}), $\hat{K}_{VS}$ ρ_{mH}^{-1} (day), and ω (ml CH_4 gVS^{-1}). Specifically, Y_H is the hydrolytic (acidogenic) biomass yield coefficient (unitless), ρ_{mH} is the maximum specific hydrolytic rate (day^{-1}), V_{CH4} is the CH_4 volume released (mL), ω is the conversion coefficient of waste into CH_4 (mL CH_4 g $mass^{-1}$), B_H is the hydrolytic (acidogenic) biomass concentration, $\widehat{K}_{VS}$ is the half-saturation coefficient (unitless). Vavilin et al. (2004) used the integrated Contois model to fit BMP test results for the putrescible fractions of MSW (Table 3-1). When compared to first order kinetics, they found that the integrated Contois model was a significantly better fit.

Monod equation (second order model)

The Monod equation is commonly used for modeling microbial uptake in biological processes. The Monod equation is a special case of Contois kinetics (Spriet, 1985). Modified forms of the Monod equation are commonly used for modeling microbial growth rates in anaerobic wastewater treatment and anaerobic digestion (Batstone et al., 2002; Bernard et al., 2001; Billington, 1988; Dochain et al., 1995; Eastman & Ferguson, 1981; Eastman et al., 1981; Lokshina et al., 2001; Sollfrank & Gujer, 1991; Vanrolleghem et al., 1995).

The Monod equation operates under several assumptions. The Monod equation may be more suitable for modeling the BMP test when there is prolonged, slower degradation at the end

of the batch test (Strömberg et al., 2014). This kinetic model is derived from the assumptions that (1) a batch digester behaves like a CSTR with a short retention time and a high OLR in the beginning, and at the end when most of the substrate is degraded, behaves like a CSTR with a low retention time and a low OLR and (2) that hydrolysis is the rate-limiting step (Koch & Drewes, 2014). The modified Monod equation for BMP tests is shown in (3-16).

$$B(t) = B_o\left(\frac{k_2 \cdot t}{1 + k_2 \cdot t}\right) \tag{3-16}$$

The parameter k_2 can be estimated by linearization of (3-16) (Koch & Drewes, 2014) and nonlinear regression (Strömberg et al., 2015) (Table 3-1).

The Quadratic Monod is another modification of Contois kinetics and has also been used for modeling BMP test results (Strömberg et al., 2015).

$$B(t) = B_o \cdot \left(\frac{t^2}{t^2 + k_{M1} \cdot t + k_{M2}}\right) \tag{3-17}$$

In Eq. (3-17), k_{M1} and k_{M2} are the rate constants. The Monod equation, while easily structurally identifiable to the biological mechanism, is not easily practically identifiable due to the lack of high quality experimental data (Dochain et al., 1995).

Chen and Hashimoto model

The Chen and Hashimoto model was developed using Contois kinetics for substrates with high total solids (TS) concentration. The Chen and Hashimoto model was a good fit for a semi-continuous mesophilic anaerobic digester receiving dairy manure (Y. R. Chen & Hashimoto, 1980). Furthermore, the Chen and Hashimoto model has been modified for batch BMP digestion systems by substituting substrate concentration with CH_4 yield as seen in Eq (3-18) (Kafle & Chen, 2016):

$$B(t) = B_o\left(1 - \frac{K_{CH}}{HRT \cdot \mu_m + K_{CH} - 1}\right) \tag{3-18}$$

where K_{CH} is the dimensionless kinetic constant, μ_m is the maximum specific growth rate (day^{-1}), and HRT is the hydraulic time (day). The parameters can be solved through linearization (Kafle & Kim, 2012; Kafle et al., 2013) or nonlinear regression (Y. R. Chen & Hashimoto, 1980; Kafle & Chen, 2016).

The Chen and Hashimoto model contains several kinetic parameters which differentiates it from the previously described models. Unlike the Monod model, the Chen and Hashimoto model accounts for the relative biodegradability of different waste materials (Billington, 1988). However, one of the drawbacks of Contois kinetics is that it is less reliable at low substrate concentrations (Billington, 1988). Of the models reviewed, only the Chen and Hashimoto model included a term for microbial growth rate. However, this term was a lumped parameter. Including parameters for specific microbial species in the model or for changes in microbial fluxes or populations could advance BMP modeling.

The Chen and Hashimoto model has been tested in literature. Kafle and Chen (2016) used the Chen and Hashimoto model to predict the CH_4 yield for several different types of livestock manure in batch mesophilic digestion (Table 3-1). When compared to the first order and Gompertz model, the Chen and Hashimoto model gave the worst prediction of CH_4 yields but was still a good fit ($R^2 > 0.97$). However, they found a relation between the model and the lignin concentration. The parameters K_{CH}, and μ_m increased as the lignin concentration of the manure decreased.

Kinetic modeling can be used for early prediction of values related to the BMP test. Short-time estimation of the biogas potential for MSW has been done by correlating biogas data with time. However, this method requires at least 14 days of data and is case specific (Ponsá, Gea, & Sánchez, 2011). Strömberg et al. (2015) used kinetic modeling to predict remaining degradation in a real time BMP experiment of several substrates including anaerobic sludge, standard compounds, household wastes, agricultural wastes, sewage sludge and lipid-rich wastes. They tested six kinetic models including the first order, first order with time dependency, combined first order, a modified Gompertz, Monod, and a quadratic Monod. For parameter estimation, they used constrained nonlinear minimization. They found that the Monod, quadratic Monod, and time-dependent first order models had more accurate predictions of the SMY than the first order, combined first order, and modified Gompertz. They suggested that these models were more accurate because they allowed for a slower decline in gas production which is typical of complex substrates. Overall, they found that mathematical modeling could reasonably predict the SMY as early as six days into the test with a reasonable error (rRMSE < 10%).

Improvements in kinetic modeling can aid BMP testing and prediction. One of the main drawbacks of the BMP test is its length. The application of kinetic modeling with an on-going BMP test could help to provide earlier predictions. However, improvements in kinetic modeling

could reduce the time needed for the BMP test. The majority of kinetic modeling uses the first order model and modified Gompertz model (Figure 3-2). There is potential for the exploration of other kinetic models for BMP test modeling. However, the predictive ability of these models assumes that the collected data is of high quality. Leakages of the biogas (Hafner & Astals, 2019) during the BMP tests can be a common issue. Poor biogas data could substantially affect the implementation of these models. Overall, attention should be paid to the BMP testing methodology.

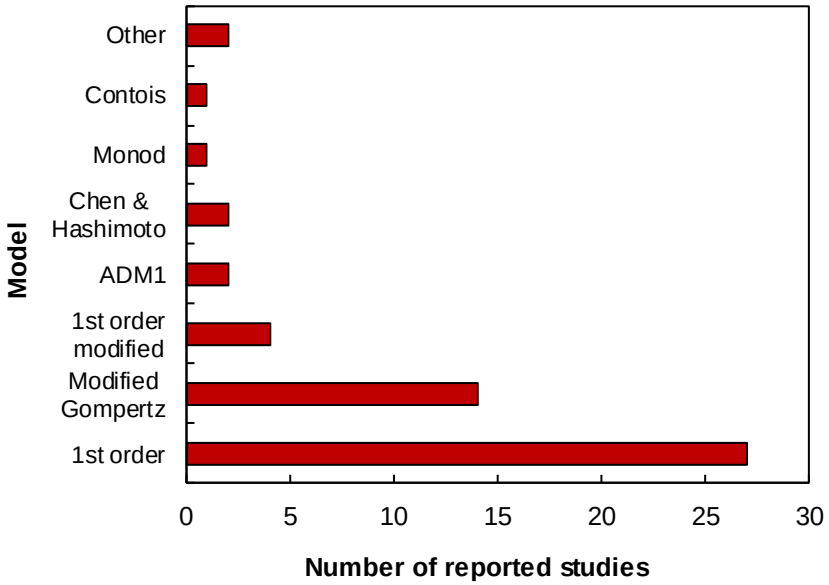

Figure 3-2. Number of reported studies for the given BMP models.

3.7 Conclusions

The following conclusions were drawn from this chapter:

1. Reliable theoretical BMP models can be selected based on the feedstock being tested and could possibly remove the need for BMP testing.
2. Substrates with higher biodegradability had higher SMY values.
3. For kinetic modeling of BMP results, the frequently used first order model lacks the nuance required for complex substrates.
4. Improvements in BMP models could reduce the time needed for the BMP test through early prediction of the SMY and other parameters.

5. Linking the function of the AD process to microbial community dynamics could further improve modeling.

3.8 References

Abbasi, T., Tauseef, S. M., & Abbasi, S. A. (2012). Anaerobic digestion for global warming control and energy generation - An overview. *Renewable and Sustainable Energy Reviews*, *16*(5), 3228–3242. https://doi.org/10.1016/j.rser.2012.02.046

Achinas, S., Li, Y., Achinas, V., & Euverink, G. J. W. (2019). Biogas Potential from the Anaerobic Digestion of Potato Peels: Process Performance and Kinetics Evaluation. *Energies*, *12*(12), 2311. https://doi.org/10.3390/en12122311

Ahmadi-Pirlou, M., Ebrahimi-Nik, M., Khojastehpour, M., & Ebrahimi, S. H. (2017). Mesophilic co-digestion of municipal solid waste and sewage sludge: Effect of mixing ratio, total solids, and alkaline pretreatment. *International Biodeterioration and Biodegradation*, *125*, 97–104. https://doi.org/10.1016/j.ibiod.2017.09.004

Alzate, M. E., Muñoz, R., Rogalla, F., Fdz-Polanco, F., & Pérez-Elvira, S. I. (2012). Biochemical methane potential of microalgae: Influence of substrate to inoculum ratio, biomass concentration and pretreatment. *Bioresource Technology*, *123*, 488–494. https://doi.org/10.1016/j.biortech.2012.06.113

Amha, Y. M., Sinha, P., Lagman, J., Gregori, M., & Smith, A. L. (2017). Elucidating microbial community adaptation to anaerobic co-digestion of fats, oils, and grease and food waste. *Water Research*, *123*, 277–289. https://doi.org/10.1016/j.watres.2017.06.065

Amon, T., Amon, B., Kryvoruchko, V., Zollitsch, W., Mayer, K., & Gruber, L. (2007). Biogas production from maize and dairy cattle manure-Influence of biomass composition on the methane yield. *Agriculture, Ecosystems and Environment*, *118*(1–4), 173–182. https://doi.org/10.1016/j.agee.2006.05.007

Angelidaki, I., Alves, M., Bolzonella, D., Borzacconi, L., Campos, J. L., Guwy, A. J., … van Lier, J. B. (2009). Defining the biomethane potential (BMP) of solid organic wastes and energy crops: A proposed protocol for batch assays. *Water Science and Technology*, *59*(5), 927–934. https://doi.org/10.2166/wst.2009.040

Angelidaki, I., Ellegraard, L., & Aharing, B. K. (1993). A mathmatical model for dynamic simulation of anaerobic digestion of complex substrates: Focusing on ammonia inhibition. *Biotechnology and Bioengineering*, *42*, 159–166. https://doi.org/10.1002/bit.26042020

Angelidaki, I., Schmidt, J. E., Ellegaard, L., & Ahring, B. K. (1998). An automatic system for simultaneous monitoring of gas evolution in multiple closed vessels. *Journal of Microbiological Methods*, *33*(1), 93–100. https://doi.org/10.1016/S0167-7012(98)00044-X

Angelidaki, Irini, Ellegaard, L., & Ahring, B. K. (1999). A comprehensive model of anaerobic bioconversion of complex substrates to biogas. *Biotechnology and Bioengineering*, *63*(3), 363–372. https://doi.org/10.1002/(SICI)1097-0290(19990505)63:3<363::AID-BIT13>3.0.CO;2-Z

Angelidaki, Irini, & Sanders, W. (2004). Assessment of the anaerobic biodegradability of macropollutants. *Reviews in Environmental Science and Biotechnology*, *3*(2), 117–129. https://doi.org/10.1007/s11157-004-2502-3

APHA. (1999). *Standard Methods for the Examination of Water and Wastewater*. (L. S. Clescerl, A. E. Greenberg, A. D. Eaton, & M. A. H. Franson, Eds.) (20th ed.). Washington D.C.: Amer Public Health Assn; American Water Works Assn; Water Environment Federation.

Astals, S., Batstone, D. J., Mata-Alvarez, J., & Jensen, P. D. (2014). Identification of synergistic impacts during anaerobic co-digestion of organic wastes. *Bioresource Technology*, *169*, 421–427. https://doi.org/10.1016/j.biortech.2014.07.024

Badshah, M., Lam, D. M., Liu, J., & Mattiasson, B. (2012). Use of an Automatic Methane Potential Test System for evaluating the biomethane potential of sugarcane bagasse after different treatments. *Bioresource Technology*, *114*, 262–269. https://doi.org/10.1016/j.biortech.2012.02.022

Batstone, D. J., Keller, J., Angelidaki, I., Kalyuzhnyi, S. V., Pavlostathis, S. G., Rozzi, A., … Vavilin, V. A. (2002). The IWA Anaerobic Digestion Model No 1 (ADM1). *Water Science and Technology*, *45*(10), 65–73. https://doi.org/10.2166/wst.2008.678

Batstone, D. J., Pind, P. F., & Angelidaki, I. (2003). Kinetics of thermophilic, anaerobic oxidation of straight and branched chain butyrate and valerate. *Biotechnology and Bioengineering*, *84*(2), 195–204. https://doi.org/10.1002/bit.10753

Batstone, D. J., Tait, S., & Starrenburg, D. (2009). Estimation of hydrolysis parameters in full-scale anerobic digesters. *Biotechnology and Bioengineering*, *102*(5), 1513–1520. https://doi.org/10.1002/bit.22163

Belle, A. J., Lansing, S., Mulbry, W., & Weil, R. R. (2015). Methane and hydrogen sulfide production during co-digestion of forage radish and dairy manure. *Biomass and Bioenergy*, *80*, 44–51. https://doi.org/10.1016/j.biombioe.2015.04.029

Beneragama, N., Iwasaki, M., & Umetsu, K. (2017). Methane production from thermophilic co-digestion of dairy manure and waste milk obtained from therapeutically treated cows. *Animal Science Journal*, *88*(2), 401–409. https://doi.org/10.1111/asj.12624

Bernard, O., Hadj-Sadok, Z., Dochain, D., Genovesi, A., & Steyer, J. P. (2001). Dynamical model development and parameter identification for an anaerobic wastewater treatment process. *Biotechnology and Bioengineering*, *75*(4), 424–438. https://doi.org/10.1002/bit.10036

Billington, R. S. (1988). A review of the kinetics of the methanogenic fermentation of lignocellulosic wastes. *Journal of Agricultural Engineering Research*, *39*(2), 71–84. https://doi.org/10.1016/0021-8634(88)90131-X

Boruff, C. S., & Buswell, A. M. (1934). The anaerobic fermentation of lignin. *Journal of the American Chemical Society*, *56*(4), 886–888. https://doi.org/10.1021/ja01319a037

Browne, J. D., & Murphy, J. D. (2013). Assessment of the resource associated with biomethane from food waste. *Applied Energy*, *104*, 170–177. https://doi.org/10.1016/j.apenergy.2012.11.017

Buffiere, P., Loisel, D., Bernet, N., & Delgenes, J.-P. (2006). Towards new indicators for the prediction of solid waste anaerobic digestion properties. *Water Science and Technology*, *53*(8), 233–241. https://doi.org/10.2166/wst.2006.254

Buswell, A. M., & Neave, S. L. (1930). *Laboratory studies of sludge digestion*. *Division of the State Water Survey*. Urbana, Illinois. https://doi.org/10.1017/CBO9781107415324.004

Buswell, M., & Muellepi, H. F. (1952). Mechanim of methane fermentation. *Industrial and Engineering Chemistry*, *44*(3), 550–552. https://doi.org/10.1021/ie50507a033

Carstensen, J., Vanrolleghem, P., Rauch, W., & Reichert, P. (1997). Terminology and methodology in modelling for water quality management - A discussion starter. *Water Science and Technology*, *36*(5), 157–168. https://doi.org/10.1016/S0273-1223(97)00470-8

Cavaleiro, A. J., Ferreira, T., Pereira, F., Tommaso, G., & Alves, M. M. (2013). Biochemical methane potential of raw and pre-treated meat-processing wastes. *Bioresource Technology*, *129*, 519–525. https://doi.org/10.1016/j.biortech.2012.11.083

Chae, K. J., Jang, A., Yim, S. K., & Kim, I. S. (2008). The effects of digestion temperature and temperature shock on the biogas yields from the mesophilic anaerobic digestion of swine manure. *Bioresource Technology*, *99*(1), 1–6. https://doi.org/10.1016/j.biortech.2006.11.063

Chen, T. H., & Hashimoto, A. G. (1996). Effects of pH and substrate:inoculum ratio on batch methane fermentation. *Bioresource Technology*, *56*(2–3), 179–186. https://doi.org/10.1016/0960-8524(96)00016-8

Chen, Y. R., & Hashimoto, A. G. (1980). Substrate Utilization Kinetic Model for Biological Treatment Processes. *Biotechnology and Bioengineering*, *XXII*, 2081–2095.

Cho, J. K., Park, S. C., & Chang, H. N. (1995). Biochemical methane potential and solid state anaerobic digestion of Korean food wastes. *Bioresource Technology*, *52*(3), 245–253. https://doi.org/10.1016/0960-8524(95)00031-9

Christ, O., Wilderer, P. A., Angerhöfer, R., & Faulstich, M. (2000). Mathematical modeling of the hydrolysis of anaerobic processes. *Water Science and Technology*, *41*(3), 61–65.

Chynoweth, D. P., Turick, C. E., Owens, J. M., Jerger, D. E., & Peck, M. W. (1993). Biochemical methane potential of biomass and waste feedstocks. *Biomass and Bioenergy*, *5*(1), 95–111. https://doi.org/10.1016/0961-9534(93)90010-2

Contois, D. E. (1959). Kinetics of bacterial growth: Relationship between population density and specific growth rate of continuous cultures. *Journal of General Microbiology*, *21*(1), 40–50. https://doi.org/10.1099/00221287-21-1-40

Costa, J. C., Oliveira, J. V., & Alves, M. M. (2016). Response surface design to study the influence of inoculum, particle size and inoculum to substrate ratio on the methane production from Ulex sp. *Renewable Energy*, *96*, 1071–1077. https://doi.org/10.1016/j.renene.2015.10.028

Curry, N., & Pillay, P. (2012). Biogas prediction and design of a food waste to energy system for the urban environment. *Renewable Energy*, *41*, 200–209. https://doi.org/10.1016/j.renene.2011.10.019

Daly, S. E., & Ni, J. (n.d.). No Title.

Davidsson, Å., Gruvberger, C., Christensen, T. H., Hansen, T. L., & Jansen, J. la C. (2007). Methane yield in source-sorted organic fraction of municipal solid waste. *Waste Management*, *27*(3), 406–414. https://doi.org/10.1016/j.wasman.2006.02.013

De Baere, L. (2000). Anaerobic digestion of solid waste: state-of-the-art. *Water Science and Technology : A Journal of the International Association on Water Pollution Research*, *41*(3), 283–290.

Dechrugsa, S., Kantachote, D., & Chaiprapat, S. (2013). Effects of inoculum to substrate ratio, substrate mix ratio and inoculum source on batch co-digestion of grass and pig manure. *Bioresource Technology*, *146*, 101–108. https://doi.org/10.1016/j.biortech.2013.07.051

Dochain, D., Vanrolleghem, P. A., & Van Daele, M. (1995). Structural identifiability of biokinetic models of activated sludge respiration. *Water Research*, *29*(11).

Donoso-Bravo, Andrés, García, G., Pérez-Elvira, S., & Fdz-Polanco, F. (2011). Initial rates technique as a procedure to predict the anaerobic digester operation. *Biochemical Engineering Journal*, *53*(3), 275–280. https://doi.org/10.1016/j.bej.2010.11.007

Donoso-Bravo, Andres, Mailier, J., Martin, C., Rodríguez, J., Aceves-Lara, C. A., & Wouwer, A. Vande. (2011). Model selection, identification and validation in anaerobic digestion: A review. *Water Research*, *45*(17), 5347–5364. https://doi.org/10.1016/j.watres.2011.08.059

Eastman, J. A., & Ferguson, J. F. (1981). Solubilization organic phase of of carbon anaerobic particulate during the digestion acid. *Journal (Water Pollution Control Federation)*, *53*(3), 352–366.

Eastman, J. A., Ferguson, J. F., Journal, S., Pollution, W., Federation, C., & Mar, P. I. (1981). Solubilization of Particulate Organic Carbon during the Acid Phase of Anaerobic Digestion. *Water Pollution Control Federation*, *53*(3), 352–366.

Edward, M., Edwards, S., Egwu, U., & Sallis, P. (2015). Bio-methane potential test (BMP) using inert gas sampling bags with macroalgae feedstock. *Biomass and Bioenergy*, *83*, 516–524. https://doi.org/10.1016/j.biombioe.2015.10.026

Elbeshbishy, E., & Nakhla, G. (2012). Batch anaerobic co-digestion of proteins and carbohydrates. *Bioresource Technology*, *116*, 170–178. https://doi.org/10.1016/j.biortech.2012.04.052

Elbeshbishy, E., Nakhla, G., & Hafez, H. (2012). Biochemical methane potential (BMP) of food waste and primary sludge: Influence of inoculum pre-incubation and inoculum source. *Bioresource Technology*, *110*, 18–25. https://doi.org/10.1016/j.biortech.2012.01.025

Erguder, T. H., Guven, E., & Demirer, G. N. (2000). Anaerobic treatment of olive mill wastewaters in batch reactors. *Process Biochemistry*, *36*(3), 243–248. https://doi.org/10.1016/S0032-9592(00)00205-3

Eskicioglu, C., & Ghorbani, M. (2011). Effect of inoculum/substrate ratio on mesophilic anaerobic digestion of bioethanol plant whole stillage in batch mode. *Process Biochemistry*, *46*(8), 1682–1687. https://doi.org/10.1016/j.procbio.2011.04.013

Fedorovich, V., Lens, P., & Kalyuzhnyi, S. (2003). Extension of Anaerobic Digestion Model No. 1. *Applied Biochemistry And Biotechnology*, *109*, 33–45. https://doi.org/https://doi.org/10.1385/ABAB

Feng, L., Li, Y., Chen, C., Liu, X., Xiao, X., Ma, X., … Liu, G. (2013). Biochemical methane potential (BMP) of vinegar residue and the influence of feed to inoculum ratios on biogas production. *BioResources*, *8*(2), 2487–2498. https://doi.org/10.15376/biores.8.2.2487-2498

Flotats, X., Ahring, B. K., & Angelidaki, I. (2003). Parameter identification of thermophilic anaerobic degradation of valerate. *Applied Biochemistry and Biotechnology*, *109*(1–3), 47–62. https://doi.org/10.1385/abab:109:1-3:47

Forster-Carneiro, T., Pérez, M., Romero, L. I., & Sales, D. (2007). Dry-thermophilic anaerobic digestion of organic fraction of the municipal solid waste: Focusing on the inoculum sources. *Bioresource Technology*, *98*(17), 3195–3203. https://doi.org/10.1016/j.biortech.2006.07.008

Gaur, R. Z., & Suthar, S. (2017). Anaerobic digestion of activated sludge, anaerobic granular sludge and cow dung with food waste for enhanced methane production. *Journal of Cleaner Production*, *164*, 557–566. https://doi.org/10.1016/j.jclepro.2017.06.201

Gavala, H. N., Angelidaki, I., & Ahring, B. K. (2003). Kinetics and Modeling of Anaerobic Digestion Process. In B. K. Ahring (Ed.), *Biomethanation I* (pp. 57–93). Berlin: Springer.

Gunaseelan, V. N. (2007). Regression models of ultimate methane yields of fruits and vegetable solid wastes, sorghum and napiergrass on chemical composition. *Bioresource Technogllogy*, *98*(6), 1270–1277. https://doi.org/10.1016/j.biortech.2006.05.014

Guwy, A. J. (2004). Equipment used for testing anaerobic biodegradability and activity. *Reviews in Environmental Science and Biotechnology*, *3*(2), 131–139. https://doi.org/10.1007/s11157-004-1290-0

Hafner, S. D., & Astals, S. (2019). Systematic error in manometric measurement of biochemical methane potential: Sources and solutions. *Waste Management*, *91*, 147–155. https://doi.org/10.1016/j.wasman.2019.05.001

Hafner, S. D., Koch, K., Carrere, H., Astals, S., Weinrich, S., & Rennuit, C. (2018). Software for biogas research: Tools for measurement and prediction of methane production. *SoftwareX*, *7*, 205–210. https://doi.org/10.1016/j.softx.2018.06.005

Hashimoto, A. G. (1989). Effect of inoculum/substrate ratio on methane yield and production rate from straw. *Biological Wastes*, *28*, 247–255. https://doi.org/10.1016/0269-7483(89)90108-0

Heo, N. H., Park, S. C., Lee, J. S., & Kang, H. (2003). Solubilization of waste activated sludge by alkaline pretreatment and biochemical methane potential (BMP) tests for anaerobic co-digestion of municipal organic waste. *Water Science and Technology*, *48*(8), 211–219.

Isci, A., & Demirer, G. N. (2007). Biogas production potential from cotton wastes. *Renewable Energy*, *32*(5), 750–757. https://doi.org/10.1016/j.renene.2006.03.018

Jensen, P. D., Ge, H., & Batstone, D. J. (2011). Assessing the role of biochemical methane potential tests in determining anaerobic degradability rate and extent. *Water Science and Technology*, *64*(4), 880–886. https://doi.org/10.2166/wst.2011.662

Jerger, D. E., Chynoweth, D. P., & Isaacson, H. R. (1987). Anaerobic digestion of sorghum biomass. *Biomass*, *14*(2), 99–113. https://doi.org/10.1016/0144-4565(87)90013-8

Kafle, G. K., & Chen, L. (2016). Comparison on batch anaerobic digestion of five different livestock manures and prediction of biochemical methane potential (BMP) using different statistical models. *Waste Management*, *48*, 492–502. https://doi.org/10.1016/j.wasman.2015.10.021

Kafle, G. K., & Kim, S. H. (2012). Kinetic Study of the Anaerobic Digestion of Swine Manure at Mesophilic Temperature : A Lab Scale Batch Operation. *Journal of Biosystems Engineering*, *37*(4), 233–244. https://doi.org/http://dx.doi.org/10.5307/JBE.2012.37.4.233

Kafle, G. K., & Kim, S. H. (2013). Anaerobic treatment of apple waste with swine manure for biogas production: Batch and continuous operation. *Applied Energy*, *103*, 61–72. https://doi.org/10.1016/j.apenergy.2012.10.018

Kafle, G. K., Kim, S. H., & Sung, K. I. (2013). Ensiling of fish industry waste for biogas production: A lab scale evaluation of biochemical methane potential (BMP) and kinetics. *Bioresource Technology*, *127*, 326–336. https://doi.org/10.1016/j.biortech.2012.09.032

Kawai, M., Nagao, N., Tajima, N., Niwa, C., Matsuyama, T., & Toda, T. (2014). The effect of the labile organic fraction in food waste and the substrate/inoculum ratio on anaerobic digestion for a reliable methane yield. *Bioresource Technology*, *157*, 174–180. https://doi.org/10.1016/j.biortech.2014.01.018

Kayhanian, M. (1999). Ammonia inhibition in high-solids biogasification: An overview and practical solutions. *Environmental Technology*, *20*(4), 355–365. https://doi.org/10.1080/09593332008616828

Koch, K., & Drewes, J. E. (2014). Alternative approach to estimate the hydrolysis rate constant of particulate material from batch data. *Applied Energy*, *120*, 11–15. https://doi.org/10.1016/j.apenergy.2014.01.050

Koch, K., Hafner, S. D., Weinrich, S., & Astals, S. (2019). Identification of Critical Problems in Biochemical Methane Potential (BMP) Tests From Methane Production Curves. *Frontiers in Environmental Science*, *7*(November), 1–8. https://doi.org/10.3389/fenvs.2019.00178

Koch, K., Lippert, T., & Drewes, J. E. (2017). The role of inoculum's origin on the methane yield of different substrates in biochemical methane potential (BMP) tests. *Bioresource Technology*, *243*, 457–463. https://doi.org/10.1016/j.biortech.2017.06.142

Kolbl, S., Paloczi, A., Panjan, J., & Stres, B. (2014). Addressing case specific biogas plant tasks: Industry oriented methane yields derived from 5L Automatic Methane Potential Test Systems in batch or semi-continuous tests using realistic inocula, substrate particle sizes and organic loading. *Bioresource Technology*, *153*, 180–188. https://doi.org/10.1016/j.biortech.2013.12.010

Kovalovszki, A., Alvarado-Morales, M., Fotidis, I. A., & Angelidaki, I. (2017). A systematic methodology to extend the applicability of a bioconversion model for the simulation of various co-digestion scenarios. *Bioresource Technology*, *235*(1), 157–166. https://doi.org/10.1016/j.biortech.2017.03.101

Labatut, R. A., Angenent, L. T., & Scott, N. R. (2011). Biochemical methane potential and biodegradability of complex organic substrates. *Bioresource Technology*, *102*(3), 2255–2264. https://doi.org/10.1016/j.biortech.2010.10.035

Lauwers, J., Appels, L., Thompson, I. P., Degrève, J., Van Impe, J. F., & Dewil, R. (2013). Mathematical modelling of anaerobic digestion of biomass and waste: Power and limitations. *Progress in Energy and Combustion Science*, *39*(4), 383–402. https://doi.org/10.1016/j.pecs.2013.03.003

Leng, L., Yang, P., Singh, S., Zhuang, H., Xu, L., Chen, W. H., … Lee, P. H. (2018). A review on the bioenergetics of anaerobic microbial metabolism close to the thermodynamic limits and its implications for digestion applications. *Bioresource Technology*, *247*, 1095–1106. https://doi.org/10.1016/j.biortech.2017.09.103

Lesteur, M., Bellon-Maurel, V., Gonzalez, C., Latrille, E., Roger, J. M., Junqua, G., & Steyer, J. P. (2010). Alternative methods for determining anaerobic biodegradability: A review. *Process Biochemistry*, *45*(4), 431–440. https://doi.org/10.1016/j.procbio.2009.11.018

Lim, S. J., & Fox, P. (2013). Biochemical methane potential (BMP) test for thickened sludge using anaerobic granular sludge at different inoculum/substrate ratios. *Biotechnology and Bioprocess Engineering*, *18*(2), 306–312. https://doi.org/10.1007/s12257-012-0465-8

Liu, G., Zhang, R., El-Mashad, H. M., & Dong, R. (2009). Effect of feed to inoculum ratios on biogas yields of food and green wastes. *Bioresource Technology*, *100*(21), 5103–5108. https://doi.org/10.1016/j.biortech.2009.03.081

Lobry, J., Rosso, L., & Flandrois, J. (1991). A fortran subroutine for the determination of parameter confidence limitis in non-linear models. *Binary*, *3*, 86–93.

Lokshina, L. Y., Vavilin, V. A., Kettunen, R. H., Rintala, J. A., Holliger, C., & Nozhevnikova, A. N. (2001). Evaluation of kinetic coefficients using integrated Monod and Haldane Models for low- temperature acetoclastic methanogens. *Water Research*, *35*(12), 2913–2922. https://doi.org/10.1016/S0043-1354(00)00595-9

López, I., & Borzacconi, L. (2010). Modelling of slaughterhouse solid waste anaerobic digestion: Determination of parameters and continuous reactor simulation. *Waste Management*, *30*(10), 1813–1821. https://doi.org/10.1016/j.wasman.2010.02.034

Luna-delRisco, M., Normak, A., & Orupõld, K. (2011). Biochemical methane potential of different organic wastes and energy crops from Estonia. *Agronomy Research*, *9*(1–2), 331–342.

Luostarinen, S., Luste, S., & Sillanpää, M. (2009). Increased biogas production at wastewater treatment plants through co-digestion of sewage sludge with grease trap sludge from a meat processing plant. *Bioresource Technology*, *100*(1), 79–85. https://doi.org/10.1016/j.biortech.2008.06.029

Luste, S., Heinonen-Tanski, H., & Luostarinen, S. (2012). Co-digestion of dairy cattle slurry and industrial meat-processing by-products - Effect of ultrasound and hygienization pre-treatments. *Bioresource Technology*, *104*, 195–201. https://doi.org/10.1016/j.biortech.2011.11.003

Ma, Y., Gu, J., & Liu, Y. (2018). Evaluation of anaerobic digestion of food waste and waste activated sludge: Soluble COD versus its chemical composition. *Science of the Total Environment*, *643*, 21–27. https://doi.org/10.1016/j.scitotenv.2018.06.187

Mao, C., Feng, Y., Wang, X., & Ren, G. (2015). Review on research achievements of biogas from anaerobic digestion. *Renewable and Sustainable Energy Reviews*, *45*, 540–555. https://doi.org/10.1016/j.rser.2015.02.032

Martín-González, L., Colturato, L. F., Font, X., & Vicent, T. (2010). Anaerobic co-digestion of the organic fraction of municipal solid waste with FOG waste from a sewage treatment plant: Recovering a wasted methane potential and enhancing the biogas yield. *Waste Management*, *30*(10), 1854–1859. https://doi.org/10.1016/j.wasman.2010.03.029

Masoud, K. (1995). Biodegradability of the organic fraction of municipal solid waste in a high-solids anaerobic digester. *Waste Management & Research*, *13*(2), 123–136. https://doi.org/10.1016/s0734-242x(95)90114-0

Mata-Alvarez, J., Dosta, J., Romero-Güiza, M. S., Fonoll, X., Peces, M., & Astals, S. (2014). A critical review on anaerobic co-digestion achievements between 2010 and 2013. *Renewable and Sustainable Energy Reviews*, *36*, 412–427. https://doi.org/10.1016/j.rser.2014.04.039

Mata-Alvarez, J., Mac, S., & Llabr, P. (2000). Anaerobic digestion of organic solid wastes. An overview of research achievements and perspectives. *Bioresource Technology*, *74*(1), 3–16. https://doi.org/10.1016/S0960-8524(00)00023-7

McCarty, P L. (1971). Energetics and Kinetics of Anaerobic Treatment. *Anaerobic Biological Treatment Processes*, 91–107.

McCarty, Perry L. (1964). Anaerobic waste treatment fundamentals. *Chemistry and Microbiology*, *95*(9), 107–112. https://doi.org/10.1300/J118v09n01_08

McEniry, J., Allen, E., Murphy, J. D., & O'Kiely, P. (2014). Grass for biogas production: The impact of silage fermentation characteristics on methane yield in two contrasting biomethane potential test systems. *Renewable Energy*, *63*, 524–530. https://doi.org/10.1016/j.renene.2013.09.052

Meng, L., Xie, L., Kinh, C. T., Suenaga, T., Hori, T., Riya, S., … Hosomi, M. (2018). Influence of feedstock-to-inoculum ratio on performance and microbial community succession during solid-state thermophilic anaerobic co-digestion of pig urine and rice straw. *Bioresource Technology*, *252*(October 2017), 127–133. https://doi.org/10.1016/j.biortech.2017.12.099

Møller, H. B., Sommer, S. G., & Ahring, B. K. (2004). Methane productivity of manure, straw and solid fractions of manure. *Biomass and Bioenergy*, *26*(5), 485–495. https://doi.org/10.1016/j.biombioe.2003.08.008

Montañés, R., Solera, R., & Pérez, M. (2015). Anaerobic co-digestion of sewage sludge and sugar beet pulp lixiviation in batch reactors: Effect of temperature. *Bioresource Technology*, *180*, 177–184. https://doi.org/10.1016/j.biortech.2014.12.056

Morris, G. R., Jewell, W. J., & Loehr, R. C. (1977). Anaerobic fermentation of animal wastes: A kinetic design evaluation. In J. M. Bell (Ed.), *Proceedings of the 32nd Industrial Waste Conference* (pp. 689–700). Lafayette, Indiana: Ann Arbor Science.

Mottet, A., François, E., Latrille, E., Steyer, J. P., Déléris, S., Vedrenne, F., & Carrère, H. (2010). Estimating anaerobic biodegradability indicators for waste activated sludge. *Chemical Engineering Journal*, *160*(2), 488–496. https://doi.org/10.1016/j.cej.2010.03.059

Neves, L., Gonçalo, E., Oliveira, R., & Alves, M. M. (2008). Influence of composition on the biomethanation potential of restaurant waste at mesophilic temperatures. *Waste Management*, *28*(6), 965–972. https://doi.org/10.1016/j.wasman.2007.03.031

Nizami, A. S., Orozco, A., Groom, E., Dieterich, B., & Murphy, J. D. (2012). How much gas can we get from grass? *Applied Energy*, *92*, 783–790. https://doi.org/10.1016/j.apenergy.2011.08.033

Nordlander, E., Thorin, E., & Yan, J. (2017). Investigating the possibility of applying an ADM1 based model to a full-scale co-digestion plant. *Biochemical Engineering Journal*, *120*, 73–83. https://doi.org/10.1016/j.bej.2016.12.014

Ohemeng-Ntiamoah, J., & Datta, T. (2018). Evaluating analytical methods for the characterization of lipids, proteins and carbohydrates in organic substrates for anaerobic co-digestion. *Bioresource Technology*, *247*(September 2017), 697–704. https://doi.org/10.1016/j.biortech.2017.09.154

Ohemeng-Ntiamoah, Juliet, & Datta, T. (2019). Perspectives on variabilities in biomethane potential test parameters and outcomes: A review of studies published between 2007 and 2018. *Science of the Total Environment*, *664*, 1052–1062. https://doi.org/10.1016/j.scitotenv.2019.02.088

Oslaj, M., Mursec, B., & Vindis, P. (2010). Biogas production from maize hybrids. *Biomass and Bioenergy*, *34*(11), 1538–1545. https://doi.org/10.1016/j.biombioe.2010.04.016

Owens, J.M. and Chynoweth, D. P. (1993). Biochemical methane potential of municipal solid waste (MSW) components. *Water Science & Technology*, *27*(2), 1–14. https://doi.org/10.2166/wst.1993.0065

Palatsi, J., Viñas, M., Guivernau, M., Fernandez, B., & Flotats, X. (2011). Anaerobic digestion of slaughterhouse waste: Main process limitations and microbial community interactions. *Bioresource Technology*, *102*(3), 2219–2227. https://doi.org/10.1016/j.biortech.2010.09.121

Petropoulos, E., Dolfing, J., Davenport, R. J., Bowen, E. J., & Curtis, T. P. (2017). Developing cold-adapted biomass for the anaerobic treatment of domestic wastewater at low temperatures (4, 8 and 15 °C) with inocula from cold environments. *Water Research*, *112*, 100–109. https://doi.org/10.1016/j.watres.2016.12.009

Ponsá, S., Gea, T., & Sánchez, A. (2011). Short-time estimation of biogas and methane potentials from municipal solid wastes. *Journal of Chemical Technology and Biotechnology*, *86*(8), 1121–1124. https://doi.org/10.1002/jctb.2615

Posmanik, R., Labatut, R. A., Kim, A. H., Usack, J. G., Tester, J. W., & Angenent, L. T. (2017). Coupling hydrothermal liquefaction and anaerobic digestion for energy valorization from model biomass feedstocks. *Bioresource Technology*, *233*, 134–143. https://doi.org/10.1016/j.biortech.2017.02.095

Ramirez, I., Volcke, E. I. P., Rajinikanth, R., & Steyer, J. P. (2009). Modeling microbial diversity in anaerobic digestion through an extended ADM1 model. *Water Research*, *43*(11), 2787–2800. https://doi.org/10.1016/j.watres.2009.03.034

Rao, M. S., Singh, S. P., Singh, A. K., & Sodha, M. S. (2000). Bioenergy conversion studies of the organic fraction of MSW: assessment of ultimate bioenergy production potential of municipal garbage. *Applied Energy*, *66*(1), 75–87. https://doi.org/10.1016/S0306-2619(99)00056-2

Raposo, F., Fernández-Cegrí, V., de la Rubia, M. A., Borja, R., Béline, F., Cavinato, C., … de Wilde, V. (2011). Biochemical methane potential (BMP) of solid organic substrates: Evaluation of anaerobic biodegradability using data from an international interlaboratory study. *Journal of Chemical Technology and Biotechnology*, *86*(8), 1088–1098. https://doi.org/10.1002/jctb.2622

Reilly, M., Dinsdale, R., & Guwy, A. (2016). The impact of inocula carryover and inoculum dilution on the methane yields in batch methane potential tests. *Bioresource Technology*, *208*, 134–139. https://doi.org/10.1016/j.biortech.2016.02.060

Richards, B. K., Cummings, R. J., White, T. E., & Jewell, W. J. (1991). Methods for kinetic-analysis of methane fermentation in high solids biomass digesters. *Biomass & Bioenergy*, *1*(2), 65–73. https://doi.org/10.1016/0961-9534(91)90028-B

Rico, J. L., García, H., Rico, C., & Tejero, I. (2007). Characterisation of solid and liquid fractions of dairy manure with regard to their component distribution and methane production. *Bioresource Technology*, *98*(5), 971–979. https://doi.org/10.1016/j.biortech.2006.04.032

Rincón, B., Banks, C. J., & Heaven, S. (2010). Biochemical methane potential of winter wheat (Triticum aestivum L.): Influence of growth stage and storage practice. *Bioresource Technology*, *101*(21), 8179–8184. https://doi.org/10.1016/j.biortech.2010.06.039

Robbins, J. E., Armold, M. T., & Lacher, S. L. (1979). Methane production from cattle waste and delignified straw. *Applied and Environmental Microbiology*, *38*(1), 175–177.

Romagnoli, F., Pastare, L., Sabūnas, A., Bāliņa, K., & Blumberga, D. (2017). Effects of pre-treatment on Biochemical Methane Potential (BMP) testing using Baltic Sea Fucus vesiculosus feedstock. *Biomass and Bioenergy*, *105*, 23–31. https://doi.org/10.1016/j.biombioe.2017.06.013

Shelton, D., & Tiedje, J. (1984). General method for determining anaerobic biodegradation potential. *Applied and Environmental Microbiology*, *47*(4), 850–857.

Sollfrank, U., & Gujer, W. (1991). Characterisation of domestic wastewater for mathmatical modelling of the activated sludge process. *Water Science and Technology*, *23*, 1057–1066.

Souza, T. S. O., Carvajal, A., Donoso-Bravo, A., Peña, M., & Fdz-Polanco, F. (2013). ADM1 calibration using BMP tests for modeling the effect ofautohydrolysis pretreatment on the performance ofcontinuous sludge digesters. *Water Research*, *47*(9), 3244–3254. https://doi.org/10.1016/j.watres.2013.03.041

Spriet, A. (1985). Structure characterization-An overview. *IFAC Proceedings Volumes*, *18*(5), 749–756. https://doi.org/10.1016/S1474-6670(17)60650-5

Strömberg, S., Nistor, M., & Liu, J. (2014). Towards eliminating systematic errors caused by the experimental conditions in Biochemical Methane Potential (BMP) tests. *Waste Management*, *34*(11), 1939–1948. https://doi.org/10.1016/j.wasman.2014.07.018

Strömberg, S., Nistor, M., & Liu, J. (2015). Early prediction of Biochemical Methane Potential through statistical and kinetic modelling of initial gas production. *Bioresource Technology*, *176*, 233–241. https://doi.org/10.1016/j.biortech.2014.11.033

Symons, G. E., & Buswell, A. M. (1933). The methane fermentation of carbohydrates. *Journal of the American Chemical Society*, *55*(5), 2028–2036. https://doi.org/10.1021/ja01332a039

Tong, X., Smith, L. H., & McCarty, P. L. (1990). Methane fermentation of selected lignocellulosic materials. *Biomass*, *21*(4), 239–255. https://doi.org/10.1016/0144-4565(90)90075-U

Triolo, J. M., Pedersen, L., Qu, H., & Sommer, S. G. (2012). Biochemical methane potential and anaerobic biodegradability of non-herbaceous and herbaceous phytomass in biogas production. *Bioresource Technology*, *125*, 226–232. https://doi.org/10.1016/j.biortech.2012.08.079

Triolo, J. M., Sommer, S. G., Møller, H. B., Weisbjerg, M. R., & Jiang, X. Y. (2011). A new algorithm to characterize biodegradability of biomass during anaerobic digestion: Influence of lignin concentration on methane production potential. *Bioresource Technology*, *102*(20), 9395–9402. https://doi.org/10.1016/j.biortech.2011.07.026

Turick, C. E., Peck, M. W., Chynoweth, D. P., Jerger, D. E., White, E. H., Zsuffa, L., & Andy Kenney, W. (1991). Methane fermentation of woody biomass. *Bioresource Technology*, *37*(2), 141–147. https://doi.org/10.1016/0960-8524(91)90202-U

Usack, J. G., & Angenent, L. T. (2015). Comparing the inhibitory thresholds of dairy manure co-digesters after prolonged acclimation periods: Part 1 – Performance and operating limits. *Water Research*, *87*, 1–12. https://doi.org/10.1016/j.watres.2015.05.055

Vanrolleghem, P. A., Van Daele, M., & Dochain, D. (1995). Practical identifiability of a biokinetic model of activated sludge respiration. *Water Research*, *29*(11), 2561–2570.

Vavilin, V. A., Fernandez, B., Palatsi, J., & Flotats, X. (2008). Hydrolysis kinetics in anaerobic degradation of particulate organic material: an overview. *Waste Management (New York, N.Y.)*, *28*(6), 939–951. https://doi.org/10.1016/j.wasman.2007.03.028

Vavilin, V. A., Lokshina, L. Y., Jokela, J. P. Y., & Rintala, J. A. (2004). Modeling solid waste decomposition. *Bioresource Technology*, *94*(1), 69–81. https://doi.org/10.1016/j.biortech.2003.10.034

Vavilin, V. A., Rytov, S. V., & Lokshina, L. Y. (1996). A description of hydrolysis kinetics in anaerobic degradation of particulate organic matter. *Bioresource Technology*, *56*, 229–237. https://doi.org/10.1016/0960-8524(96)00034-X

Vedrenne, F., Béline, F., Dabert, P., & Bernet, N. (2008). The effect of incubation conditions on the laboratory measurement of the methane producing capacity of livestock wastes. *Bioresource Technology*, *99*(1), 146–155. https://doi.org/10.1016/j.biortech.2006.11.043

Veeken, A., & Hamelers, B. (1999). Effect of temperature on hydrolysis rates of selected biowaste components. *Bioresource Technology*, *69*(3), 249–254. https://doi.org/10.1016/S0960-8524(98)00188-6

Veluchamy, C., & Kalamdhad, A. S. (2017). Biochemical methane potential test for pulp and paper mill sludge with different food / microorganisms ratios and its kinetics. *International Biodeterioration and Biodegradation*, *117*, 197–204. https://doi.org/10.1016/j.ibiod.2017.01.005

Venkiteshwaran, K., Bocher, B., Maki, J., & Zitomer, D. (2016). Relating anaerobic digestion microbial community and process function. *Microbiology Insights*, *8*, 37–44. https://doi.org/10.4137/MBI.S33593

Vidal, G., Carvalho, A., Méndez, R., & Lema, J. M. (2000). Influence of the content in fats and proteins on the anaerobic biodegradability of dairy wastewaters. *Bioresource Technology*, *74*(3), 231–239. https://doi.org/10.1016/S0960-8524(00)00015-8

Wagner, A. O., Lins, P., Malin, C., Reitschuler, C., & Illmer, P. (2013). Impact of protein-, lipid- and cellulose-containing complex substrates on biogas production and microbial communities in batch experiments. *The Science of the Total Environment*, *458–460*, 256–266. https://doi.org/10.1016/j.scitotenv.2013.04.034

Wandera, S. M., Qiao, W., Algapani, D. E., Bi, S., Yin, D., Qi, X., … Dong, R. (2018). Searching for possibilities to improve the performance of full scale agricultural biogas plants. *Renewable Energy*, *116*, 720–727. https://doi.org/10.1016/j.renene.2017.09.087

Wang, Q. L., Li, W., Gao, X., & Li, S. J. (2016). Life cycle assessment on biogas production from straw and its sensitivity analysis. *Bioresource Technology*, *201*(X), 208–214. https://doi.org/10.1016/j.biortech.2015.11.025

Wang, Y., Odle, W. S. I., Eleazer, W. E., & Barlaz, M. A. (1997). Methane potential of food waste and anaerobic toxicity of leachate produced during food wase decomposition. *Waste Management and Research*, *15*, 149–167. https://doi.org/10.1006/wmre.1996.0073

Wickham, R., Galway, B., Bustamante, H., & Nghiem, L. D. (2016). Biomethane potential evaluation of co-digestion of sewage sludge and organic wastes. *International Biodeterioration and Biodegradation*, *113*, 3–8. https://doi.org/10.1016/j.ibiod.2016.03.018

Yan, Y., Zhang, L., Feng, L., Sun, D., & Dang, Y. (2018). Comparison of varying operating parameters on heavy metals ecological risk during anaerobic co-digestion of chicken manure and corn stover. *Bioresource Technology*, *247*(July 2017), 660–668. https://doi.org/10.1016/j.biortech.2017.09.146

Yoon, Y. M., Kim, S. H., Shin, K. S., & Kim, C. H. (2014). Effects of substrate to inoculum ratio on the biochemical methane potential of piggery slaughterhouse wastes. *Asian-Australasian Journal of Animal Sciences*, *27*(4), 600–607. https://doi.org/10.5713/ajas.2013.13537

Zaher, U., Li, R., Jeppsson, U., Steyer, J. P., & Chen, S. (2009). GISCOD: General Integrated Solid Waste Co-Digestion model. *Water Research*, *43*(10), 2717–2727. https://doi.org/10.1016/j.watres.2009.03.018

Zeng, S., Yuan, X., Shi, X., & Qiu, Y. (2010). Effect of inoculum/substrate ratio on methane yield and orthophosphate release from anaerobic digestion of Microcystis spp. *Journal of Hazardous Materials*, *178*(1–3), 89–93. https://doi.org/10.1016/j.jhazmat.2010.01.047

Zhang, B., Zhang, L. L., Zhang, S. C., Shi, H. Z., & Cai, W. M. (2005). [Influence of temperature on hydrolysis and acidogenesis of kitchen wastes in two-phase anaerobic digestion]. *Environmental Technology*, *26*(3), 329–339.

Zhang, Q., Hu, J., & Lee, D. J. (2016). Biogas from anaerobic digestion processes: Research updates. *Renewable Energy*, *98*, 108–119. https://doi.org/10.1016/j.renene.2016.02.029

Zhang, R., El-Mashad, H. M., Hartman, K., Wang, F., Liu, G., Choate, C., & Gamble, P. (2007). Characterization of food waste as feedstock for anaerobic digestion. *Bioresource Technology*, *98*(4), 929–935. https://doi.org/10.1016/j.biortech.2006.02.039

Zhu, B., Gikas, P., Zhang, R., Lord, J., Jenkins, B., & Li, X. (2009). Characteristics and biogas production potential of municipal solid wastes pretreated with a rotary drum reactor. *Bioresource Technology*, *100*(3), 1122–1129. https://doi.org/10.1016/j.biortech.2008.08.024

Zwietering, M. H., Jongenburger, I., Rombouts, F. M., & Van, T. R. K. (1990). Modeling of the bacterial growth curve. *Applied and Environmental Microbiology*, *56*(6), 1875–1881.

CHAPTER 4. MODELING OF HYDROGEN SULFIDE PRODUCTION IN BIOCHEMICAL METHANE POTENTIAL TESTS

4.1 Abstract

Hydrogen sulfide (H_2S) is an unwanted byproduct in biogas from anaerobic digestion (AD). However, the modeling of H_2S production in AD is complex and often relies on the sulfate reduction processes in the digester liquid. This study examined H_2S production in six biochemical methane potential (BMP) tests and one precipitation test to investigate interactions of iron, sulfate, phosphorus and the anaerobic microbial community in AD. The H_2S final specific production (FSP, H_2S production per g VS) over the digestion period was examined using a generalized additive model (gam). The results showed that highly soluble, carbohydrate-based wastes had a high H_2S FSP. The H_2S production as a time series was successfully modelled using a gam model ($R^2 > 0.82$). Additionally, the H_2S FSP was negatively correlated with the initial Fe(II) : S ratio in the digester liquid. The results indicated that FeS precipitation was preferred in the presence of an anaerobic community.

4.2 Introduction

There is increasing interest about renewable energy production and concern about greenhouse gas (GHG) emissions from organic waste materials. Anaerobic digestion (AD) is a solution for both issues. It is a mature and cost-effective technology that uses a mixed microbial community to convert pre-existing wasted biomass to biogas. Biogas is composed mainly of methane (CH_4) (50-70%) and carbon dioxide (CO_2) (30-50%) (NREL, 2013). It can be used as a renewable energy to provide heat or generate electricity, thereby replacing conventional fossil fuel energy sources. Capturing biogas for energy use reduces GHG emissions. In 2018, landfills containing organic waste accounted for 17.4% of CH_4 emissions in the United States, while manure management accounted for 9.7% (EPA, 2020). In 2019, AD systems on livestock farms were able to reduce GHG emissions by 4.63 million metric tons of CO_2 equivalent (U.S. EPA, 2020).

Hydrogen sulfide is the third most important component in biogas but not a desired product. It is generated during the AD process and its concentration is usually <1% (<10,000 ppm) in biogas.

Hydrogen sulfide can be explosive, highly flammable, corrosive, and fouling at certain concentrations (Barrera, Spanjers, Dewulf, Romero, & Rosa, 2013; OSHA, n.d.). It is extremely toxic to humans and animals at concentrations greater than 1000 ppm. To protect the equipment in combined heat and power (CHP) generation and boiler applications, H_2S concentrations should be kept below 1000 ppm. Hydrogen sulfide should be removed almost entirely for vehicle fuel or natural gas use (Appels et al., 2008; Rasi, Läntelä, & Rintala, 2011).

Formation of H_2S in AD requires a sulfur source, which can cause potential for sulfur inhibition in AD. There are different mechanisms for sulfur inhibition in AD. Sources of sulfur in AD include the introduction of sulfur-rich feedstock and the degradation of amino acids and the subsequent release of sulfur. Even though sulfide is a required nutrient for bacteria, high concentrations of sulfide (> 200 mg L^{-1}) can pose a toxicity problem in AD (Lin, King, Williams, & Hu, 2017; Omil, Méndez, & Lema, 1995; B. G. F. Parkin & Owen, 1987). One cause of this toxicity is when sulfate reducing bacteria (SRB) out-compete methanogens for acetate and hydrogen to produce H_2S (*i.e.*, primary inhibition) (Chen, Cheng, & Creamer, 2008; Harada, Uemura, & Momonoi, 1994; Harper & Pohland, Frederick, 1986; Moestedt, Nilsson Påledal, & Schnürer, 2013). Sulfate reduction is generally favored over methanogenesis. Compared to methanogens, SRBs have higher specific growth rates and greater affinities for substrate utilization and removal (Chen et al., 2008; Harada et al., 1994; Oude Elferink, Visser, Hulshoff Pol, & Stams, 1994). A secondary inhibition can also occur when sulfide precipitates metals and thus inhibits methanogenesis by depriving microorganisms of essential nutrients (Chen et al., 2008; Mountfort & Asher, 1979; Winfrey & Zeikus, 1977).

There are several methods for preventing H_2S production in AD. They include the addition of Fe^{3+} salts, the addition of sulfur scavenging microorganisms, adsorption with activated carbon systems, and the addition of oxygen into the digester (Appels et al., 2008; Barber & Mcquitty, 1977; Chen et al., 2008; Cirne, Van Der Zee, Fernandez-Polanco, & Fernandez-Polanco, 2008; Z. Song, Williams, & Edyvean, 2001). However, these methods can be expensive and inefficient or cause other side-effects (Peu et al., 2012). Hence, H_2S is typically scrubbed from the biogas rather than preventing its formation in the AD process (Choudhury, Shelford, Felton, Gooch, & Lansing, 2019; Peu et al., 2012).

The H_2S production can be studied in biochemical methane potential (BMP) tests. The BMP test is a controlled batch lab-scale digestion study whose purpose is to examine the CH_4 and

biogas production from a given substrate (Angelidaki et al., 2009). Though the BMP test usually focuses on CH_4 production, H_2S production can also be examined. Using the information from BMP tests, the H_2S production has been modeled based on the C : S ratio of the agricultural feedstocks (Peu et al., 2012).

However, connecting H_2S production only to the introduction of sulfur-rich substrates can oversimplify the other influences on H_2S production. For example, the presence of metals can influence the conversion of sulfur. High iron concentrations could precipitate sulfide, which could prevent the precipitation of other essential metals by microorganisms through secondary inhibition (Gupta, Flora, Sayles, & Suidan, 1994). However, metal concentrations can also inhibit H_2S production. Batch digester tests of dairy manure showed that iron and copper played a role in reducing H_2S concentrations in the biogas through sulfide-metal precipitation (Lin et al., 2017). This reduction in H_2S production was attributed to sulfide-metal precipitation. Additionally, the pH, COD : Sulfate, and sulfate concentrations can influence CH_4 inhibition and sulfate conversion to H_2S in AD (Guerrero, Chamy, Jeison, Montalvo, & Huiliñir, 2013; Vavilin, Vasiliev, Rytov, & Ponomarev, 1994). For example, the inhibition of sulfide on acetoclastic methanogenesis intensifies at acidic pH values (Koster, Rinzema, de Vegt, & Lettinga, 1986). Moreover, H_2S production in AD could be related to different types of feedstock (Belle, Lansing, Mulbry, & Weil, 2015).

The goal of this study is to improve understanding of H_2S production in lab-scale batch tests through identifying influential factors on H_2S production that can serve as indicators for potential digester inhibition. The specific objectives of the study were: 1.) Examining biogas production and digester liquid pH; 2.) Studying dynamic behaviors of H_2S production and digester liquid pH; and 3.) Determining influential factors for controlling H_2S production.

4.3 Materials and methods

4.3.1 Sources of substrate and inoculum

Field digesters for substrate and inoculum

Substrate and inoculum used in the experiment were collected from four industrial-scale digesters (Digesters F, B, L, and W) in Indiana State. Collections occurred at seven dates between January 2018 and November 2019 for seven laboratory tests (Table 4-1). The substrate and

inoculum were taken at different locations within the field digesters. After collection, they were transported to Purdue University and immediately used in the laboratory tests.

Table 4-1. Characteristics of the four industrial anaerobic digesters, and substrate and innoculum collections for laboratory tests.

Description	**Industrial anaerobic digester**			
	Digester F	**Digester B**	**Digester L**	**Digester W**
Digester design	Mixed plug flow	Mixed plug flow	Completely mixed	Completely mixed
Digester type	Agriculture	Agricultural co-digestion	WWTP	WWTP
Digester feedstock	Dairy manure slurry	Beef cattle manure, food waste, glycerin, industrial wastes, and biodiesel waste	WAS, PS	WAS, food waste, grease
Digester HRT (days)	15	28-32	15-30	ND
Digestion T (°C)	41.6	38.3	36	Mesophilic
Biogas production ($m^3\ d^{-1}$)	~34,000	~61,000	~1900	~1500
Collection date (m/d/y)	1/18/18	6/5/18, 8/9/18, 10/24/18, 2/18/19	5/17/19	11/15/19
Materials collected	DM, EF, EF-R	INF, DL-E, DL-W, EF-E, EF-W, EF-L	INF, EF	EF
Used in lab test (#)	1	2-5	6	7 (precipitation)

Note: WWTP = wastewater treatment plant; WAS = waste activated sludge; PS = primary sludge; ND = no data.

Digester F

Digester F was a mixed plug-flow digester treating dairy manure (DM) at mesophilic conditions (41.6°C) and a hydraulic retention time (HRT) of 15 days (Table 4-1). Digester F produced about 34,000 m^3 of biogas daily (Table 4-1). Three types of substrate and inoculum were collected in January 2018 from the influent that was mainly DM, digester effluent (EF) and effluent after solid separation and phosphorus recovery (EF-R).

Digester B

Digester B was also a mixed plug-flow design, consisting of three parallel and isolated digester bodies. It operated at 38.3°C and an HRT of 28-32 days and produced about 61,000 m^3 of biogas daily (Table 4-1). Digester B received beef cattle manure (~50%) with other co-digested materials including food waste, glycerin, industrial waste (IW), and biodiesel waste, resulting in

variable influent to the digester. Therefore it provided unique conditions to study the effect of different influent composition on the performance of AD. Effluent from Digester B was processed to remove solids and left a liquid portion of effluent (EF-L).

Substrate and inoculum were collected from Digester B at four dates on 6/5/18, 8/9/18, 10/24/18, and 2/18/19, and used in Tests 2, 3, 4, and 5, respectively. Digester B was reported as experiencing foaming at the first three collection times. Additionally, glycerin loads were reported as being reduced during the last collection.

Six types of materials were taken at different locations of the digester system. These materials were 1) digester influent (INF) in the equalization pit after feedstock mixing, 2) and 3) digester liquid in the middle of the east (DL-E) and west (DL-W) digesters, 4) and 5) digester effluent in the effluent pits of the east (EF-E) and west (EF-W) digesters, and 6) liquid fraction of digester effluent (EF-L) after solids removal using a roller press, slope screen, and centrifuge (Figure 4-1).

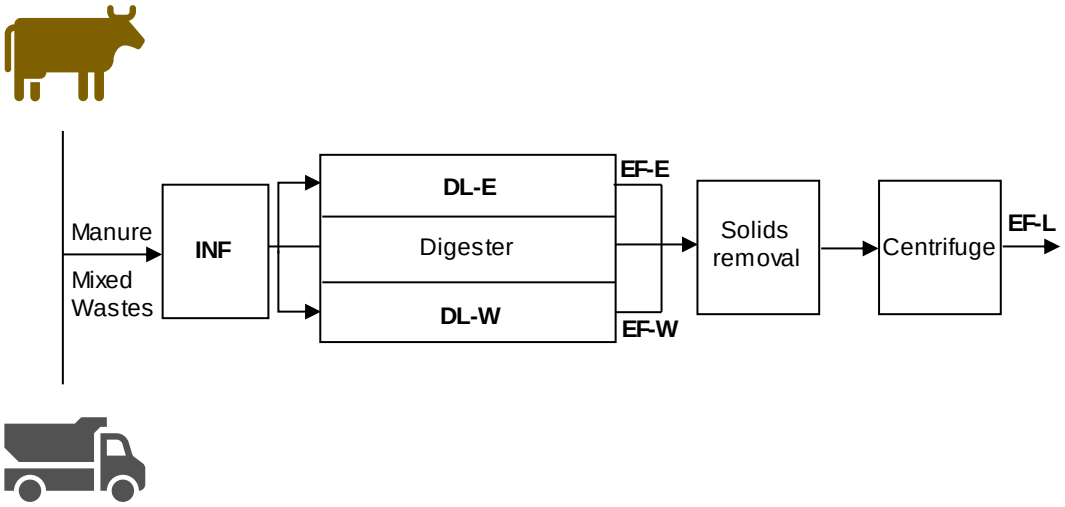

Figure 4-1. Overview of field digester sampling locations (in bold letters).

Digester L

Digester L was at a wastewater treatment plant (WWTP), operating at 36°C and an HRT of 15-30 days. It treated waste activated sludge (WAS) and primary sludge (PS) and produced about 1900 m^3 of biogas daily. Influent and effluent at Digester L were collected in May 2019 and used in lab Test 6.

Additionally, three types of dry and powdered cornstarch-based co-digestion wastes (identified as S1, S2, and S3) from the facility were used as the substrate for Test 6. Substrate SM (Table 4-2) was an equal mix by mass of S1, S2, and S3.

Digester W

Digester W was a mesophilic digester at another WWTP. It treated WAS and other co-digestion wastes, including food waste and grease, and produced about 1500 m^3 of biogas daily (Table 4-1). Substrate and inoculum were collected at Digester W in November 2019 and used in a precipitation test (Test 7).

4.3.2 Substrate and inoculum characterization

The substrate and inoculum were thoroughly characterized after collection (Day 0 of each test) to determine several chemical and physical parameters (Table A-1). The total chemical oxygen demand (TCOD), soluble chemical oxygen demand (SCOD), total volatile fatty acids (TVFAs), total alkalinity (TALK), total sulfate, total phosphorus (TP), Total Kjeldahl Nitrogen (TKN), Total Nitrogen (TN), inorganic N, iron, copper, and nickel were measured using TNTplus™ Vial test kits and a Hach DR3900 Benchtop Spectrophotometer (Hach Company, Loveland, CO). Other Hach test kits used in the lab tests included orthophosphate (OP) (Hach Orthophosphate Test Kit Model PO-19), tannic acid (Hach Method 8193), and TAN (Hach Method 8038).

The measurement of TS, fixed solids (FS), and volatile solids (VS) followed methods described in (APHA, 1999). A Jenco Digital pH Meter (Model 60 with Cole-Parmer electrode Cat No 05993-00) was used to measure pH. Conductivity was measured with a Hanna Instruments HI 9813-6N EC Meter.

Measurements necessitating particulate samples (pH, solids, conductivity, TCOD, sulfate, tannic acid, TAN, and TP) were thoroughly mixed with a magnetic stir bar to ensure consistency. Measurements requiring soluble samples were filtered with a cellulose acetate filter of either 0.2 μm (SCOD) or 0.45 μm (TKN, TVFA, TALK, OP, Fe, Cu, Ni) (Table A-1). Soluble samples were filtered with either a 0.2 μm cellulose acetate filter or a 0.45 μm cellulose acetate μm filter. Dilutions were performed on a g g^{-1} basis.

4.3.3 Lab-digester set-up

The laboratory tests were conducted in customized digesters. For experiments involving materials from Digesters F and B (Tests 1 through 5), the digesters were made of 1000 mL (with 6.75 mm OD barb side outlet port) or 500 mL (with 6.35 mm OD barb side outlet port) flasks (Bomex borosilicate glass filtering flasks). The 1000 mL digesters was sealed with #10 rubber stoppers and the 500 mL digesters was sealed with #8 rubber stoppers.

A piece of pipe, cut from a 10 mL Falcon Pipet (#357551), was inserted through each rubber stopper and used as an operation port for sampling and measurement. When the digesters were sealed with the stoppers, the lower end of the pipe extended to below the digester liquid so the biogas produced in the digesters could not escape from the operation port. The side outlet port in the digester body was used as a biogas collection port. Two 500 mL gas bags in parallel were attached to the side outlet port using a Tee.

For experiments involving materials from Digesters L and W (Tests 6 and 7), the digesters were made of 1000 mL Corning polycarbonate square bottles. The original 45 mm screw cap of the bottles were replaced with #8 rubber stoppers. In addition to the operation port, a biogas port was added by inserting a short piece of pipe, cut from a 2 mL polystyrene Falcon Pipet (#357507), through the stopper. The lower end of the pipe opened at the headspace of the digester to release the biogas. The top end of the pipe was connected to a 3-L or a 1-L Tedlar bag, depending on the biogas production rates during different stages of AD, to collect the biogas. To ensure air tightness, the pipes were sealed to the stopper using a silicone sealant.

4.3.4 Lab-digester operation

Immediately after loading the digesters with influent (the mixture of substrate, inoculum, and RO water when necessary), the digesters were randomly placed in several water baths (GEMMYCo Model YCW-010, and PolyScience Model WB28A11B). The temperatures of the water baths were controlled at 38.3°C ± 0.1 for Tests 1-5, and 7 and at 36°C ± 0.1 for Test 6. The tests were ended when the CH_4 daily production was less than 1% of its cumulative production.

The biogas volume and composition were measured for the first three days daily, and then at intervals of no more than three days until the end of the tests. Before detaching from the

digesters, the gas bags were sealed with metal screw clamps (16 mm x 19 mm). The bags were immediately replaced with new bags.

The volumes of biogas in the bags were measured using a custom-made device and a 200 mL syringe (SEALY Model VS 404). All biogas volumes were converted to Standard Temperature and Pressure (1 atm, 0°C) before data processing. Biogas compositions were measured with a 5000 Gas Analyzer (LANDTEC North America, Inc., Colton, CA), which has detection ranges of CH_4 (0-100%); CO_2 (0-100%); O_2 (0-25%), and H_2S (0-10,000 ppm). The specific methane yield (SMY) was calculated by dividing the final cumulative CH_4 volume by the grams of the initial volatile solids.

The pH of the digester liquid was measured through the operation port using a Jenco Model 60 Digital pH meter (Cole-Parmer electrode Cat No 05993-00) on the same days when the biogas volume and concentration were measured. The liquid in the digesters were thoroughly mixed with a magnetic stir bar before pH measurement.

4.3.5 BMP tests

Tests 1 through 6 were regular BMP tests that were conducted with different combinations of substrate and inoculum (Table 4-2). The substrate included DM, EF-R, INL, and mixture of PS and WAS. The inoculum was either EF, EF-R, or DL to ensure the necessary microbial consortia for CH_4. Additionally, digesters with 100% inoculum to determine the activity of the different stages of the AD system were used. The DL from Digester B experienced foaming issues in Test 2 so, in subsequent tests, the DL was diluted with reverse osmosis (RO) water to 50% in the digesters.

The six BMP tests were all performed in triplicate, except for blanks which were in duplicate. For each test, a "blank" control with inoculum and water was used to determine the production of CH_4 from the inoculum.

The SMY was calculated by dividing the final cumulative CH_4 volume by the grams of the initial volatile solids.

Table 4-2. Sample collection location and % volume of materials loaded in each lab-digester in each batch of collected materials (lab-digester group No.).

Field digester	Lab- digester group No.	RO water (% V)	Substrate (% V)	Inoculum (% V)
F	1-1	0	DM (100)	0
F	1-2	0	DM (90)	EF (10)
F	1-3	0	0	EF-R (100)
F	1-4	0	EF-R (90)	EF (10)
F	1-5	0	0	EF (100)
F	1-6**	90	0	EF (10)
B	2-7	0	INL (90)	EF (10)
B	2-8	0	INL (90)	DL-W (10)
B	2-9*	0	0	DL-W (100)
B	2-10	0	0	EF-W (100)
B	2-11**	90	0	EF-W (10)
B	2-12**	90	0	DL-W (10)
B	3-13	0	INL (90)	EF-W (10)
B	3-14	0	INL (90)	DL-W (10)
B	3-15	0	0	EF-W (100)
B	3-16	50	0	DL-W (50)
B	3-17**	90	0	EF-W (10)
B	3-18**	90	0	DL-W (10)
B	4-19	0	INL (80)	EF-W (20)
B	4-20	50	0	DL-W (50)
B	4-21	50	0	DL-E (50)
B	4-22	0	0	EF (100)
B	4-23**	80	0	EF-W (20)
B	5-24	0	INL (80)	EF-W (20)
B	5-25	50	0	DL-W (50)
B	5-26	50	0	DL-E(50)
B	5-27	0	0	EF (100)
B	5-28**	0	0	EF-W (20)
L	6-29	0	PS+ WAS mix (33.3)+Cellulose (0.02)	EF (66.7)
L	6-30	0	PS+WAS mix (33.3)	EF (66.7)
L	6-31	13.3	PS+ WAS mix (28.7)+S1 (0.7%)	EF (57.3)
L	6-32	23.4	PS+WAS mix (25.1)+S1 (1.3)	EF (50.2)
L	6-33	31.2	PS+WAS mix (22.4)+S1 (1.7)	EF (44.7)
L	6-34	11.3	PS+WAS mix (29.4)+S2 (0.7)	EF (58.7)
L	6-35	27.3	PS+WAS mix (23.7)+S2 (1.6)	EF (47.4)
L	6-36	12.7	PS+WAS mix (28.9)+S3 (7)	EF (57.7)
L	6-37	22.4	PS+WAS mix (25.5)+S3 (1.2)	EF (50.9)
L	6-38	30.0	PS+WAS mix (22.8)+S3 (1.6)	EF (45.6)
L	6-39	14.3	PS+WAS mix (28.3)+SM (0.8)	EF (56.6)
L	6-40	1.4	PS+WAS mix (24.6)+SM (1.4)	EF (49.2)
L	6-41	33	PS+WAS mix (21.7)+SM (1.8)	EF (43.5)
L	6-42	48.9	PS+WAS mix (16.1)+SM (2.7)	EF (32.3)
L	6-43	23.5	PS+WAS mix (24.6)+SM (2.8)	EF (49.2)
L	6-44	0	0	EF (100)
L	6-45	0	PS+WAS mix (80)	EF (20)

*Each digester group contains 3 individual digesters, except for blanks which contain 2. * Digesters in this group foamed over during the experiment and were removed. **Digesters in this group were blanks. DL = digester liquid, DM = dairy manure, EF = effluent, EF-R = effluent with phosphorus and solids recovered, PS = primary sludge, WAS = waste activated sludge.*

4.3.6 Precipitation tests

Based on the results of Tests 1 through 6, an experiment was designed to gain more insight into the role of iron, phosphorus, and sulfide in AD. Ferric chloride hexahydrate (VWR analytical) was the iron source, phosphoric acid 85% (Mallinckrodt Chemicals) was the phosphorus source, and sodium sulfide nonahydrate (ACS, 98.0% min, Crystalline, Na_2S $9H_2O$, Alfa Aesar) was the sulfide source. The inoculum was obtained from Digester W as described in the previous section 4.3.1. The inoculum was 10% of the volume in the 1 L working volume used. The digester set-up was described in the previous sections 4.3.3 and 4.3.4.

The conditions of this test were selected to be similar to conditions in Tests 1 through 6. To test FeS precipitation, the sulfide concentration was limiting since sulfide concentrations were naturally limiting in the previous BMP tests. To test $Fe_3(PO_4)_2$, formation, Fe was limiting as that was what occurred in the previous BMP batch tests. The experimental set-up is described in more detail in Table 4-3. Additionally, on Day 0, each digester received 3 grams of sodium bicarbonate (Mallinckrodt Chemicals) and 0.001 gram of resazurin sodium salt (Thermo Fisher Scientific) as a buffer and oxygen indicator, respectively. Each treatment was performed in duplicate. Biogas volume and pH were measured at intervals of no less than 2 days and the gas concentrations were measured as needed using methods described in section 4.3.4.

Table 4-3. The experimental design of the precipitation tests.

Treatment	**Ferric Chloride (g)**	**Sodium Sulfide (g)**	**Phosphoric Acid (mL)**	**Inoculum (g)**
Fe Reduction + Inoculum	0.5809			100
Fe Reduction	0.5809			
Fe Reduction+ FeS Precipitation + Inoculum	0.5809	0.2434		100
Fe Reduction +FeS Precipitation	0.5809	0.2434		
Fe-P Precipitation + Inoculum	0.5809		0.7205	100
Fe-P Precipitation	0.5809		0.7205	
Inoculum only				100

4.3.7 Data analysis

Result data

The tests resulted in data that included characterizations of the lab-digester liquid (Tables A-2 through A-5), the final specific H_2S production calculations (Table 4-4), the H_2S and pH time series data, and the qualitative variables of the substrate and the inoculum (substrate type, collection date, location, inoculum, foaming). Numerical calculations, statistics, and modeling were performed in Microsoft Excel and R version 3.6.3 (2020-02-29) (x86_64-w64-mingw32/x64 (64-bit)).

Calculations

To have a uniform comparison between the different digesters, the final specific H_2S production (FSP) was calculated using Eq. (4-1):

$$FSP = \frac{\sum_{i=1}^{n} C_{H_2S,i} \cdot V_{Biogas,i}}{1000 \cdot W_{VS}} \quad (4\text{-}1)$$

where FSP is the final specific H_2S production, mL g VS^{-1}; C_{H2S} is the concentration of H_2S in the biogas, ppm; V_{Biogas} is the volume of the biogas, L; W_{VS} is the initial weight of VS fed into the digester, g; *n*, is the number of biogas collections during the test; and *i* is *i*th collection of biogas produced from the digester. Eq (4-1) was modified from calculations for the SMY from the batch digestion tests.

The concentration of H_2S in the liquid phase was calculated using Henry's Law and the related coefficients from the literature (Isa, Grusenmeyer, & Vestraete, 1986; Lawrence, McCarty, & Guerin, 1964). Using Henry's law, the total dissolved sulfide concentration (TDS) was calculated from the H_2S concentration measured in the biogas during the lab-digester tests as shown in Eq. (4-2):

$$[H_2S]_l = \alpha[H_2S]_g \quad (4\text{-}2)$$

where α is the absorption coefficient which is 1.73 at 38.3°C and 1.80 at 36.0°C and H_2S concentrations are expressed in moles per liter of liquid and moles per liter of gas, respectively.

The theoretical partition of H_2S between the gas and liquid phases of the digester were calculated based on the measured pH and H_2S concentrations using Eq. (4-3):

$$\boldsymbol{f}=\left(1+\frac{\mathrm{K}_d}{10^{-\mathrm{pH}}}\right)^{-1} \quad (4\text{-}3)$$

where f is the fraction of free H_2S gas to TDS ($H_2S(l)$ + HS^- + S^{2-}) and K_d is the equilibrium dissociation constant for H_2S which was 1.639 x 10^{-7} at 38.3°C and 1.535 x 10^{-7} at 36.0°C (Isa et al., 1986; Lawrence et al., 1964).

The total dissolved sulfide (TDS) concentration was calculated using the concentration of H_2S in the liquid and the pH in Eq. (4-4) (Isa et al., 1986; Lawrence et al., 1964).

$$TDS = \frac{[K_d][H_sS(l)]}{10^{-pH}} + [H_2S(l)] \quad (4\text{-}4)$$

The COD removal by SRB was calculated from the initial and final TCOD and sulfate concentrations as shown in Eq (4-5) (Guerrero et al., 2013).

$$COD\text{removal by SRB} = \frac{0.67 * \left[SO^{-2}_{4,\text{initial}} - SO^{-2}_{4,\text{final}}\right]}{COD_{i\,n\text{tial}}} \quad (4\text{-}5)$$

Regression analysis

Different regression analyses were performed on the data. Ridge, LASSO (Least Absolute Shrinkage and Selection Operator), and partial least squares (PLS) regression was performed in Rstudio. Ridge, LASSO, and PLS regression can be used for data which displays multicollinearity. The package FactomineR was used to develop a multiple linear regression model of qualitative characteristics (substrate type, collection date, location, inoculum, foaming) on the final specific H_2S production data. Pearson and spearman correlation tests between the FSPs and initial characterizations were also performed using the cor() function in Rstudio.

Statistical tests

The data from the precipitation tests were analyzed using statistical tests. Due to the small sample sizes ($n < 30$) for each treatment in the precipitation test, the data was first tested for normality using the Shapiro-Wilk test, which is a commonly used normality test and is

recommended for smaller sample sizes (Ghasemi & Zahediasl, 2012). If the data was not normally distributed ($P < .05$), then a Wilcoxon signed-rank test was applied. If the data was normally distributed, then a paired *t*-test was applied. Both the Wilcoxon signed-rank test and the paired *t*-test are commonly used analyses for data in which there are two independent variables (Date, Treatment) and one dependent variable (Fe). They are commonly used to determine differences between "before" and "after" data from different treatments (McDonald, 2014). The *P* values were corrected with a Bonferroni correction method, which is popular and the most conservative *P* values correction method (Jafari & Ansari-Pour, 2019).

Model development

Local Regression (loess) and Generalized Additive Model (gam) were used for modeling the final specific H_2S productions (S. Wood, 2011; S. N. Wood, 2004). The models were developed using RStudio package mcgv (S. N. Wood, 2001). Loess is a non-parametric method that uses data points of less than 1000 to predict the local y value through fitting multiple regressions in a local neighborhood of numerical data. Gam uses nonlinear regression to fit local y values in a local neighborhood of numeric data and is a more generalized version of loess. The gam model is shown in Eq (4-6):

$$s(E((Y)) = \beta_0 + f_1(x_1) \dots f_m(x_m) \quad (4\text{-}6)$$

where β_0 is the intercept, f_m is the smoothing function, and s is the link function which was identity.

4.4 Results and discussion

4.4.1 Hydrogen sulfide production

Hydrogen sulfide production from 43 digester groups in the six tests showed a considerable variability (Table 4-4). The lowest specific H_2S productions ranged from non-detectable (Table 4-4, lab-digester group #1-6 that had 90% RO water) to 1.29 mL g VS^{-1} (#6-41). The lowest five lab-digester groups producing < 0.001 mL g VS^{-1} were those which tested either effluent from Digester F (#1-5) or diluted digester liquid from the middle of Digester B. The digesters that produced ≥ 0.2 mL H_2S g VS^{-1} were all from Test 6. These digesters also received co-digestion

substrate S1, or S2, or SM. Digester groups # 6-41 and 6-43 were the highest with 1.29 and 0.75 mL g VS^{-1}, respectively.

The time series of H_2S concentrations are shown in Figure 4-2. In most cases, the highest H_2S concentrations were observed within the first ten days of the experiments. Notably, the H_2S concentrations exceeded 1000 ppm in Tests 3, 5, and 6. In the lab, BMP digester operators should note that BMP tests can produce biogas with high H_2S concentrations. If the biogas has a large volume and leaks in the lab room air, it could pose a potential risk and the room air should be vented accordingly.

Table 4-4. Specific hydrogen sulfide productions from 43 digester groups in the six tests.

FD-T-LD	Substrate (% V)	Inoculum (% V)	RO water (% V)	H_2S production (mL g VS^{-1})
F-1-1	DM (100)			0.01 ± 0.0052
F-1-2	DM (90)	EF (10)		0.012 ± 0.0055
F-1-3		EF-R (100)		0.0033 ± 0.0021
F-1-4	EF-R (90)	EF (10)		0.0029 ± 0.0022
F-1-5		EF (100)		4e-04 ± NA
F-1-6		EF (10)	(90)	NA
B-2-7	INL (90)	EF (10)		0.003 ± 0.0012
B-2-8	INL (90)	DL-W (10)		0.0038 ± 0
B-2-9*		DL-W (100)		
B-2-10		EF-W (100)		0.40 ± 0.80
B-2-11		EF-W (10)	(90)	0.0045 ± NA
B-2-12		DL-W (10)	(90)	0.0035 ± 0.0031
B-3-13	INL (90)	EF-W (10)		0.0019 ± 0.0019
B-3-14	INL (90)	DL-W (10)		0.0011 ± 0.0015
B-3-15		EF-W (100)		0.0083 ± 0.011
B-3-16		DL-W (50)	(50)	6e-04 ± 7e-04
B-3-17		EF-W (10)	(90)	6e-04 ± 4e-04
B-3-18		DL-W (10)	(90)	8e-04 ± 8e-04
B-4-19	INL (80)	EF-W (20)		0.0054 ± NA
B-4-20		DL-W (50)	(50)	0.0027 ± 0.0021
B-4-21		DL-E (50)	(50)	0.0039 ± 0.0019
B-4-22		EF (100)		0.0028 ± 0.0029
B-4-23		EF-W (20)	80	9e-04 ± 0
B-5-24	INL (80)	EF-W (20)		0.025 ± 0.012
B-5-25		DL-W (50)	(50)	0.014 ± 0.0098
B-5-26		DL-E(50)	(50)	0.016 ± 0.0057
B-5-27		EF (100)		0.0026 ± 7e-04
B-5-28		EF-W (20)		0.0064 ± 0.0061
L-6-29	SL (33.3)+Cellulose (0.02)	EF (66.7)		0.080 ± NA
L-6-30	SL (33.3)	EF (66.7)		0.092 ± NA
L-6-31	SL (28.7)+S1 (0.7%)	EF (57.3)	(13.3)	0.20 ± 0.10
L-6-32	SL (25.1)+S1 (1.3)	EF (50.2)	(23.4)	0.30 ± NA
L-6-33	SL (22.4)+S1 (1.7)	EF (44.7)	(31.2)	
L-6-34	SL (29.4)+S2 (0.7)	EF (58.7)	(11.3)	0.074 ± NA

Table 4-4 continued.

FD-T-LD	Substrate (% V)	Inoculum (% V)	RO water (% V)	H_2S production (mL g VS^{-1})
L-6-35	SL (23.7)+S2 (1.6)	EF (47.4)	(27.3)	0.24 ± 0.053
L-6-36	SL (28.9)+S3 (7)	EF (57.7)	(12.7)	0.043 ± NA
L-6-37	SL (25.5)+S3 (1.2)	EF (50.9)	(22.4)	0.14 ± 0.12
L-6-38	SL (22.8)+S3 (1.6)	EF (45.6)	(30)	0.29 ± NA
L-6-39	SL (28.3)+SM (0.8)	EF (56.6)	(14.3)	0.040 ± NA
L-6-40	SL (24.6)+SM (1.4)	EF (49.2)	(1.4)	0.50 ± NA
L-6-41	SL (21.7)+SM (1.8)	EF (43.5)	(33)	1.29 ± NA
L-6-42	SL (16.1)+SM (2.7)	EF (32.3)	(48.9)	0.20 ± NA
L-6-43	SL (24.6)+SM (2.8)	EF (49.2)	(23.5)	0.75 ± 0.9933
L-6-44		EF (100)		0.10 ± NA
L-6-45	SL (80)	EF (20)		0.061 ± 0.048

Each digester group contains 3 individual digesters, except for blanks that contains 2. FD-T-LD = Field digester - Test number - Lab digester group number, DL = digester liquid, DM = dairy manure, EF = effluent, EF-R = effluent after solids removal and phosphorus recovery, SL = sludge, a mixture of primary sludge and waste activated sludge.

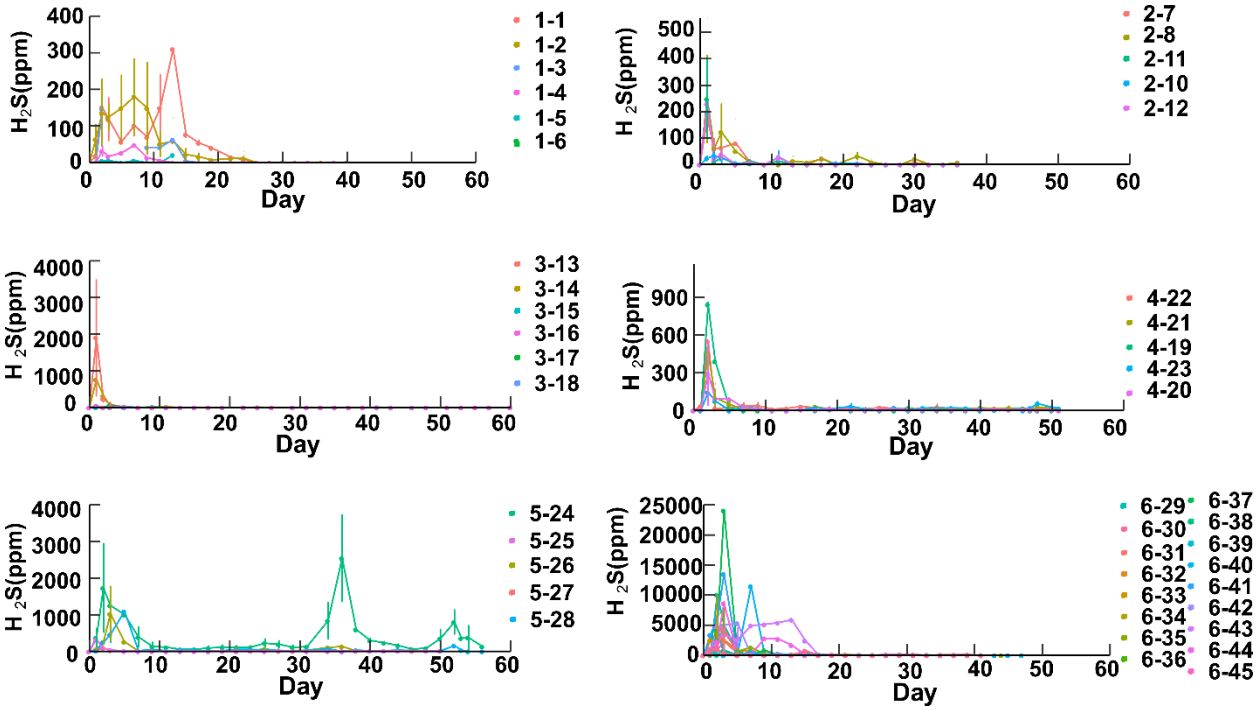

Figure 4-2. The average measured H_2S concentration (ppm) and standard deviation over time from the lab-digester groups.

4.4.2 Correlations between H_2S production and digester influent characteristics

Correlation calculation results showed that the most important influences on the final specific H_2S productions, disregarding those characteristics containing solids measurements, were the initial Fe(II) : S and OP concentrations (Table 4-5). Sulfate itself was not highly correlated

with the final specific H_2S productions, but its relation to iron was. Additionally, concentrations of the initial copper and different forms of nitrogen were correlated with H_2S production. Since the majority of H_2S was produced relatively early in the experiment (Figure 4-2), the initial concentrations of these metals and nutrients may have a complex effect on H_2S production.

Table 4-5. Correlation coefficients between the final specific H_2S productions and the day 0 digester influent characteristics.

Characteristic	Correlation Coefficient	Test	*P* value	Significance
FE(II) : S	-0.65	spearman	< .001	***
SCOD : TCOD	-0.63	spearman	< .001	***
TCOD : TKN	0.54	spearman	< .001	***
TCOD : TN : TP	0.54	spearman	< .001	***
SCOD	-0.52	spearman	< .001	***
OP	-0.52	spearman	< .001	***
Inorganic N	-0.50	spearman	< .001	***
TN	-0.48	spearman	< .001	***
TAN : TKN	0.46	spearman	< .001	***
TKN	-0.46	spearman	< .001	***
OP : TP	-0.46	spearman	< .001	***
Fe(II) : TP	0.35	spearman	< .001	***
Fe	0.34	spearman	.0011	**
TVFA	-0.32	pearson	.024	**
Cu	-0.22	pearson	.036	*
TAN	-0.22	pearson	.037	*
Conductivity	-0.15	spearman	.16	
Ni	0.14	spearman	.19	
TP	-0.11	spearman	.31	
Sulfate	-0.09	spearman	.39	
pH	-0.08	spearman	.43	
TALK	-0.08	pearson	.43	
TCOD : Sulfate	0.08	spearman	.47	
TVFA : TALK	-0.06	spearman	.58	
Tannic Acid	0.01	spearman	.91	

** P < .05, ** P < .01, *** P < .001*

TCOD to sulfate ratio and H_2S production

The TCOD : Sulfate ratios also varied among different lab-digesters. The digesters containing DM and DL (lab-digester group numbers 1-1, 1-2, 2-7, 2-8, 3-13, 3-14, 4-19, 5-24) had initial TCOD : Sulfate ratios greater than 10, suggesting that sulfide inhibition was unlikely from those particular digesters (Table A-4). Lab-digesters with an initial TCOD : Sulfate less than 10 included materials containing digester influent and liquid from field Digester B (lab-digester group numbers 3-15, 3-16, 4-21, 5-25, 5-26, 5-27) and lab-digester group numbers 6-29, 6-30, 6-45 from

field Digester L (Table A-4). The recorded pH for group numbers 6-29, 6-30, and 6-45 from Digester L, and 3-16 and 4-21 from Digester B were below neutral (Table A-4).

The TCOD : Sulfate ratio has been commonly used as an indicator for the likelihood of SRB and methanogen competition. After sulfate reduction, sulfide could present as H_2S in the gas phase and liquid phase. For wastewater, it has been suggested that a TCOD : Sulfate ratio below 10 would exceed the free H_2S concentration limit of 150 mg L^{-1} (Isa et al., 1986; Kalyuzhnyi, Fedorovich, Lens, Hulshoff Pol, & Lettinga, 1998). Other studies have cited 1.7 or 1 as ratios for SRB dominance in anaerobic digesters (Choi & Rim, 1991; McCartney & Oleszkiewicz, 1993). Overall, the TCOD : Sulfate ratio was generally a better predictor of TCOD removal than final specific H_2S productions.

TCOD destruction

The TCOD removal varied greatly between different substrate collection days and digester types (Figure 4-3). The majority of cases had TCOD removal by methanogenesis (Figure 4-3). The amount and type of TCOD destruction varied considerably. The digesters in Test 5 had some of the lowest TCOD removal rates, with rates of less than 22% (Table A-7) with the exception of lab-digester group number 5-28 (Figure 4-3). Lab-digester group number 5-28 was the blank and subsequently had a low initial TS concentration (12 g L^{-1}) compared to the other digesters in the test (34-138 g L^{-1}) (Table A-2). In the majority of tests, TCOD was removed by methanogenesis (Figure 4-3). However, the Test 5 cases had some of the highest percentages of COD removal by SRB, most likely attributed to the low initial TCOD : Sulfate ratio (Table A-4). These high removal rates did not result in particularly high FSP values (Table 4-4). However, there were relatively high concentrations of H_2S in the biogas from these Test 5 samples (Figure 4-2). Lab-digester group numbers 2-7, 2-8, and 2-10, had little TCOD removal and was even calculated as being negative (Table A-7) for methanogen removal. Minimal changes in the VS : TS ratio were observed in these digesters (Table A-5) and TCOD increased slightly (Table A-2). Most likely, there was minimal CH_4 production and solids conversion; when combined with laboratory error, this most likely resulted in this slight increase. Overall, the TCOD : Sulfate ratio was generally a better predictor of TCOD removal than final specific H_2S productions.

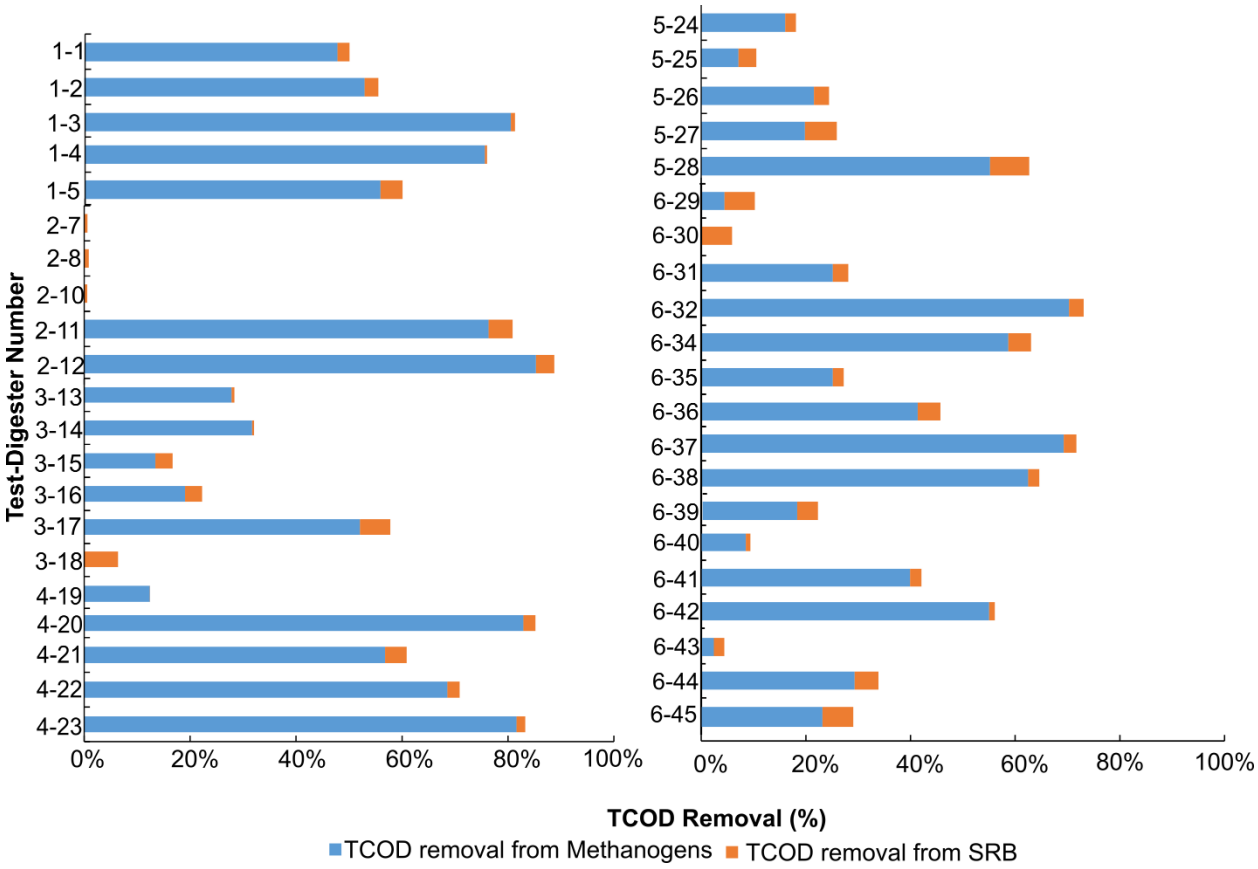

Figure 4-3. The average final percent TCOD removal by methanogens and sulfate-reducing bacteria (SRB) for each lab-digester group.

Iron and H_2S production

Increased FSP values were negatively correlated with Fe(II) : S ratios. Some of the highest FSP productions, such as in 6-38 and 6-43, had Fe(II) : S ratios that were 0 (Table A-5). Therefore, the relationships with iron and sulfur were examined further to uncover the mechanism of H_2S production.

The results of the change in digester liquid over the BMP test time are summarized in Table A-6. The analysis of the changes in concentrations over time identified that in 44% of cases, the iron concentrations increased over time (Table A-6). The iron measurements in this study were soluble (Table A-1). Since the majority of soluble iron was Fe(II), this increase in iron suggests that an iron reduction process was occurring (Figure 4-4). In the remaining cases, the iron concentration decreased over time. This suggests that an iron precipitation process occurred (Figure 4-4).

The two most common ways in which iron precipitation occurs in AD is through combining with sulfide or phosphorus. At below 0.1 g L^{-1}, Fe can release P; but at higher concentrations, Fe can react with PO_4^{3-} and form a precipitant (Yanchen Liu, Shi, Li, Hou, & He, 2011; Peng et al., 2014). Fe(II) will combine with sulfide to form FeS and will follow a pseudo-first order reaction when Fe(II) is limiting (Ya Liu et al., 2017). There was a possibility that in these batch tests, iron was most likely being reduced through FeS precipitation since the sulfate concentrations decreased in most cases (Table A-6).

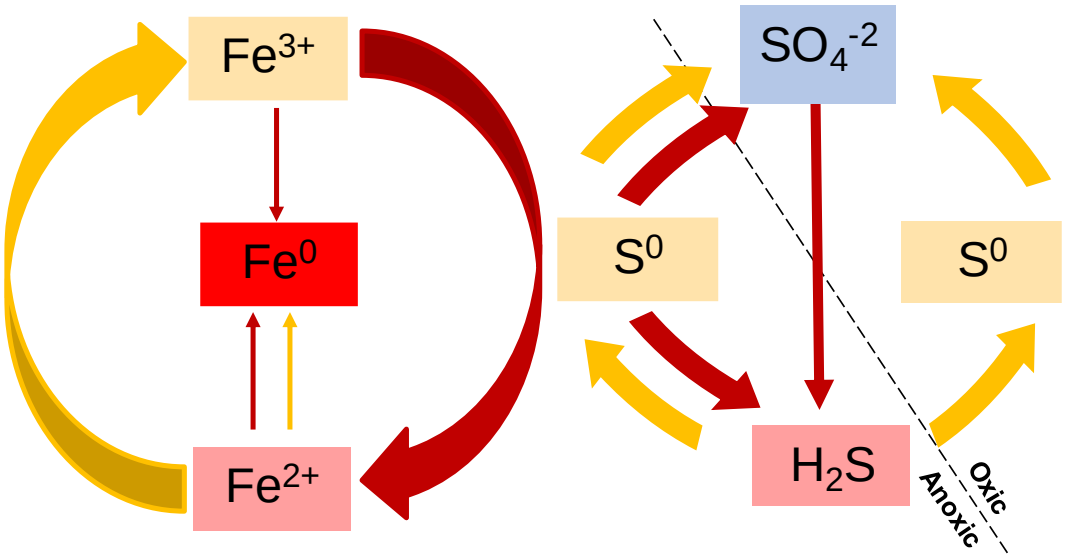

Adapted from (Madigan & Martinko, 2006).

Figure 4-4. Representation of the iron and sulfate cycles. Red arrows indicate reduction processes and yellow arrows indicate oxidation processes.

Initial sulfate concentration

Several important characteristics of sulfate were shown. Overall, the starting sulfate concentrations varied for different lab-digester group numbers from 0.57 g L^{-1} to 10.48 g L^{-1} (Table A-3). However, most starting concentrations exceeded 2 g L^{-1} (Table A-3). Notably, Test 5 had sulfate concentrations exceeding 4 g L^{-1} for lab-digester group numbers 5-24 through 5-27 (Table A-3). The H_2S concentration in the biogas exceeded 1000 ppm for lab-digester group numbers 5-24, 5-26, 5-28 (Figure 4-2). However, this did not necessarily result in high FSP values (Table 4-4). Influent sulfate concentrations in AD above 2 g SO_4^2 L^{-1} can result in high concentrations of undissociated H_2S and subsequent methanogenesis inhibition (Sarti, Pozzi, Chinalia, Ono, &

Foresti, 2010). In another study with a high rate anaerobic digester, sulfate toxicity was reported above 5 g L^{-1} (Isa et al., 1986). In this study, there were no significant correlations between initial sulfate concentration and the FSP value (Table 4-5). Therefore, there was no clear cut relationship between initial sulfate concentration and H_2S concentration.

pH and dynamics of H_2S production

Interactions between H_2S concentrations and pH were observed. When the pH was below 7, the fraction of H_2S gas produced was modeled to be higher (Figure 4-5). Additionally, in the case of Test 5, H_2S concentration demonstrated oscillations in H_2S production after Day 30 (Figure 4-2). Higher pH values, particularly in Test 4, corresponded with lower final specific H_2S productions (Table 4-4). Increases in H_2S concentrations have been shown to trigger a positive feedback loop with sulfate and acetate resulting in a subsequent decline in pH in chemostats (Fomichev & Vavilin, 1997; Vavilin et al., 1994). For example, methanogens and SRB may exhibit oscillating behavior for 5-20 days near system failure (Fomichev & Vavilin, 1997; Vavilin et al., 1994). Sulfate concentration and pH has been shown to affect SRB and methanogen concentrations (O'Flaherty, Mahony, O'Kennedy, & Colleran, 1998) which may be contributing to these oscillations.

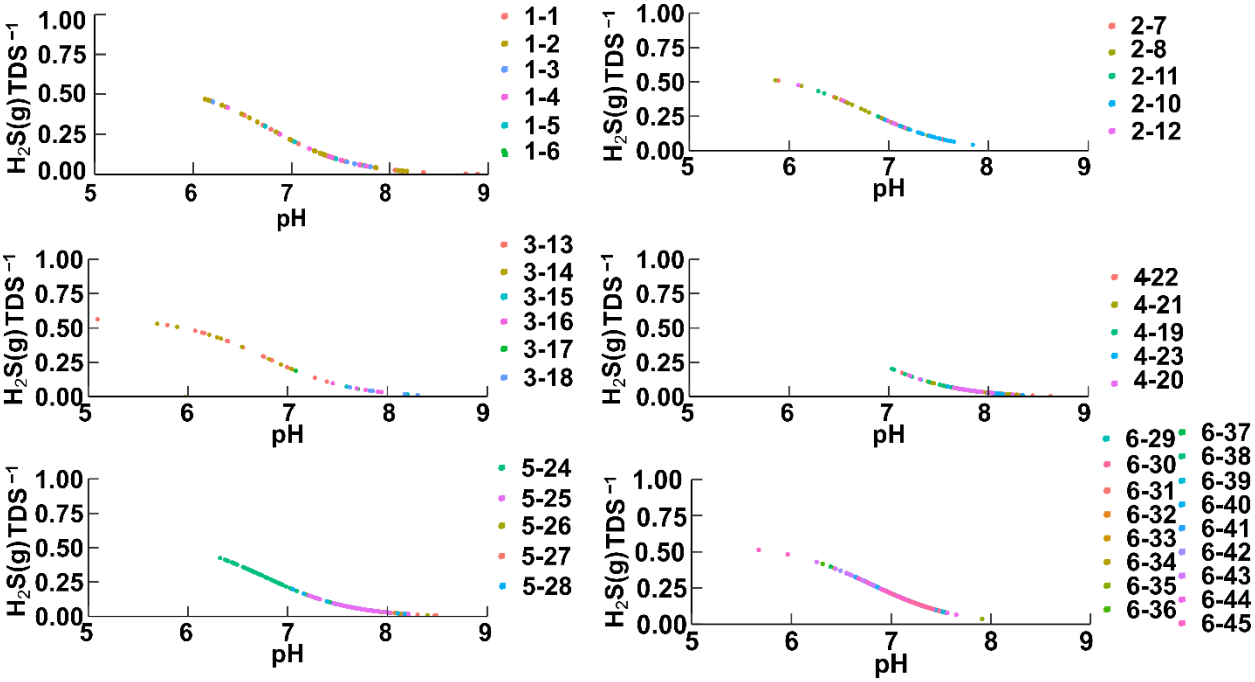

Figure 4-5. The average fraction of free H_2S gas to TDS versus pH for each lab-digester group.

4.4.3 Material collection locations on final specific H_2S productions

Several different types of regression analyses were performed (Table 4-6). None of the regression methods had R^2 values or root mean square error (RMSE) values which indicated a good fit. For the qualitative variables, location of the field digester where materials were collected was the most significant predictor of the final specific H_2S productions (Table 4-7). The adjusted R^2 value was still low (0.11) on this, however. Therefore, the data was fitted with a more complex model.

Table 4-6. Errors from PCA, PLS, Ridge, OLS, and Lasso regression analyses for the final specific H_2S production (mL g VS^{-1}).

	RMSE	**R^2**
pca	1.5	0.0086
PLS	1.9	0.0064
ridge	2.51	0.0005
ols	98.51	0.0005
lasso	0.72	0.0005

Table 4-7. FactoMine R results and significance.

	Intercept	**Field digester location**
Estimate	-0.095	0.12
Standard error	0.065	0.034
***t*-value**	-1.5	3.4
***P* value**	.15	.001
Significance		**

** P < .05, ** P < .01, *** P < .001*

4.4.4 Precipitation

The *t*-tests revealed significant changes in Fe(II), TP, and sulfate concentrations over the digestion period in the precipitation test (Table 4-8). When iron reduction was tested, the Fe(II) concentrations only significantly increased in the treatments without inoculum ($P = .026$) (Table 4-8, Table A-8). Phosphorus precipitation only occurred in treatments without inoculum. For example, total phosphorus concentrations significantly decreased ($P < .001$) in the phosphorus treatment without inoculum (Table 4-8, Table A-8). Sulfate precipitation was less clear. For example, sulfate significantly decreased in the FeS treatment ($P = .001$) with inoculum (Table 4-8, Table A-8). The soluble Fe concentration significantly ($P = .009$) increased in the FeS treatment

without inoculum but sulfate significantly increased (P = .029) (Table 4-8, Table A-8). Therefore, Fe-S precipitation appears to be mediated by the anaerobic community as it was not observed in the non-inoculum treatment.

Table 4-8. The P values and their significance from precipitation tests for the changes in Fe(II), TP, and sulfate concentrations between Day 0 and Day 26 for each treatment.

Treatment	**Fe (II)**	**TP**	**Sulfate**	**Treatment confirmed?**
Fe Reduction w Inoculum	.763	.047 *	<.001 ***	No
Fe Reduction w/o Inoculum	.026*	NA	NA	Yes
Fe Reduction+ FeS Precipitation w Inoculum	.18	0 ***	.003 **	Yes
Fe Reduction +FeS Precipitation w/o Inoculum	.009 **	NA	.029 *	Yes
Fe-P Precipitation w Inoculum	.053	<.001***	.001 **	Yes
Fe-P Precipitation w/o Inoculum	<.001 ***	<.001 ***	NA	Yes
Inoculum only	.535	.009 **	.002**	NA

* P < .05, ** P < .01, *** P < .001

The differences in Fe(II) concentrations between inoculum treatments (Table 4-8) suggests that the presence of the anaerobic community may prevent iron reduction, thereby explaining why iron reduction occurred less often in the previous batch tests. However, the anaerobic community did not seem to prevent Fe-P precipitation since phosphorus concentrations were observed to decrease in both the absence and presence of an anaerobic community (Table A-6). The anaerobic community appears to be necessary in the case of Fe-S precipitation as a decrease in sulfate concentration was not observed in the non-inoculum treatment (Table A-6). In other words, iron reduction and iron-phosphorus precipitation seem to occur without the presence of an anaerobic community, while FeS precipitation seems to require an anaerobic community.

Iron reduction was less likely to occur in the presence of an anaerobic microbial community, therefore, an iron-precipitation process was favored in the anaerobic community. The soluble concentrations of 0.20-16.0 mg L^{-1} Fe, 0.15-1.92 mg L^{-1} Co, and 0.05-0.40 mg L^{-1} for Ni are considered sufficient to prevent secondary inhibition by metal availability (G. F. Parkin, Lynch, Kuo, Van Keuren, & Bhattacharya, 1990). Ferrous and copper have been used to control H_2S concentrations in biogas from a batch digester containing dairy manure, but copper lost its effectiveness after 45 days and severely inhibited microbial activity (Lin et al., 2017). Therefore,

this is an explanation for the negative correlation with the Fe(II) S^{-1} ratio and the final specific H_2S productions (Table 4-5).

4.4.5 Modeling H_2S productions

The gam and loess models and their results are summarized in Table 4-9. Between the two models, the gam models had a better fit (Table 4-9). The gam model has the ability to fit the H_2S production even when the production curves vary considerably between tests (Figures A-1 through A-8). In most digesters, the H_2S production increased rapidly during the first ten days and then leveled off (Figures A.1 through A-8). Lab-digester group number 4-23, however, experienced a linear increase over time (Figure A-4). Lab-digester group number 3-15 experienced a drop due to one of the replicates being removed during the test (Figure A-3) and had lower goodness of fit values (Table 4-9).

The coefficients from the gam model can be obtained to predict H_2S production in future studies. Both gam and loess models have been used in environmental modeling (Thakur et al., 2018; S. N. Wood & Augustin, 2002) due to their ability to fit smooth curves to complex data. Overall, the initial increase in H_2S production during the first 10 days was the most challenging to model. The results benefitted from modeling processes which do not rely on comparative selection processes for defined models but, rather on smoothing processes with penalties (S. N. Wood, 2001).

There have been few studies modeling H_2S production kinetics from batch digester systems. The H_2S production in one mesophilic batch study was 0.76 mL g VS^{-1} for dairy manure and 2.23 mL g VS^{-1} for radish (Belle et al., 2015). The plot of the H_2S data (%) as a time series depicted initial increases in H_2S concentrations and then a decline starting after Day 1 (Belle et al., 2015). This increase then decline was attributed to the depletion of sulfate concentration in the digester (Belle et al., 2015). In this study, there were "spikes" of H_2S concentration (ppm) past day 10 (Tests 1, 5, 6) which were most likely attributed to low pH (Figure 4-2). In all digesters, there was sulfate at the end of the digestion period (Table A-3), so the depletion of sulfate is not an adequate explanation for H_2S decrease over time. Rather, the decline in H_2S production may indicate an adjustment of the digester to more favorable conditions for methanogenesis.

Table 4-9. Goodness of fit measurements from the gam and loess models for each lab-digester group.

Lab-digester group No.	R^2 (gam)	R^2 (loess)	RMSE (loess)	RMSE (gam)
1-1	1	0.99	0.00017	0.00014
1-2	1	14	0.00017	0.00014
1-3	0.96	0.91	0.00017	0.00014
1-4	0.98	0.97	0.00017	0.00014
1-5	0.97	0.97	0.00017	0.00014
2-7	0.93	0.81	0.00043	0.00025
2-8	0.93	0.83	0.00043	0.00025
2-10	0.99	0.92	0.00043	0.00025
2-11	0.82	0.59	0.00043	0.00025
2-12	0.89	0.69	0.00043	0.00025
3-13	0.54	0.35	5.75E-05	2.40E-05
3-14	0.59	0.38	5.75E-05	2.40E-05
3-15	0.85	0.40	5.75E-05	2.40E-05
3-16	0.96	0.80	5.75E-05	2.40E-05
3-17	0.94	0.83	5.75E-05	2.40E-05
3-18	0.96	0.85	5.75E-05	2.40E-05
4-19	0.91	0.74	0.00020	8.57E-05
4-20	0.98	0.90	0.00020	8.57E-05
4-21	0.96	0.83	0.00020	8.57E-05
4-22	0.98	0.95	0.00020	8.57E-05
4-23	0.99	0.96	0.00020	8.57E-05
5-24	0.97	0.91	0.0016	0.0012
5-25	0.77	0.58	0.0016	0.0012
5-26	0.96	0.85	0.0016	0.0012
5-27	0.96	0.84	0.0016	0.0012
5-28	0.98	0.91	0.0016	0.0012
6-29	0.92	0.84	0.011	0.0055
6-30	0.94	0.75	0.011	0.0055
6-31	0.97	0.94	0.011	0.0055
6-32	0.88	0.70	0.011	0.0055
6-34	0.94	0.81	0.011	0.0055
6-35	0.90	0.66	0.011	0.0055
6-36	0.90	0.69	0.011	0.0055
6-37	0.95	0.82	0.011	0.0055
6-38	0.92	0.79	0.011	0.005
6-39	0.93	0.75	0.011	0.0055
6-40	0.83	0.64	0.011	0.0055
6-41	0.98	0.83	0.011	0.0055
6-42	0.92	0.87	0.011	0.0055
6-43	0.99	0.95	0.011	0.0055
6-44	0.93	0.88	0.011	0.0055
6-45	0.95	0.84	0.011	0.0055

4.5 Conclusions

The following conclusions were drawn from this chapter:

1. Hydrogen sulfide production showed a considerable variability, ranging from non-detectable to 1.29 mL g VS^{-1}. Higher H_2S concentrations in the produced biogas were observed within the first ten days of AD.
2. There were no significant correlations between the initial sulfate concentrations and the final specific H_2S productions.
3. Another commonly cited indicator of final specific H_2S production, *i.e.*, TCOD : Sulfate ratio, was not shown as a reliable predictor. This ratio was generally a better indicator of TCOD removal than H_2S production.
4. The most important influences on the final specific H_2S productions were the initial Fe(II) : S ratio and OP concentrations. Sulfate, phosphorus, and iron in the anaerobic microbial community were important for the understanding of H_2S production.
5. Iron reduction and iron-phosphorus precipitation seemed to occur without the presence of an anaerobic community, whereas FeS precipitation seemed to require an anaerobic community.
6. The gam model could be applied to model the H_2S production for a variety of different substrate types with high R^2 values.

4.6 References

Angelidaki, I., Alves, M., Bolzonella, D., Borzacconi, L., Campos, J. L., Guwy, A. J., … van Lier, J. B. (2009). Defining the biomethane potential (BMP) of solid organic wastes and energy crops: A proposed protocol for batch assays. *Water Science and Technology*, *59*(5), 927–934. https://doi.org/10.2166/wst.2009.040

APHA. (1999). *Standard Methods for the Examination of Water and Wastewater*. (L. S. Clescerl, A. E. Greenberg, A. D. Eaton, & M. A. H. Franson, Eds.) (20th ed.). Washington D.C.: Amer Public Health Assn; American Water Works Assn; Water Environment Federation.

Appels, L., Baeyens, J., Degrève, J., & Dewil, R. (2008). Principles and potential of the anaerobic digestion of waste-activated sludge. *Progress in Energy and Combustion Science*, *34*(6), 755–781. https://doi.org/10.1016/j.pecs.2008.06.002

Barber, E. M., & Mcquitty, J. B. (1977). Chemical Control of Hydrogen Sulfide From Anaerobic Swine Manure. II. Oxidizing Agents. *Canadian Agricultural Engineering*, *19*(1), 15–19.

Barrera, E. L., Spanjers, H., Dewulf, J., Romero, O., & Rosa, E. (2013). The sulfur chain in biogas production from sulfate-rich liquid substrates: A review on dynamic modeling with vinasse as model substrate. *Journal of Chemical Technology and Biotechnology*, *88*(8), 1405–1420. https://doi.org/10.1002/jctb.4071

Belle, A. J., Lansing, S., Mulbry, W., & Weil, R. R. (2015). Methane and hydrogen sulfide production during co-digestion of forage radish and dairy manure. *Biomass and Bioenergy*, *80*, 44–51. https://doi.org/10.1016/j.biombioe.2015.04.029

Chen, Y., Cheng, J. J., & Creamer, K. S. (2008). Inhibition of anaerobic digestion process: A review. *Bioresource Technology*, *99*(10), 4044–4064. https://doi.org/10.1016/j.biortech.2007.01.057

Choi, E., & Rim, J. M. (1991). Competition and inhibition of sulfate reducers and methane producers in anaerobic treatment. *Water Science and Technology*, *23*(7–9), 1259–1264.

Choudhury, A., Shelford, T., Felton, G., Gooch, C., & Lansing, S. (2019). Evaluation of Hydrogen Sulfide Scrubbing Systems for Anaerobic Digesters on Two U.S. Dairy Farms. *Energies*, *12*, 4605.

Cirne, D. G., Van Der Zee, F. P., Fernandez-Polanco, M., & Fernandez-Polanco, F. (2008). Control of sulphide during anaerobic treatment of S-containing wastewaters by adding limited amounts of oxygen or nitrate. *Reviews in Environmental Science and Biotechnology*, *7*(2), 93–105. https://doi.org/10.1007/s11157-008-9128-9

EPA. (2020). *Inventory of U.S. Greenhouse Gas Emissions and Sinks*.

Fomichev, A. O., & Vavilin, V. A. (1997). The reduced model of self-oscillating dynamics in an anaerobic system with sulfate-reduction. *Ecological Modelling*, *95*(2–3), 133–144. https://doi.org/10.1016/S0304-3800(96)00041-5

Ghasemi, A., & Zahediasl, S. (2012). Normality tests for statistical analysis: A guide for non-statisticians. *International Journal of Endocrinology and Metabolism*, *10*(2), 486–489. https://doi.org/10.5812/ijem.3505

Guerrero, L., Chamy, R., Jeison, D., Montalvo, S., & Huiliñir, C. (2013). Behavior of the anaerobic treatment of tannery wastewater at different initial pH values and sulfate concentrations. *Journal of Environmental Science and Health - Part A Toxic/Hazardous Substances and Environmental Engineering*, *48*(9), 1073–1078. https://doi.org/10.1080/10934529.2013.773827

Gupta, A., Flora, J. R. V., Sayles, G. D., & Suidan, M. T. (1994). Methanogenesis and sulfate reduction in chemostats-II. Model development and verification. *Water Research*, *28*(4), 795–803. https://doi.org/10.1016/0043-1354(94)90086-8

Harada, H., Uemura, S., & Momonoi, K. (1994). Interaction between sulfate-reducing bacteria and methane-producing bacteria in UASB reactors fed with low strength wastes containing different levels of sulfate. *Water Research*, *28*(2), 355–367. https://doi.org/10.1016/0043-1354(94)90273-9

Harper, S. R., & Pohland, Frederick, G. (1986). Recent developments in hydrogen management during anaerobic biological wastewater treatment. *Biotechnology and Bioengineering*, *28*, 585–602. https://doi.org/10.1007/Bfb0000691

Isa, Z., Grusenmeyer, S., & Vestraete, W. (1986). Sulfate reduction relative to methane production in high-rate anaerobic digestion: Technical aspects. *Applied and Environmental Microbiology*, *51*(3), 572–579.

Jafari, M., & Ansari-Pour, N. (2019). Why, when and how to adjust your P values? *Cell Journal*, *20*(4), 604–607. https://doi.org/10.22074/cellj.2019.5992

Kalyuzhnyi, S., Fedorovich, V., Lens, P., Hulshoff Pol, L., & Lettinga, G. (1998). Mathematical modelling as a tool to study population dynamics between sulfate reducing and methanogenic bacteria. *Biodegradation*, *9*(3–4), 187–199.

Koster, I. W., Rinzema, A., de Vegt, A. L., & Lettinga, G. (1986). Sulfide inhibition of the methanogenic activity of granular sludge at various pH-levels. *Water Research*, *20*(12), 1561–1567. https://doi.org/10.1016/0043-1354(86)90121-1

Lawrence, A. W., McCarty, P. L., & Guerin, F. J. A. (1964). Effects of sulfides on anaerobic treatment. In *Proceedings of the nineteenth Industrial Waste Conference* (pp. 343–357). West Lafayette, IN: Purdue University.

Lin, H., King, A., Williams, N., & Hu, B. (2017). Hydrogen sulfide removal via appropriate metal ions dosing in anaerobic digestion. *Environmental Progress and Sustainable Energy*, *36*(5), 1405–1416. https://doi.org/10.1002/ep.12587

Liu, Ya, Zhang, Z., Bhandari, N., Dai, Z., Yan, F., Ruan, G., … Tomson, M. B. (2017). New Approach to Study Iron Sulfide Precipitation Kinetics, Solubility, and Phase Transformation. *Industrial and Engineering Chemistry Research*, *56*(31), 9016–9027. https://doi.org/10.1021/acs.iecr.7b01615

Liu, Yanchen, Shi, H., Li, W., Hou, Y., & He, M. (2011). Inhibition of chemical dose in biological phosphorus and nitrogen removal in simultaneous chemical precipitation for phosphorus removal. *Bioresource Technology*, *102*(5), 4008–4012. https://doi.org/10.1016/j.biortech.2010.11.107

Madigan, M. T., & Martinko, J. M. (2006). *Brock Biology of Microorganisms*. (G. Carlson, Ed.) (11th ed.). Upper Saddle River: Prentice Hall.

McCartney, D. M., & Oleszkiewicz, J. A. (1993). Competition between methanogens and sulfate reducers: effect of COD:sulfate ratio and acclimation. *Water Environment Research*, *65*(5), 655–664. https://doi.org/10.2175/wer.65.5.8

McDonald, J. H. (2014). *Handbook of Biological Statistics* (3rd ed.). Baltimore, Maryland: Sparky House Publishing.

Moestedt, J., Nilsson Påledal, S., & Schnürer, A. (2013). The effect of substrate and operational parameters on the abundance of sulphate-reducing bacteria in industrial anaerobic biogas digesters. *Bioresource Technology*, *132*(May 2014), 327–332. https://doi.org/10.1016/j.biortech.2013.01.043

Mountfort, D. O., & Asher, R. A. (1979). Effect of inorganic sulfide on the growth and metabolism of Methanosarcina barkeri strain DM. *Applied and Environmental Microbiology*, *37*(4), 670–675. https://doi.org/10.1128/aem.37.4.670-675.1979

NREL. (2013). *Biogas Potential in the United States (Fact Sheet)*. *Related Information: Energy Analysis, NREL (National Renewable Energy Laboratory)*. Golden, CO. https://doi.org/10.2172/1097303

O'Flaherty, V., Mahony, T., O'Kennedy, R., & Colleran, E. (1998). Effect of pH on growth kinetics and sulphide toxicity thresholds of a range of methanogenic, syntrophic and sulphate-reducing bacteria. *Process Biochemistry*, *33*(5), 555–569. https://doi.org/10.1016/S0032-9592(98)00018-1

Omil, F., Méndez, R., & Lema, J. M. (1995). Anaerobic treatment of saline wastewaters under high sulphide and ammonia content. *Bioresource Technology*, *54*(3), 269–278. https://doi.org/10.1016/0960-8524(95)00143-3

OSHA. (n.d.). Hydrogen Sulfide. https://doi.org/10.1016/B978-0-12-386454-3.00513-3

Oude Elferink, S. J. W. H., Visser, A., Hulshoff Pol, L. W., & Stams, A. J. M. (1994). Sulfate reduction in methanogenic bioreactors. *FEMS Microbiology Reviews*, *15*(2–3), 119–136. https://doi.org/10.1111/j.1574-6976.1994.tb00130.x

Parkin, B. G. F., & Owen, W. F. (1987). Fundamentals of anaerobic digestion of wastewater sludges. *Journal of Environmental Engineering*, *112*(5), 867–920.

Parkin, G. F., Lynch, N. A., Kuo, W.-C., Van Keuren, E. L., & Bhattacharya, S. K. (1990). Interaction between acetate fed sulfate reducers and methanogens. *Research Journal of the Water Pollution Control Federation*, *62*(6), 780–788. https://doi.org/10.1016/0043-1354(95)00238-3

Peng, S. C., Xue, J., Shi, C. B., Wang, J., Chen, T. H., & Yue, Z. B. (2014). Iron-enhanced anaerobic digestion of cyanobacterial biomass from Lake Chao. *Fuel*, *117*(PART A), 1–4. https://doi.org/10.1016/j.fuel.2013.09.006

Peu, P., Picard, S., Diara, A., Girault, R., Béline, F., Bridoux, G., & Dabert, P. (2012). Prediction of hydrogen sulphide production during anaerobic digestion of organic substrates. *Bioresource Technology*, *121*, 419–424. https://doi.org/10.1016/j.biortech.2012.06.112

Rasi, S., Läntelä, J., & Rintala, J. (2011). Trace compounds affecting biogas energy utilisation - A review. *Energy Conversion and Management*, *52*(12), 3369–3375. https://doi.org/10.1016/j.enconman.2011.07.005

Sarti, A., Pozzi, E., Chinalia, F. A., Ono, A., & Foresti, E. (2010). Microbial processes and bacterial populations associated to anaerobic treatment of sulfate-rich wastewater. *Process Biochemistry*, *45*(2), 164–170. https://doi.org/10.1016/j.procbio.2009.09.002

Song, Z., Williams, C. J., & Edyvean, R. G. J. (2001). Coagulation and anaerobic digestion of tannery wastewater. *Process Safety and Environmental Protection*, *79*(January), 23–28. https://doi.org/https://doi.org/10.1205/095758201531103

Thakur, M. P., Reich, P. B., Hobbie, S. E., Stefanski, A., Rich, R., Rice, K. E., … Eisenhauer, N. (2018). Reduced feeding activity of soil detritivores under warmer and drier conditions. *Nature Climate Change*, *8*(1), 75–78. https://doi.org/10.1038/s41558-017-0032-6

U.S. EPA. (2020). Potential for Anaerobic Digestion on Livestock Farms in the United States. Retrieved April 15, 2020, from https://www.epa.gov/agstar/agstar-data-and-trends#adpotential

Vavilin, V. A., Vasiliev, V. B., Rytov, S. V, & Ponomarev, A. V. (1994). Self- oscillating coexistence of methanogens and sulphate-reducers under hydrogen sulphide inhibition and the pH-regulating effect. *Bioresource Technol*, *49*, 105–119.

Winfrey, M. R., & Zeikus, J. G. (1977). Effect of sulfate on carbon and electron flow during microbial methanogenesis in freshwater sediments. *Applied and Environmental Microbiology*, *33*(2), 275–281. https://doi.org/10.1128/aem.33.2.275-281.1977

Wood, S. (2011). Fast stable restricted maximum likelihood and marginal likelihood estimation of semiparametric generalized linear models. *Journal of the Royal Statistical Society Series B*, *73*(1), 3–36. https://doi.org/https://www.jstor.org/stable/41057423

Wood, S. N. (2001). mgcv: GAMs and Generalized Ridge Regression for R. *R News*, *1*, 20–25.

Wood, S. N. (2004). Stable and efficient multiple smoothing parameter estimation for generalized additive models. *Journal of the American Statistical Association*, *99*(467), 673–686. https://doi.org/10.1198/016214504000000980

Wood, S. N., & Augustin, N. H. (2002). GAMs with integrated model selection using penalized regression splines and applications to environmental modelling. *Ecological Modelling*, *157*(2–3), 157–177. https://doi.org/10.1016/S0304-3800(02)00193-X

CHAPTER 5. IDENTIFICATION OF KEY PROCESS PARAMETERS ON ANAEROBIC DIGESTER FOAMING

5.1 Abstract

Foaming is an issue in co-digested AD systems and can cause instability and significant economic loss. However, the causes of foaming are not completely understood. In this study, an investigation of a field mesophilic digester, which experienced unpredictable foaming events, four batches of laboratory experiments, and a machine learning in data analysis were conducted. The ratios of Fe(II) : S, Fe(II) : TP, and TVFA : TALK; and the concentrations of Cu were identified as influential parameters in both the field digester and lab-digesters. These characteristics could model predictions of whether a digester would foam with 87% accuracy. A model was developed for "foaming potential" of lab-digesters with a root mean square error (RMSE) of 0.048.

5.2 Introduction

Increasing global energy demand, increasing concerns about greenhouse gas (GHG) emissions from fossil fuels, concerns about energy security, and the limited quantity of oil have contributed to the development of sustainable energy technologies (IEA, 2019; UNEP, 2019). The deployment of renewable energy technologies has increased globally in the past decade (IEA, 2019). It is projected that the demand for biogas technologies will increase substantially by 2040 (IEA, 2019).

Anaerobic digestion (AD) is an environmentally sustainable technology that uses a mixed microbial community to convert organic wastes to methane gas (CH_4) and carbon dioxide (CO_2). Anaerobic digestion systems can accept a diverse composition of organic wastes including livestock manure, waste activated sludge, food waste, industrial wastes, pharmaceutical wastes, and crop residues. Therefore, AD captures CH_4, a GHG, and generates a fuel source. The CH_4 potential from landfilled materials, animal manure, wastewater, and other waste streams could displace 5% or 56% of natural gas consumption in the electric power or transportation sectors (NREL, 2013).

The main stages of AD are hydrolysis, acidogenesis, acetogenesis, and methanogenesis. Basically, large particles are biodegraded into smaller, soluble monomers (hydrolysis) which are

converted to short chain fatty acids, CO_2, hydrogen gas (H_2), (acidogenesis, acetogenesis) and finally CH_4 (methanogenesis). In order for the digester to function efficiently, the rate of reaction in each stage must remain in balance with the other stages. However, differences in feedstock composition, digester design, shape, temperature, loading rates, and retention time can affect each stage and overall digester function.

Foam may be generated in imbalanced AD systems. Foams in lab-scale digesters and in field digesters are countless tiny bubbles which are generated faster than their decay in a liquid (Vardar-sukan, 1998). These bubbles are surrounded by a liquid film that thins but does not rupture when the gas bubbles approach each other. In AD, CO_2 is more likely to be trapped in foams than CH_4 due to its higher density and solubility (Kanu, Aspray, & Adeloye, 2015).

Foaming is a problem in AD systems. It can occur in both industrial digesters and lab-scale digesters and result in reduced biogas production, volatile solid (VS) destruction, and pH (Ross & Ellis, 1992). Foaming can cause odor problems, fouling of gas collection compressors and other equipment, gas binding in sludge recirculating pumps, and solids inversion (Ganidi, Tyrrel, & Cartmell, 2009). Not surprisingly, foaming can result in economic loss for an AD system (Ganidi et al., 2009).

Insight into foaming in AD systems has been gained through investigation of foaming in activated sludge systems. Foaming in activated sludge systems has been described as a three-phase system which consists of a gas, liquid, and solid phase (Davenport & Curtis, 2002; Ganidi et al., 2009; Ganidi, Tyrrel, & Cartmell, 2011). In the three-phase system, a particle becomes attached to the gas bubble and rises with it through the liquid, thereby preventing bubble coalescence and increasing foam stability (Bikerman, 1973). Typically, these particles are small, surface active agents or microorganisms whose hydrophobic ends are attracted to the air-liquid interface of the bubble (Bikerman, 1973; Ganidi et al., 2009, 2011; Kanu et al., 2015; Vardar-sukan, 1998). Surface active agents also lower the surface tension of the liquid which decreases the tendency for gas bubbles to rupture. Examples of surface active agents include proteins, lipids, particulate matter (e.g., sand, metals), volatile fatty acids, or detergents (Ganidi et al., 2009). Filamentous organisms can also attach to the gas bubbles and act as a foam stabilizer due to their hydrophobic properties (Ganidi et al., 2009).

However, changes in surface tension from the presence of surface active agents or filamentous organisms may not be the sole explanation for foaming. For example, measurements

of surface tension and hydrophobicity did not show consistent correlations with changes in total solids (TS) concentrations or compounds in raw dairy manure foaming (Boe, Kougias, Pacheco, O-Thong, & Angelidaki, 2012). The presence of certain organic compounds, such as Na^+ and NH_4^+ increased surface tension but demonstrated an increased tendency to foam (Boe et al., 2012). Additionally, lipids did not increase the tendency to foam in raw dairy manure, suggesting that it is their organic load which may be correlated with foaming in AD (Boe et al., 2012). Moreover, increased TS concentrations increased foaming tendency but did not affect surface tension significantly (Boe et al., 2012).

Therefore, other factors besides the presence of surface active agents or filamentous organisms should also be considered. For example, foaming in continuously stirred digesters in a full-scale biogas plant was attributed to the chemical properties of the influent substrate, including alkalinity and protein content, and mixing patterns, rather than microbial community differences (Kougias, Boe, O-Thong, Kristensen, & Angelidaki, 2014). Additionally, the presence of filamentous microorganisms could not be correlated to foam stabilization in a lab-scale digester receiving feed from an activated sludge plant (Ganidi et al., 2011). Furthermore, temperature or excessive CO_2 production from digester imbalance has been suggested as other possible factors influencing foaming formation and processes in AD systems (Ganidi et al., 2009; Kanu et al., 2015; Kougias et al., 2014; Murk, Frieling, Tortorici, & Dietrich, 1980). Therefore, the framework of the three-part system explains the main mechanisms of foam formation but requires more in-depth analysis about the role of digester influent and subsequent AD processes.

Due to the complexity of the foaming process in AD systems, knowledge-based approaches will be needed to model them. Knowledge-based approaches is a broadly defined term for approaches which involve knowledge acquisition, representation, and management (Poch, Comas, Rodríguez-Roda, Sànchez-Marrè, & Cortés, 2004). Knowledge-based approaches are suited towards prediction tasks in wastewater treatment plant (WWTP) systems due to their ability to handle complexity and uncertainty (Poch et al., 2004). Artificial intelligence techniques (e.g., neural networks, fuzzy logic) can be combined with knowledge-based systems to create hybrid knowledge-based systems (Poch et al., 2004; Wen & Vassiliadis, 1998). Hybrid knowledge-based systems have been used to predict foaming risk in anaerobic digesters (Jordi Dalmau, Comas, Rodríguez-Roda, Pagilla, & Steyer, 2010), acidification states (Carrasco, Rodríguez, Punal, Roca, & Lema, 2004), and CH_4 yields (Cakmakci, 2007). In other words, these systems can handle a

large number of qualitative and quantitative variables (*i.e.*, "knowledge"), develop complex connections between these variables, and then simulate AD processes to aide with control and operation.

The goal of this study was to obtain new insights into the effect of the digester liquid's chemical and physical characteristics on foaming in AD systems. It was also to propose the creation of a hybrid knowledge-based approach to model digester foaming with particular interest in digester influent.

5.3 Materials and methods

5.3.1 Overview

This study consisted of an investigation of an industrial-scale field digester and a laboratory experiment on foaming. Test materials were all obtained at the same field digester. The field digester was studied at foaming and non-foaming time points to determine influential physical and chemical characteristics on foaming. The role of gas production was examined in lab-scale foaming digesters. Additionally, machine learning was used to identify influential variables on foaming and to develop a model for foaming

5.3.2 Field digester investigation

The field digester of this study was an industrial-scale mixed plug-flow digester system in Indiana State. The system produced about 61,000 m^3 of biogas daily for electricity generation and heating. The system had three 9085 m^3 anaerobic digesters that operated in parallel at mesophilic (38.3°C) conditions and a hydraulic retention time (HRT) of 28-32 days. The field digester system treated beef cattle manure (~50%) with other co-digested materials including food waste, glycerin, industrial wastes, and biodiesel waste depending on availability. The variable composition of the influent provided unique opportunities to investigate the effect of influent compositions on foaming.

Five batches of samples were collected during incidents of foaming and non-foaming operations from October 2017 to February 2019 (Table 4-2). Batches 1 and 5 were collected during non-foaming times. Batches 2, 3, and 4 were collected at the times that the digesters were

experiencing foaming. Additionally, at the time of Batch 5 collection, glycerin loads to the digesters were nearly negligible.

Six types of samples were taken at six locations of the digester system. These samples were 1) digester influent (INF) in the equalization pit that stored digester influent after feedstock mixing, 2) and 3) digester liquid in the middle of east and west digesters (DL-E and DL-W, respectively), 4) and 5) digester effluent in the effluent pits of east and west digesters (EF-E and EF-W, respectively), and 6) liquid fraction of digester effluent (EF-L) after solids removal using a roller press, slope screen, and centrifuge (Figure 4-1).

After collection, the samples were transported to Purdue University and immediately characterized to determine relationships between the physical/chemical characteristics and the origins of foaming. Detailed methods of characterization are presented in Section 4.3 and Table A-1.

5.3.3 Lab-digester experiment

Lab-digester set-up

The lab-digesters were customized for the tests. They were made of glass borosilicate flasks (Bomex). For Batch 1, the digesters had a working volume of 500 mL. However, the gas bags in Batch 1 tests experienced leakage so no CH_4 yield data was collected and used in this chapter. For Batches 2-5, the digesters had a working volume of 1000 mL. Details about the lab-digester setup are described in Section 4.3.3 for Digester B.

Lab experimental design

The samples from the field digester underwent anaerobic digestion in four batches of lab-scale digesters. In each of the Batches 2 through 5 tests (Table 5-1), a "blank" control with 10% or 20% volume inoculum and the remaining volume as reverse osmosis (RO) water was used to determine the contribution of CH_4 from inoculum (Table 5-1). There were also digesters with 50% or 100% inoculum to determine the activity of the different stages of the field digester (Table 5-1). The experiments were performed in triplicate, except the blanks which were performed in duplicate (Table 5-1).

Table 5-1. Description of materials loaded into each lab-digester group.

Lab-Digester Group No.	Substrate (% V)	Inoculum (% V)	Inoculum Type	RO water (% V)
2-1	90	10	EF-W	0
2-2	90	10	DL-W	0
2-3*	0	100	DL-W	0
2-4	0	100	EF-W	0
2-5**	0	10	DL-W	90
2-6**	0	10	EF-W	90
3-7	90	10	EF-W	0
3-8	90	10	DL-W	0
3-9	0	50	DL-W	50
3-10	0	100	EF-W	0
3-11**	0	10	DL-W	90
3-12**	0	10	EF-W	90
4-13	80	20	DL-W	0
4-14	0	100	EF-E	0
4-15	0	50	DL-W	50
4-16	0	50	DL-E	50
4-17**	0	20	EF-W	80
5-18	80	20	EF-W	0
5-19	0	100	EF-E	0
5-20	0	50	DL-E	50
5-21	0	50	DL-W	50
5-22**	0	20	EF-W	80

*Each digester group contains 3 individual digesters, except for blanks that contains 2. *This lab-digester group foamed over during the experiment and was removed before completing the test. **Digesters in this group were blanks. NA = not applicable.*

The substrate to all lab-digesters was the INF from the field digester. The inoculum to all lab-digesters came from the field digester liquid (DL-E, DL-W) and effluent (EF-E, EF-W) (Figure 4-1). The inoculum ensured the necessary microbial consortia for CH_4 production in the lab-digesters. The characteristics of substrate and inoculum were the same as determined for the field digester on Day 0 and described in Section 4.3. On the final day of each test, the lab-digester liquid was thoroughly mixed, sampled, and characterized using the same methods as on Day 0 (Tables B.1 through B.4).

During the lab tests, the lab-digesters were randomly assigned to several water baths (GEMMYCo Model YCW-010 and PolyScience Model WB28) and incubated at 38.3°C ± 0.1 until the volume of daily CH_4 production from the lab-digester was less than 1% of the volume of cumulative CH_4 production from the same digester.

Biogas collection and measurement

The biogas from the lab-digesters was collected in plastic bags. The bags were connected with silicone rubber tubing. Two 500 mL gas bags were attached to the side outlet port of the digester to collect the biogas. When a gas bag was removed from a lab-digester for biogas volume and gas composition measurement, it was immediately replaced with an empty bag.

Biogas volume and biogas composition were measured for the first three days daily, and then at intervals of no more than three days. Biogas volume was determined using a custom-made device and a 200 mL syringe (Sealey Model VS 404, Jack Sealey Ltd, Suffolk, UK). All biogas volumes were converted to Standard Temperature and Pressure (0°C, 1 atm). The biogas composition was measured with a Biogas Analyzer (Model 5000, LANDTEC North America, Inc., Colton, CA) with detection ranges of CH_4 (0-100%), CO_2 (0-100%), O_2 (0-25%), and H_2S (0-10,000 ppm). The specific methane yield (SMY) was calculated by dividing the cumulative CH_4 volume by grams of initial volatile solids in the digester in $m^3\ g^{-1}$ VS.

Digester liquid pH measurement

The digester liquid pH was measured at the same instances as the biogas was collected and measured, *i.e.,* for the first three days daily, and then at intervals of no more than three days. The pH measurement was conducted through the operational port during the experiment using a pH probe (Cole-Parmer electrode Cat No 05993-00) and a pH meter (Model 60, Jenco Digital pH Meter). The measurement was done after the contents of the digester were thoroughly mixed with the magnetic stir bar in each lab-digester and a magnetic stirrer.

5.3.4 Data and software

The data used in statistical analysis and model development were from the chemical characterizations of the field digesters and lab-digesters (Tables B-2 through B-9), SMY (Table B-9) results from the lab-digester tests and qualitative variables (primary digester liquid, collection date, substrate to inoculum ratio (S:I), foaming). Rstudio (version 3.6.3, (2020-02-29 Platform: x86_64-w64-mingw32/x64, 64-bit) and Microsoft Excel were used for data analysis.

t-tests

Differences in the chemical characteristics between foaming and non-foaming time-points for the field digester samples were examined using RStudio. First, the normality of the data was checked using the Shapiro-Wilk Normality test. If the data was not normally distributed ($P < 0.05$), then the non-parametric Wilcoxon signed-rank test was applied. Otherwise, a pairwise *t*-test with a Bonferroni correction was performed.

Qualitative factors analysis

Differences between the CH_4 production potentials from the lab-digesters were examined using Rstudio. The package FactoMineR in Rstudio was used to develop a multiple linear regression model of the influence of qualitative variables on SMY. The data for the FactomineR was the final SMY value (Table B-9) and the qualitative information on the sample collection (Table 5-1 and Table 4-1). Specifically, this was inputted as the primary digester liquid (INF, EFFL, DL) added to the digester, digester material collection date, substrate to inoculum (S:I) ratio, and whether the materials were taken from the digester during foaming or nonfoaming timepoints. The primary digester liquid was the highest percentage of materials added to the digester, excluding RO water.

A principle component analysis (PCA) biplot of the lab test results was generated in the factoextra package in RStudio. To determine whether foaming or another quantitative factor influenced the decreased SMY, PCA and regression analyses on the SMY and Day 0 characterizations (Tables B.1 through B.4) of the digester liquid were performed.

Foaming potential

In this particular study, a foaming potential of each lab-digester group was determined using Eq. 5-1 from Kanu et al. (2015). The lower the foaming potential value, the increased likelihood of foaming. This equation is motivated by the fact that surfactant concentration typically increases when the feed to the digester increases, thereby decreasing foaming potential. Additionally, total biogas production is likely to be lower in foaming digesters due to gas entrapment. In this study, the feedstock volume was converted to mass (g) of total solids so the foaming potential was (mL g feed TS^{-1}).

$$\text{Foaming potential} = \left[\frac{\text{Volume of biogas produced}}{\text{Volume of feedstock to the digester}}\right] \quad (5\text{-}1)$$

5.3.5 Machine learning

Machine learning to predict foaming classification

The foaming classification data was obtained from the field digester and included INFL and DL materials (Tables B-5 through B-8). The foaming classification was defined as "yes" or "no" and referred to whether the digester was "yes, foaming" or "no, non-foaming". The foaming classification data was only taken from INFL and DL locations in the field digester because these areas were experiencing visible foaming and digester overspill at the time of collection.

Machine learning was performed using the caret package in RStudio (Kuhn, 2008) to predict the state of the digesters (foaming v. non-foaming) (Figure 5-1). Missing data were determined through *k*-nearest neighbor imputation. The foaming state was converted to a dummy variable of "0" (non-foaming) or "1" (foaming). All the data was centered and scaled before modeling. Recursive feature modeling with repeated cross validation was used to determine the top five numerical predictors. Recursive feature modeling is a wrapper method that is used to determine the best performing subset when there are many factors. The recursive feature modeling process was repeated 11 times with a random seed each time in order to determine the best subset of six predictor variables. Wrapper methods tend to be more robust than traditional filter methods (e.g., Pearson correlation, ANOVA). Each model was trained using a supervised machine learning model with 5-fold cross-validation repeated 100 times using the train() function in RStudio.

Several classification and regression models were tested. These models included neural net (NN), multinomial logistic regression (MULTINOM), *k*-nearest neighbor (KNN), classification and regression trees (CART), support vector machines (SVM) with radial basis function kernel, Brieman's random forest algorithm (RF), and the generalized linear model via penalized maximum likelihood (Glmnet). Accuracy and the kappa statistic were used to evaluate the predictive ability of the models (Banerjee, Capozzoli, McSweeney, & Sinha, 1999).

The test and training data were obtained by randomly partitioning the data (67% training, 33% testing) using the function createDataPartition in RStudio. The test data was used to evaluate the model. The predictive accuracies and kappa statistics were determined using the predict function

in RStudio. The model's results were compared to the testing data to determine the model's accuracy and kappa values.

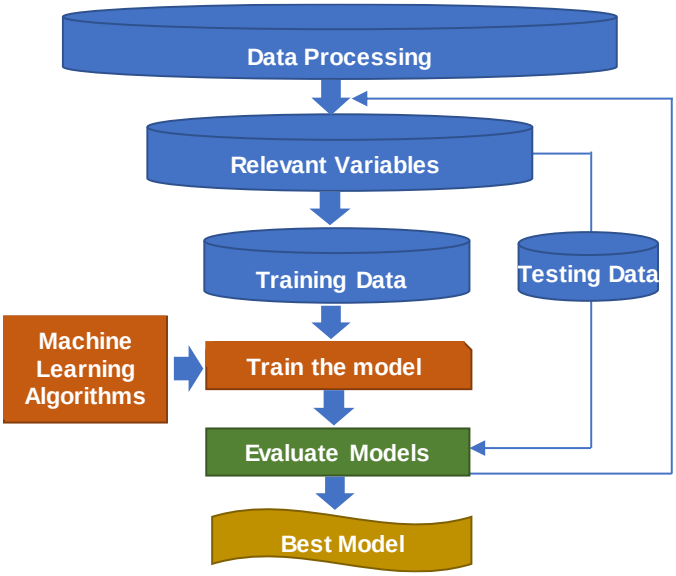

Figure 5-1. Overview of machine learning.

Machine learning algorithms for foaming classification

Foaming classification was developed by using the neural net model in the nnet package in RStudio and different machine learning algorithms. The model was a feed-forward neural network with a single hidden layer (Ripley, 1996; Venables & Ripley, 2002). Neural networks consist of several layers of interconnected elements (neurons) that are connected by weights, which receive inputs from previous layers or external sources (Figure 5-2). Only the "input" and "output" neurons interact with the outside world; the "hidden" neurons are intermediate neurons, which are not visible to the user. A neural network is a type of black-box modeling, which can be created by summing the product of the inputs and the weighted connections, adding a bias, and then passing the result through an output function. The value of the weights provide information on the relationships between the interconnected elements. "Training" the network refers to determining the weights and unit thresholds of the network. In the feed-forward process, the computation process starts in the first layer and proceeds with each consecutive layer until the output layer (Figure 5-2). The training process used in this study was a quasi-Newton optimization procedure (Bergmeir & Benítez, 2012).

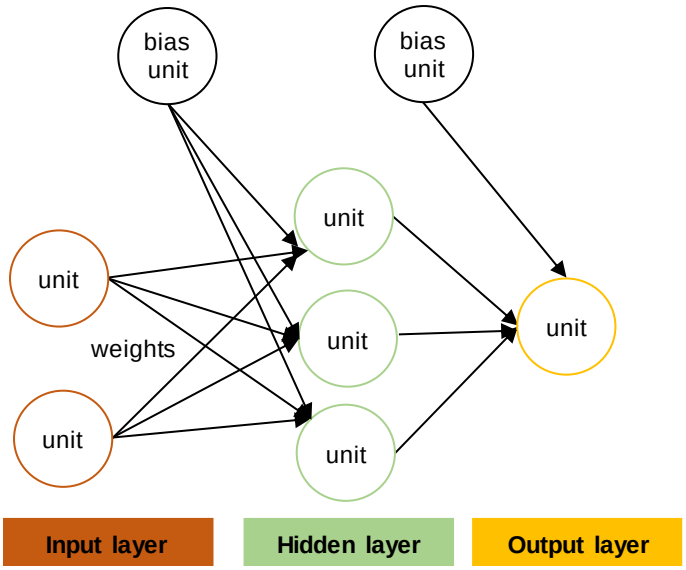

Figure 5-2. A single layer of a 2-3-1 feed-forward neural network.

Additional algorithms are described as follows:

The MULTINOM algorithm in RStudio uses neural networks to fit nominal (categorial) variables to log-linear models (Venables & Ripley, 2002). The appeal of the MULTINOM algorithm is that it does not assume linearity, normality, or homoscedasticity of the data (Starkweather & Moske, 2011). The tuning parameter was decay, which is a regularization parameter. The predictive accuracy was used to select the optimal model using the largest value. The final predictive accuracy value used for the model had a decay value of 1e-04.

The KNN algorithm is a supervised non-parametric algorithm that is primarily used for classification. The KNN algorithm examines the classes of its *k*-nearest examples in a reference set and then assigns a classification based on the majority classification (Ripley, 1996; Venables & Ripley, 2002). The benefits of KNN is that it accounts for the class of the data. The tuning parameter was k, and k values between 5 and 23 were tested. The predictive accuracy with the largest value was used to select the optimal model. The final predictive accuracy value used for the model had a k value of 5.

The CART algorithm uses decision trees to classify and partition the data using a Gini index as the criterion (L. Breiman, Friedman, Olshen, & Stone, 1984). The CART algorithm is a flexible classification method for data with highly ordered variables (L. Breiman et al., 1984). Maxdepth was the tuning parameter and was the maximum depth to which the decision tree could

"grow". The CART model only converged on one solution because the program held maxdepth at a constant value of 1.

The SVM with radial basis function kernel algorithm uses a Gaussian kernel function to map the data nonlinearly in space and then construct a hyperplane to classify the data (Schölkopf et al., 1997). The SVM algorithm is well-suited for data with separable classes (Schölkopf et al., 1997). The tuning parameters were sigma and c. Sigma was the scale parameter, and c was a regularization parameter. The predictive accuracy was used to select the optimal model using the largest value. The final predictive accuracy value used for the model had a sigma of 0.40 and a c value of 8.

The RF algorithm uses an ensemble of decision trees to determine class prediction (Leo Breiman, 2001). The benefits of the RF algorithm include its randomness which generates a "forest" of uncorrelated trees and its inability to overfit data (Leo Breiman, 2001). The tuning parameter is the mtry value which is the number of randomly sampled variables that are sampled as candidates at each split in the random forest model. The predictive accuracy was used to select the optimal model using the largest value. The final predictive accuracy value used for the model had a mtry value of 2.

The GLMNET algorithm fits a generalized linear model with lasso, ridge, or elastic (combination of lasso and ridge) net penalties (Friedman, Hastie, & Tibshirani, 2010). The benefits of the GLMNET algorithm include its efficiency as well as its mixture of lasso and ridge methods which can reduce the effect of highly correlated data (Friedman et al., 2010). The tuning parameters were alpha and lambda. Alpha is the elasticnet mixing parameter and varied between 0 and 1. Lambda is the parameter which controls penalization in the model. The predictive accuracy was used to select the optimal model using the largest value. The final predictive accuracy value used for the model had an alpha value of 0.4 and lambda value of 0.0001.

Machine learning to predict foaming potential

The hybrid neural fuzzy inference system (HYFIS) model in the frbs package in RStudio was used to model the foaming potential (mL g TS^{-1}) from individual BMP digesters (Bergmeir & Ben, 2015). The previous equation 5-1, relies on data which is collected at the end of the experiment. If foaming potential could be tied to an influent Day 0 characteristic, then the potential to foam could be determined before the BMP test begins. The machine learning model thus

developed connections between the Day 0 characteristics from the BMP digesters (Tables B-1 to B-5) and the foaming potential data (Table B-9).

The HYFIS model combines the neural network structure and fuzzy logic in what is known as a neuro-fuzzy model. The HYFIS model is used to deal with systems with uncertainty, imprecision or non-linearity. The HYFIS model was selected due to lower R^2 values and high RMSE values (Table B-14) using the previously mentioned algorithms from section "Machine learning algorithms for foaming classification".

The HYFIS model uses Wang and Mendel techniques for knowledge acquisition (L. X. Wang & Mendel, 1992). First, structure identification and parameter estimation (mean and variance) of the training data was performed through gradient descent-based learning algorithms (Kim & Kasabov, 1999). A knowledge base was then generated. The test data then underwent the prediction phase. First, the input data underwent a "fuzzification" process (Figure 5-3). The data was mapped to a value between 0 and 1 using a selected membership function. In more detail, "0" indicated that the variable was not a member and "1" indicated complete membership. The data was then assigned a label which indicates the degree of membership. For example, a value of 0.01 might be labelled as "low" membership. A value of 0.99 might be labelled as "high" membership. In other words, the data were roughly subdivided into categories. The HYFIS model used a Gaussian membership function. Next, there was the inference process (Figure 5-3). This was when a set of linguistic IF-THEN rules were determined based on the data and the selected inference method. For example, a rule would be "IF A is high THEN B is low". This resulted in much greater flexibility for modeling and a greater tolerance of variance. Next, the decision making unit would interpret the inputted values and then assign an output value using these "IF-THEN" rules. The HYFIS model uses Mamdani fuzzy logic techniques as its inference system. Finally, there was a defuzzification process which then converts the data back into crisp, numerical values (Figure 5-3).

The variable selection method was a backward-elimination strategy (Kohavi & John, 1997) as used for determining the biological risk of foaming in AD (J. Dalmau, Comas, Rodríguez-Roda, Latrille, & Steyer, 2008; J. Dalmau, Comas, Rodriguez-Roda, Latrille, & Steyer, 2009). First, the HYFIS model was run with every single predictor variable and the reference RMSE was obtained. Then, the model was re-run with one variable removed and the RMSE was obtained and compared to the reference RMSE. If the RMSE increased when that variable was dropped, then the variable

was deemed as relevant to the model. Once a subset of relevant variables was chosen, combinations of these variables were tested by adding one variable at a time to the HYFIS model. First, the variable with the highest RMSE was then selected and trained again with the HYFIS model. If the RMSE was less than the reference RMSE, then the variable was deemed as essential. The variable with the next highest RMSE was added and the process was repeated until all variables were tested (*i.e.*, forward elimination).

Once the relevant variables were selected, the final model was evaluated using RMSE and R^2 values. This was accomplished using the predict function in RStudio to compare the model to the testing data.

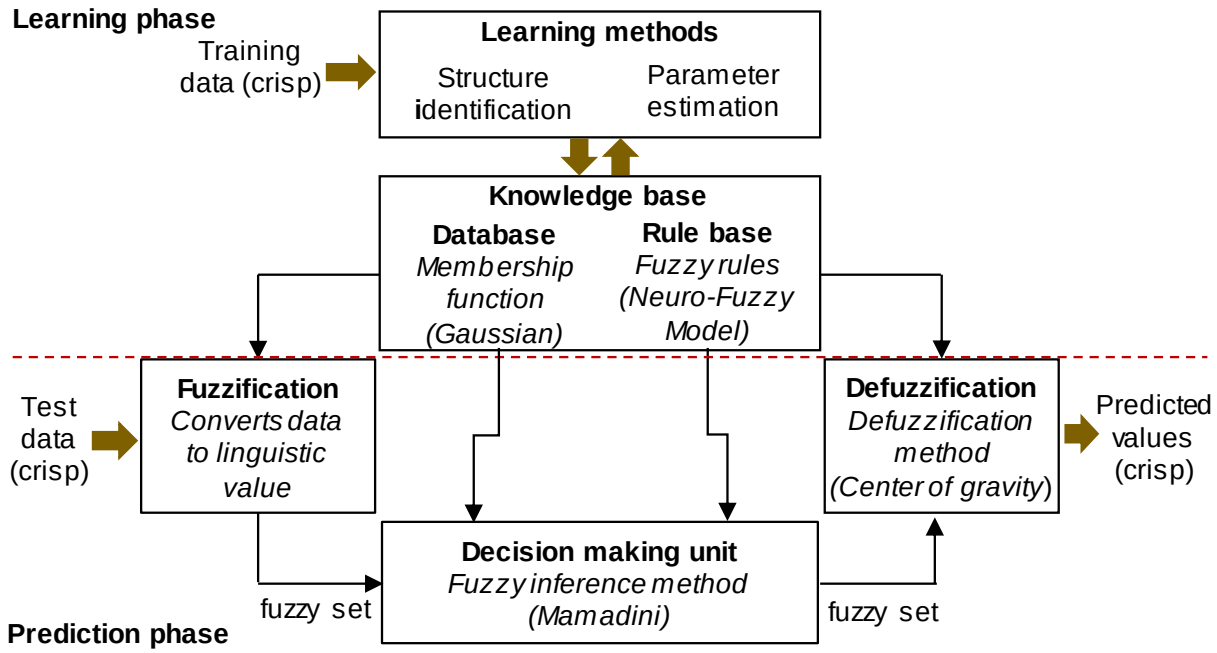

Adapted from (Bergmeir & Ben, 2015; Cakmakci, 2007; Jang, 1993)

Figure 5-3. Overview of the HYFIS model.

5.4 Results and discussion

5.4.1 Field digester characteristics

Some significant differences in the digester influent were found. Influents related to digester foaming had significantly lower OP, iron, nickel, and ammonia concentrations in the digester influent and significantly higher total alkalinity concentrations (Table 5-2). Foaming-

causing influents additionally had significantly lower Fe(II) : S, Fe(II) : TP, OP : TP, and SCOD : TCOD ratios and higher VS : TS ratios (Figure 5-1, Tables B-7 through B-8).

Table 5-2. The *P* values and significance levels of the measured Day 0 chemical concentrations for the non-foaming (n = 3) and foaming INFL (n = 3) field digester samples.

Characteristic	Non-foaming (g L^{-1})	Foaming (g L^{-1})	*P* value	Significance
Cu	0.007 ± 0.004	0.005 ± 0.002	.349	
Fe	0.178 ± 0.07	0.03 ± 0.014	< .001	***
Ni	0.011 ± 0.002	0.007 ± 0.002	.006	**
TP	6.58 ± 1.7	5.28 ± 0.64	.054	
OP	3.3 ± 0.24	2.1 ± 0.47	< .001	***
TKN	1.81 ± 0.69	1.33 ± 0.46	.14	
NH_3N	1.89 ± 0.19	1.5 ± 0.2	.001	**
Sulfate	8.08 ± 3.45	6.78 ± 0.65	.281	
TS	141 ± 17	309 ± 287	1	
VS	80.21 ± 32.21	287.48 ± 287.25	.066	
pH	6.25 ± 1.05	6.81 ± 0.18	.394	
TCOD	223 ± 34	249 ± 134	.628	
SCOD	83 ± 25	71 ± 49	.381	
TALK	2.2 ± 1.53	4.77 ± 1.07	.007	**
TVFA	14.6 ± 1.4	16.3 ± 5.1	.465	
Conductivity	8.11 ± 0.17	8.42 ± 1.83	.839	
Tannic Acid	2.64 ± 0.81	2.35 ± 0.28	.323	
TN	1.15 ± 1.41	1.38 ± 0.49	.657	
Inorganic N	0.89 ± 0.77	0.08 ± 0.06	.077	
SCOD : TCOD	0.41 ± 0.11	0.27 ± 0.04	.022	*
OP : TP	0.53 ± 0.13	0.41 ± 0.05	.044	*
TCOD : TN : TP	255.2 ± 237.31	35.77 ± 36.35	.034	*
TVFA : TALK	8.44 ± 3.51	3.74 ± 1.89	.016	*
TAN : TKN	1.08 ± 0.37	1.23 ± 0.33	.445	
TCOD : Sulfate	33.39 ± 17.16	36.39 ± 21.08	.731	
FS : TS	0.4 ± 0.3	0.13 ± 0.08	.022	*
VS : TS	0.6 ± 0.3	0.87 ± 0.08	.022	*
FE(II) : S	0.055 ± 0.042	0.008 ± 0.004	.008	**
Fe(II) : TP	0.05 ± 0.033	0.01 ± 0.005	.003	**
TCOD : TKN	1.81 ± 0.69	1.33 ± 0.46	1	

** P < .05, ** P < .01, *** P < .001*

The differences in the digester influent could explain the tendency to foam. The SCOD : TCOD ratio was lower at foaming incidents (Table 5-2,Table B-3), suggesting that non-foaming digesters were receiving material which was more solubilized and thus primed for methanogenesis. Additionally, an increased percentage of organic matter (Table 5-2, Table B-4) was present in foaming samples, indicating possible digester overload. A relationship between elevated VS : TS

content and foaming in sludge samples has been demonstrated (Jiang, Qi, Hao, McIlroy, & Nielsen, 2018). Additionally, the elevated alkalinity concentrations may have been a surface active agent in the foaming digesters. High alkalinity concentrations have been positively correlated with a tendency to foam due to decreasing the surface tension of the digester liquid (Gerardi, 2003; Kougias et al., 2014; Nges & Liu, 2010; Niekerk, Kawahigashi, Reichlin, Malea, & Niekerk, 1987). Additionally, increased alkalinity concentrations increases CO_2 solubility, thereby increasing the likelihood of its entrapment in the digester liquid (Murk et al., 1980). These characteristics suggest that there were differences in the digester INFL materials that caused foaming.

Digesters receiving mixed waste streams could be more vulnerable to foaming. For example, co-digestion of manure with lipid-rich substrates such as food waste, slaughterhouse waste, and glycerol can cause digester instability and foaming (Atandi & Rahman, 2012; Fierro et al., 2016; Usack & Angenent, 2015). The field Digester B reportedly had lipid-rich wastes in the influent. Specifically, glycerin wastes were reported as present in the influent for all cases except in Batch 5 (a non-foaming case). Biodiesel wastes were reported as present in all cases. However, there were other differences in the samples that more closely isolated the causes of foaming. Because the influent was a co-digested mix of various waste streams, chemical characterization was the best solution to determine differences between foaming and non-foaming samples.

5.4.2 Lab-digester characteristics

Digester substrate, inoculum, and liquid

The Day 0 analysis of the lab-digesters indicate some important characteristics in digester substrate and inoculum. The VS : TS ratios were generally high for all of the materials (greater than 50%) which were loaded into the digesters (Table B-4). Some of the highest VS : TS ratios were in digesters taken from foaming samples (> 0.8) (Table B-4). A high VS : TS ratio indicates that these samples had high organic strength and suggests that there may have been overloading of the digester. The initial pH varied from 5.9 to 7.95 (Table B-1). The optimal pH for methanogenesis is 6.5 to 7.6 (Parkin & Owen, 1987), and most samples fell within this range. Digesters using materials taken from foaming time points generally had lower pH values below 7 (Table B-1). The initial sulfate concentrations were also generally high (> 2 g L^{-1}) in almost all of the digesters (Table B-2).

The digester liquid underwent degradation during the digestion period. The SCOD : TCOD ratios generally increased between Day 0 and the final day (Table B-3). In fact, the SCOD : TCOD ratios only decreased in digesters receiving samples from foaming incidents. The OP and TN concentrations increased in most cases (Table B-2), with the decrease in OP only occurring in digesters receiving samples from foaming incidents. Therefore, the solubilization of the organic matter as well as the degradation of amino acids evidently occurred, with a greater extent in foaming samples. Some of the organic matter was utilized as evidenced by the general decrease in VS : TS ratios (Table B-4). Additionally, the pH increased in most cases over the digestion period (Table B-1). The decrease in sulfate concentration over the digestion period (Table B-2) also indicated sulfate reduction.

Specific methane yield

The SMY from the BMP digesters varied considerably. The digesters containing influent samples had generally low SMY results for both foaming and non-foaming cases (less than 11 mL CH_4 g VS^{-1}) (Figure 5-4). For example, manure slurries have had SMYs from 165 to 530 mL CH_4 g VS^{-1} (Møller, Sommer, & Ahring, 2004). The digesters in Batch 5 that received materials from the field digester during non-foaming events had significantly higher SMYs (Figure B-2, Table B-13) for all digesters except for digesters containing field digester influent (Figure 5-4). The fact that the foaming potential was a high value (indicating low foaming potential) in the digester liquid and effluent samples indicates that the microbial community in the digester was viable, but that a characteristic of the digester liquid might be inhibiting CH_4 production, rather than the foaming itself. For example, the elevated total alkalinity concentrations might have contributed to excess CO_2 production and gas entrapment.

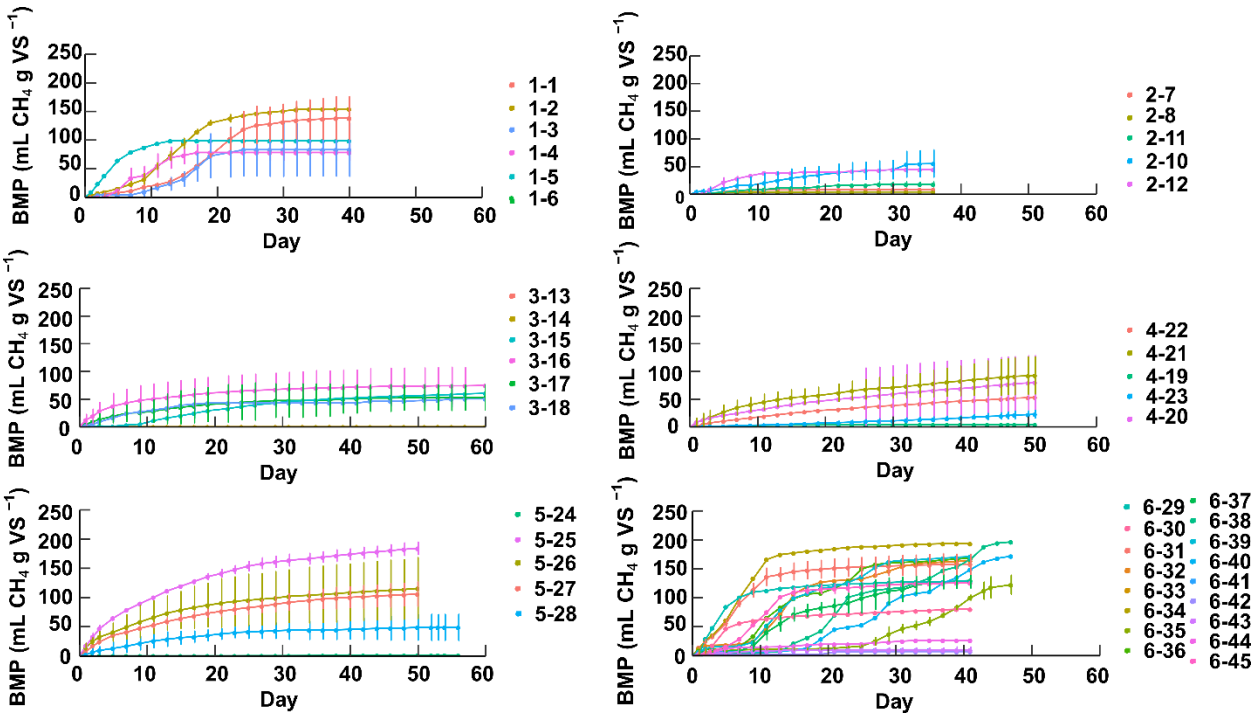

Figure 5-4. Specific methane yields and standard deviations over time from BMP tests for each lab-digester group.

5.4.3 Qualitative variable from FactoMineR analysis

The qualitative variables of collection date (batch), foaming, S:I, and primary digester liquid (INF, EFFL, DL) showed some differences in the regression model from the FactoMineR analysis of the Day 0 characteristics and the SMY. The two most influential variables on SMY were the S : I ($P < .001$) and the primary digester liquid ($P < .001$). However, the adjusted R^2 of the overall FactoMineR model was 0.59, indicating that the choice of a linear model may not be the best for determining the qualitative influences on CH_4 yield.

Digester liquid characteristic from PCA analysis

The PCA analysis revealed that there were distinct differences in the digester liquid characteristics (Tables B-2 through B-6). This was evident in the PCA plot (Figure 5-5), although there was no distinct clustering between the foaming and non-foaming samples from the lab-digesters. Different clusters of vectors could explain correlations in the results. For example, the initial VS : TS and SCOD : TCOD ratios had a negative correlation with the CH_4 yield (Figure

5-5), which would be the opposite of what would be expected. However, the relationship of these variables to foaming may be conflated with the SMY.

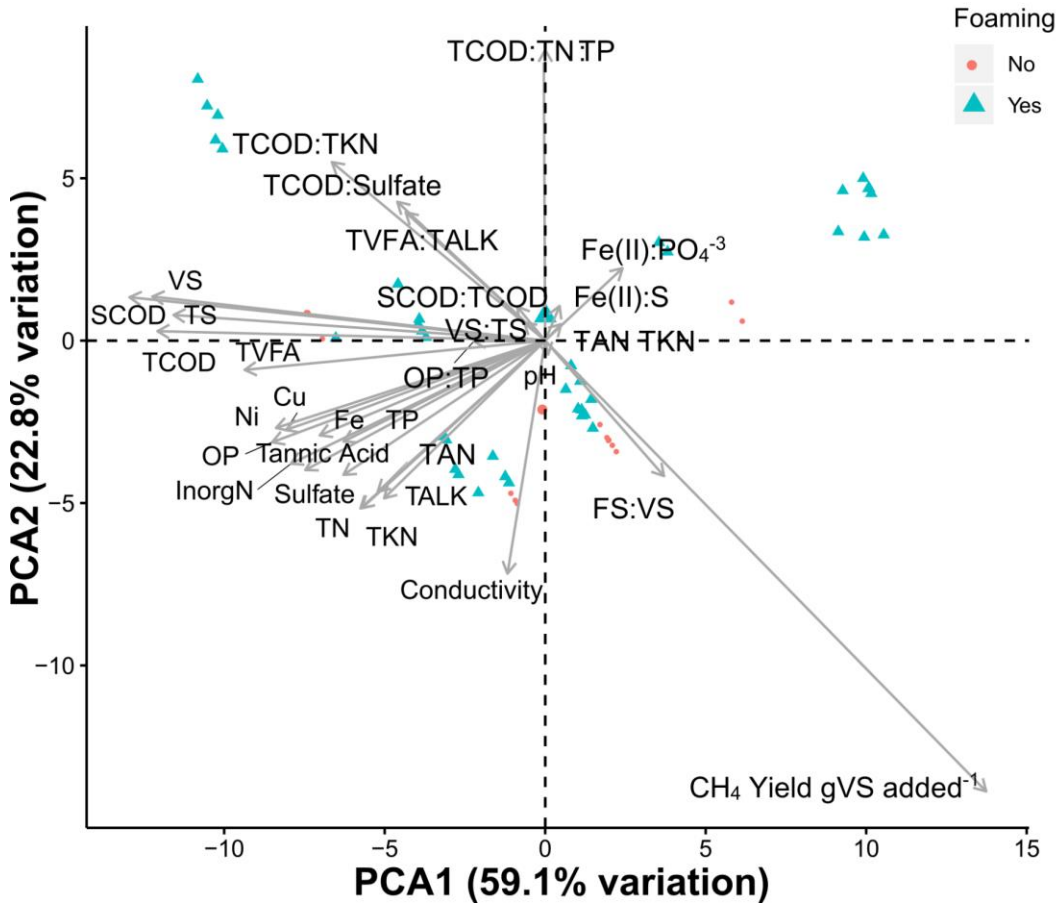

The angle between two vectors represents the correlation between those variables and the principle component. The length of the arrow indicates the contribution to the PCA. Two principle components are shown. PCA1 explained 58.5% of the variation and PCA2 explained 22.9% of the variation. The colors of each circle represent the foaming condition (blue triangle = Yes; red circle = No).

Figure 5-5. Biplot of the lab test results with each vector (line with arrow) representing the characterizations.

Foaming potential

The foaming potential results indicated differences among lab-digesters. Low foaming potential values (below 20 mL g TS^{-1}) were clearly indicated in lab-digester group numbers 3-7, 3-8, 4-13, and 5-18 (Figure 5-6, Table B-9). These digesters started with 90% or 80% of their

volume as INF. These digesters also had low SMYs (Figure 5-4) with a larger percentage of their biogas composed of CO_2. The CO_2 was most likely trapped in the liquid, resulting in foaming.

These foaming potential values aligned with what was observed. These digesters exhibited foaming during the course of the experiment. In fact, lab-digester group numbers 4-13, 3-8, 3-10, and 2-2 also had one replicate within their group which was removed due to foaming. Lab-digester group number 2-3 was not included in the foaming potential calculations because all replicates were removed during the experiment due to overflow from foaming. The foam in the lab-digesters consisted of very small bubbles that rose rapidly within the first 72 hours of the experiment.

In general, there were differences in foaming potential values and the primary digester liquid. In all cases, foaming potential values were lower in digesters containing materials from the foaming field digester (Figure B-1, Table B-12). Specifically, DL samples had significantly lower foaming potential during times of foaming (Figure B-1). The digester contents would have contained the most biologically-active materials from the field digester system. The digester liquid may have foamed due to digester imbalance and the middle samples contained these conditions. Therefore, the observed foaming was somewhat confirmed by the foaming potential calculations and suggests that the material from the field digester has properties which might cause foaming.

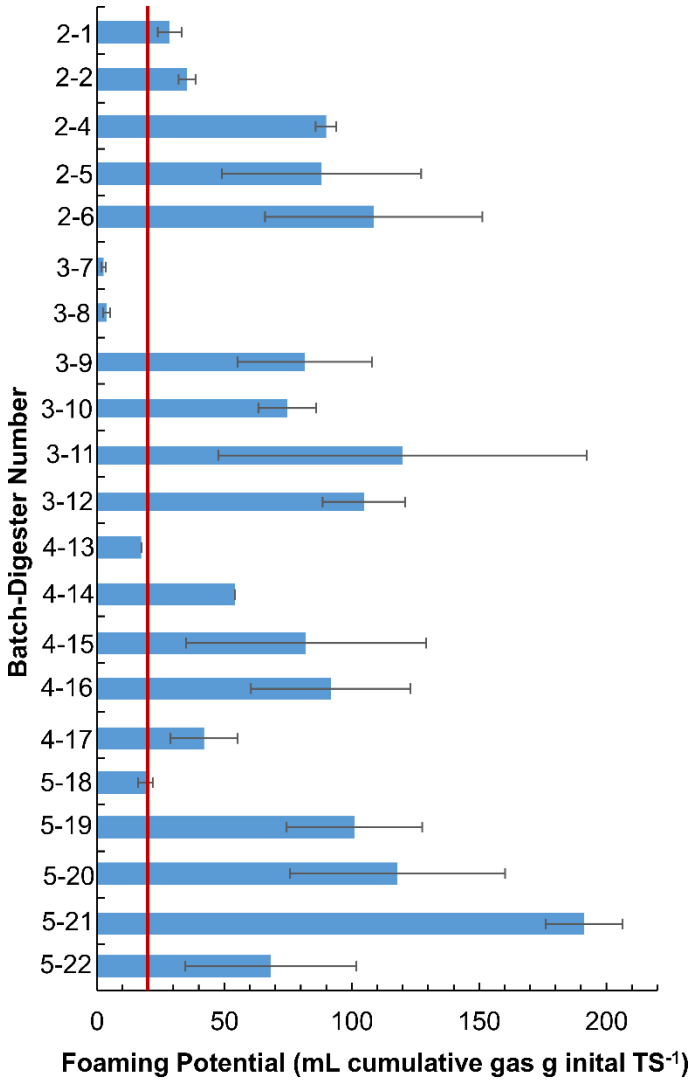

Figure 5-6. The final average foaming potential and standard deviation for each lab-digester group number.

5.4.4 Foaming classification and foaming potential from machine learning

Foaming classification

Recursive feature modeling identified the most significant predictor variables as Fe(II) : S, Fe(II) : TP, TCOD, Fe, TVFA : TALK and Cu. Since only samples from the influent and digester liquid were examined in this analysis, these variables align with the *t*-test results. Most of these variables, except for Cu and TCOD, were identified as influential variables on foaming in the influent (Table 5-2). In the DL samples, Cu and TCOD were identified as significant on foaming

classification (Table B-10). Hence, the recursive feature modeling process was able to narrow down the most relevant predictor variables of all the process parameters with an 89% accuracy.

The model with the highest predictive accuracies for foaming classification ("yes", "no") were the KNN (80%) and SVM (87%) models (Table 5-3). The NN and MULTINOM models had some of the lowest predictive accuracies of 73% (Figure 5-7). The weighted values were < 0.50 for the NN model, except for Fe(II) : S which had a weight of 0.68. The SVM and KNN algorithms are specialized models for the classification of data which is most likely why they had the best predictive accuracies.

These results improved on findings from previous studies. A study compared the KNN, SVM with radial kernel, RF, and GLMNET models to predict CH_4 production based on influent characteristics (total carbon, TN, carbon to nitrogen ratio, cellulose, xylan, lignin, glucan, temperature) (L. Wang, Long, Liao, & Liu, 2020). Their best predictive accuracy was 73% with the GLMNET model (L. Wang et al., 2020). Another study examined biomethane production from an industrial co-digested system using RF, elastic net, and extreme gradient boosting and reported R^2 values between 0.80 and 0.88 (De Clercq et al., 2020). By examining a broader range of characteristics and more machine learning algorithms, the method in this study was able to develop a machine learning model for foaming classification.

Table 5-3. Models used for supervised machine learning of foaming classification in the field digester and their predictive accuracy and kappa value.

Model tested	Type of Model	Tuning Parameter	Accuracy	Kappa
MULTINOM	classification	decay	0.73	0.46
KNN	classification, regression	k	0.80	0.59
CART	classification, regression	maxdepth	0.60	0.18
NN	classification, regression	size, decay	0.73	0.46
SVM	classification, regression	sigma, c	0.87	0.74
RF	classification, regression	mtry	0.73	0.46
GLMNET	classification, regression	alpha, lambda	0.73	0.46

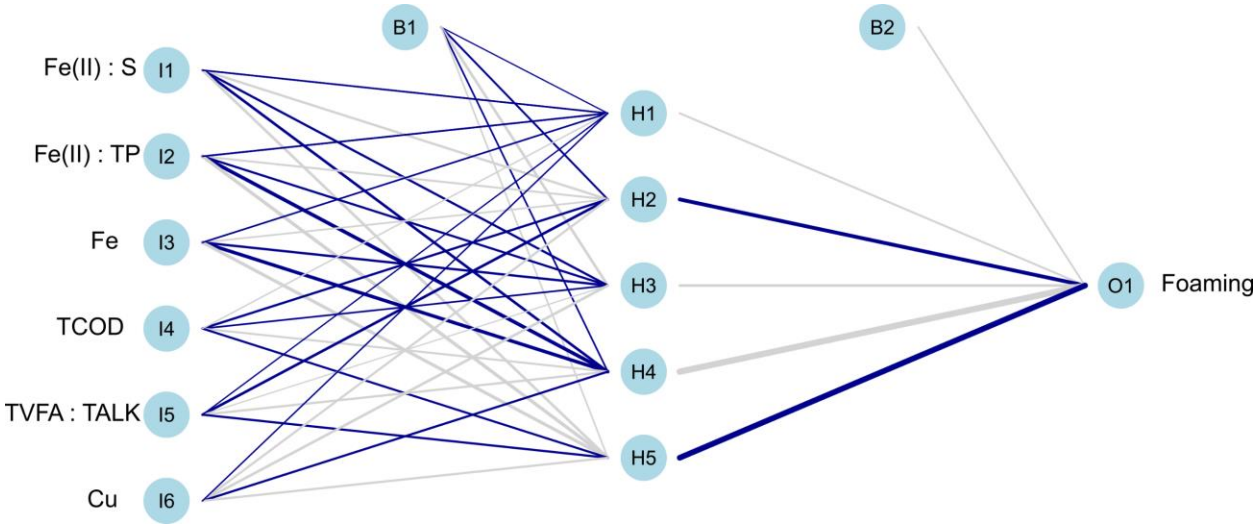

Figure 5-7. NN model for foaming classification.

Foaming potential

Using the backward-elimination strategy, the most relevant subset of variables for predicting foaming potential were SCOD : TCOD, TCOD : Sulfate, sulfate, copper, conductivity, VS, Fe(II) : S, Inorganic N, Fe(II) : TP, TVFA : TALK, and tannic acid (Figure 5-8)

After applying the forward elimination strategy to this subset, the combination of predictor variables with the lowest RMSE was Cu, sulfate, TCOD : Sulfate, SCOD : TCOD, and conductivity, with a RMSE of 0.048 (Table 5-4). Therefore, those were the predictor variables used in the final HYFIS model.

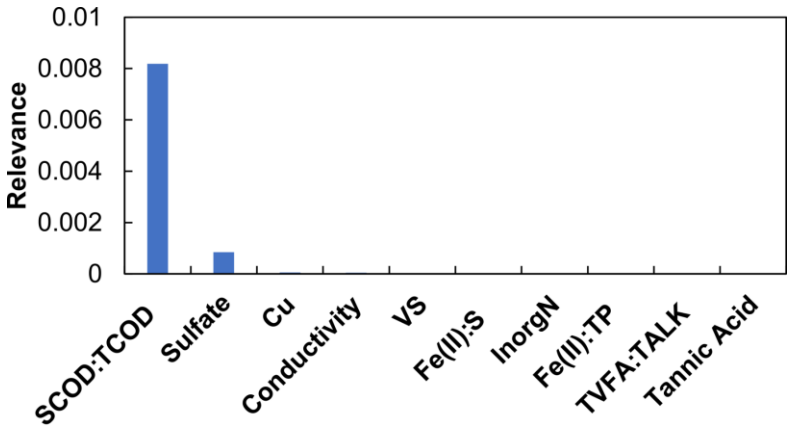

The relevance was determined by subtracting the RMSE value of the HYFIS model without that variable from the RMSE value of the HYFIS model for all the variables. The more positive the number the more relevant the variable.

Figure 5-8. The most relevant variables for determining foaming potential using the HYFIS model.

Table 5-4. RMSE values for the HYFIS models with different combinations of predictor variables.

Predictor Variables	RMSE
All	0.0830
SCOD : TCOD + Sulfate	0.0683
SCOD : TCOD + Sulfate + Cu	0.0489
SCOD : TCOD + Sulfate + Cu + Conductivity	0.0481
SCOD : TCOD + Sulfate + Cu + Conductivity + VS	0.0486
SCOD : TCOD + Sulfate + Cu + Conductivity + VS + Fe(II) : S	0.0520
SCOD : TCOD + Sulfate + Cu + Conductivity + VS + Fe(II) : S + Inorganic N	0.0510
SCOD : TCOD + Sulfate + Cu + Conductivity + VS + Fe(II) : S + Inorganic N + Fe(II) : TP	0.0510
SCOD : TCOD + Sulfate + Cu + Conductivity + VS + Fe(II) : S + Inorganic N + Fe(II) : TP +TVFA : TALK	0.0492

The optimal HYFIS model had 7 labels, 100 iterations, a 0.03 step size, and center of gravity (COG) as a defuzzification method. The model's predictions were compared with the test values from the data set (Figure 5-9). The R^2 value for the model was 81% and the RMSE was 0.048. This RMSE is lower than the one obtained in (J. Dalmau et al., 2008). In that study, the inflow rate, TVFA concentration, total organic carbon (TOC) concentration, pH in influent, pH in digester, CO_2, and CH_4 percentages were the only variables considered (J. Dalmau et al., 2008).

Simulation and validation of this study's model indicated that the foaming potential for individual digesters was more difficult to predict and required a fuzzy-logic method which was

more suited to the variability of the different digester combinations. Since foaming potential uses biogas volume and TS data, it could provide a useful metric for AD operators.

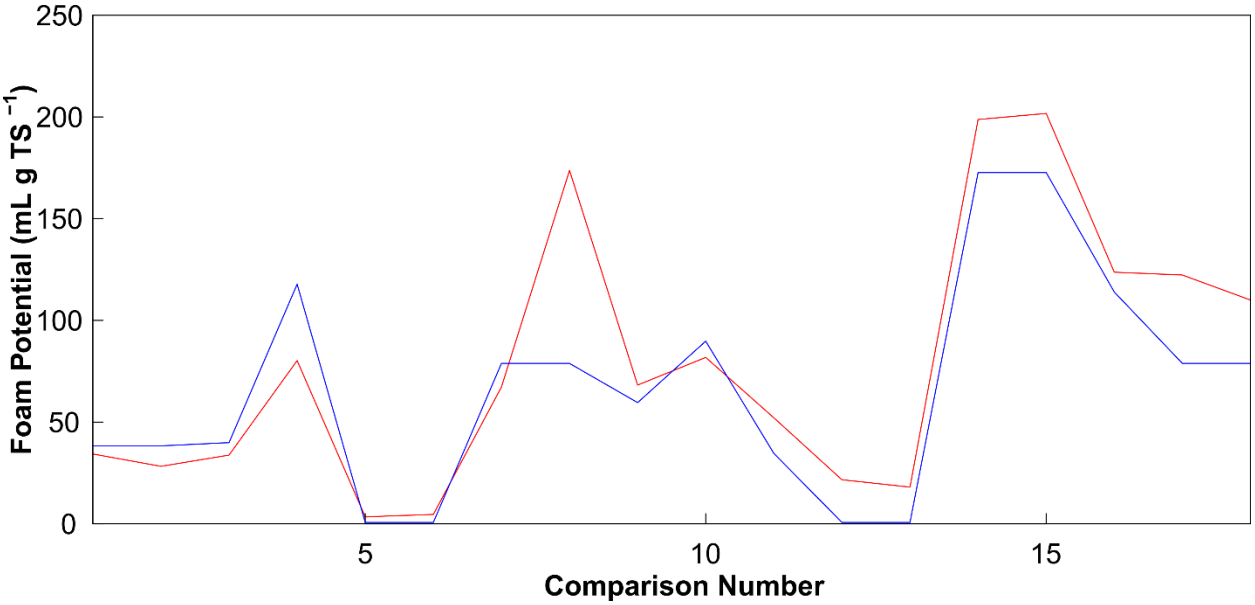

Figure 5-9. Comparison of the measured data (red) and the predictions (blue) from the HYFIS model for foam potential from the lab- digesters.

In both machine learning scenarios, TVFA : TALK, Fe(II) : S, Fe(II) : TP, and Cu were influential variables. The TVFA concentrations were significantly higher in the digester liquid (Table B-10) and effluent (Table B-11) samples during foaming, though not in the influent (Table 5-2). Elevated TVFA : TALK ratios have been observed in foaming lab-digesters (Ross & Ellis, 1992). The TVFAs are surface active agents which can contribute to foaming (Ganidi et al., 2009). The Fe(II) : S and Fe(II) : TP ratios were both significantly lower in the influent during foaming (Table 5-2). Therefore, less soluble iron was available relative to the sulfur and total phosphorus concentrations. The Cu concentration was significantly lower in the digester liquid samples during foaming (Table B-10). In the lab and field digesters, the microorganisms may have experienced a nutrient deficiency, which resulted in AD process imbalance and subsequent foaming. Additionally, copper and iron can also play a role in foam formation. In a simulated study of foaming in a gelatin mixture, the presence of copper sulfide shortened the time for foam collapse while the presence of ferric hydroxide ($FeOH_3$) increased foam height (Bikerman, 1973).

The most influential chemical parameters on foaming, which were identified using machine learning in this study, improved the understanding of causes of digester foaming. While

the chemical characteristics chosen in this study provided broad insight into the AD process, they were only recorded at discrete time-points. In the future, more studies on digester foaming are needed in modeling using larger datasets from more diversified digester feedstock and digester operation conditions. Controlled experiments which analyze the relationships discovered in this study can be developed to define the mechanisms of foaming.

5.5 Conclusions

The following conclusions were drawn from this chapter:

1. There were significant differences in the influent and digester liquid of a field digester during times of foaming and non-foaming.
2. Substrate and inoculum taken from foaming field digesters resulted in lower SMY values in lab-scale tests.
3. Important characteristics for predicting foaming were Fe(II) : S, Fe(II) : TP, TVFA : TALK, and Cu.
4. Machine learning predicted the foaming status of the industrial-scale digester with a predictive accuracy of 87% and the foaming potential of individual lab-scale digesters with an RMSE of 0.048 based on the influent characteristics.

5.6 References

Atandi, E., & Rahman, S. (2012). Prospect of anaerobic co-digestion of dairy manure: a review. *Environmental Technology Reviews*, *1*(1), 127–135. https://doi.org/10.1080/09593330.2012.698654

Banerjee, M., Capozzoli, M., McSweeney, L., & Sinha, D. (1999). Beyond kappa: A review of interrater agreement measures. *Canadian Journal of Statistics*, *27*(1), 3–23. https://doi.org/10.2307/3315487

Bergmeir, C., & Ben, M. (2015). frbs : Fuzzy Rule-Based Systems for Classification. *Journal of Statistical Software*, *65*(6), 1–30.

Bergmeir, C., & Benítez, J. M. (2012). Neural Networks in R Using the Stuttgart Neural Network Simulator: RSNNS. *Journal of Statistical Software*, *46*(7), 1–26. https://doi.org/10.18637/jss.v021.i05

Bikerman, J. J. (1973). Three-Phase Foams. In *Foams* (pp. 149–158). New York: Springer-Verlag. https://doi.org/https://doi.org/10.1007/978-3-642-86734-7

Boe, K., Kougias, P. G., Pacheco, F., O-Thong, S., & Angelidaki, I. (2012). Effect of substrates and intermediate compounds on foaming in manure digestion systems. *Water Science and Technology*, *66*(10), 2146–2154. https://doi.org/10.2166/wst.2012.438

Breiman, L., Friedman, J. H., Olshen, R. A., & Stone, C. J. (1984). Classification Algorithms and Regression Trees. In *Classification and Regression Trees* (pp. 29–33, 103–113). New York: Chapman & Hall / CRC Press (Formerly Monterey: Wadsworth and Brooks/Cole).

Breiman, Leo. (2001). Random forests. In R. E. Schapire (Ed.), *Machine Learning* (Vol. 45, pp. 5–32). Kluwer Academic Publishers. https://doi.org/10.1023/A:1010933404324

Cakmakci, M. (2007). Adaptive neuro-fuzzy modelling of anaerobic digestion of primary sedimentation sludge. *Bioprocess and Biosystems Engineering*, *30*(5), 349–357. https://doi.org/10.1007/s00449-007-0131-2

Carrasco, E. F., Rodríguez, J., Punal, A., Roca, E., & Lema, J. M. (2004). Diagnosis of acidification states in an anaerobic wastewater treatment plant using a fuzzy-based expert system. *Control Engineering Practice*, *12*(1), 59–64. https://doi.org/10.1016/S0967-0661(02)00304-0

Dalmau, J., Comas, J., Rodríguez-Roda, I., Latrille, E., & Steyer, J.-P. (2008). A neural network approach for selecting the most relevant variables for foaming in anaerobic digestion. *Proc. IEMSs 4th Biennial Meeting - Int. Congress on Environmental Modelling and Software: Integrating Sciences and Information Technology for Environmental Assessment and Decision Making, IEMSs 2008*, *3*, 1799–1804.

Dalmau, J., Comas, J., Rodriguez-Roda, I., Latrille, E., & Steyer, J. P. (2009). Validation of knowledge-based risk model for biological foaming in anaerobic digestion simulation. In *AiAi-2009 5th IFIP Conference on Artificial Intelligence and Innovations* (pp. 322–332). Thessaloniki, Greece.

Dalmau, Jordi, Comas, J., Rodríguez-Roda, I., Pagilla, K., & Steyer, J. P. (2010). Model development and simulation for predicting risk of foaming in anaerobic digestion systems. *Bioresource Technology*, *101*(12), 4306–4314. https://doi.org/10.1016/j.biortech.2010.01.056

Davenport, R. J., & Curtis, T. P. (2002). Are filamentous mycolata important in foaming? *Water Science and Technology*, *46*(1–2), 529–533.

De Clercq, D., Wen, Z., Fei, F., Caicedo, L., Yuan, K., & Shang, R. (2020). Interpretable machine learning for predicting biomethane production in industrial-scale anaerobic co-digestion. *Science of the Total Environment*, *712*, 134574. https://doi.org/10.1016/j.scitotenv.2019.134574

Fierro, J., Martinez, E. J., Rosas, J. G., Fernández, R. A., López, R., & Gomez, X. (2016). Co-Digestion of Swine Manure and Crude Glycerine: Increasing Glycerine Ratio Results in Preferential Degradation of Labile Compounds. *Water, Air, and Soil Pollution*, *227*(3). https://doi.org/10.1007/s11270-016-2773-7

Friedman, J., Hastie, T., & Tibshirani, R. (2010). Regularization Paths for Generalized Linear Models via Coordinate Descent. *Journal of Statistical Software*, *33*(1), 1–22.

Ganidi, N., Tyrrel, S., & Cartmell, E. (2009). Anaerobic Digestion foaming causes-A review. *Bioresource Technol*, *100*, 5546–5554. https://doi.org/10.1016/j.biortech.2009.06.024

Ganidi, N., Tyrrel, S., & Cartmell, E. (2011). The effect of organic loading rate on foam initiation during mesophilic anaerobic digestion of municipal wastewater sludge. *Bioresource Technology*, *102*(12), 6637–6643. https://doi.org/10.1016/j.biortech.2011.03.057

Gerardi, M. H. (2003). *The Microbiology of Anaerobic Digesters*. Hoboken, NJ: John Wiley & Sons, Inc. https://doi.org/10.1002/0471468967

IEA. (2019). *World Energy Outlook 2019*. Paris.

Jang, J. R. (1993). ANFIS : Adaptive-Network-Based Fuzzy Inference System. *IEEE Transactions on Systems, Man, and Cybernetics*, *23*(3). https://doi.org/10.1109/21.256541

Jiang, C., Qi, R., Hao, L., McIlroy, S. J., & Nielsen, P. H. (2018). Monitoring foaming potential in anaerobic digesters. *Waste Management*, *75*, 280–288. https://doi.org/10.1016/j.wasman.2018.02.021

Kanu, I. R., Aspray, T. J., & Adeloye, A. J. (2015). Understanding and Predicting Foam in Anaerobic Digester. *International Journal of Bioengineering and Life Sciences*, *9*(10), 1056–1060.

Kim, J., & Kasabov, N. (1999). HyFIS: Adaptive neuro-fuzzy inference systems and their application to nonlinear dynamical systems. *Neural Networks*, *12*(9), 1301–1319. https://doi.org/10.1016/S0893-6080(99)00067-2

Kohavi, R., & John, G. H. (1997). Wrappers for feature subset selection. *Artificial Intelligence*, *97*, 273–324. https://doi.org/10.1007/978-3-642-39038-8-27

Kougias, P. G., Boe, K., O-Thong, S., Kristensen, L. A., & Angelidaki, I. (2014). Anaerobic digestion foaming in full-scale biogas plants: A survey on causes and solutions. *Water Science and Technology*, *69*(4), 889–895. https://doi.org/10.2166/wst.2013.792

Kuhn, M. (2008). Building Predictive Models in R Using the caret Package. *Journal Of Statistical Software*, *28*(5), 1–26. https://doi.org/10.18637/jss.v028.i05

Møller, H. B., Sommer, S. G., & Ahring, B. K. (2004). Methane productivity of manure, straw and solid fractions of manure. *Biomass and Bioenergy*, *26*(5), 485–495. https://doi.org/10.1016/j.biombioe.2003.08.008

Murk, J. S., Frieling, J. L., Tortorici, L. D., & Dietrich, C. C. (1980). Use of bench-scale digesters to evaluate full-scale digester performance. *Journal of the Water Pollution Control Federation*, *52*(11), 2709–2716.

Nges, I. A., & Liu, J. (2010). Effects of solid retention time on anaerobic digestion of dewatered-sewage sludge in mesophilic and thermophilic conditions. *Renewable Energy*, *35*(10), 2200–2206. https://doi.org/10.1016/j.renene.2010.02.022

Niekerk, A. Van, Kawahigashi, J., Reichlin, D., Malea, A., & Niekerk, A. Van. (1987). Foaming in anaerobic digesters - a survey and laboratory investigation. *Water Pollution Control Federation*, *59*(5), 249–253.

NREL. (2013). *Biogas Potential in the United States (Fact Sheet)*. *Related Information: Energy Analysis, NREL (National Renewable Energy Laboratory)*. Golden, CO. https://doi.org/10.2172/1097303

Parkin, B. G. F., & Owen, W. F. (1987). Fundamentals of anaerobic digestion of wastewater sludges. *Journal of Environmental Engineering*, *112*(5), 867–920.

Poch, M., Comas, J., Rodríguez-Roda, I., Sànchez-Marrè, M., & Cortés, U. (2004). Designing and building real environmental decision support systems. *Environmental Modelling and Software*, *19*(9), 857–873. https://doi.org/10.1016/j.envsoft.2003.03.007

Ripley, B. D. (1996). *Pattern Recognition via Neural Networks*. Cambridge: Cambridge University Press.

Ross, R. D., & Ellis, L. A. M. (1992). Laboratory-scale investigation of foaming in anaerobic digesters. *Water Environment Research*, *64*(2), 154–162. https://doi.org/10.2175/wer.64.2.9

Schölkopf, B., Sung, K. K., Burges, C. J. C., Girosi, F., Niyogi, P., Poggio, T., & Vapnik, V. (1997). Comparing support vector machines with gaussian kernels to radial basis function classifiers. *IEEE Transactions on Signal Processing*, *45*(11), 2758–2765. https://doi.org/10.1109/78.650102

Starkweather, J., & Moske, A. K. (2011). Multinomial logistic regression. https://doi.org/10.1080/10543406.2012.756500

UNEP. (2019). *Emissions Gap Report 2019*. Nairobi.

Usack, J. G., & Angenent, L. T. (2015). Comparing the inhibitory thresholds of dairy manure co-digesters after prolonged acclimation periods: Part 1 – Performance and operating limits. *Water Research*, *87*, 1–12. https://doi.org/10.1016/j.watres.2015.05.055

Vardar-sukan, F. (1998). Foaming : Consequences, Prevention and Destruction. *Biotechology Advances*, *16*(5), 913–948. https://doi.org/https://doi.org/10.1016/S0734-9750(98)00010-X

Venables, W. N., & Ripley, B. D. (2002). *Modern Applied Statistics with S Fourth edition by*. *World* (Fourth, Vol. 53). Springer. https://doi.org/10.2307/2685660

Wang, L., Long, F., Liao, W., & Liu, H. (2020). Prediction of anaerobic digestion performance and identification of critical operational parameters using machine learning algorithms. *Bioresource Technology*, *298*(December 2019), 122495. https://doi.org/10.1016/j.biortech.2019.122495

Wang, L. X., & Mendel, J. M. (1992). Generating Fuzzy Rules by Learning from Examples. *IEEE Transactions on Systems, Man and Cybernetics*, *22*(6), 1414–1427. https://doi.org/10.1109/21.199466

Wen, C. H., & Vassiliadis, C. A. (1998). Applying hybrid artificial intelligence techniques in wastewater treatment. *Engineering Applications of Artificial Intelligence*, *11*(6), 685–705. https://doi.org/10.1016/s0952-1976(98)00036-0

CHAPTER 6. BIOCHEMICAL METHANE POTENTIAL TEST COMPARATIVE MODELING AND DEVELOPMENT OF MODELS FOR EARLY PREDICTION OF ANAEROBIC DIGESTER PERFORMANCE

6.1 Abstract

Anaerobic digestion (AD) is a technical solution for reducing odor, pathogens, and greenhouse gas (GHG) emissions from organic wastes. Biochemical methane potential (BMP) tests are used to determine the suitability of a given substrate for AD. Several BMP tests were conducted using a variety of substrate and inoculum types. The BMP test results were fitted using several kinetic models and the parameters were calculated. Several time-series forecasting algorithms were tested for early estimation of the specific methane yield (SMY). The experimental results revealed differences in methane production curves, hydrolysis rates, and time to reach the specific methane yield (SMY). No one kinetic model could be applied to every scenario. The Autoregressive Integrated Moving Average (ARIMA) algorithm most often produced the model with the lowest root mean square error (RMSE). The SMY could be predicted 25% ahead of the total test time.

6.2 Introduction

Anaerobic Digestion (AD) treats complex, organic wastes using a mixed microbial community. The AD process consists of four stages including hydrolysis, acidogenesis, acetogenesis, and methanogenesis (Parkin & Owen, 1987; Pavlostathis & Giraldo-Gomez, 1991). Hydrolysis is the breakdown of complex, organic molecules, such as polysaccharides, lipids, and proteins, by hydrolytic extracellular enzymes released by bacteria to smaller, soluble molecules which can be taken up by the cell membranes of microorganisms. The solubilized molecules then undergo conversion to volatile fatty acids (VFAs) (*i.e.*, acetate, propionate, isobutyrate, butyrate, valerate, isovalerate), alcohols, lactate, formate, carbon dioxide (CO_2), hydrogen (H_2), and ammonia. Next, some compounds from the acidogenesis stage, such as propionate, butyrate, isobutyrate, valerate, isovalerate, and ethanol are further degraded to acetic acid, formate, H_2 and CO_2. During methanogenesis, methane (CH_4) is produced from cleavage of the acetate molecule, a process known as acetoclastic methanogenesis, and the reduction of CO_2 by H_2 or formate, a

process known as hydrogenotrophic methanogenesis. The resulting biogas contains about 50-70% CH_4, 30-50% CO_2, and trace gases (NREL, 2013). The biogas can then be captured and used as a fuel source. AD technology can therefore stabilize organic wastes and be used as an alternative to fossil fuels.

The BMP test is a frequently used analysis to determine the feasibility of a substrate for AD. Organic waste materials have heterogeneous physical, chemical, and microbiological properties which can adversely affect the stability of the AD system, as indicated by decreased biogas production. The BMP test provides the maximum CH_4 yield (mL g VS^{-1}) for a substrate under conditions which are favorable conditions for fermentation (Owen, Stuckev, Healy, Young, & Mccarty, 1979). Because the test is performed at lab-scale in batch mode, it allows the researcher to easily modify the experimental design to determine the optimal conditions for continuous or semi-continuous AD. These conditions include retention time, organic loading rate (OLR), and dilution ratios. However, the BMP test can overestimate CH_4 yields or generally fail to replicate the unique conditions of a continuous AD system (Jerger, Chynoweth, & Isaacson, 1987; Labatut, Angenent, & Scott, 2011). There is interest in using kinetic modeling in combination with the BMP test to improve its predictive applicability to AD. More descriptive models may provide better insight into substrate hydrolysis and biodegradability while reducing the time needed for the BMP test.

One of the challenges of BMP test modeling is that the CH_4 production curves can vary greatly among batch BMP tests. Changes in operational parameters can affect the dynamic behavior of batch anaerobic digesters (Zhang et al., 2019) as well as differences in substrate type (Chynoweth, Turick, Owens, Jerger, & Peck, 1993; Turick et al., 1991). This presents unique challenges in modeling BMP tests. Early prediction of CH_4 production has been accomplished using the Monod equation (Donoso-Bravo, García, Pérez-Elvira, & Fdz-Polanco, 2011) and other kinetic equations (Dai, Duan, Dong, & Dai, 2013; Strömberg, Nistor, & Liu, 2015). However, differences in CH_4 production curves may mean that one kinetic equation does not fit all. Additionally, differences in operational parameters, substrates, and initial conditions can be difficult to isolate, obtain data from, or replicate.

Predicting CH_4 production using artificial intelligence tools may result in a better prediction. Time series forecasting is an area of machine learning which uses historical data to predict future values by analyzing trends in the data (Hyndman, R.J. Athanasopoulos, 2018). There are various

time series forecasting models which can be selected, fitted, and evaluated to the data set (Hyndman, R.J. Athanasopoulos, 2018). These models can then be used to predict future values. Thus, this process does not require knowledge of the substrate characteristics or information about the microbial or physical chemical processes in the digester.

Few studies have used time series forecasting to predict outcomes in AD systems. For decades, times series techniques have been recognized as useful for analyzing continuous high-quality digester data (Monteith & Stephenson, 1981). However, few studies have applied it. In one case, time series forecasting has been used to predict H_2 and CH_4 flowrate one hour in advance in an AD system (Ruiz, Castellano, González, Roca, & Lema, 2004). In that study, the auto-regressive integrated moving average with explanatory variable (ARIMAX) model was selected to model the data from a continuously-fed hybrid UASB-UAF digester with reportedly low error rates. Another study used fractal analysis of times series data of pH from an anaerobic sequencing batch reactor (AnSBR) digester and correlated the results to other process parameters such as CH_4 production and chemical oxygen demand (COD) (Sánchez-García et al., 2018). Ultimately, early prediction of CH_4 data can save time for AD operators. Little or no attention has been suggested for forecasting SMY.

The objectives of this chapter were to 1) evaluate CH_4 production curves related to different substrates in BMP tests; 2) pinpoint influential factors on CH_4 yields; 3) identify the best modeling method of BMP tests.

6.3 Materials and methods

6.3.1 Data and data preparation

The data used in this Chapter are part of the laboratory experimental data described in Chapter 4, section 4.3. Only sources of substrate and inoculum from Digesters F, B, and L (Section 4.3.1) and relevant result data from six lab tests (Table 4-2) were used in model development in this Chapter.

The data were composed of the BMP data, qualitative variables, and lab-digester liquid characterizations (Tables A-2 to A-5). The qualitative variables included 6 types of primary digester liquid by volume (INFL DM, EF, DL, WAS+PS, EF-R), 6 batch numbers (1-6), three

field digester collection locations (Digester F, B, L), two inoculum conditions (yes, no), and two digester foaming conditions (yes, no).

The BMP data was used for times series forecasting. Specifically, this BMP data included the measured methane yield (mL CH_4 g VS added $^{-1}$) for each sampling day for each BMP digester. In total, there were 100 different time series which were tested and 290 data points.

Before time series forecasting, the BMP data were transformed to stationary data by differencing the log-transformed data. Each BMP digester times series was tested individually. For the forecasting analysis, 75% of each time series for each BMP digester was used as training data and the remaining 25% was used for testing data. The root mean square error (RMSE) values were calculated from the forecasted and test data for each model type.

6.3.2 **Statistical methods and kinetic calculations**

All data analysis was conducted in Microsoft Excel and Rstudio (version 3.6.3 ((2020-02-29 Platform: x86_64-w64-mingw32/x64,64-bit).

The collected BMP data was evaluated using kinetic models. These models were identified as being frequently used for modeling in literature (Eqs. 6-1 to 6-5).

These kinetic models were fitted to the BMP data using nonlinear curve fitting in Excel. The models that were fitted included the first order model (Eq. 6-1), combined first order (Eq. 6-2), second order (Eq. 6-3), Chen & Hashimoto (Eq. 6-4), and modified Gompertz (Eq. 6-5). The RMSE value between the fitted and actual CH_4 yield was used as the objective function. The objective function was set to minimization. The fitted and measured values were compared using adjusted R^2 and RMSE to determine the accuracy of the model. These kinetic parameters were obtained using the GRG nonlinear Solver method in Excel.

The first order model was selected for fitting the BMP data as shown in Eq. 6-1 (Strömberg et al., 2015):

$$B = B_o[1 - \exp(-k_1 t)] \quad (6\text{-}1)$$

where k_1 is the rate coefficient (day^{-1}), t is time (days), B is the methane yield (mL g VS^{-1}), and B_o is the SMY (mL g VS^{-1}).

The combined first order model was selected for fitting the BMP data as shown in Eq. 6-2 (Strömberg et al., 2015):

$$B(t) = B_o\left(1 - f_d \cdot exp(-k_{1mod} \cdot t) - (1 - f_d) \cdot \exp(-k_{2mod} \cdot t)\right) \quad (6\text{-}2)$$

where k_{1mod} and k_{2mod} are the rate coefficients (day^{-1}), f_d is the biodegradable fraction (unitless), t is time (days), B is the methane yield (mL g VS^{-1}), and B_o is the SMY (mL g VS^{-1}).

The second order model was selected for fitting the BMP data as shown in Eq 6-3 (Strömberg et al., 2015):

$$B(t) = B_o\left(\frac{k_2 \cdot t}{1 + k_2 \cdot t}\right) \quad (6\text{-}3)$$

where k_2 is the rate coefficient (day^{-1}), t is time (days), B is the methane yield (mL g VS^{-1}), and B_o are the SMY (mL g VS^{-1}).

The Chen and Hashimoto model was selected for fitting the BMP data as shown in Eq. 6-4 (Kafle & Chen, 2016):

$$B(t) = B_o\left(1 - \frac{K_{CH}}{HRT \cdot \mu_m + K_{CH} - 1}\right) \quad (6\text{-}4)$$

where K_{CH} is the Chen and Hashimoto kinetic constant (unitless), HRT is the hydraulic retention time (days), μ_m is the maximum specific growth rate (day^{-1}), t is time (days), B is the methane yield (mL g VS^{-1}), and B_o are the SMY (mL g VS^{-1}).

The modified Gompertz model was selected for fitting the BMP data as shown in Eq. 6-5 (Strömberg et al., 2015):

$$B_{(t)} = B_o \cdot exp\left\{-exp\left[\frac{R_m.e}{H}(\lambda - t) + 1\right]\right\} \quad (6\text{-}5)$$

where λ is the lag phase (days), H is the Gompertz CH_4 production potential (mL CH_4 g VS^{-1}), R_m is the maximum specific CH_4 production rate (mL CH_4 g VS^{-1} day^{-1}), t is time (days), B is the methane yield (mL g VS^{-1}), and B_o is the SMY (mL g VS^{-1}).

Information on the BMP behavior was obtained from the BMP data. The time to reach 80% (T_{80}) and 90% (T_{90}) of the biogas production was calculated from the biogas data in Excel. The hydrolysis constant (k_h) from the first order time-dependency (Eq. 6-6) (Koch & Drewes, 2014) was also calculated for the lab-scale digesters in Excel:

$$k_h = \frac{t - 100}{t - t^2} \tag{6-7}$$

where k_h is the hydrolysis coefficient and t is time (days).

Effect calculations were used to assess the comparative fit of the different kinetic models. The effects of fitting the BMP data to the five different kinetic models (Eqs. 6-1 to 6-5) were calculated based on the method from (Strömberg et al., 2015) in which the RMSE of the fitted and measured data are calculated for each model type and then the average differences between each model type (Eq. 6-8):

$$E_{M1} = -\frac{1}{4} \cdot \left(\sum RMSE_{M1} - \sum_{i=M2:M5} RMSE_i \right) \tag{6-8}$$

where M is the model number.

The RMSE was calculated by Eq. (6-9):

$$RMSE = \frac{\sqrt{\sum \frac{(y_i - \hat{y}_i)^2}{n}}}{\bar{y}} \tag{6-9}$$

where n is the number of samples, y_i is the measured value, $\hat{y}_i$ is the predicted value, and $\bar{y}$ is the mean of the measured samples.

6.3.3 **New model development**

The package FactomineR in RStudio was used to develop a multiple linear regression model of the qualitative variables and the SMY data.

Machine learning was used for early prediction of BMP data through time series forecasting. Five time series algorithms were chosen for the forecasting of the BMP data. The *forecast* and *TSA* package in RStudio was used to develop an Autoregressive Integrated Moving Average (ARIMA(p, d, q)) model of CH_4 yield. The ARIMA model is expressed as (Hyndman, R.J. Athanasopoulos, 2018) (Eq. 6-10):

$$\grave{y_t} = c + \varphi_1 \grave{y_{t-1}} + \ldots + \varphi_p \grave{y_{t-p}} + \theta_1 \varepsilon_{t-1} + \ldots + \theta_q \varepsilon_{t-q} + \varepsilon_t \tag{6-10}$$

where y_t` is the differenced time series, p is the autoregressive parameter, or number of lags to use, d is the degrees of differencing (subtracting current value from previous value d times) to get a stationary data set, q is the moving average component error in mode and determines the number of terms to use, ε is the previous error terms, ϕ is the slope coefficient, and θ is the moving average parameter.

The ARIMA model is a popular forecasting model. The ARIMA model assumes stationary data (Bisgaard & Kulahci, 2011), identifies a model, estimates parameters, and then forecasts. The *auto.arima* function in Rstudio was used (Hyndman, R.J. Athanasopoulos, 2018; Hyndman & Khandakar, 2008).

Additionally, the Extreme Learning Machine (ELM) model was used for time series forecasting using the *nnfor* package in RStudio. ELM uses an algorithm for fitting single layer feed forward neural networks (Huang, Zhu, & Siew, 2006).

Neural networks were used to forecast the BMP data. *Nnetar* was in the forecast package in Rstudio for fitting feed-forward neural networks with a single hidden layer (Kourentzes, Barrow, & Crone, 2014).

The KNN model was used for forecasting in the tsfknn package in Rstudio (Martinez, Frias, 2019). The KNN model uses the *k*-nearest neighbor regression for forecasting.

The multi-layer perceptron (MLP) model was generated using the RSNNS package in RStudio. This model consists of connected feed-forward networks.

6.4 Results and discussion

6.4.1 Methane yield

The CH_4 yield results varied considerably among the different lab-digester groups. Predominantly, first- and second-order type curves were evident in Batches 2-5. There was a rapid increase in CH_4 yield and then a gradual levelling off. The CH_4 yield curves also varied considerably from the Digester L samples, most likely due to the variety of different treatment types. Several lab-digesters from Batches 1 and 6 experienced Gompertz-type growth curves with short lags before a rapid increase in CH_4 production and then a leveling off. All lab-digesters in Batch 1 except lab-digester group number 1-5 demonstrated this lag (Figure 6-1). Lab-digester group numbers 6-32, 6-35 through 6-40, and 6-42 also demonstrated this lag (Figure 6-1). The

lags in Batch 6 may be attributed to relatively low initial pH values (6.46-6.85) which increased over time to neutral values (Table A-2). However, the curves for treatments 6-35 through 6-38 indicate polyauxic behavior, in which there are extended lags and multiple lags and CH_4 production. These types of curves indicate an "unhealthy" BMP digester with inhibition (Koch, Hafner, Weinrich, & Astals, 2019). The inhibition may be due to low pH or an inadequate ISR ratio. The lags in Batch 1 may be attributed to the presence of dairy manure which is less readily degradable than other types of manure (Hill, 1982; Kafle & Chen, 2016).

The SMY values also varied for the different lab-digester group numbers. The final SMY for dairy manure was higher than for the mixed industrial wastes from Digester B (Table 6-2). The SMY for dairy manure with inoculum was higher (154 mL g VS^{-1}) than without (138 mL g VS^{-1}) (Table 6-2). Digesters containing influent from Digester B had unusually low CH_4 production despite having active cumulative gas production. The final SMY values were 9 mL g VS^{-1} for lab-digester group number 2-7, 4 mL g VS^{-1} for lab-digester group number 2-8 (Table 6-2). The final SMY values for Digester B from Batch 3 were 0.17 mL g VS^{-1} for lab-digester group numbers 3-13, 0.21 g VS^{-1} for lab-digester group numbers 3-15, 61 mL g VS^{-1}, and 74 mL g VS^{-1} (lab-digester group number 3-16) (Table 6-2). Higher SMYs were obtained from the Batch 5 test. The substrate and inoculum for the Batch 5 tests were collected from a field digester which was not foaming. There was a lot of variation in BMP yields from the Batch 6 lab-scale digesters (Figure 6-1). The low SMY (7.2-10 mL g VS^{-1}) values came from SM samples with a 50% COD loading or higher (lab-digester group numbers 6-41 through 6-43) (Table 6-2). The highest SMY value was 196 mL g VS^{-1} from a digester with 75% COD from an S3 sample (lab-digester group number 6-38).

The low SMY yields from digesters containing Digester B influent may be attributed to the source of the influent. The influent was a co-digested mixture of several different feedstocks. Generally, BMP tests can fail to represent the synergistic and antagonistic effects of co-digested substrates (Koch, Hafner, Weinrich, Astals, & Holliger, 2020). In real life, the Digester B influent is gradually added to the functioning digester, and therefore, the microbial community would be better acclimated than in this batch BMP test.

The variability of the CH_4 yields in this study is reflective of variability of CH_4 yields in literature. Dairy manure slurry produces approximately 126-243 mL CH_4 g VS^{-1} (Amon et al., 2007; Kafle & Chen, 2016; Labatut et al., 2011; Møller, Sommer, & Ahring, 2004; Usack & Angenent, 2015; Vedrenne, Béline, Dabert, & Bernet, 2008), which corresponds with the values

in this study (Table 6-2). Primary sludge (PS) and waste activated sludge (WAS) can have SMYs which range from 108-132 mL g VS or COD^{-1} (Amha, Sinha, Lagman, Gregori, & Smith, 2017; Elbeshbishy, Nakhla, & Hafez, 2012; Ohemeng-Ntiamoah & Datta, 2018). Starch has had SMYs of 315 mL g COD^{-1} (Elbeshbishy & Nakhla, 2012) and 320 mL g VS^{-1} (Raposo et al., 2011). The variability of the Test 6 samples which contained mixtures of WAS, PS, and cornstarch-based wastes reflect these differences. Most likely, the presence of PS and WAS decreased the SMY value of the cornstarch-based substrates. However, the lower values in lab-digester group numbers 6-41 through 6-43 may have been due to antagonistic effects of the SM mixture.

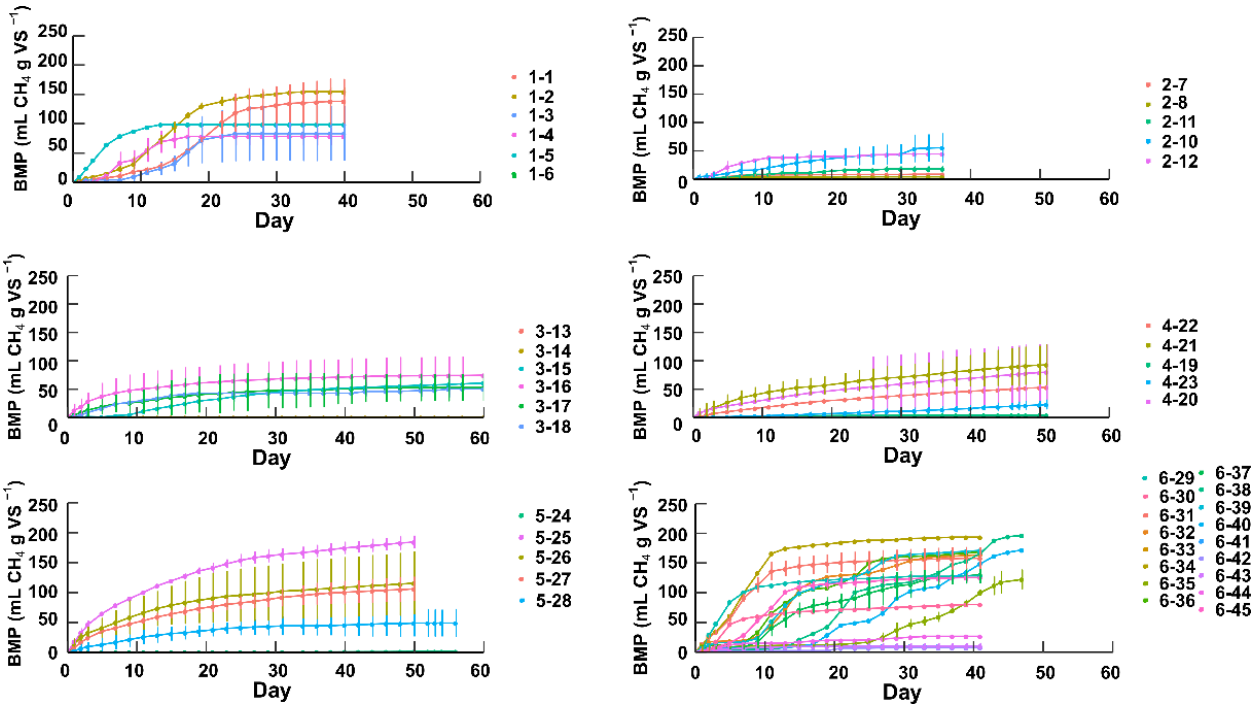

Figure 6-1. The average methane yields (mL CH_4 g VS^{-1}) and standard deviation over time from each lab-digester group.

6.4.2 Influential factors on methane yield

There were differences in the CH_4 yield results between different batches. The most influential qualitative variable on final SMY (mL g VS^{-1}) from the FactomineR analysis was foaming ($P < .001$) (Table 6-1). The substrate and inoculum collected for the BMP tests Batches 2-4 were collected from field digesters experiencing foaming, and thus experienced lower CH_4 yields. However, the adjusted R^2 value was 0.27 indicating that this model was a poor fit. The FactomineR results use a linear model, which was not the best model to predict future BMP data.

Table 6-1. FactoMineR results for the lab-digesters.

	Intercept	**Foaming**
Estimate	183.55	-70.60
Std. Error	18.40	12.18
***t*-value**	9.98	-5.80
***P* value**	< .001	< .001
Significance	***	***

** P < .05, ** P < .01, *** P < .001*

6.4.3 Kinetic models

There were considerable differences among the fitted SMYs for the different model types. Almost all lab-digester group numbers had at least one fitted SMY with an R^2 value greater than 0.90 (Table 6-2). The Chen and Hashimoto model had a negative effect in nearly all cases (Figure 6-2, Table C-1) and was the worst performing model. Batches 1 and 6 had reliable predictions from the Gompertz model (Table 6-2). Batches 2-6 had particularly good fits from the first and second order models (Table 6-2). However, lab-digester group numbers 3-13, 6-41, and 6-42, did not have good SMY predictions for any model type (Table 6-2). All three of these lab-digester treatments had very low SMY values and most likely experienced inhibition (Table 6-2). Therefore, predicting SMY values can be a challenge when there is a source of inhibition.

The kinetic parameters and their adjusted R^2 values from Equations 6-1 through 6-6 are summarized in (Table 6-3). The kinetic parameters calculated using the Chen and Hashimoto model generally had poor R^2 values (-0.15-0.89) (Table 6-3). The lag times for CH_4 production from the modified Gompertz model varied from 0 to 71 days (Table 6-3). Not surprisingly, first order and second order models had high R^2 values (> 0.90) in many cases. Many of the CH_4 yield curves from Batches 2-5 had first and second order shaped curves. In most cases, the first order curve was a better fit than the first order modified.

Calculations from the biogas data demonstrated the differences in digester treatments. The T_{90} values ranged from 7-50 for all lab-scale digesters, indicating the variability in time required to reach full biogas production (Table 6-4). The T_{90} values for Batches 2-5 were generally higher (23 to 50 days) than Batches 1 and 6 (7 to 42 days) which were reflective of the gradual increase of their first-order and second order CH_4 yield curves (Table 6-4). Inclusion of full biogas data analysis can provide further insight into the microbial activity of the system.

The hydrolysis coefficients also provided insight to the CH_4 yield data. The hydrolysis constant, k_h ranged from 0.01-0.31, though most samples had lower k_h values (0.04-0.01 day^{-1})

(Table 6-4). These relatively low k_h values coincided with the length of time required for the batch tests (greater than 30 days) as well as the lag time for CH_4 production in many cases. This is most likely due to the presence of recalcitrant materials which required additional time to hydrolyze.

In summary, there were noticeable differences among the different waste types. The variability in lag times as well as the time to reach 80% and 90% of total biogas production (T_{80}, T_{90}) can have implications for the length of future BMP testing. In this study, all tests required longer than 30 days, and Batch 3 required 60 days to reach the SMY. Additionally, the generally low hydrolysis values suggest that a long time is required for complete CH_4 production as hydrolysis can be the limiting step. In fact, some studies recommend performing BMP testing for as long as 80 or 100 days (Ponsá, Gea, & Sánchez, 2011; Vedrenne et al., 2008) to ensure complete results. Overall, there was no one model which fit every different type of CH_4 production. Awareness of substrate type may be essential before choosing a predictive model.

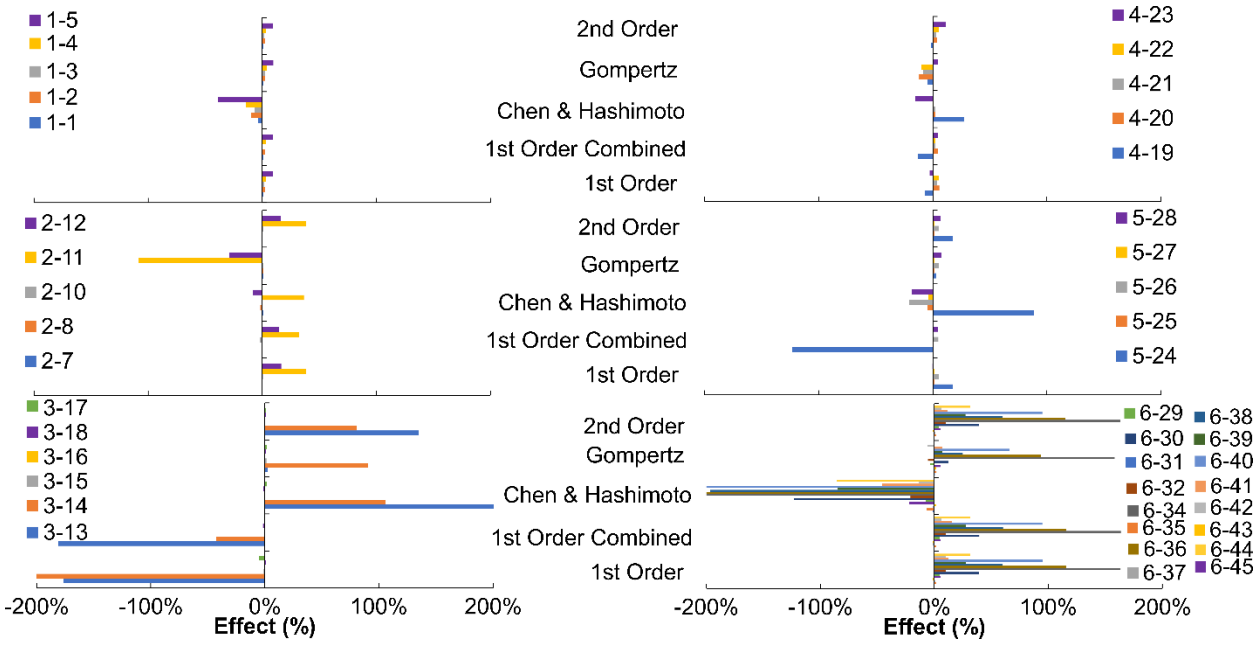

Figure 6-2. The effect (%) calculations of how well each BMP model from literature fitted the measured BMP data (mL CH_4 g VS^{-1}) for each lab-digester group.

Table 6-2. The measured and fitted SMY values with the adjusted R^2 in parenthesis for each lab-digester group number.

Lab-digester Group No.	**SMY**	**SMY Chen & Hashimoto**	**SMY Modified Gompertz**	**SMY 1st order**	**SMY 2nd order**	**SMY 1st order modified**
1-1	138	156(0.94)	153(0.86)	80(0.94)	81(0.94)	78(0.94)
1-2	154	186(0.78)	164(0.98)	143(0.94)	143(0.94)	138(0.94)
1-3	83	79(0.86)	97(0.93)	27(0.89)	27(0.89)	50(0.89)
1-4	78	82(0.92)	78(0.99)	67(0.97)	67(0.97)	67(0.97)
1-5	99	0.18(-0.15)	94(1)	110(0.96)	111(0.96)	109(0.97)
2-7	8.8	9.0(0.91)	8.6(0.97)	9.9(0.8)	11(0.78)	9.9(0.8)
2-8	4.3	4.9(0.48)	4.5(0.93)	4.5(0.9)	4.7(0.87)	4.5(0.9)
2-10	55	0.23(0.99)	52(0.98)	52(0.99)	52(0.99)	52(0.35)
2-11	18	18(0.98)	40(0.92)	20(0.98)	20(0.98)	18(0.42)
2-12	45	54(0.15)	195(0.97)	47(0.74)	47(0.7)	45(0.53)
3-13	0.17	0.15(-0.05)	0.15(0.76)	0.17(0.72)	0.17(0.84)	0.017(0.62)
3-14	0.21	0.21(0.18)	0.2(1)	0.21(0.2)	0.21(0.97)	0.17(0.82)
3-15	61	66(0.97)	59(0.99)	61(0.05)	33(0.93)	0.94(0.12)
3-16	75	74.66(1)	67(0.9)	75(0.96)	74(1)	42(0.89)
3-17	53	52(1)	48(0.85)	50(0.99)	76(0.85)	16(0.85)
3-18	50	46(0.99)	44(0.92)	50(0.95)	53(0.92)	4(0.72)
4-19	4.1	4.1(0.92)	4(0.93)	0.67(1)	1.3(0.76)	0.028(0.97)
4-20	80	90(0.81)	95(0.92)	70(0.92)	130(0.99)	18(0.96)
4-21	93	94(0.99)	80(0.93)	83(0.97)	122(0.93)	24(0.47)
4-22	53	62(0.8)	45(0.95)	52(1)	54(1)	4.1(-0.02)
4-23	23	0.18(NA)	21(0.99)	19(0.99)	19(0.99)	2.0(-0.03)
5-24	1.2	2.0(-0.02)	0.99(0.91)	0.95(1)	0.93(0.9)	0.042(0.03)
5-25	184	216(0.66)	166(0.96)	171(0.98)	181(1)	40(0.94)
5-26	116	0(NA)	103(0.95)	105(0.97)	165(0.84)	66(0.97)
5-27	106	123(0.71)	95(0.95)	98(0.98)	104(1)	19(-0.03)
5-28	49	0.3(NA)	44(0.97)	49(1)	70(0.85)	0.042(0.46)
6-29	129	6.7(0.82)	120(0.97)	190(0.6)	192(0.59)	153(0.71)
6-30	80	575(0.07)	104(0.6)	115(0.65)	114(0.65)	80(0.95)
6-31	158	167(0.96)	157(1)	248(0.71)	250(0.7)	254(0.54)
6-32	164	0(0.79)	740(0.66)	182(0.91)	189(0.91)	179(0.91)
6-34	193	393(0.88)	195(0.99)	293(0.68)	28(0.18)	212(0.92)
6-35	115	147(0.89)	91(0.97)	44(0.8)	44(0.8)	44(0.8)
6-36	169	103.18(-0.04)	189(0.96)	168(0.93)	34(0.94)	165(0.93)
6-37	130	140(0.97)	146(0.95)	99(0.96)	99(0.96)	254(0.96)
6-38	196	195(0.87)	137(0.9)	34(0.93)	35(0.93)	40(0.95)
6-39	171	209(0.87)	194(0.96)	174(0.94)	35(0.95)	14(0.06)
6-40	172	162(0.86)	214(0.93)	49(0.93)	48(0.92)	6.5(0)
6-41	10	25(0.48)	12(0.65)	15(0.69)	11(0.73)	7.6(0.74)
6-42	7.2	9.8(0.7)	8.8(0.77)	8.3(0.84)	11(0.87)	2.3(0.08)
6-43	9.8	10.1(0.97)	12(0.55)	15.6(0.87)	15(0.63)	15(0.62)
6-44	27	38(0.77)	42(0.65)	37(0.88)	36(0.89)	29(0.95)
6-45	126	11(-0.05)	105(0.99)	108(0.77)	105(0.79)	109(0.75)

Table 6-3. The fitted kinetic parameters and their R^2 value in parenthesis for each lab-digester group.

No	μ_m Day^{-1} Eq. 6-4	K_{chen} Day^{-1} Eq. 6-4	k_1 Day^{-1} Eq. 6-1	k_2 Day^{-1} Eq. 6-3	k_{1mod} Day^{-1} Eq. 6-2	k_{2mod} Day^{-1} Eq. 6-2	Lag Day^{-1} Eq. 6-5	R_m mL g VS day^{-1} Eq. 6-5
1-1	0.31 (0.94)	105(0.94)	0.0016 (0.94)	0.00037 (0.94)	0.0024 (0.94)	0.0024 (0.94)	7.5(0.87)	5.9(0.87)
1-2	0.00021(0.78)	0.99(0.78)	0.00068(0.94)	0.00041(0.94)	0.0035 (0.94)	0.0035 (0.94)	4.0(0.98)	7.6(0.98)
1-3	0.27(0.86)	179049(0.86)	0.0015(0.89)	0.0056(0.89)	0.10(0.89)	0.40(0.89)	27(0.93)	27(0.93)
1-4	0.00059(0.92)	0.99(0.92)	0.00043(0.97)	0.0039(0.97)	0.013(0.97)	0.013(0.97)	3.5 (0.99)	7.8(0.99)
1-5	0.000048(-0.15)	0.33(-0.15)	0.060(0.97)	0.031(0.96)	0.063(0.97)	0.063(0.97)	0.60(1)	16(1)
2-7	0.86(0.91)	3.7(0.91)	0.048(0.80)	0.028(0.78)	0.048(0.80)	0.048(0.80)	1.3(0.97)	0.96(0.97)
2-8	0.00022(0.48)	0.99(0.48)	0.12(0.90)	0.086(0.87)	0.12(0.90)	0.12(0.90)	0.0 (0.93)	0.44(0.93)
2-10	959 (0.99)	74701 (0.99)	0.032(0.99)	0.020(0.99)	6.9(0.10)	3.6(0.10)	0.24(0.98)	2.0(0.98)3.
2-11	1.326 (0.98)	68(0.98)	0.032(0.98)	0.019(0.98)	6.0(0.42)	3.0(0.42)	3.5(0.92)	4.1(0.92)
2-12	0.000019(0.15)	1.0(0.15)	0.00065(0.74)	0.00014(0.70)	5.9(0.53)	3.0(0.53)	2.3(0.97)	44(0.97)
3-13	1.1(-0.053)	0.31(-0.53)	8.2 e-07(0.72)	0.41(0.84)	0.040(0.62)	0.18(0.62)	2.8(0.76)	1.0(0.76)
3-14	0.00068(0.18)	0.88(0.18)	1.6e-06(0.20)	2.3(0.97)	0.40(0.82)	0.21(0.82)	0.031(1)	0.15(1)
3-15	1.73(0.97)	1502(0.97)	0.00015(0.05)	0.000055(0.93)	0.010(0.12)	0.16(0.12)	7.6(0.99)	2.2(0.99)
3-16	8251(1)	53940(1)	0.16(0.96)	0.17(1)	0.010(0.89)	0.098(0.89)	0.0(0.90)	7.9(0.90)
3-17	6268(1)	82624(1)	0.093(0.99)	0.00037(0.85)	0.010(0.85)	0.13(0.85)	0.0(0.96)	3.2(0.96)
3-18	2134(1)	26212(0.99)	0.063(0.95)	0.045(0.92)	0.010(0.71)	0.187(0.71)	1.2(0.98)	4.0(0.98)
4-19	0.55(0.92)	5.2(0.92)	0.00099(1)	0.000012(0.76)	0.010(0.97)	0.083(0.97)	4.3(0.93)	0.35(0.93)
4-20	0.000084(0.81)	0.99(0.81)	0.064(0.92)	0.064(0.99)	0.10(0.96)	0.13(0.96)	0.0(0.93)	1.9(0.93)
4-21	3015 (0.99)	103485(0.99)	0.074(0.97)	0.00024(0.93)	0.010(0.47)	0.12(0.47)	0.0(0.93)	4.3(0.93)
4-22	0.00013(0.80)	0.99(0.80)	0.033(1)	0.023(1)	0.010(-0.025)	0.17(-0.025)	1.7(0.95)	2.1(0.95)
4-23	0.26(0)	0(0)	0.00012(0.99)	0.00016(0.99)	0.010(-0.027)	0.11(-0.027)	6.6(0.99)	0.51(0.99)
5-24	0.14(-0.018)	0.031(-0.018)	0.00014(1)	0.00087(0.90)	0.010(0.026)	0.17(0.026)	7.4(0.91)	0.026(0.91)
5-25	0.00013(0.66)	0.99(0.66)	0.092(0.98)	0.082(1)	0.100(0.94)	0.16(0.94)	0.0 (0.96)	11(0.96)
5-26	0.015(0)	110(0)	0.11(0.97)	0.00034(0.84)	0.010(0.97)	0.09(0.97)	0.0(0.95)	7.5(0.95)
5-27	0.000075(0.7218)	0.99(0.71)	0.079(0.98)	0.066(1)	0.010(-0.033)	21(-0.033)	0.0(0.95)	5.4(0.95)
5-28	412177(0)	0(0)	0.059(1)	0.00033(0.85)	0.010(0.46)	0.13(0.46)	0.92(0.97)	2.8(0.97)
6-29	0.97(0.82)	2.75(0.82)	0.0039(0.60)	0.00083(0.59)	0.19(0.71)	0.13(0.71)	1.3(0.54)	31(0.54)
6-30	0.00014(0.07)	0.99(0.07)	0.00045(0.65)	0.00027(0.65)	0.12(0.95)	0.00(0.95)	0.0(0.77)	2.5(0.77)
6-31	1.03(0.96)	6.25(0.96)	0.0048(0.71)	0.0011(0.70)	0(0.54)	0.0092(54)	0.48(1)	14(1)
6-32	0.078(0.79)	820(0.79)	0.00060(0.91)	0.0013(0.91)	0.0025(0.91)	0.0025(0.91)	43(0.66)	106(0.66)
6-34	1257095(0.88)	12507832(0.88)	0.0010(0.68)	20016452(0.18)	0.075(0.92)	0.0027(0.92)	0.98(0.99)	17(0.99)
6-35	0.00045(0.89)	0.98(0.89)	0.00015(0.80)	0.000091(0.80)	0.00076(0.80)	0.00076(0.80)	71(0.96)	16(0.96)

Table 6-3 continued.

No	μ_m Day^{-1} Eq. 6-4	K_{chen} Day^{-1} Eq. 6-4	k_1 Day^{-1} Eq. 6-1	k_2 Day^{-1} Eq. 6-3	k_{1mod} Day^{-1} Eq. 6-2	k_{2mod} Day^{-1} Eq. 6-2	Lag Day^{-1} Eq. 6-5	R_m mL g VS day^{-1} Eq. 6-5
6-36	0.50(-0.04)	2.0E-05(-0.04)	0.0055(0.93)	0.00040(0.94)	0.0018(0.93)	0.0018(0.93)	4.4(0.97)	6.7(0.97)
6-37	305(0.97)	35000(0.97)	0.0035(0.96)	0.0013(0.96)	0.10(0.96)	0.40(0.96)	6.0(0.95)	4.9(0.95)
6-38	0.18(0.87)	107619(0.87)	0.00011(0.93)	0.00040(0.93)	0.00051(0.95)	0.00051(0.95	28(0.90)	13(0.90)
6-39	689(0.87)	118491654(0.87)	0.00057(0.94)	0.00040(0.95)	956(0.06)	2679(0.06)	4.5(0.96)	6.4(0.96)
6-40	0.14(0.86)	152841(0.86)	0.00014(0.93)	0.00040(0.92)	459(0.005)	808(0.005)	65(0.93)	55(0.93)
6-41	490(0.48)	511042841(0.48)	0.000059(0.69)	0.00040(0.73)	11(0.74)	20(0.74)	0(0.75)	3.1(0.75)
6-42	1583(0.70)	2312898273(0.70)	0.000027(0.84)	0.00040(0.87)	170(0.08)	271(0.08)	39(0.80)	0.57(0.80)
6-43	13781(0.97)	52016(0.97)	0.000041(0.87)	0.000036(0.63)	0.00091(0.62)	0(0.62)	0.0(0.55)	0.29(0.55)
6-44	1342(0.77)	532843585(0.77)	0.00012(0.88)	0.00040(0.89)	0.036(0.95)	0.036(0.95)	1.3(0.82)	3.2(0.82)
6-45	0.35(-0.050)	0(-0.050)	0.00035(0.77)	0.0070(0.79)	0.00026(0.75)	0.00026(0.75)	3.5(0.99)	9.9(0.99)

Table 6-4. Calculated values for each lab-digester group.

Lab-digester group No.	**K_h Day^{-1} Eq. 6-7**	**T_{80} day**	**T_{90} day**
1-1	0.04	16	22
1-2	0.05	17	26
1-3	0.11	0	7
1-4	0.31	26	31
1-5	0.4	28	35
2-7	0.07	8	23
2-8	0.11	27	31
2-10	0.05	27	31
2-11	0.1	29	31
2-12	0.07	30	31
3-13	0.05	9	30
3-14	0.09	13	35
3-15	0.01	31	43
3-16	0.01	18	29
3-17	0.02	34	42
3-18	0.02	42	50
4-19	0.04	24	31
4-20	0.02	34	43
4-21	0.02	33	41
4-22	0.02	35	42
4-23	0.02	42	47
5-24	0.02	38	44
5-25	0.02	22	32
5-26	0.02	24	36
5-27	0.02	27	34
5-28	0.02	28	42
6-29	0.04	7	12
6-30	0.04	12	23
6-31	0.04	9	11
6-32	0.04	23	25
6-34	0.04	10	13
6-35	0.04	29	33
6-36	0.04	24	26
6-37	0.04	28	33
6-38	0.02	40	42
6-39	0.04	25	27
6-40	0.02	39	42
6-41	0.05	13	16
6-42	0.04	21	21
6-43	0.04	12	13
6-44	0.04	26	29
6-45	0.04	8	17

6.4.4 Times series forecasting

The results of the time series forecasting are summarized in (Table 6-5). No one forecasting model worked for all lab-digesters. In some cases (lab-digester group numbers 1-1, 2-7, 3-13, 4-19, 6-29), the RMSE values between the real and predicted data were very high, indicating a poor prediction. For these lab-digester treatments, the other replicates showed better RMSE values. The forecasted values were based on 75% of the previous values, which was 9 to 15 days in advance for all batches (Figures C-1 through C-7).

The ARIMA model was most frequently the best time series forecasting model (Table 6-5). Both neural network models and time series models have been used to forecast in an up-flow anaerobic sludge blanket (UASB) scale steady-state digester (Ruiz et al., 2004). Lab-scale digesters are not "steady-state" and therefore have changing CH_4 yield production with time. The ARIMA model is unique because it accounts for the autocorrelations in the data and is flexible for many different types of time series patterns (Hyndman, R.J. Athanasopoulos, 2018). The model is able to use previous data to predict future data points which is an optimal scenario in AD.

Table 6-5. Optimal forecasting model and RMSE value for each lab-scale digester.

Lab-digester group No.	Replicate	Best Model	RMSE
1-1	B	NNETAR	1.819
1-1	C	ARIMA	0
1-2	A	ARIMA	0.038
1-2	B	ELM	0.003
1-2	C	ARIMA	0.015
1-3	A	ARIMA	0.006
1-3	B	ARIMA	0
1-3	C	ELM	0
1-4	A	ARIMA	0
1-4	B	ARIMA	0
1-4	C	ARIMA	0
1-5	A	ARIMA	0
2-7	A	NNETAR	1.779
2-7	B	ARIMA	0
2-7	C	ARIMA	0.101
2-8	A	ARIMA	0
2-8	C	ARIMA	0
2-10	A	KNN	0
2-10	B	ARIMA	0
2-10	C	ARIMA	0.258
2-11	A	ARIMA	0.119
2-11	B	ARIMA	0
2-12	A	ARIMA	0
2-12	B	MLP	0.005

Table 6-5 continued.

Lab-digester group No.	Replicate	Best Model	RMSE
3-13	A	KNN	2.282
3-13	B	ARIMA	0
3-13	C	ARIMA	0
3-14	A	ARIMA	0
3-14	B	ARIMA	0
3-15	B	ARIMA	0
3-15	C	KNN	0.065
3-16	A	ARIMA	0.010
3-16	B	NNETAR	0.057
3-16	C	ARIMA	0.008
3-17	A	ARIMA	0.023
3-17	B	ARIMA	0
3-18	A	ARIMA	0
3-18	B	KNN	0.064
4-19	B	ARIMA	1.581
4-20	A	ARIMA	0
4-20	B	MLP	0.014
4-20	C	ARIMA	0.069
4-21	A	ARIMA	0.050
4-21	B	KNN	0.034
4-21	C	ELM	0.017
4-22	A	ARIMA	0.020
4-22	B	ELM	0.023
4-22	C	ELM	0.030
4-23	A	NNETAR	0.048
4-23	B	NNETAR	0.072
5-24	A	NNETAR	1.660
5-24	B	ARIMA	0.075
5-24	C	KNN	0
5-25	A	ELM	0.081
5-25	B	NNETAR	0.012
5-25	C	ELM	0.012
5-26	A	ELM	0.011
5-26	B	MLP	0.012
5-26	C	KNN	0.011
5-27	A	ARIMA	0.018
5-27	B	ARIMA	0.015
5-27	C	ELM	0.011
5-28	A	MLP	0.010
5-28	B	MLP	0.028
6-29	A	ARIMA	2
6-30	A	ARIMA	0.005
6-31	A	KNN	0.011
6-31	B	MLP	0.004
6-31	C	ARIMA	0
6-32	A	ARIMA	0
6-34	A	ARIMA	0.006
6-35	A	ARIMA	0.001
6-35	B	NNETAR	0.157
6-35	C	ELM	0.198
6-36	C	MLP	0.088

Table 6-5 continued.

Lab-digester group No.	Replicate	Best Model	RMSE
6-37	A	NNETAR	0.009
6-37	B	ARIMA	0.010
6-37	C	ARIMA	0.006
6-38	A	ARIMA	0.008
6-39	A	NNETAR	0.052
6-40	A	ARIMA	0.008
6-41	A	MLP	0.051
6-42	A	ELM	0.010
6-43	A	ARIMA	0
6-43	B	MLP	0.027
6-43	C	ARIMA	0
6-44	A	ARIMA	0.001
6-45	A	ARIMA	0
6-45	B	ARIMA	0.002

A unique array of materials were chosen for this study. This is evidenced in the CH_4 yield results which indicate a variety of CH_4 production curves (Figure 6-1) as well as the differences in hydrolysis coefficients and T_{80} and T_{90} values (Table 6-4). Therefore, the time series forecasting and models included several different scenarios. Specifically, the models predicted several final SMY values with high R^2 values.

This study is novel because it developed an approach for the early prediction of BMP data. The use of time series forecasting only requires previously collected SMY values and thus is not limited by the initial substrate characteristics. This study demonstrates that the selection of the forecasting model is important in predicting future values. This study could be improved through the use of a continuous data acquisition system for CH_4 production, which would provide a greater number of data points for the predictions. Ultimately, time series forecasting could reduce the time needed for the BMP test.

6.5 Conclusions

The following conclusions were drawn from this chapter:

1. A variety of different substrates investigated through BMP testing had different CH_4 production curves. Differences in these CH_4 production curves had different best-fit models.
2. The k_h, $T_{80,}$ and T_{90} values varied considerably for the different BMP tests, indicating the need for close BMP test monitoring.

3. Using time series forecasting to predict future BMP yields, ARIMA was found to be the best fitted model in 59% of cases and predicted SMY values in the final 25% of the batch BMP test time.

6.6 References

Amha, Y. M., Sinha, P., Lagman, J., Gregori, M., & Smith, A. L. (2017). Elucidating microbial community adaptation to anaerobic co-digestion of fats, oils, and grease and food waste. *Water Research*, *123*, 277–289. https://doi.org/10.1016/j.watres.2017.06.065

Amon, T., Amon, B., Kryvoruchko, V., Zollitsch, W., Mayer, K., & Gruber, L. (2007). Biogas production from maize and dairy cattle manure-Influence of biomass composition on the methane yield. *Agriculture, Ecosystems and Environment*, *118*(1–4), 173–182. https://doi.org/10.1016/j.agee.2006.05.007

APHA. (1999). *Standard Methods for the Examination of Water and Wastewater*. (L. S. Clescerl, A. E. Greenberg, A. D. Eaton, & M. A. H. Franson, Eds.) (20th ed.). Washington D.C.: Amer Public Health Assn; American Water Works Assn; Water Environment Federation.

Bisgaard, Sø., & Kulahci, M. (2011). *Time Series Analysis and Forecasting By Example*. Wiley.

Chynoweth, D. P., Turick, C. E., Owens, J. M., Jerger, D. E., & Peck, M. W. (1993). Biochemical methane potential of biomass and waste feedstocks. *Biomass and Bioenergy*, *5*(1), 95–111. https://doi.org/10.1016/0961-9534(93)90010-2

Dai, X., Duan, N., Dong, B., & Dai, L. (2013). High-solids anaerobic co-digestion of sewage sludge and food waste in comparison with mono digestions: Stability and performance. *Waste Management*, *33*(2), 308–316. https://doi.org/10.1016/j.wasman.2012.10.018

Donoso-Bravo, A., García, G., Pérez-Elvira, S., & Fdz-Polanco, F. (2011). Initial rates technique as a procedure to predict the anaerobic digester operation. *Biochemical Engineering Journal*, *53*(3), 275–280. https://doi.org/10.1016/j.bej.2010.11.007

Elbeshbishy, E., & Nakhla, G. (2012). Batch anaerobic co-digestion of proteins and carbohydrates. *Bioresource Technology*, *116*, 170–178. https://doi.org/10.1016/j.biortech.2012.04.052

Elbeshbishy, E., Nakhla, G., & Hafez, H. (2012). Biochemical methane potential (BMP) of food waste and primary sludge: Influence of inoculum pre-incubation and inoculum source. *Bioresource Technology*, *110*, 18–25. https://doi.org/10.1016/j.biortech.2012.01.025

Hill, D. T. (1982). Optimum operational design criteria for anaerobic digestion of animal manure. *Transactions of the ASAE*, *25*(4), 1029–1032. https://doi.org/10.13031/2013.33661

Huang, G. Bin, Zhu, Q. Y., & Siew, C. K. (2006). Extreme learning machine: Theory and applications. *Neurocomputing*, *70*(1–3), 489–501. https://doi.org/10.1016/j.neucom.2005.12.126

Hyndman, R.J. Athanasopoulos, G. (2018). *Forecasting: principles and practice*.

Hyndman, R. J., & Khandakar, Y. (2008). *Automatic Time Series Forecasting: The forecast Package for R*. *Journal of Statistical Software* (Vol. 27). Hoboken, NJ.

Jerger, D. E., Chynoweth, D. P., & Isaacson, H. R. (1987). Anaerobic digestion of sorghum biomass. *Biomass*, *14*(2), 99–113. https://doi.org/10.1016/0144-4565(87)90013-8

Kafle, G. K., & Chen, L. (2016). Comparison on batch anaerobic digestion of five different livestock manures and prediction of biochemical methane potential (BMP) using different statistical models. *Waste Management*, *48*, 492–502. https://doi.org/10.1016/j.wasman.2015.10.021

Koch, K., & Drewes, J. E. (2014). Alternative approach to estimate the hydrolysis rate constant of particulate material from batch data. *Applied Energy*, *120*, 11–15. https://doi.org/10.1016/j.apenergy.2014.01.050

Koch, K., Hafner, S. D., Weinrich, S., & Astals, S. (2019). Identification of Critical Problems in Biochemical Methane Potential (BMP) Tests From Methane Production Curves. *Frontiers in Environmental Science*, *7*(November), 1–8. https://doi.org/10.3389/fenvs.2019.00178

Koch, K., Hafner, S. D., Weinrich, S., Astals, S., & Holliger, C. (2020). Power and Limitations of Biochemical Methane Potential (BMP) Tests. *Frontiers in Energy Research*, *8*(April), 1–4. https://doi.org/10.3389/fenrg.2020.00063

Kourentzes, N., Barrow, D. K., & Crone, S. F. (2014). Neural network ensemble operators for time series forecasting. *Expert Systems with Applications*, *41*(9), 4235–4244. https://doi.org/10.1016/j.eswa.2013.12.011

Labatut, R. A., Angenent, L. T., & Scott, N. R. (2011). Biochemical methane potential and biodegradability of complex organic substrates. *Bioresource Technology*, *102*(3), 2255–2264. https://doi.org/10.1016/j.biortech.2010.10.035

Martinez, Frias, C. dan R. (2019). Time Series Forecasting with KNN in R : the tsfknn Package. *The R Journal*, *20*(1), 1–14.

Møller, H. B., Sommer, S. G., & Ahring, B. K. (2004). Methane productivity of manure, straw and solid fractions of manure. *Biomass and Bioenergy*, *26*(5), 485–495. https://doi.org/10.1016/j.biombioe.2003.08.008

Monteith, H. D., & Stephenson, J. P. (1981). Mixing efficiencies in full-scale anaerobic digesters by tracer methods. *Journal of the Water Pollution Control Federation*, *53*(1), 78–84. https://doi.org/10.2166/wqrj.1978.011

NREL. (2013). *Biogas Potential in the United States (Fact Sheet)*. *Related Information: Energy Analysis, NREL (National Renewable Energy Laboratory)*. Golden, CO. https://doi.org/10.2172/1097303

Ohemeng-Ntiamoah, J., & Datta, T. (2018). Evaluating analytical methods for the characterization of lipids, proteins and carbohydrates in organic substrates for anaerobic co-digestion. *Bioresource Technology*, *247*(September 2017), 697–704. https://doi.org/10.1016/j.biortech.2017.09.154

Owen, W. F., Stuckev, D. C., Healy, J. B., Young, L. Y., & Mccarty, P. L. (1979). Bioassay for monitering biochemical methane potential and anaerobic toxicity. *Water Research*, *13*(6), 485–492. https://doi.org/10.1016/0043-1354(79)90043-5

Parkin, B. G. F., & Owen, W. F. (1987). Fundamentals of anaerobic digestion of wastewater sludges. *Journal of Environmental Engineering*, *112*(5), 867–920.

Pavlostathis, S. G., & Giraldo-Gomez, E. (1991). Kinetics of anaerobic treatment: A critical review. *Critical Reviews in Environmental Control*, *21*(5–6), 411–490. https://doi.org/10.1080/10643389109388424

Ponsá, S., Gea, T., & Sánchez, A. (2011). Short-time estimation of biogas and methane potentials from municipal solid wastes. *Journal of Chemical Technology and Biotechnology*, *86*(8), 1121–1124. https://doi.org/10.1002/jctb.2615

Raposo, F., Fernández-Cegrí, V., de la Rubia, M. A., Borja, R., Béline, F., Cavinato, C., … de Wilde, V. (2011). Biochemical methane potential (BMP) of solid organic substrates: Evaluation of anaerobic biodegradability using data from an international interlaboratory study. *Journal of Chemical Technology and Biotechnology*, *86*(8), 1088–1098. https://doi.org/10.1002/jctb.2622

Ruiz, G., Castellano, M., González, W., Roca, E., & Lema, J. M. (2004). Transient State Detection and Prediction of Organic Overload in Anaerobic Digestion Process Using Statistical Tools. *IFAC Proceedings Volumes*, *37*(3), 357–362. https://doi.org/10.1016/s1474-6670(17)32607-1

Sánchez-García, D., Hernández-García, H., Mendez-Acosta, H. O., Hernández-Aguirre, A., Puebla, H., & Hernández-Martínez, E. (2018). Fractal Analysis of pH Time-Series of an Anaerobic Digester for Cheese Whey Treatment. *International Journal of Chemical Reactor Engineering*, *16*(11). https://doi.org/10.1515/ijcre-2017-0261

Strömberg, S., Nistor, M., & Liu, J. (2015). Early prediction of Biochemical Methane Potential through statistical and kinetic modelling of initial gas production. *Bioresource Technology*, *176*, 233–241. https://doi.org/10.1016/j.biortech.2014.11.033

Turick, C. E., Peck, M. W., Chynoweth, D. P., Jerger, D. E., White, E. H., Zsuffa, L., & Andy Kenney, W. (1991). Methane fermentation of woody biomass. *Bioresource Technology*, *37*(2), 141–147. https://doi.org/10.1016/0960-8524(91)90202-U

Usack, J. G., & Angenent, L. T. (2015). Comparing the inhibitory thresholds of dairy manure co-digesters after prolonged acclimation periods: Part 1 – Performance and operating limits. *Water Research*, *87*, 1–12. https://doi.org/10.1016/j.watres.2015.05.055

Vedrenne, F., Béline, F., Dabert, P., & Bernet, N. (2008). The effect of incubation conditions on the laboratory measurement of the methane producing capacity of livestock wastes. *Bioresource Technology*, *99*(1), 146–155. https://doi.org/10.1016/j.biortech.2006.11.043

Zhang, W., Li, L., Xing, W., Chen, B., Zhang, L., Li, A., … Yang, T. (2019). Dynamic behaviors of batch anaerobic systems of food waste for methane production under different organic loads, substrate to inoculum ratios and initial pH. *Journal of Bioscience and Bioengineering*, *128*(6), 733–743. https://doi.org/10.1016/j.jbiosc.2019.05.013

CHAPTER 7. GENERAL CONCLUSIONS

Biochemical methane potential tests are a useful laboratory method that can assist with the optimization of operational strategies for field AD systems. However, there are still many challenges for improving the technical aspects of this method and the mathematical models of test results. Moreover, the ability of the BMP method to gain new insights into anaerobic digester performance has still not been fully exploited.

Significant variabilities in reported BMP methodologies were uncovered in the comprehensive literature review. These variabilities were primarily demonstrated in BMP test setup, digester operation and control, biogas collection and quantification, and BMP calculation and expressions. Moreover, the lack of reporting on key operational parameters made the reported tests and test results difficult to be reproduced. Understanding these variabilities led to the conclusion that developing and implementing standardized BMP test practices are needed for making the BMP tests a better tool to serve the growing number of field AD systems.

Modeling has also been applied in BMP tests to explain the physical and chemical properties of the liquid, to predict SMY, to mathematically describe the changes in a defined system, and to forecast future events. Among the variety of mathematical models reviewed in this dissertation, the most frequently used first order model lacks the nuance required for complex substrates. Improvements in nonlinear modeling could reduce the time needed for the BMP test. Linking the function of the AD process to the microbial community dynamics could further improve modeling. Moreover, models and calculations should be carefully chosen based on substrate types.

Laboratory BMP tests could be a supportive approach to gain new insights into some operational issues in field AD systems, such as H_2S production. Hydrogen sulfide productions in the lab-digesters showed considerable variability, ranging from non-detectable to 1.29 mL g VS^{-1}. Higher H_2S concentrations in the biogas were observed within the first ten days of AD. Unlike in previous studies, initial sulfate concentrations and the final specific H_2S productions were not significantly correlated, and the TCOD : Sulfate ratio was not a reliable H_2S production predictor. Instead, the initial Fe(II) : S ratio and OP concentrations had important influences on H_2S productions. Iron reduction and iron-phosphorus precipitation could have occurred without the presence of an anaerobic community, whereas FeS precipitation seemed to require an anaerobic

community. Sulfate, phosphorus, and iron in the anaerobic microbial community were important for understanding the H_2S production.

When combined with field investigation and machine learning, the BMP test enabled the identification of key parameters in digester foaming. Influents related to the field digester foaming had significantly lower OP, iron, nickel, and NH_3 concentrations in the digester influent and significantly higher total alkalinity concentrations. Important parameters of digester influents related to digester foaming were the ratios of Fe(II) : S, Fe(II) : TP, and TVFA : TALK; and the concentrations of Cu. Digesters receiving mixed waste streams could be more vulnerable to foaming. In the lab tests, digesters receiving substrates from the field digester during non-foaming events had significantly higher SMYs but lower CO_2 concentrations in the produced biogas. Foaming in the lab-digesters occurred within the first 72 hours of the experiment. Machine learning revealed that the ratios of TVFA : TALK, Fe(II) : S, Fe(II) : TP, and the concentrations of Cu were influential variables.

In addition to the findings from the BMP modeling literature review, the studies on the field investigation and lab experimental results also led to the conclusion that models should be carefully chosen based on the modeling objectives. In the H_2S production research, the gam model was the most applicable to a variety of different substrates. In the digester foaming study, a hybrid knowledge-based approach predicted the foaming status of the field digester and the foaming potential of individual lab-scale digesters. To investigate the CH_4 productions in lab BMP tests, it was demonstrated that differences in CH_4 production curves were an important factor for model selection. The application of time series forecasting to the early prediction of BMP data had several successful predictions with low RMSE values, particularly with the ARIMA algorithm.

Over the past decades, BMP testing has been slow in the development of new knowledge and new technologies. However, many research gaps, some of which have been identified in this dissertation, still exist. The BMP test could be expanded to examine other aspects of digester function including H_2S production and foaming. Filling these gaps requires continuous efforts in scientific research. Successes in expanding BMP testing will make the BMP test a valuable tool in AD development and application for a healthy world.

APPENDIX A. CHAPTER 4 SUPPLEMENTARY

Table A-1. Methods for characterization of substrate, inoculum, and digester effluent.

Parameter	Unit	Method	Matter
pH	Unitless	Jenco Digital pH Meter (Model 60) with Cole-Parmer electrode Cat No 05993-00	Particulate
TS	g L^{-1}	Standard Methods for the Examination of Wastewater (20^{th} edition) Method 2540 B	Particulate
VS, FS	g L^{-1}	Standard Methods for the Examination of Wastewater (20^{th} edition) Method 2540E	Particulate
Conductivity	mS cm^{-1}	Hanna Instruments HI 9813-6N EC Meter	Particulate
COD	g L^{-1}	Adapted USEPA Reactor Digestion Method (250-15,000 mg COD L^{-1}) for TNTplus™ Vial Test TNT823 Method 10212*	TCOD = Particulate SCOD=Soluble (0.2µm filter)
TVFA	g Acetic Acid L^{-1}	Adapted Esterification Method (50-2,500 mg Acetic Acid L^{-1}) for TNTplus™ Vial Test TNT 872 Method 10240*	Soluble (0.45µm filter)
TALK	g $CaCO_3$ L^{-1}	Adapted Colorimetric Method (25-400 mg $CaCO_3$ L^{-1}) for TNTplus™ Vial Test TNT 870 *	Soluble (0.45µm filter)
Sulfate	g SO_4^{-2} L^{-1}	Adapted Turbidimetric Method (40-150 mg SO_4^{2-} L^{-1}) TNTplus Vial Test for TNTplus™ 864 Method 10227 *	Particulate
Tannic Acid	g L^{-1}	Adapted Tyrosine Method (0.1-9.0 mg Tannic Acid L^{-1}) for Hach Method 8193*	Particulate
OP	g PO_4 L^{-1}	Hach Orthophosphate Test Kit Model PO-19	Soluble (0.45µm filter)
TAN	g NH_3-N L^{-1}	Adapted USEPA Nessler Method (0.02-2.50 mg NH_3-N L^{-1}) For Hach Method 8038*	Particulate
TP	g PO_4^{3-} L^{-1}	Adapted USEPA PhosVer®3 with Acid Persulfate Digestion Method (0.02-1.10 mg PO_4^{3-} L^{-1}) for Test N' Tube™ Vials Method 8190 * *	Particulate
TKN, TN, Inorganic N	g L^{-1}	Simplified TKN Method (0-16 mg N L^{-1}) for TNTplus™ 880 Method 10242 *	Soluble (0.45µm filter)
Fe	g L^{-1}	Adapted Phenanthroline Method (0.2-6.0 mg Fe L^{-1}) for TNTplus™ 858 Method 10229 *	Soluble (0.45µm filter)
Cu	g L^{-1}	Adapted Bathocuproine Method (0.1 to 8.0 mg Cu L^{-1}) for TNTplus™ 860 Method 10238 *	Soluble (0.45µm filter)
Ni	g L^{-1}	Adapted Dimethylglyoxime Method (0.1 to 6.0 mg Ni L^{-1}) for TNTplus™ 856 Method 10220 *	Soluble (0.45µm filter)

*Note: *Measured with Hach DR3900 Benchtop Spectrophotometer (Hach Company, Loveland, CO).*

Table A-2. The mean ± standard deviation of digester influent (day zero) and effluent (final day) characteristics for each lab-digester group (1).

Day	No.	pH	Conductivity	TS	VS	TCOD	SCOD	TVFA	TALK	TKN
Final	1-1	7.88 ± 0.04	6.49 ± 0.15	24 ± 4	14.61 ± 3.77	28 ± 3	12.44 ± 8.02	4.2 ± 1.5	14.61 ± 4.01	2.9 ± 0.73
Zero	1-1	7.72 ± 0.15	8.56 ± 0	47 ± 0	36.51 ± 0	55 ± 0	32.59 ± 0	5.9 ± 0	8.44 ± 0	2.27 ± 0
Final	1-2	7.85 ± 0.08	6.45 ± 0.01	21 ± 2	11.69 ± 1.78	25 ± 6	6.65 ± 1.03	2.6 ± 0.1	10.47 ± 1.17	2.01 ± 0.2
Zero	1-2	7.64 ± 0.12	8.5 ± 0	45 ± 0	34.39 ± 0	53 ± 0	33.03 ± 0	5.8 ± 0	8.52 ± 0	2.27 ± 0
Final	1-3	7.82 ± 0.08	6.3 ± 0.06	9 ± 0	3.69 ± 0.07	5 ± 0	10.31 ± 6.89	3 ± 0.7	9.86 ± 1.67	2.04 ± 0.37
Zero	1-3	7.72 ± 0.05	8.85 ± 0	12 ± 0	6.07 ± 0	25 ± 0	49.33 ± 0	4.8 ± 0	8.97 ± 0	1.68 ± 0
Final	1-4	7.7 ± 0.15	6.36 ± 0.09	10 ± 0	4.28 ± 0.25	7 ± 1	7.49 ± 2.67	2.6 ± 0.1	8.8 ± 1.45	1.78 ± 0.18
Zero	1-4	7.66 ± 0.12	8.76 ± 0	13 ± 0	6.99 ± 0	27 ± 0	48.1 ± 0	4.8 ± 0	8.99 ± 0	1.74 ± 0
Final	1-5	7.96 ± NA	6.35 ± NA	17 ± NA	9.37 ± NA	16 ± NA	5.19 ± NA	3.8 ± NA	22.66 ± NA	1.56 ± NA
Zero	1-5	7.75 ± 0.28	7.96 ± 0	23 ± 0	15.24 ± 0	37 ± 0	37.07 ± 0	4.9 ± 0	9.24 ± 0	2.32 ± 0
Final	2-7	7.52 ± 0.37	6.95 ± 0.04	82 ± 6	64.48 ± 5.58	192 ± 61	42.07 ± 4.51	19 ± 0.4	8.33 ± 3.4	3.65 ± 0.09
Zero	2-7	6.54 ± 0.05	9.91 ± 0	99 ± 0	80.83 ± 0	150 ± 0	37.69 ± 0	9.3 ± 0	6.56 ± 0	1.53 ± 0
Final	2-8	7.85 ± 0.76	6.87 ± 0.17	94 ± 2	74.89 ± 1.76	155 ± 6	40.75 ± 0.07	18.9 ± 0.2	10.16 ± 1.7	4.53 ± 1.03
Zero	2-8	6.94 ± 0.04	9.86 ± 0	100 ± 0	81.01 ± 0	152 ± 0	37.29 ± 0	9.2 ± 0	6 ± 0	1.45 ± 0
Final	2-10	8.03 ± 0.24	6.34 ± 3.14	44 ± 29	29.98 ± 19.35	67 ± 47	12.58 ± 7.8	5.4 ± 3.3	11.14 ± 7.39	2.15 ± 1.39
Zero	2-10	7.5 ± 0.3	8.34 ± 4.84	51 ± 30	36.2 ± 21.02	52 ± 30	12.5 ± 7.26	4.8 ± 2.8	9.45 ± 5.49	1.87 ± 1.09
Final	2-11	7.46 ± NA	1.94 ± NA	2 ± NA	0.91 ± NA	2 ± NA	2.98 ± NA	0.52 ± NA	0.75 ± NA	0.23 ± NA
Zero	2-11	7.15 ± NA	1.08 ± NA	7 ± NA	4.67 ± NA	7 ± NA	1.61 ± NA	0.62 ± NA	1.22 ± NA	0.24 ± NA
Final	2-12	7.65 ± 0.14	2.18 ± 0.02	2 ± 0	0.85 ± 0.12	1 ± 0	2.66 ± 0.25	0.22 ± 0	0.8 ± 0.12	0.3 ± 0
Zero	2-12	7 ± 0.05	1.02 ± 0	8 ± 0	4.85 ± 0	10 ± 0	1.21 ± 0	0.53 ± 0	0.66 ± 0	0.16 ± 0
Final	3-13	7.14 ± 0.6	4.27 ± 1.45	205 ± 156	185.41 ± 155.4	353 ± 67	75.14 ± 16.03	19.5 ± 2	6.58 ± 3.73	1.23 ± 0.11
Zero	3-13	6.62 ± 0.2	1 ± 1.13	628 ± 0	605.95 ± 0	490 ± 0	150.72 ± 0	20.2 ± 0	4.18 ± 0	0.92 ± 0
Final	3-14	7.5 ± 0.14	0.93 ± 0.92	146 ± 42	122.45 ± 35.09	340 ± 36	72.82 ± 11.84	18.5 ± 0.2	3.79 ± 0.81	1.05 ± 0.37
Zero	3-14	6.02 ± 0.07	1.89 ± 0.92	627 ± 0	605.5 ± 0	498 ± 0	150.86 ± 0	19.3 ± 0	4.3 ± 0	0.92 ± 0
Final	3-15	7.65 ± 0	7.81 ± 0.1	33 ± 18	18.59 ± 13.45	59 ± 28	46.54 ± 18.21	6 ± 0.1	11.37 ± 0.81	2.75 ± 0.23
Zero	3-15	7.95 ± 0.03	7.63 ± 0.02	74 ± 0	52.89 ± 0	70 ± 0	18.43 ± 0	21.5 ± 0	7.31 ± 0	2.23 ± 0
Final	3-16	7.55 ± 0.04	7.06 ± 0.15	20 ± 9	12.43 ± 6.69	27 ± 12	9.04 ± 1.36	5.2 ± 2.4	5.06 ± 0.64	1.46 ± 0.37
Zero	3-16	5.99 ± 0.01	6.5 ± 0.13	35 ± 0	24.22 ± 0	35 ± 0	9.21 ± 0	10.8 ± 0	3.66 ± 0	1.12 ± 0
Final	3-17	7.65 ± 0	2.78 ± 1.21	4 ± 1	2.49 ± 0.45	3 ± 1	1.48 ± 0.78	0.89 ± 0.42	1.35 ± 0.19	0.18 ± 0.05
Zero	3-17	7.21 ± 0.01	2.45 ± 0.19	7 ± 0	5.29 ± 0	7 ± 0	1.84 ± 0	2.2 ± 0	0.73 ± 0	0.22 ± 0
Final	3-18	6.84 ± 1.29	3.11 ± 0.22	5 ± 0	2.78 ± 0.08	5 ± 2	1.27 ± 0.08	0.71 ± 0	1.04 ± 0.02	0.24 ± 0.04
Zero	3-18	5.92 ± 0	1.93 ± 0.67	7 ± 0	4.84 ± 0	3 ± 0	1.88 ± 0	1.2 ± 0	0.89 ± 0	0.23 ± 0
Final	4-19	7.16 ± NA	7.96 ± NA	108 ± NA	82.49 ± NA	199 ± NA	62.03 ± NA	26.2 ± NA	8.3 ± NA	2.38 ± NA

Table A-2 continued.

Day	No.	pH	Conductivity	TS	VS	TCOD	SCOD	TVFA	TALK	TKN
Zero	4-19	6.95 ± NA	8.67 ± NA	137 ± NA	114.91 ± NA	227 ± NA	58.86 ± NA	16.4 ± NA	6.06 ± NA	1.83 ± NA
Final	4-20	7.83 ± 0.09	6.87 ± 0.06	23 ± 9	14.39 ± 7.46	10 ± 3	6.4 ± 0.64	3.6 ± 0.9	4.34 ± 0.7	1.09 ± 0.12
Zero	4-20	6.85 ± 0.05	7.51 ± 0.14	45 ± 0	33.82 ± 0	68 ± 0	9.46 ± 0	3 ± 0	5.54 ± 0	1 ± 0
Final	4-21	8.15 ± 0.05	6.89 ± 0.04	26 ± 14	15.9 ± 10.28	16 ± 8	8.63 ± 1.73	2.8 ± 1.3	13.8 ± 2.37	1.11 ± 0.3
Zero	4-21	6.98 ± 0.06	7.63 ± 0.2	48 ± 0	35.41 ± 0	41 ± 0	9.24 ± 0	4.1 ± 0	5.52 ± 0	1.32 ± 0
Final	4-22	8.16 ± 0.07	7.84 ± 0.2	37 ± 3	19.58 ± 2.76	29 ± 5	13.5 ± 2.41	5 ± 0.2	12.9 ± 5.1	1.88 ± 0.39
Zero	4-22	7.34 ± 0.13	8.53 ± 0.03	83 ± 0	58.29 ± 0	99 ± 0	17.85 ± 0	6.2 ± 0	8.85 ± 0	2.12 ± 0
Final	4-23	8.01 ± 0.13	4.49 ± 0.27	6 ± 0	3.18 ± 0.63	5 ± 2	4.44 ± 0.04	4.4 ± 4.9	2.35 ± 0.53	0.69 ± 0.29
Zero	4-23	7.11 ± 0.01	4.26 ± 0.89	28 ± 0	26.59 ± 0	32 ± 0	3.4 ± 0	1.2 ± 0	1.88 ± 0	0.4 ± 0
Final	5-24	6.43 ± 0.04	6.63 ± 0.31	86 ± 11	69.39 ± 9.07	147 ± 12	81.2 ± 16.18	35.8 ± 10.2	5.91 ± 1.37	3.72 ± 0.37
Zero	5-24	7.12 ± 0.59	7.36 ± 0.56	138 ± 0	119.73 ± 0	180 ± 0	59.84 ± 0	12 ± 0	2.78 ± 0	2.49 ± 0
Final	5-25	7.73 ± 0.07	7.19 ± 0.07	17 ± 6	10.77 ± 4.48	31 ± 2	9 ± 1.82	5.3 ± 0.2	8.95 ± 0.98	2.12 ± 1.25
Zero	5-25	7.62 ± 0.22	7.08 ± 0.24	34 ± 0	25.56 ± 0	35 ± 0	7.64 ± 0	2.6 ± 0	4.07 ± 0	1.11 ± 0
Final	5-26	7.73 ± 0.12	6.85 ± 0.54	27 ± 2	18.22 ± 1.75	27 ± 5	6.84 ± 0.65	3.3 ± 0.6	6.12 ± 1.88	1.29 ± 0.35
Zero	5-26	7.54 ± 0.18	7.29 ± 0.08	35 ± 0	25.27 ± 0	36 ± 0	4.61 ± 0	2.1 ± 0	4.67 ± 0	1.33 ± 0
Final	5-27	7.95 ± 0.24	8.2 ± 0.07	43 ± 6	27.61 ± 4.7	39 ± 11	14.15 ± 2.62	8 ± 3.3	15.04 ± 1.79	3.36 ± 0.95
Zero	5-27	7.88 ± 0.05	7.92 ± 0.1	61 ± 0	43.3 ± 0	52 ± 0	8.84 ± 0	3.9 ± 0	7.14 ± 0	2.02 ± 0
Final	5-28	7.09 ± 0.11	4.23 ± 0.17	5 ± 2	3.17 ± 1.55	4 ± 1	3.26 ± 0.34	0.7 ± 0.01	2.35 ± 0.1	0.53 ± 0.02
Zero	5-28	7.86 ± 0.12	4.61 ± 0.29	12 ± 0	11.27 ± 0	12 ± 0	2.07 ± 0	0.87 ± 0	1.78 ± 0	0.46 ± 0
Final	6-29	7.08 ± NA	5.2 ± NA	35 ± NA	16.66 ± NA	35 ± NA	1.91 ± NA	0.36 ± NA	3.39 ± NA	0.67 ± NA
Zero	6-29	6.74 ± NA	6.14 ± NA	37 ± NA	20.56 ± NA	38 ± NA	1.98 ± NA	3.9 ± NA	4.18 ± NA	0.09 ± NA
Final	6-30	7.18 ± NA	5.04 ± NA	28 ± NA	13.23 ± NA	43 ± NA	2.47 ± NA	0.36 ± NA	6.11 ± NA	0.45 ± NA
Zero	6-30	6.75 ± NA	6.31 ± NA	37 ± NA	20.37 ± NA	38 ± NA	1.98 ± NA	3.9 ± NA	4.18 ± NA	0.09 ± NA
Final	6-31	7.09 ± 0.08	4.45 ± 0.23	36 ± 10	17.37 ± 4.96	32 ± 2	1.86 ± 0.33	0.42 ± 0.05	5.65 ± 1.71	0.49 ± 0.09
Zero	6-31	6.88 ± 0.03	5.27 ± 0.24	43 ± 0	24.13 ± 0	45 ± 0	1.7 ± 0	3.3 ± 0	3.6 ± 0	0.08 ± 0
Final	6-32	7.18 ± NA	4.65 ± NA	24 ± NA	11.54 ± NA	14 ± NA	2.65 ± NA	0.51 ± NA	3.71 ± NA	0.58 ± NA
Zero	6-32	6.94 ± NA	4.66 ± NA	50 ± NA	28.03 ± NA	52 ± NA	1.49 ± NA	2.9 ± NA	3.16 ± NA	0.07 ± NA
Zero	6-33	6.64 ± NA	4.46 ± NA	56 ± NA	32.05 ± NA	59 ± NA	1.33 ± NA	2.6 ± NA	2.82 ± NA	0.06 ± NA
Final	6-34	7.09 ± NA	4.84 ± NA	24 ± NA	11.48 ± NA	16 ± NA	2.4 ± NA	0.45 ± NA	3.93 ± NA	0.8 ± NA
Zero	6-34	6.86 ± NA	5.02 ± NA	42 ± NA	23.52 ± NA	44 ± NA	1.75 ± NA	3.4 ± NA	3.69 ± NA	0.08 ± NA
Final	6-35	7.26 ± 0.15	3.34 ± 0.27	34 ± 6	18.22 ± 3.58	41 ± 16	6.66 ± 1.49	2.2 ± 0.1	2.69 ± 0.22	0.46 ± 0.08
Zero	6-35	6.93 ± 0.06	4.08 ± 0.32	52 ± 0	30.12 ± 0	56 ± 0	1.41 ± 0	2.8 ± 0	3 ± 0	0.07 ± 0
Final	6-36	7.07 ± NA	4.85 ± NA	7 ± NA	2.69 ± NA	24 ± NA	2.31 ± NA	0.45 ± NA	4.94 ± NA	0.74 ± NA
Zero	6-36	6.85 ± NA	5.05 ± NA	43 ± NA	23.99 ± NA	45 ± NA	1.72 ± NA	3.4 ± NA	3.63 ± NA	0.08 ± NA
Final	6-37	7.19 ± 0.14	4.2 ± 0.26	22 ± 10	10.67 ± 5.27	23 ± 2	2.1 ± 0.3	0.54 ± 0.18	3.69 ± 0.95	0.63 ± 0.06
Zero	6-37	6.91 ± 0.05	4.57 ± 0.14	49 ± 0	27.75 ± 0	51 ± 0	1.51 ± 0	3 ± 0	3.2 ± 0	0.07 ± 0

Table A-2 continued.

Day	No.	pH	Conductivity	TS	VS	TCOD	SCOD	TVFA	TALK	TKN
Final	6-38	7.54 ± NA	4.39 ± NA	31 ± NA	14.85 ± NA	21 ± NA	2.62 ± NA	0.61 ± NA	4.1 ± NA	0.59 ± NA
Zero	6-38	6.87 ± NA	4.53 ± NA	55 ± NA	31.64 ± NA	58 ± NA	1.35 ± NA	2.7 ± NA	2.86 ± NA	0.06 ± NA
Final	6-39	6.89 ± NA	4.53 ± NA	35 ± NA	17.31 ± NA	36 ± NA	2.01 ± NA	0.48 ± NA	4.64 ± NA	0.37 ± NA
Zero	6-39	6.85 ± NA	5.21 ± NA	44 ± NA	24.52 ± NA	46 ± NA	1.68 ± NA	3.3 ± NA	3.56 ± NA	0.08 ± NA
Final	6-40	7.43 ± NA	3.46 ± NA	34 ± NA	16.71 ± NA	48 ± NA	2.65 ± NA	0.54 ± NA	3.02 ± NA	0.52 ± NA
Zero	6-40	6.86 ± NA	4.47 ± NA	51 ± NA	28.83 ± NA	53 ± NA	1.46 ± NA	2.9 ± NA	3.1 ± NA	0.07 ± NA
Final	6-41	7.12 ± NA	3.84 ± NA	33 ± NA	20.52 ± NA	35 ± NA	15.48 ± NA	7 ± NA	1.68 ± NA	0.29 ± NA
Zero	6-41	6.46 ± NA	3.92 ± NA	58 ± NA	33.3 ± NA	61 ± NA	1.29 ± NA	0.02 ± NA	2.74 ± NA	0.06 ± NA
Final	6-42	7.08 ± NA	4.13 ± NA	30 ± NA	19.78 ± NA	37 ± NA	25.34 ± NA	10.2 ± NA	1.67 ± NA	0.17 ± NA
Zero	6-42	6.93 ± NA	4.76 ± NA	81 ± NA	47.69 ± NA	85 ± NA	0.96 ± NA	1.9 ± NA	2.04 ± NA	0.05 ± NA
Final	6-43	7.09 ± 0.23	4.21 ± 0.2	42 ± 8	28.26 ± 5.72	53 ± 12	26.58 ± 5.1	10.1 ± 1.6	2.22 ± 0.26	0.35 ± 0.06
Zero	6-43	6.93 ± 0.02	4.08 ± 0.24	53 ± 2	31.28 ± 2.12	56 ± 2	1.46 ± 0	2.9 ± 0	3.12 ± 0.02	0.07 ± 0
Final	6-44	7.17 ± NA	5.04 ± NA	32 ± NA	14.82 ± NA	25 ± NA	1.6 ± NA	0.43 ± NA	4.79 ± NA	0.69 ± NA
Zero	6-44	6.88 ± NA	6.51 ± NA	31 ± NA	15.53 ± NA	38 ± NA	1.99 ± NA	2.6 ± NA	5.29 ± NA	0.48 ± NA
Final	6-45	7.29 ± 0.13	4.45 ± 0.21	34 ± 4	16.43 ± 2.5	27 ± 3	2.53 ± 0.53	0.46 ± 0.15	5.06 ± 0.32	0.53 ± 0.15
Zero	6-45	6.83 ± 0.1	3.49 ± 0.02	44 ± 0	27.13 ± 0	38 ± 0	0.4 ± 0	1.7 ± 0	2.64 ± 0	0.15 ± 0

Units are in g L^{-1} except for conductivity (mS cm^{-1}) and pH (unitless). n = 3).

Table A-3. The mean ± standard deviation of digester influent (day zero) and effluent (final day) characteristics for each lab-digester group (2).

Day	No.	TAN	Sulfate	Tannin	TP	OP	Fe	Ni	Cu	TN
Final	1-1	1.95 ± 0.08	3.4 ± 0.04	1.26 ± 0.03	0.94 ± 0.06	0.1 ± 0.03	0.01 ± 0.002	0.002 ± 0.001	0.002 ± 0	2.935 ± 0.734
Zero	1-1	1.32 ± 0	5.19 ± 0	1.79 ± 0	0.21 ± 0	0.23 ± 0	0.008 ± 0	0.003 ± 0	0.006 ± 0	2.388 ± 0
Final	1-2	1.74 ± 0.07	3.13 ± 0.25	1.11 ± 0.15	0.71 ± 0.15	0.06 ± 0.02	0.008 ± 0	0.001 ± 0	0.003 ± 0	2.038 ± 0.203
Zero	1-2	1.37 ± 0	5.11 ± 0	1.79 ± 0	0.23 ± 0	0.22 ± 0	0.008 ± 0.001	0.003 ± 0	0.004 ± 0.001	2.393 ± 0
Final	1-3	1.36 ± 0.02	1.11 ± 0.02	0.51 ± 0.05	0.17 ± 0.08	0.03 ± 0.01	0.003 ± 0.004	0.001 ± 0.001	0.001 ± 0.001	2.071 ± 0.374
Zero	1-3	1.61 ± 0	1.38 ± 0	1.01 ± 0	0.05 ± 0	0.06 ± 0	0.003 ± 0	0.001 ± 0	0.001 ± 0	2.434 ± 0
Final	1-4	1.4 ± 0.05	1.03 ± 0.16	0.49 ± 0.04	0.16 ± 0.06	0.02 ± 0	0.002 ± 0	0.005 ± 0.002	0.002 ± 0	1.803 ± 0.184
Zero	1-4	1.64 ± 0	1.69 ± 0	1.09 ± 0	0.08 ± 0	0.07 ± 0	0.005 ± 0	0.001 ± 0	0.001 ± 0	2.434 ± 0
Final	1-5	1.43 ± NA	2.19 ± NA	0.73 ± NA	0.53 ± NA	0.04 ± NA	0.008 ± NA	0 ± NA	0.004 ± NA	1.589 ± NA
Zero	1-5	1.86 ± 0	4.42 ± 0	1.76 ± 0	0.35 ± 0	0.14 ± 0	0.016 ± 0	0.003 ± 0	0.002 ± 0	2.434 ± 0
Final	2-7	2.63 ± 0.18	5.65 ± 0.26	2.12 ± 1.36	6.48 ± 0.93	3.87 ± 0.61	0.005 ± 0.001	0.006 ± 0	0.005 ± 0.001	3.708 ± 0.104
Zero	2-7	1.81 ± 0	6.97 ± 0	2.43 ± 0	2.12 ± 0	2.12 ± 0	0.014 ± 0	0.004 ± 0	0.004 ± 0	1.55 ± 0
Final	2-8	2.65 ± 0.17	5.03 ± 1.18	2.58 ± 0.53	6.67 ± 0.38	3.6 ± 0	0.013 ± 0.011	0.004 ± 0	0.003 ± 0.001	4.6 ± 1.106
Zero	2-8	1.75 ± 0	6.99 ± 0	2.34 ± 0	2.06 ± 0	2.06 ± 0	0.012 ± 0	0.004 ± 0	0.004 ± 0	1.474 ± 0
Final	2-10	3.05 ± 1.97	3.85 ± 2.63	3.1 ± 2.1	4.69 ± 2.94	1.2 ± 0.8	0.008 ± 0.013	0.002 ± 0.001	0.002 ± 0.001	2.248 ± 1.434
Zero	2-10	2.61 ± 1.52	4.39 ± 2.55	2.88 ± 1.67	3.39 ± 1.97	1.32 ± 0.76	0.048 ± 0.028	0.003 ± 0.002	0.002 ± 0.001	1.886 ± 1.095
Final	2-11	0.14 ± NA	0.11 ± NA	0.37 ± NA	2.03 ± NA	0.02 ± NA	0 ± NA	0 ± NA	0 ± NA	0.246 ± NA
Zero	2-11	0.34 ± NA	0.57 ± NA	0.37 ± NA	0.44 ± NA	0.17 ± NA	0.006 ± NA	0 ± NA	0 ± NA	0.243 ± NA
Final	2-12	0.2 ± 0.02	0.09 ± 0.01	0.06 ± 0.01	0.93 ± 0.07	0.4 ± 0	0.001 ± 0	0 ± 0	0 ± 0	0.342 ± 0.005
Zero	2-12	0.28 ± 0	0.58 ± 0	0.28 ± 0	1.25 ± 0	0.11 ± 0	0.005 ± 0	0 ± 0	0 ± 0	0.168 ± 0
Final	3-13	2.56 ± 0.24	2.51 ± 0.2	1.97 ± 0.18	6.92 ± 0.68	1.67 ± 0.31	0.025 ± 0.011	0.005 ± 0.002	0.003 ± 0.001	1.268 ± 0.082
Zero	3-13	1.34 ± 0	6.39 ± 0	2.49 ± 0	4.96 ± 0	1.76 ± 0	0.039 ± 0	0.007 ± 0	0.007 ± 0	0.953 ± 0
Final	3-14	1.84 ± 0.08	3.75 ± 0.94	2.34 ± 0.01	5.99 ± 0.17	2.6 ± 0	0.065 ± 0.015	0.006 ± 0	0.005 ± 0	1.093 ± 0.383
Zero	3-14	1.35 ± 0	6.37 ± 0	2.43 ± 0	5.01 ± 0	1.75 ± 0	0.039 ± 0	0.008 ± 0	0.007 ± 0	0.952 ± 0
Final	3-15	3.02 ± 0.42	4.11 ± 0.52	2.82 ± 0.93	3.18 ± 1.27	2.5 ± 0.14	0.019 ± 0.02	0.007 ± 0.003	0.007 ± 0.002	2.845 ± 0.238
Zero	3-15	2.32 ± 0	7.48 ± 0	4.35 ± 0	6.24 ± 0	1.4 ± 0	0.043 ± 0	0.003 ± 0	0.002 ± 0	2.26 ± 0
Final	3-16	1.28 ± 0.13	2.08 ± 1.31	1.62 ± 0.68	3.01 ± 0.77	1.27 ± 0.23	0.014 ± 0.011	0.003 ± 0.001	0.004 ± 0.001	1.527 ± 0.395
Zero	3-16	1.16 ± 0	3.74 ± 0	2.18 ± 0	3.12 ± 0	0.7 ± 0	0.021 ± 0	0.001 ± 0	0.001 ± 0	1.13 ± 0
Final	3-17	0.26 ± 0.12	0.15 ± 0	0.26 ± 0.22	1.21 ± 0.48	0.6 ± 0.28	0.006 ± NA	0.001 ± NA	0.001 ± NA	0.218 ± 0.061
Zero	3-17	0.23 ± 0	0.75 ± 0	0.44 ± 0	0.62 ± 0	0.14 ± 0	0.004 ± 0	0 ± 0	0 ± 0	0.226 ± 0
Final	3-18	0.34 ± 0.05	0.42 ± 0.3	0.24 ± 0.04	0.96 ± 0.17	1.4 ± 1.41	0.005 ± NA	0 ± NA	0.001 ± NA	0.276 ± 0.017
Zero	3-18	0.25 ± 0	0.72 ± 0	0.43 ± 0	0.67 ± 0	0.14 ± 0	0.004 ± 0	0.001 ± 0	0.001 ± 0	0.228 ± 0
Final	4-19	2.93 ± NA	6.85 ± NA	3.78 ± NA	6.61 ± NA	3.6 ± NA	0.025 ± NA	0.007 ± NA	0.003 ± NA	2.452 ± NA
Zero	4-19	1.88 ± NA	6.94 ± NA	3.03 ± NA	5.98 ± NA	2.56 ± NA	0.035 ± NA	0.007 ± NA	0.006 ± NA	1.932 ± NA
Final	4-20	1.2 ± 0.04	0.84 ± 0.45	0.92 ± 0.03	1.56 ± 0.23	1.93 ± 1.14	0.01 ± 0.001	0.003 ± 0	0.003 ± 0.001	1.147 ± 0.109

Table A-3 continued.

Day	No.	TAN	Sulfate	Tannin	TP	OP	Fe	Ni	Cu	TN
Zero	4-20	1.37 ± 0	3.14 ± 0	2.65 ± 0	3.02 ± 0	0.7 ± 0	0.011 ± 0	0.002 ± 0	0.001 ± 0	1.032 ± 0
Final	4-21	1.37 ± 0.15	1.62 ± 1.15	1.13 ± 0.28	1.7 ± 0.12	2 ± 0.53	0.013 ± 0.005	0.004 ± 0.002	0.003 ± 0.003	1.187 ± 0.306
Zero	4-21	1.26 ± 0	4.09 ± 0	1.99 ± 0	2.72 ± 0	1 ± 0	0.019 ± 0	0.001 ± 0	0.001 ± 0	1.342 ± 0
Final	4-22	2.3 ± 0.71	3.63 ± 0.58	2.24 ± 0.25	2.97 ± 0.13	1.87 ± 0.61	0.031 ± 0.016	0.009 ± 0.004	0.011 ± 0.006	2.024 ± 0.44
Zero	4-22	3.02 ± 0	7.04 ± 0	5.23 ± 0	7.55 ± 0	1.47 ± 0	0.029 ± 0	0.003 ± 0	0.005 ± 0	2.21 ± 0
Final	4-23	0.33 ± 0.01	0.6 ± 0.37	0.36 ± 0	0.74 ± 0.03	1 ± 0	0.013 ± 0.003	0.002 ± 0.001	0.003 ± 0.001	0.725 ± 0.276
Zero	4-23	0.58 ± 0	1.38 ± 0	1.05 ± 0	1.22 ± 0	0.32 ± 0	0.006 ± 0	0.001 ± 0	0.002 ± 0	0.425 ± 0
Final	5-24	2.24 ± 0.45	4.93 ± 0.72	2.37 ± 0.47	6.71 ± 1.2	6.27 ± 1.22	0.069 ± 0.07	0.009 ± 0.001	0.008 ± 0.001	3.701 ± 0.347
Zero	5-24	2.16 ± 0	10.48 ± 0	3.12 ± 0	7.32 ± 0	3.09 ± 0	0.118 ± 0	0.011 ± 0	0.006 ± 0	2.64 ± 0
Final	5-25	1.32 ± 0.2	2.38 ± 0.25	1.17 ± 0.26	1.51 ± 0.28	1.27 ± 0.12	0.015 ± 0.002	0.005 ± 0.002	0.005 ± 0.002	2.073 ± 1.218
Zero	5-25	1.45 ± 0	4.19 ± 0	1.52 ± 0	2.4 ± 0	0.8 ± 0	0.017 ± 0	0.005 ± 0	0.005 ± 0	1.279 ± 0
Final	5-26	1.37 ± 0.5	3.14 ± 0.81	1.65 ± 0.64	3.13 ± 1.45	1.13 ± 0.12	0.015 ± 0.006	0.011 ± 0.012	0.015 ± 0.009	1.272 ± 0.359
Zero	5-26	1.46 ± 0	4.71 ± 0	1.47 ± 0	2.64 ± 0	0.77 ± 0	0.016 ± 0	0.005 ± 0	0.005 ± 0	1.308 ± 0
Final	5-27	3.22 ± 0.37	4.37 ± 0.56	3.21 ± 1.34	4.03 ± 1.8	2.07 ± 0.23	0.024 ± 0.005	0.005 ± 0.001	0.005 ± 0	3.264 ± 0.917
Zero	5-27	2.79 ± 0	9.23 ± 0	3.07 ± 0	4.29 ± 0	1.4 ± 0	0.033 ± 0	0.009 ± 0	0.01 ± 0	2.084 ± 0
Final	5-28	0.52 ± 0.06	0.22 ± 0.03	0.36 ± 0.11	0.7 ± 0.1	0.44 ± 0.06	0.009 ± 0.001	0.001 ± 0	0.001 ± 0	0.512 ± 0.001
Zero	5-28	1.6 ± 0	1.6 ± 0	0.61 ± 0	0.86 ± 0	0.32 ± 0	0.008 ± 0	0.002 ± 0	0.002 ± 0	0.476 ± 0
Final	6-29	0.73 ± NA	0.65 ± NA	1.18 ± NA	1.53 ± NA	0 ± NA	0.007 ± NA	0.001 ± NA	0 ± NA	0.683 ± NA
Zero	6-29	0.76 ± NA	3.96 ± NA	2.55 ± NA	2.1 ± NA	0 ± NA	0.039 ± NA	0.003 ± NA	0.001 ± NA	0.117 ± NA
Final	6-30	0.82 ± NA	0.67 ± NA	6.11 ± NA	2.55 ± NA	0 ± NA	0.01 ± NA	0.002 ± NA	0.003 ± NA	0.45 ± NA
Zero	6-30	7.59 ± NA	3.96 ± NA	2.55 ± NA	2.1 ± NA	0 ± NA	0.039 ± NA	0.003 ± NA	0.001 ± NA	0.092 ± NA
Final	6-31	0.73 ± 0.02	1.4 ± 0.51	2.41 ± 0.4	3.11 ± 0.73	0 ± 0	0.008 ± 0.001	0.001 ± 0.001	0.001 ± 0	0.501 ± 0.094
Zero	6-31	1.64 ± 1.7	3.41 ± 0	2.19 ± 0	1.8 ± 0	0 ± 0	0.033 ± 0	0.002 ± 0	0.001 ± 0	0.1 ± 0
Final	6-32	0.56 ± NA	0.81 ± NA	1.45 ± NA	0.71 ± NA	0 ± NA	0.017 ± NA	0.002 ± NA	0 ± NA	0.604 ± NA
Zero	6-32	0.37 ± NA	2.99 ± NA	1.92 ± NA	1.58 ± NA	0 ± NA	0.029 ± NA	0.002 ± NA	0.001 ± NA	0.088 ± NA
Zero	6-33	0.51 ± NA	2.66 ± NA	1.71 ± NA	1.41 ± NA	0 ± NA	0.026 ± NA	0.002 ± NA	0.001 ± NA	0.078 ± NA
Final	6-34	0.77 ± NA	0.65 ± NA	2.42 ± NA	2.4 ± NA	0 ± NA	0.005 ± NA	0.001 ± NA	0.001 ± NA	0.803 ± NA
Zero	6-34	0.67 ± NA	3.49 ± NA	2.24 ± NA	1.85 ± NA	0 ± NA	0.034 ± NA	0.003 ± NA	0.001 ± NA	0.103 ± NA
Final	6-35	1.44 ± 1.48	1.09 ± 0.24	2.19 ± 0.99	1.89 ± 1.23	0 ± 0	0.035 ± 0.006	0.002 ± 0	0.001 ± 0	0.474 ± 0.074
Zero	6-35	0.54 ± 0	2.82 ± 0	1.81 ± 0	1.49 ± 0	0 ± 0	0.028 ± 0	0.002 ± 0	0.001 ± 0	0.083 ± 0
Final	6-36	0.71 ± NA	0.55 ± NA	1.37 ± NA	3.05 ± NA	0 ± NA	0.009 ± NA	0.001 ± NA	0.001 ± NA	0.759 ± NA
Zero	6-36	0.66 ± NA	3.44 ± NA	2.21 ± NA	1.82 ± NA	0 ± NA	0.034 ± NA	0.002 ± NA	0.001 ± NA	0.101 ± NA
Final	6-37	2.33 ± 1.66	0.66 ± 0.17	1.2 ± 0.48	2.5 ± 1.41	0 ± 0	0.011 ± 0.004	0.002 ± 0.001	0.002 ± 0	0.643 ± 0.065
Zero	6-37	0.39 ± 0.34	3.03 ± 0	1.95 ± 0	1.6 ± 0	0 ± 0	0.03 ± 0	0.002 ± 0	0.001 ± 0	0.089 ± 0
Final	6-38	0.56 ± NA	0.86 ± NA	2.16 ± NA	0.47 ± NA	0 ± NA	0.012 ± NA	0.001 ± NA	0.001 ± NA	0.611 ± NA
Zero	6-38	0.52 ± NA	2.71 ± NA	1.74 ± NA	1.43 ± NA	0 ± NA	0.026 ± NA	0.002 ± NA	0.001 ± NA	0.08 ± NA

Table A-3 continued.

Day	No.	TAN	Sulfate	Tannin	TP	OP	Fe	Ni	Cu	TN
Final	6-39	0.59 ± NA	0.67 ± NA	1.84 ± NA	2.05 ± NA	0 ± NA	0.008 ± NA	0.001 ± NA	0.001 ± NA	0.385 ± NA
Zero	6-39	0.64 ± NA	3.37 ± NA	2.16 ± NA	1.78 ± NA	0 ± NA	0.033 ± NA	0.002 ± NA	0.001 ± NA	0.099 ± NA
Final	6-40	0.59 ± NA	2.22 ± NA	2.58 ± NA	4.1 ± NA	0 ± NA	0.017 ± NA	0.001 ± NA	0 ± NA	0.52 ± NA
Zero	6-40	0.56 ± NA	2.93 ± NA	1.88 ± NA	1.55 ± NA	0 ± NA	0.029 ± NA	0.002 ± NA	0.001 ± NA	0.086 ± NA
Final	6-41	0.35 ± NA	0.59 ± NA	2.02 ± NA	1.93 ± NA	100 ± NA	0.15 ± NA	0.005 ± NA	0.002 ± NA	0.298 ± NA
Zero	6-41	0.5 ± NA	2.59 ± NA	1.66 ± NA	1.37 ± NA	0 ± NA	0.025 ± NA	0.002 ± NA	0.001 ± NA	0.077 ± NA
Final	6-42	0.25 ± NA	0.54 ± NA	1.12 ± NA	1.99 ± NA	180 ± NA	0.15 ± NA	0.007 ± NA	0.003 ± NA	0.212 ± NA
Zero	6-42	0.37 ± NA	1.92 ± NA	1.23 ± NA	1.01 ± NA	0 ± NA	0.019 ± NA	0.001 ± NA	0 ± NA	0.057 ± NA
Final	6-43	1.84 ± 1.24	1.25 ± 0.75	2.86 ± 1.23	2.75 ± 0.6	100 ± 40	0.273 ± 0.043	0.014 ± 0.006	0.006 ± 0.002	0.358 ± 0.059
Zero	6-43	0.56 ± 0	2.93 ± 0	1.88 ± 0	1.55 ± 0	0 ± 0	0.029 ± 0	0.7 ± 1.209	0.2 ± 0.345	0.087 ± 0.001
Final	6-44	0.94 ± NA	0.92 ± NA	1.29 ± NA	2.57 ± NA	0 ± NA	0.009 ± NA	0.002 ± NA	0.002 ± NA	0.611 ± NA
Zero	6-44	0.99 ± NA	3.51 ± NA	3.06 ± NA	2.2 ± NA	0 ± NA	0.021 ± NA	0.002 ± NA	0.001 ± NA	0.157 ± NA
Final	6-45	3.26 ± 0.14	1.25 ± 0.79	1.28 ± 1.62	3.36 ± 0	0 ± 0	0.009 ± 0.002	0.002 ± 0	0.001 ± 0	0.544 ± 0.173
Zero	6-45	0.38 ± 0	4.6 ± 0	1.83 ± 0	2.4 ± 0	0 ± 0	0.064 ± 0	0.004 ± 0	0.001 ± 0	0.148 ± 0

Units are in g L^{-1}. n = 3.

Table A-4. The mean ± standard deviation of digester influent (day zero) and effluent (final day) characteristics for each lab-digester group (3).

Day	No.	InorgN	SCOD : TCOD	OP : TP	TCOD : TN : TP	TVFA : TALK	TAN : TKN	TCOD: Sulfate	TCOD : TKN
Final	1-1	0.035 ± 0.001	0.45 ± 0.32	0.11 ± 0.02	10.6 ± 2.42	0.31 ± 0.19	0.7 ± 0.2	8.32 ± 0.63	9.97 ± 1.66
Zero	1-1	0.12 ± 0	0.6 ± 0	1.07 ± 0	107.87 ± 0	0.7 ± 0	0.58 ± 0	10.55 ± 0	24.13 ± 0
Final	1-2	0.032 ± 0.004	0.28 ± 0.04	0.09 ± 0.04	16.99 ± 2.34	0.25 ± 0.03	0.88 ± 0.13	7.89 ± 2.24	12.51 ± 4.53
Zero	1-2	0.12 ± 0	0.62 ± 0	0.97 ± 0	98.07 ± 0	0.68 ± 0	0.6 ± 0	10.37 ± 0	23.31 ± 0
Final	1-3	0.035 ± 0.005	1.89 ± 1.26	0.19 ± 0.13	18.25 ± 8.37	0.31 ± 0.07	0.68 ± 0.12	4.94 ± 0.25	2.76 ± 0.58
Zero	1-3	0.116 ± 0	1.94 ± 0	1.22 ± 0	212.89 ± 0	0.53 ± 0	0.96 ± 0	18.34 ± 0	15.1 ± 0
Final	1-4	0.028 ± 0.004	1.09 ± 0.31	0.14 ± 0.07	27.23 ± 13.88	0.3 ± 0.04	0.79 ± 0.07	6.61 ± 0.63	3.84 ± 0.58
Zero	1-4	0.116 ± 0	1.81 ± 0	0.86 ± 0	138.76 ± 0	0.53 ± 0	0.94 ± 0	15.74 ± 0	15.23 ± 0
Final	1-5	0.024 ± NA	0.33 ± NA	0.08 ± NA	18.53 ± NA	0.17 ± NA	0.91 ± NA	7.18 ± NA	10.02 ± NA
Zero	1-5	0.116 ± 0	0.99 ± 0	0.4 ± 0	44.27 ± 0	0.53 ± 0	0.8 ± 0	8.43 ± 0	16.08 ± 0
Final	2-7	0.056 ± 0.025	0.24 ± 0.09	0.61 ± 0.16	8.08 ± 3	2.53 ± 0.92	0.72 ± 0.04	34.3 ± 12.04	52.41 ± 16.64
Zero	2-7	0.053 ± 0	0.25 ± 0	1 ± 0	45.52 ± 0	1.41 ± 0	1.18 ± 0	21.45 ± 0	97.77 ± 0
Final	2-8	0.066 ± 0.076	0.26 ± 0.01	0.54 ± 0.03	5.16 ± 0.75	1.89 ± 0.3	0.6 ± 0.18	31.84 ± 8.7	34.96 ± 6.55
Zero	2-8	0.055 ± 0	0.24 ± 0	1 ± 0	50.21 ± 0	1.53 ± 0	1.21 ± 0	21.81 ± 0	105.13 ± 0
Final	2-10	0.12 ± 0.007	0.78 ± 1.19	0.21 ± 0.13	6.54 ± 2.93	0.62 ± 0.27	1.27 ± 0.57	16.3 ± 6.84	26.66 ± 18.01
Zero	2-10	0.04 ± 0	0.24 ± 0	0.39 ± 0	20.65 ± 28.59	0.51 ± 0	1.39 ± 0	11.95 ± 0	28.04 ± 0
Final	2-11	0.025 ± 0.016	1.9 ± NA	0.01 ± NA	3.15 ± NA	0.7 ± NA	0.61 ± NA	13.92 ± NA	6.78 ± NA
Zero	2-11	0.004 ± 0	0.24 ± NA	0.39 ± NA	63.54 ± NA	0.51 ± NA	1.39 ± NA	11.95 ± NA	28.04 ± NA
Final	2-12	0.043 ± 0.004	2.23 ± 0.2	0.43 ± 0.03	3.79 ± 0.91	0.28 ± 0.04	0.68 ± 0.07	13.21 ± 0.54	4.02 ± 0.73
Zero	2-12	0.006 ± 0	0.13 ± 0	0.09 ± 0	46.01 ± 0	0.81 ± 0	1.71 ± 0	16.6 ± 0	59.71 ± 0
Final	3-13	0.042 ± 0.029	0.22 ± 0.05	0.24 ± 0.07	40.39 ± 7.93	3.47 ± 1.36	2.09 ± 0.09	140.85 ± 29.02	292.4 ± 78.33
Zero	3-13	0.119 ± 0	0.31 ± 0	0.35 ± 0	103.55 ± 0	4.84 ± 0	1.47 ± 0	76.6 ± 0	535.08 ± 0
Final	3-14	0.044 ± 0.016	0.21 ± 0.01	0.43 ± 0.01	54.59 ± 15.17	5 ± 1.11	1.88 ± 0.73	92.65 ± 13.83	339.24 ± 84.63
Zero	3-14	0.099 ± 0	0.3 ± 0	0.35 ± 0	104.46 ± 0	4.5 ± 0	1.47 ± 0	78.25 ± 0	542.84 ± 0
Final	3-15	0.095 ± 0.013	0.81 ± 0.08	0.86 ± 0.39	6.42 ± 1.11	0.53 ± 0.03	1.11 ± 0.24	13.95 ± 5.08	21.84 ± 12.02
Zero	3-15	0.6 ± 0	0.26 ± 0	0.22 ± 0	4.99 ± 0	2.94 ± 0	1.04 ± 0	9.39 ± 0	31.48 ± 0
Final	3-16	0.063 ± 0.032	0.42 ± 0.29	0.43 ± 0.04	6.64 ± 4.37	1.04 ± 0.55	0.92 ± 0.28	15.29 ± 5.05	18.47 ± 6.99
Zero	3-16	0.3 ± 0	0.26 ± 0	0.22 ± 0	9.97 ± 0	2.94 ± 0	1.04 ± 0	9.39 ± 0	31.48 ± 0
Final	3-17	0.034 ± 0.01	0.47 ± 0.16	0.49 ± 0.04	12.74 ± 5.83	0.64 ± 0.22	1.36 ± 0.25	19.55 ± 3.66	16.56 ± 1.07
Zero	3-17	0.06 ± 0	0.26 ± 0	0.22 ± 0	49.85 ± 0	2.94 ± 0	1.04 ± 0	9.39 ± 0	31.48 ± 0
Final	3-18	0.036 ± 0.027	0.26 ± 0.12	1.35 ± 1.23	19.76 ± 5.43	0.68 ± 0.01	1.43 ± 0.03	14.32 ± 5.26	23.18 ± 12.75
Zero	3-18	0.002 ± 0	0.6 ± 0	0.21 ± 0	20.59 ± 0	1.37 ± 0	1.12 ± 0	4.37 ± 0	13.96 ± 0
Final	4-19	0.073 ± NA	0.31 ± NA	0.54 ± NA	12.27 ± NA	3.16 ± NA	1.23 ± NA	29.03 ± NA	83.54 ± NA
Zero	4-19	0.154 ± NA	0.26 ± NA	0.43 ± NA	19.65 ± NA	2.71 ± NA	1.03 ± NA	32.69 ± NA	124.26 ± NA

Table A-4 continued.

Day	No.	InorgN	SCOD : TCOD	OP : TP	TCOD : TN : TP	TVFA : TALK	TAN : TKN	TCOD: Sulfate	TCOD : TKN
Final	4-20	0.028 ± 0.02	0.66 ± 0.17	1.19 ± 0.54	5.54 ± 0.14	0.86 ± 0.32	1.11 ± 0.12	13.11 ± 3.38	9.19 ± 1.72
Zero	4-20	0.051 ± 0	0.14 ± 0	0.23 ± 0	21.77 ± 0	0.55 ± 0	1.37 ± 0	21.59 ± 0	68.09 ± 0
Final	4-21	0.103 ± 0.053	0.6 ± 0.21	1.19 ± 0.36	7.59 ± 1.2	0.21 ± 0.1	1.26 ± 0.17	12.18 ± 6.2	13.88 ± 2.83
Zero	4-21	0.062 ± 0	0.23 ± 0	0.37 ± 0	11.17 ± 0	0.74 ± 0	0.96 ± 0	9.95 ± 0	30.96 ± 0
Final	4-22	0.148 ± 0.048	0.47 ± 0.05	0.63 ± 0.21	4.92 ± 1.03	0.45 ± 0.23	1.29 ± 0.54	8.24 ± 2.72	15.79 ± 3.76
Zero	4-22	0.102 ± 0	0.18 ± 0	0.19 ± 0	5.94 ± 0	0.7 ± 0	1.42 ± 0	14.1 ± 0	46.68 ± 0
Final	4-23	0.031 ± 0.01	0.89 ± 0.32	1.36 ± 0.06	11.64 ± 8.42	1.68 ± 1.71	0.51 ± 0.2	9.82 ± 2.9	9 ± 6.44
Zero	4-23	0.022 ± 0	0.11 ± 0	0.26 ± 0	61.47 ± 0	0.62 ± 0	1.43 ± 0	23.02 ± 0	78.72 ± 0
Final	5-24	0.02 ± 0.024	0.56 ± 0.15	0.97 ± 0.35	6.03 ± 0.99	6.5 ± 2.84	0.61 ± 0.16	30.42 ± 6.76	39.95 ± 7.02
Zero	5-24	0.067 ± 0	0.33 ± 0	0.42 ± 0	9.32 ± 0	4.3 ± 0	0.87 ± 0	17.19 ± 0	72.37 ± 0
Final	5-25	0.044 ± 0.04	0.29 ± 0.08	0.86 ± 0.16	12.46 ± 6.51	0.6 ± 0.07	0.73 ± 0.26	13.3 ± 1.99	17.87 ± 7.91
Zero	5-25	0.031 ± 0	0.22 ± 0	0.33 ± 0	11.44 ± 0	0.63 ± 0	1.31 ± 0	8.37 ± 0	31.73 ± 0
Final	5-26	0.021 ± 0.019	0.26 ± 0.05	0.42 ± 0.19	9.13 ± 7.32	0.56 ± 0.1	1.04 ± 0.14	8.69 ± 0.7	22.86 ± 11.29
Zero	5-26	0.032 ± 0	0.13 ± 0	0.29 ± 0	10.37 ± 0	0.44 ± 0	1.1 ± 0	7.61 ± 0	27 ± 0
Final	5-27	0.098 ± 0.031	0.38 ± 0.06	0.62 ± 0.37	3.9 ± 3.03	0.52 ± 0.16	1 ± 0.25	9.03 ± 3.09	12.54 ± 5.8
Zero	5-27	0.065 ± 0	0.17 ± 0	0.33 ± 0	5.86 ± 0	0.55 ± 0	1.38 ± 0	5.67 ± 0	25.95 ± 0
Final	5-28	0.018 ± 0.024	0.75 ± 0.09	0.63 ± 0	12.29 ± 1.04	0.3 ± 0.02	0.97 ± 0.06	20.75 ± 7.46	8.32 ± 1.45
Zero	5-28	0.017 ± 0	0.17 ± 0	0.37 ± 0	29.69 ± 0	0.49 ± 0	3.49 ± 0	7.62 ± 0	26.58 ± 0
Final	6-29	0.011 ± NA	0.06 ± NA	0 ± NA	33.07 ± NA	0.11 ± NA	1.09 ± NA	52.75 ± NA	51.42 ± NA
Zero	6-29	0.025 ± NA	0.05 ± NA	0 ± NA	157.3 ± NA	0.93 ± NA	8.25 ± NA	9.69 ± NA	417.29 ± NA
Final	6-30	0.003 ± NA	0.06 ± NA	0 ± NA	37.07 ± NA	0.06 ± NA	1.84 ± NA	63.25 ± NA	95.13 ± NA
Zero	6-30	0.025 ± NA	0.05 ± NA	0 ± NA	198.16 ± NA	0.93 ± NA	82.47 ± NA	9.64 ± NA	415.22 ± NA
Final	6-31	0.013 ± 0.01	0.06 ± 0.01	0 ± 0	22.3 ± 7.49	0.08 ± 0.04	1.52 ± 0.25	25.97 ± 12.16	67.34 ± 8.62
Zero	6-31	0.021 ± 0	0.04 ± 0	0 ± 0	249.38 ± 0	0.93 ± 0	20.67 ± 21.52	13.21 ± 0	568.8 ± 0
Final	6-32	0.023 ± NA	0.19 ± NA	0 ± NA	32.97 ± NA	0.14 ± NA	0.96 ± NA	17.34 ± NA	24.2 ± NA
Zero	6-32	0.019 ± NA	0.03 ± NA	0 ± NA	374.45 ± NA	0.92 ± NA	5.3 ± NA	17.4 ± NA	748.91 ± NA
Zero	6-33	0.017 ± NA	0.02 ± NA	0 ± NA	536.98 ± NA	0.92 ± NA	8.25 ± NA	22.22 ± NA	956.25 ± NA
Final	6-34	0.007 ± NA	0.15 ± NA	0 ± NA	8.49 ± NA	0.11 ± NA	0.97 ± NA	25.05 ± NA	20.51 ± NA
Zero	6-34	0.022 ± NA	0.04 ± NA	0 ± NA	231.45 ± NA	0.93 ± NA	8.24 ± NA	12.59 ± NA	541.44 ± NA
Final	6-35	0.014 ± 0.011	0.17 ± 0.03	0 ± 0	57.83 ± 33.89	0.82 ± 0.04	2.86 ± 2.53	37.38 ± 11.45	86.66 ± 20.11
Zero	6-35	0.018 ± 0	0.03 ± 0	0 ± 0	449.25 ± 0	0.92 ± 0	8.22 ± 0	19.81 ± 0	850.19 ± 0
Final	6-36	0.016 ± NA	0.1 ± NA	0 ± NA	10.51 ± NA	0.09 ± NA	0.95 ± NA	44.54 ± NA	32.62 ± NA
Zero	6-36	0.021 ± NA	0.04 ± NA	0 ± NA	243.6 ± NA	0.93 ± NA	8.25 ± NA	13 ± NA	559.91 ± NA
Final	6-37	0.009 ± 0.008	0.09 ± 0.02	0 ± 0	18.32 ± 10.82	0.15 ± 0.06	3.78 ± 2.74	37.14 ± 14.24	36.27 ± 3.12

Table A-4 continued.

Day	No.	InorgN	SCOD : TCOD	OP : TP	TCOD : TN : TP	TVFA : TALK	TAN : TKN	TCOD: Sulfate	TCOD : TKN
Zero	6-37	0.019 ± 0	0.03 ± 0	0 ± 0	359.31 ± 0	0.93 ± 0	5.5 ± 4.76	16.92 ± 0	728.41 ± 0
Final	6-38	0.016 ± NA	0.13 ± NA	0 ± NA	72.43 ± NA	0.15 ± NA	0.94 ± NA	23.97 ± NA	34.67 ± NA
Zero	6-38	0.017 ± NA	0.02 ± NA	0 ± NA	508.08 ± NA	0.93 ± NA	8.24 ± NA	21.41 ± NA	921.29 ± NA
Final	6-39	0.012 ± NA	0.06 ± NA	0 ± NA	45.05 ± NA	0.1 ± NA	1.57 ± NA	52.93 ± NA	95.4 ± NA
Zero	6-39	0.021 ± NA	0.04 ± NA	0 ± NA	258.14 ± NA	0.93 ± NA	8.23 ± NA	13.54 ± NA	582.19 ± NA
Final	6-40	NA ± NA	0.05 ± NA	0 ± NA	22.61 ± NA	0.18 ± NA	1.12 ± NA	21.74 ± NA	92.54 ± NA
Zero	6-40	0.018 ± NA	0.03 ± NA	0 ± NA	397.48 ± NA	0.93 ± NA	8.22 ± NA	18.17 ± NA	779.7 ± NA
Final	6-41	0.005 ± NA	0.44 ± NA	51.69 ± NA	61.21 ± NA	4.16 ± NA	1.18 ± NA	59.71 ± NA	120.3 ± NA
Zero	6-41	0.016 ± NA	0.02 ± NA	0 ± NA	580.89 ± NA	0.01 ± NA	8.21 ± NA	23.54 ± NA	1008.43 ± NA
Final	6-42	0.04 ± NA	0.68 ± NA	90.26 ± NA	88.83 ± NA	6.12 ± NA	1.46 ± NA	69.83 ± NA	218.43 ± NA
Zero	6-42	0.012 ± NA	0.01 ± NA	0 ± NA	1463.1 ± NA	0.93 ± NA	8.17 ± NA	44.38 ± NA	1890.47 ± NA
Final	6-43	0.013 ± 0.018	0.51 ± 0.1	38 ± 16.54	56.31 ± 18.47	4.63 ± 1.17	5.41 ± 4.13	53.16 ± 30.88	151.34 ± 8.76
Zero	6-43	0.018 ± 0	0.03 ± 0	0 ± 0	412.83 ± 13.3	0.92 ± 0.01	8.17 ± 0.04	19.09 ± 0.8	813.2 ± 29.02
Final	6-44	0.016 ± NA	0.06 ± NA	0 ± NA	16.13 ± NA	0.09 ± NA	1.35 ± NA	27.5 ± NA	36.54 ± NA
Zero	6-44	0.029 ± NA	0.05 ± NA	0 ± NA	110.46 ± NA	0.49 ± NA	2.06 ± NA	10.9 ± NA	79.36 ± NA
Final	6-45	0 ± NA	0.09 ± 0.01	0 ± 0	15.82 ± 6.39	0.09 ± 0.04	6.48 ± 2.09	27.71 ± 19.39	54.17 ± 19.99
Zero	6-45	0.002 ± 0	0.01 ± 0	0 ± 0	107.3 ± 0	0.65 ± 0	2.59 ± 0	8.28 ± 0	258.45 ± 0

Unitless except for InorgN (g L^{-1}). n = 3.

Table A-5. The mean ± standard deviation of digester influent (day zero) and effluent (final day) characteristics for each lab-digester group (4).

Day	No.	FS : TS	VS : TS	Fe(II) : S	Fe(II) : TP
Final	1-1	0.39 ± 0.06	0.61 ± 0.06	0.005 ± 0.001	0.018 ± 0.005
Zero	1-1	0.22 ± 0	0.78 ± 0	0.003 ± 0	0.063 ± 0
Final	1-2	0.43 ± 0.02	0.57 ± 0.02	0.004 ± 0	0.019 ± 0.003
Zero	1-2	0.23 ± 0	0.77 ± 0	0.003 ± 0	0.059 ± 0.006
Final	1-3	0.59 ± 0.02	0.41 ± 0.02	0.004 ± 0.006	0.039 ± 0.06
Zero	1-3	0.5 ± 0	0.5 ± 0	0.004 ± 0	0.117 ± 0
Final	1-4	0.58 ± 0.01	0.42 ± 0.01	0.003 ± 0	0.025 ± 0.016
Zero	1-4	0.47 ± 0	0.53 ± 0	0.005 ± 0	0.1 ± 0
Final	1-5	0.46 ± NA	0.54 ± NA	0.007 ± NA	0.027 ± NA
Zero	1-5	0.34 ± 0	0.66 ± 0	0.006 ± 0	0.079 ± 0
Final	2-7	0.21 ± 0.01	0.79 ± 0.01	0.001 ± 0	0.001 ± 0.001
Zero	2-7	0.18 ± 0	0.82 ± 0	0.003 ± 0	0.011 ± 0
Final	2-8	0.2 ± 0	0.8 ± 0	0.005 ± 0.005	0.003 ± 0.003
Zero	2-8	0.19 ± 0	0.81 ± 0	0.003 ± 0	0.01 ± 0
Final	2-10	0.34 ± 0.03	0.66 ± 0.03	0.003 ± 0.005	0.002 ± 0.003
Zero	2-10	0.29 ± 0	0.71 ± 0	0.019 ± 0	0.024 ± 0
Final	2-11	0.45 ± NA	0.55 ± NA	0 ± NA	0 ± NA
Zero	2-11	0.29 ± NA	0.71 ± NA	0.019 ± NA	0.024 ± NA
Final	2-12	0.48 ± 0	0.52 ± 0	0.023 ± 0.002	0.002 ± 0
Zero	2-12	0.37 ± 0	0.63 ± 0	0.014 ± 0	0.007 ± 0
Final	3-13	0.13 ± 0.08	0.87 ± 0.08	0.017 ± 0.006	0.006 ± 0.002
Zero	3-13	0.03 ± 0	0.97 ± 0	0.01 ± 0	0.013 ± 0
Final	3-14	0.16 ± 0	0.84 ± 0	0.03 ± 0.001	0.018 ± 0.004
Zero	3-14	0.03 ± 0	0.97 ± 0	0.011 ± 0	0.013 ± 0
Final	3-15	0.48 ± 0.13	0.52 ± 0.13	0.009 ± 0.01	0.013 ± 0.016
Zero	3-15	0.29 ± 0	0.71 ± 0	0.01 ± 0	0.012 ± 0
Final	3-16	0.41 ± 0.09	0.59 ± 0.09	0.01 ± 0.006	0.009 ± 0.009
Zero	3-16	0.3 ± 0	0.7 ± 0	0.01 ± 0	0.012 ± 0
Final	3-17	0.4 ± 0.01	0.6 ± 0.01	0.061 ± NA	0.299 ± 0.414
Zero	3-17	0.29 ± 0	0.71 ± 0	0.01 ± 0	1.082 ± 1.514
Final	3-18	0.41 ± 0.03	0.59 ± 0.03	0.015 ± NA	0.358 ± 0.494
Zero	3-18	0.3 ± 0	0.7 ± 0	0.01 ± 0	0.617 ± 0.858
Final	4-19	0.23 ± NA	0.77 ± NA	0.006 ± NA	0.007 ± NA
Zero	4-19	0.16 ± NA	0.84 ± NA	0.009 ± NA	0.01 ± NA
Final	4-20	0.41 ± 0.1	0.59 ± 0.1	0.025 ± 0.014	0.011 ± 0.003
Zero	4-20	0.26 ± 0	0.74 ± 0	0.006 ± 0	0.006 ± 0
Final	4-21	0.43 ± 0.09	0.57 ± 0.09	0.018 ± 0.013	0.012 ± 0.004
Zero	4-21	0.26 ± 0	0.74 ± 0	0.008 ± 0	0.012 ± 0
Final	4-22	0.48 ± 0.03	0.52 ± 0.03	0.015 ± 0.006	0.018 ± 0.01
Zero	4-22	0.3 ± 0	0.7 ± 0	0.007 ± 0	0.006 ± 0
Final	4-23	0.49 ± 0.07	0.51 ± 0.07	0.042 ± 0.017	0.03 ± 0.009
Zero	4-23	0.06 ± 0	0.94 ± 0	0.007 ± 0	0.008 ± 0
Final	5-24	0.19 ± 0.01	0.81 ± 0.01	0.02 ± 0.024	0.02 ± 0.022
Zero	5-24	0.13 ± 0	0.87 ± 0	0.019 ± 0	0.027 ± 0
Final	5-25	0.37 ± 0.04	0.63 ± 0.04	0.044 ± 0.04	0.018 ± 0.003
Zero	5-25	0.24 ± 0	0.76 ± 0	0.007 ± 0	0.012 ± 0
Final	5-26	0.32 ± 0.01	0.68 ± 0.01	0.021 ± 0.019	0.009 ± 0.005
Zero	5-26	0.27 ± 0	0.73 ± 0	0.006 ± 0	0.01 ± 0

Table A-5 continued.

Day	No.	FS : TS	VS : TS	Fe(II) : S	Fe(II) : TP
Final	5-27	0.36 ± 0.02	0.64 ± 0.02	0.098 ± 0.031	0.012 ± 0.006
Zero	5-27	0.28 ± 0	0.72 ± 0	0.006 ± 0	0.013 ± 0
Final	5-28	0.44 ± 0.09	0.56 ± 0.09	0.018 ± 0.024	0.022 ± 0.001
Zero	5-28	0.09 ± 0	0.91 ± 0	0.008 ± 0	0.015 ± 0
Final	6-29	0.52 ± NA	0.48 ± NA	0 ± NA	0.008 ± NA
Zero	6-29	0.44 ± NA	0.56 ± NA	0 ± NA	0.031 ± NA
Final	6-30	0.53 ± NA	0.47 ± NA	0 ± NA	0.007 ± NA
Zero	6-30	0.44 ± NA	0.56 ± NA	0 ± NA	0.031 ± NA
Final	6-31	0.52 ± 0	0.48 ± 0	0 ± 0	0.005 ± 0.001
Zero	6-31	0.44 ± 0	0.56 ± 0	0 ± 0	0.031 ± 0
Final	6-32	0.52 ± NA	0.48 ± NA	0 ± NA	0.041 ± NA
Zero	6-32	0.43 ± NA	0.57 ± NA	0 ± NA	0.031 ± NA
Zero	6-33	0.43 ± NA	0.57 ± NA	0 ± NA	0.031 ± NA
Final	6-34	0.52 ± NA	0.48 ± NA	0 ± NA	0.004 ± NA
Zero	6-34	0.43 ± NA	0.57 ± NA	0 ± NA	0.031 ± NA
Final	6-35	0.46 ± 0	0.54 ± 0	0 ± 0	0.044 ± 0.033
Zero	6-35	0.42 ± 0	0.58 ± 0	0 ± 0	0.031 ± 0
Final	6-36	0.6 ± NA	0.4 ± NA	0 ± NA	0.005 ± NA
Zero	6-36	0.44 ± NA	0.56 ± NA	0 ± NA	0.031 ± NA
Final	6-37	0.51 ± 0.01	0.49 ± 0.01	0 ± 0	0.011 ± 0.01
Zero	6-37	0.43 ± 0	0.57 ± 0	0 ± 0	0.031 ± 0
Final	6-38	0.52 ± NA	0.48 ± NA	0 ± NA	0.043 ± NA
Zero	6-38	0.43 ± NA	0.57 ± NA	0 ± NA	0.031 ± NA
Final	6-39	0.51 ± NA	0.49 ± NA	0 ± NA	0.007 ± NA
Zero	6-39	0.44 ± NA	0.56 ± NA	0 ± NA	0.031 ± NA
Final	6-40	0.51 ± NA	0.49 ± NA	0 ± NA	0.007 ± NA
Zero	6-40	0.43 ± NA	0.57 ± NA	0 ± NA	0.031 ± NA
Final	6-41	0.37 ± NA	0.63 ± NA	0 ± NA	0.132 ± NA
Zero	6-41	0.43 ± NA	0.57 ± NA	0 ± NA	0.031 ± NA
Final	6-42	0.33 ± NA	0.67 ± NA	0 ± NA	0.128 ± NA
Zero	6-42	0.41 ± NA	0.59 ± NA	0 ± NA	0.031 ± NA
Final	6-43	0.33 ± 0.01	0.67 ± 0.01	0 ± 0	0.177 ± 0.062
Zero	6-43	0.41 ± 0.02	0.59 ± 0.02	0 ± 0	0.031 ± 0
Final	6-44	0.54 ± NA	0.46 ± NA	0 ± NA	0.006 ± NA
Zero	6-44	0.5 ± NA	0.5 ± NA	0 ± NA	0.016 ± NA
Final	6-45	0.52 ± 0.02	0.48 ± 0.02	0 ± 0	0.004 ± 0.001
Zero	6-45	0.38 ± 0	0.62 ± 0	0 ± 0	0.045 ± 0

Unitless. n = 3.

Table A-6. Fraction of increases and decreases for each parameter over time.

Parameter	Decrease	Increase
pH	0.19	0.90
Conductivity	0.71	0.31
TS	0.69	0.33
VS	0.73	0.29
TCOD	0.72	0.30
SCOD	0.44	0.63
TVFA	0.61	0.43
TALK	0.40	0.68
TKN	0.36	0.73
TN	0.37	0.72
Inorganic N	0.58	0.46
TAN	0.44	0.63
Sulfate	0.84	0.15
Tannic Acid	0.64	0.39
TP	0.41	0.67
OP	0.29	0.80
Fe	0.60	0.44
Ni	0.52	0.54
Cu	0.45	0.62

Table A-7. The percentage of each type of COD removal for each lab-digester group.

Lab-digester group No.	COD removal from Methanogens, %	COD removal from SRB,%
1-1	46.16	2.19
1-2	51.19	2.51
1-3	77.73	0.73
1-4	72.96	0.40
1-5	53.91	4.02
2-7	-28.75	0.59
2-8	-2.62	0.86
2-10	-32.56	0.57
2-11	75.36	4.47
2-12	84.16	3.41
3-13	27.46	0.53
3-14	31.29	0.35
3-15	13.25	3.21
3-16	18.79	3.16
3-17	51.37	5.67
3-18	-73.88	6.30
4-19	12.39	0.03
4-20	82.91	2.27
4-21	56.81	4.06
4-22	68.57	2.30
4-23	81.62	1.65
5-24	16.32	2.06
5-25	7.22	3.46
5-26	21.86	2.93
5-27	20.11	6.22
5-28	56.05	7.59
6-29	4.35	5.77
6-30	-17.04	5.77
6-31	25.01	2.99
6-32	70.14	2.81
6-34	58.56	4.33
6-35	25.03	2.08
6-36	42.25	4.33
6-37	69.18	2.39
6-38	62.34	2.14
6-39	18.06	3.96
6-40	8.39	0.89
6-41	39.78	2.19
6-42	54.88	1.09
6-43	2.24	1.99
6-44	29.17	4.53
6-45	23.07	5.89

Table A-8. Percent increase and decrease for each characteristic for the precipitation tests.

Treatment	pH	Sulfate	TP	Fe	Ni	Cu
Fe Reduction w/ Inoculum	2.68	-76.52	99.24	17.05	-123.31	-116.1
Fe Reduction w/o Inoculum	3.31	NA	NA	Inf	NA	NA
Fe Reduction +FeS Precipitation w/ Inoculum	0.98	-33.61	112.29	225.2	-129.55	-116.44
Fe Reduction + FeS Precipitation w/o Inoculum	0.69	5150.85	NA	Inf	NA	NA
Fe-P Precipitation w/ Inoculum	-1.04	-61.49	-36.34	30.7	-120.15	-115.47
Fe-P Precipitation w/o Inoculum	-1.52	NA	-37.75	Inf	NA	NA
Inoculum only	-0.48	-47.8	139.52	-46.45	-131.85	-111.91

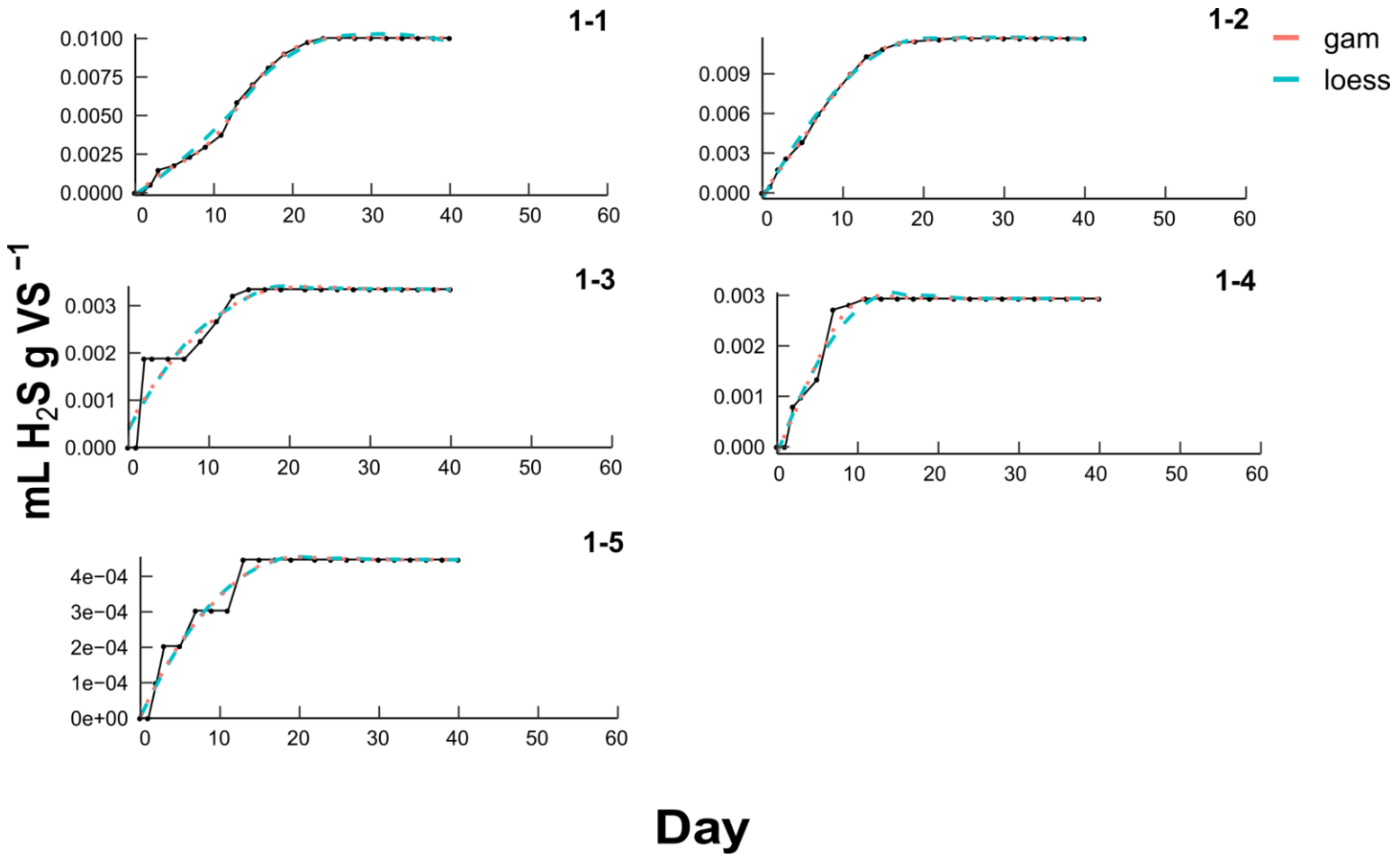

Figure A-1. The specific H_2S productions and the fitted gam and loess models for the lab-digesters for Batch 1.

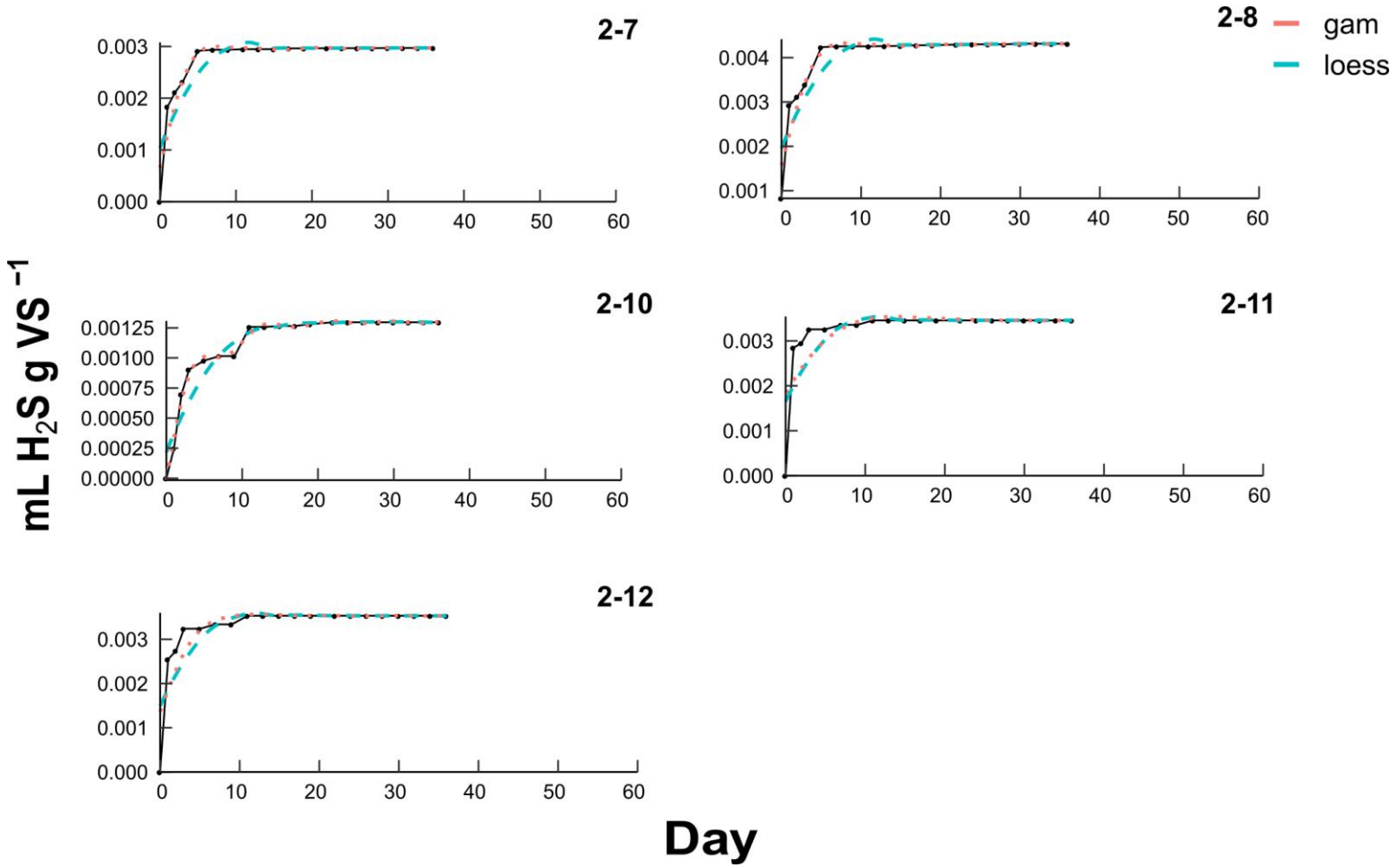

Figure A-2. The specific H_2S productions and the fitted gam and loess models for the lab-digesters for Batch 2.

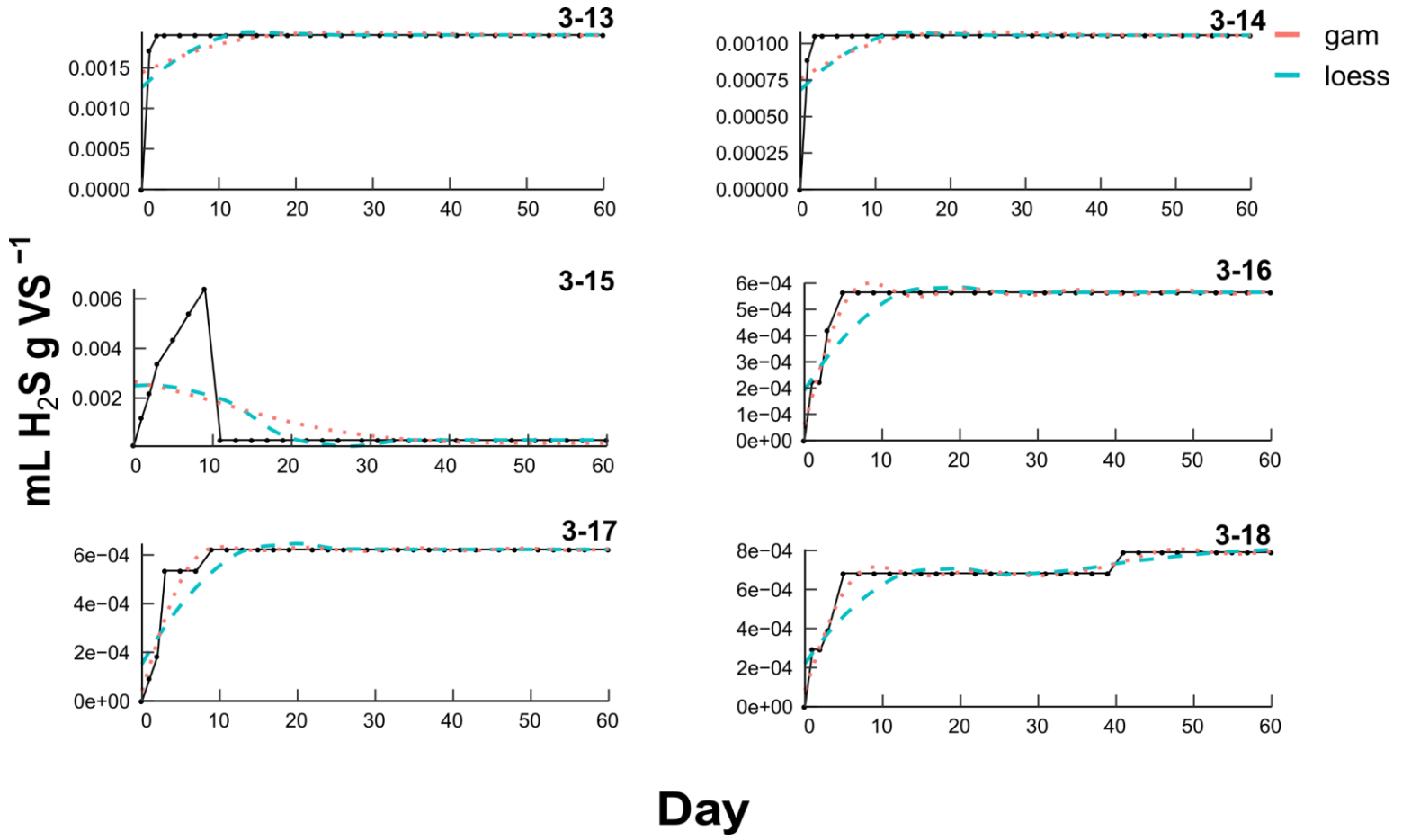

Figure A-3. The specific H_2S production and the fitted gam and loess models for the lab-digesters for Batch 3.

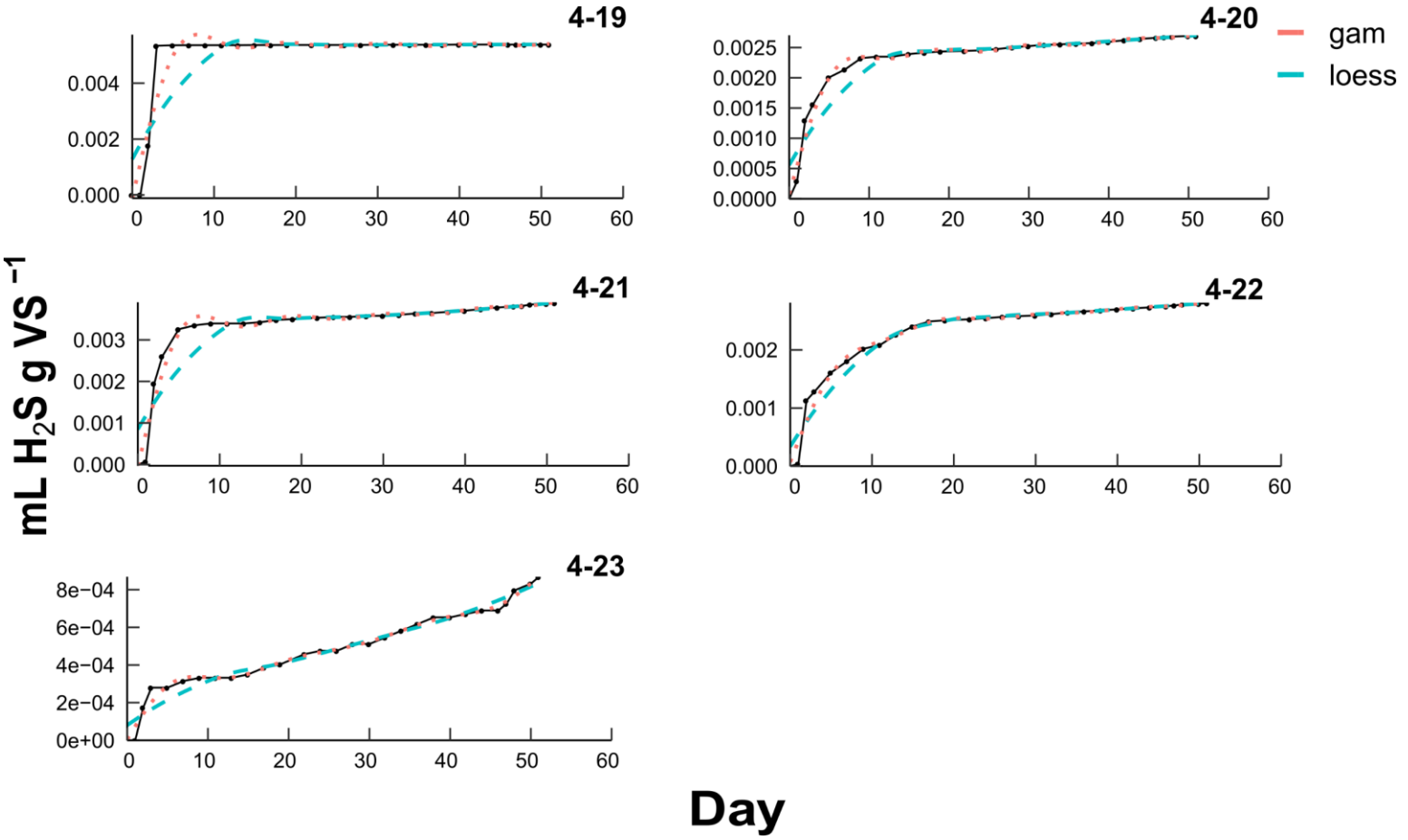

Figure A-4. The specific H_2S production and the fitted gam and loess models for the lab-digesters for Batch 4.

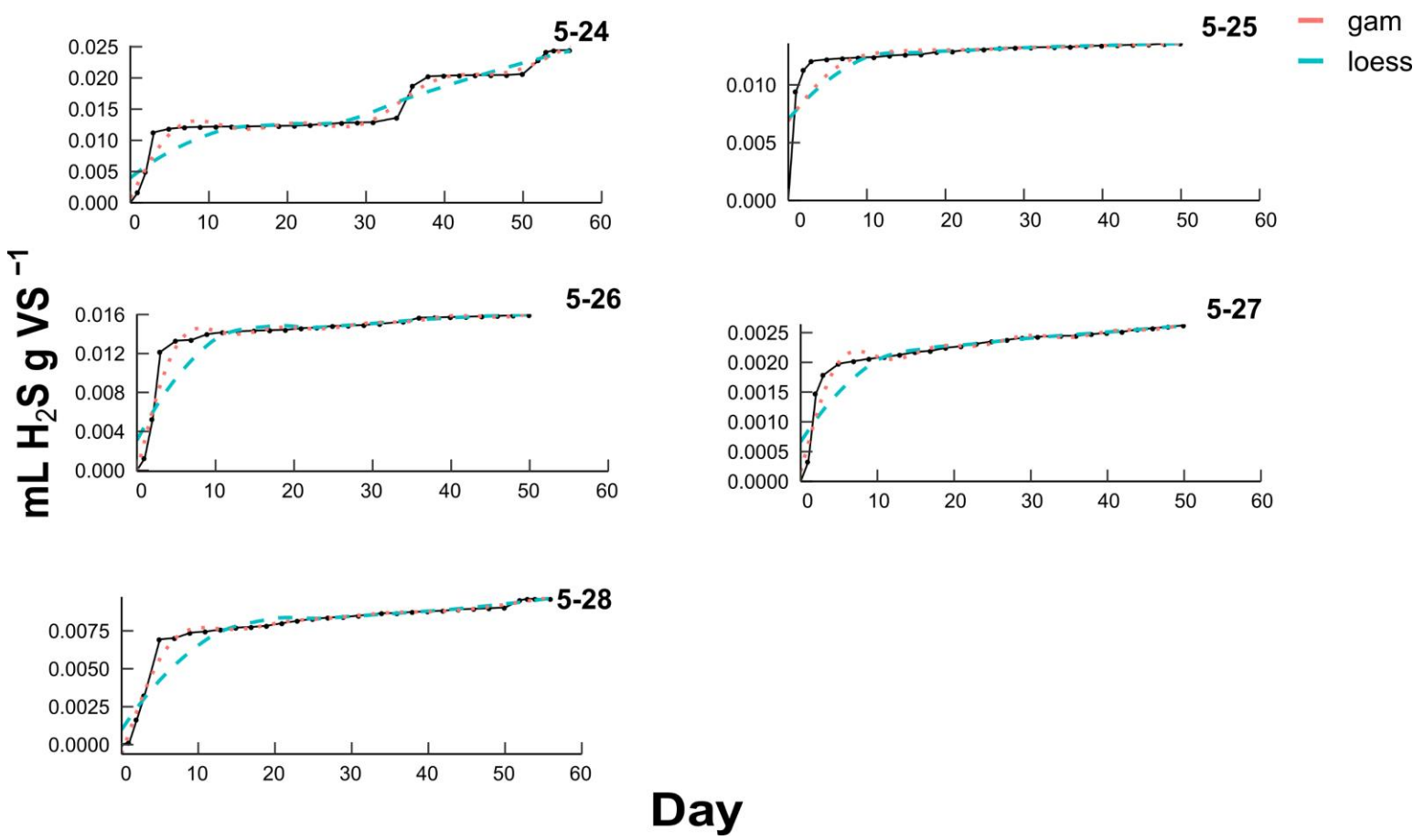

Figure A-5. The specific H_2S production and the fitted gam and loess models for the lab-digester groups for Batch 5.

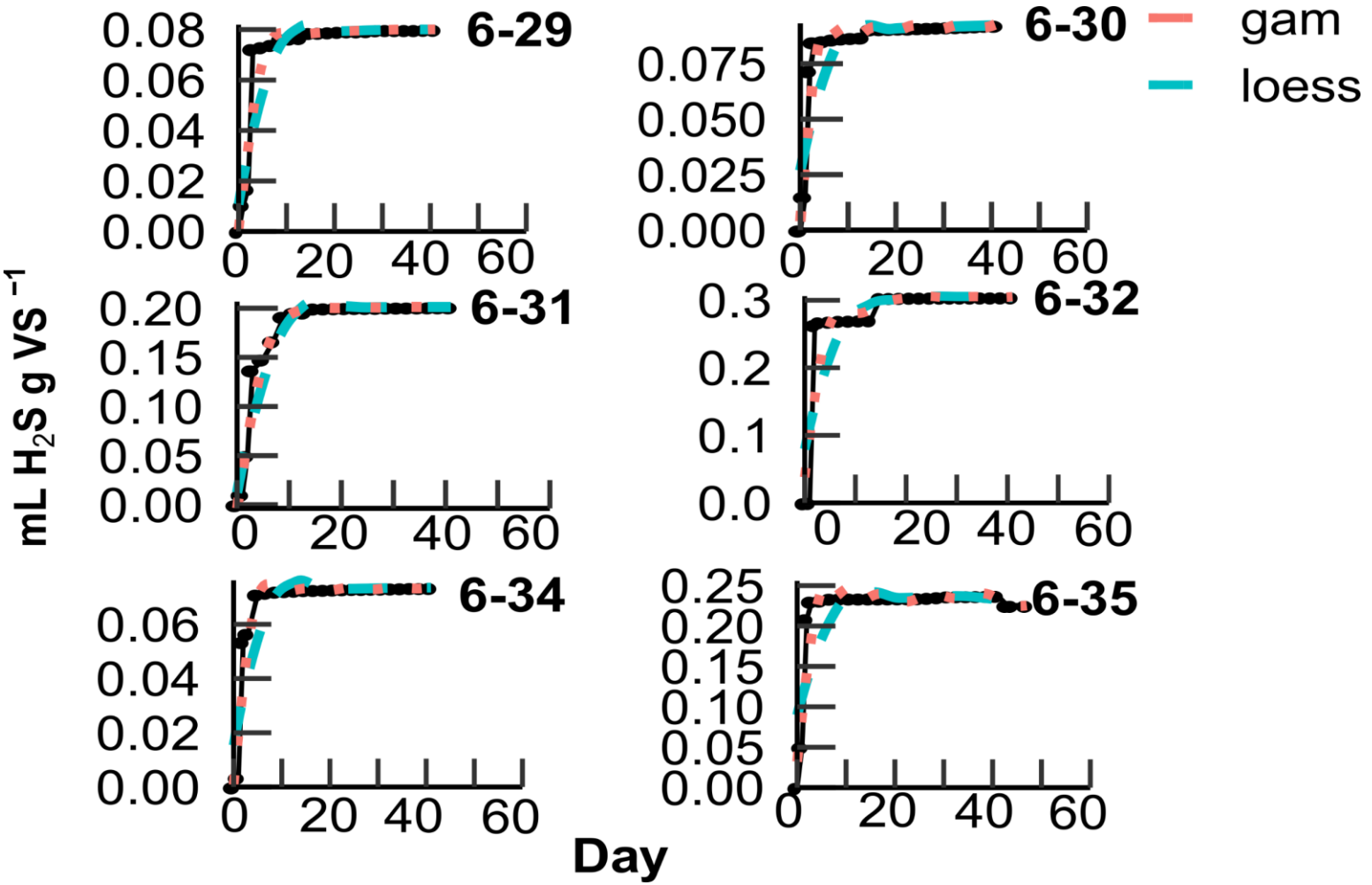

Figure A-6. The specific H_2S production and the fitted gam and loess models for the lab-digester groups for Batch 6 (1).

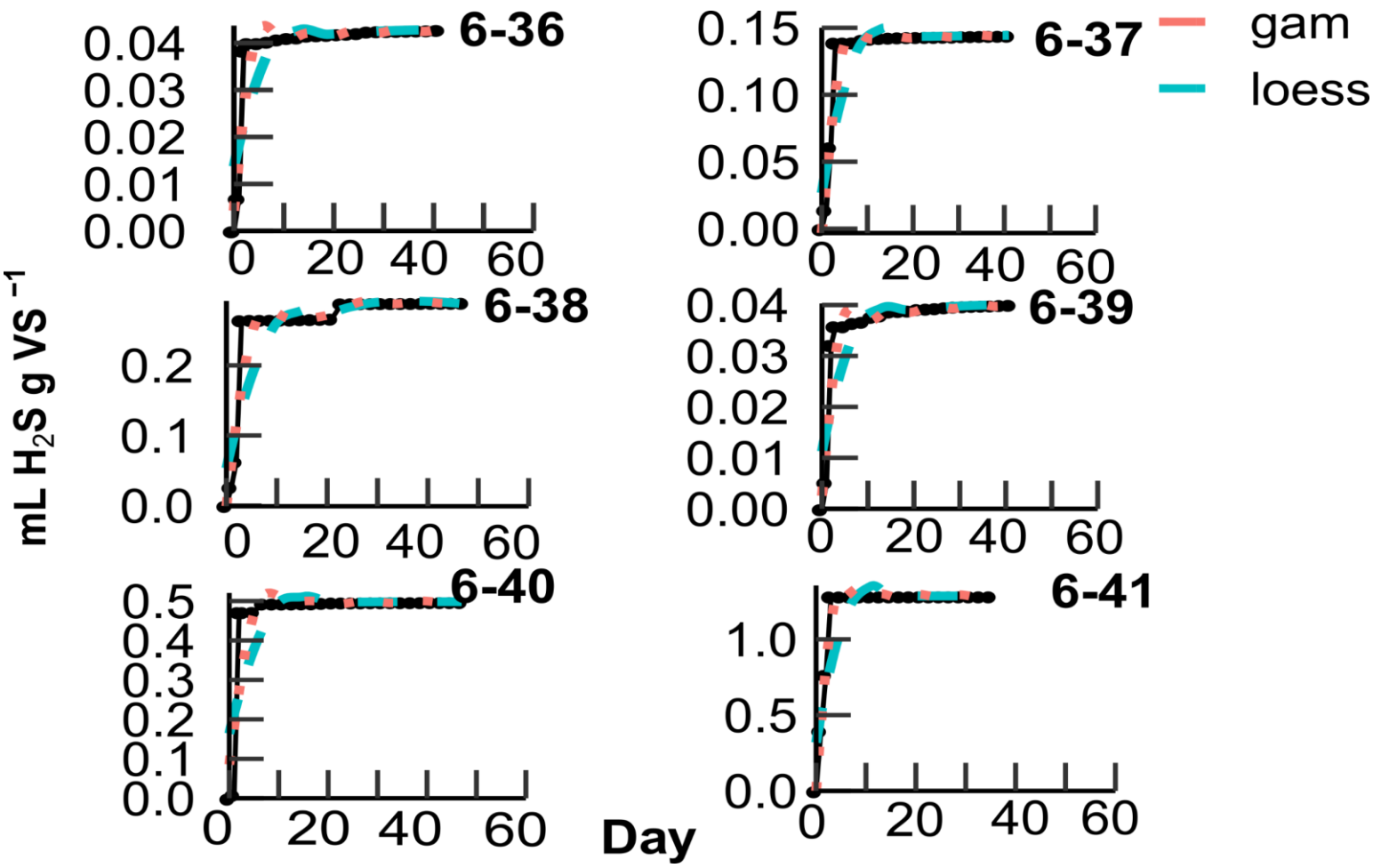

Figure A-7. The specific H_2S production and the fitted gam and loess models for the lab-digester groups for Batch 6 (2).

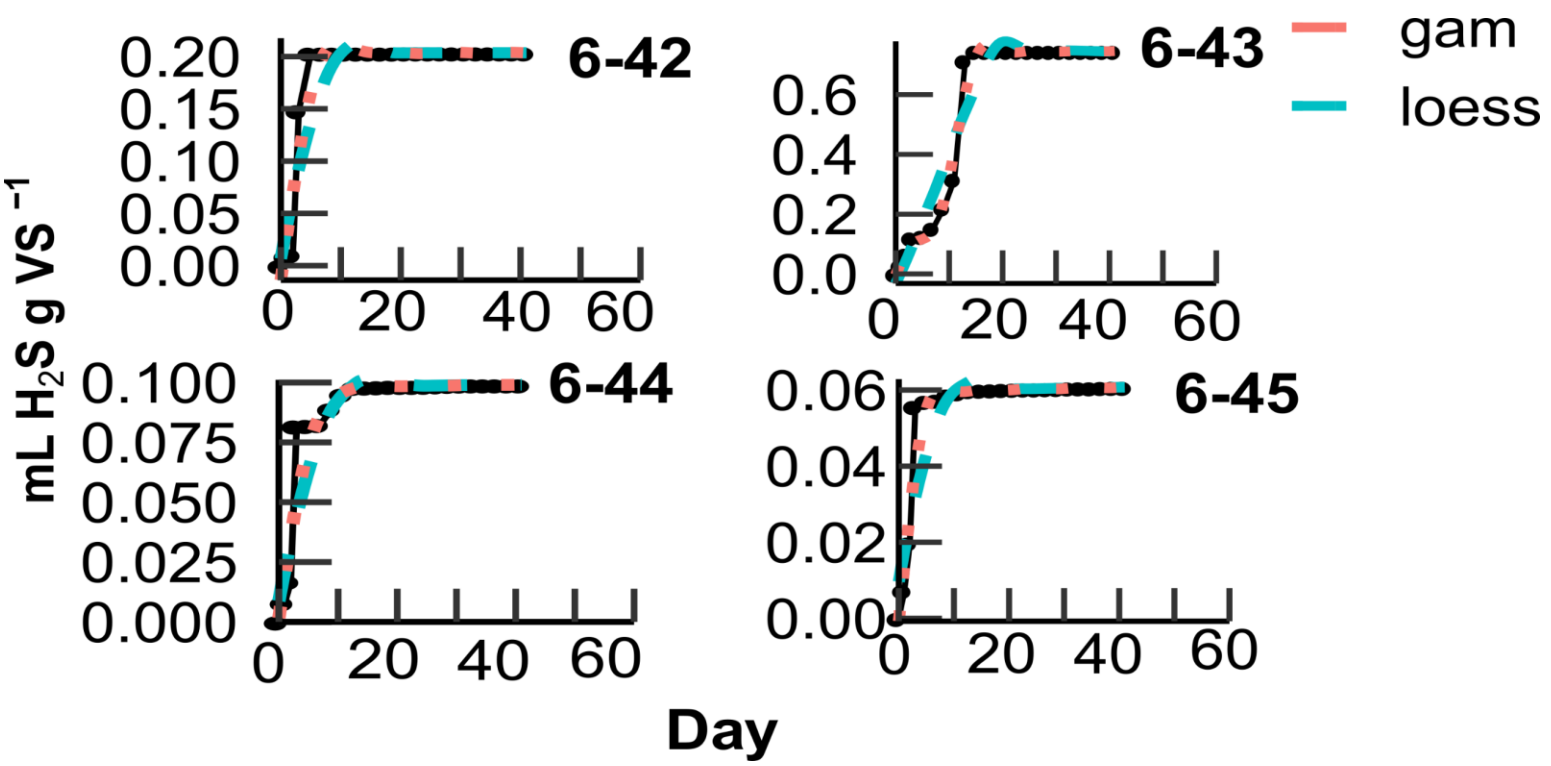

Figure A-8. The specific H_2S production and the fitted gam and loess models for the lab-digester groups for Batch 6 (3).

APPENDIX B. CHAPTER 5 SUPPLEMENTARY

Table B-1. The mean ± standard deviation of digester influent (day zero) and effluent (final day) characteristics for each lab-digester group (1).

Day	No.	pH	Conductivity	TS	VS	TCOD	SCOD	TVFA	TALK
Final	2-1	7.52 ± 0.37	6.95 ± 0.04	82 ± 6	64.48 ± 5.58	192 ± 61	42.07 ± 4.51	19 ± 0.4	8.33 ± 3.4
Zero	2-1	6.54 ± 0.05	9.91 ± 0	99 ± 0	80.83 ± 0	150 ± 0	37.69 ± 0	9.3 ± 0	6.56 ± 0
Final	2-2	7.85 ± 0.76	6.87 ± 0.17	94 ± 2	74.89 ± 1.76	155 ± 6	40.75 ± 0.07	18.9 ± 0.2	10.16 ± 1.7
Zero	2-2	6.94 ± 0.04	9.86 ± 0	100 ± 0	81.01 ± 0	152 ± 0	37.29 ± 0	9.2 ± 0	6 ± 0
Final	2-4	8.14 ± 0.15	7.87 ± 0.8	59 ± 1	39.65 ± 0.59	89 ± 19	15.77 ± 5.46	7 ± 0.6	14.68 ± 2.59
Zero	2-4	7.64 ± 0.02	10.77 ± 0	66 ± 0	46.7 ± 0	68 ± 0	16.12 ± 0	6.2 ± 0	12.19 ± 0
Final	2-5	7.65 ± 0.14	2.18 ± 0.02	2 ± 0	0.85 ± 0.12	1 ± 0	2.66 ± 0.25	0.22 ± 0	0.8 ± 0.12
Zero	2-5	7 ± 0.05	1.02 ± 0	8 ± 0	4.85 ± 0	10 ± 0	1.21 ± 0	0.53 ± 0	0.66 ± 0
Final	2-6	7.58 ± 0.18	1.83 ± 0.15	2 ± 0	0.94 ± 0.04	1 ± 0	2.98 ± 0	0.52 ± 0	0.64 ± 0.16
Zero	2-6	7.1 ± 0.07	1.08 ± 0	7 ± 0	4.67 ± 0	7 ± 0	1.61 ± 0	0.62 ± 0	1.22 ± 0
Final	3-7	7.14 ± 0.6	4.27 ± 1.45	205 ± 156	185.41 ± 155.4	353 ± 67	75.14 ± 16.03	19.5 ± 2	6.58 ± 3.73
Zero	3-7	6.62 ± 0.2	1 ± 1.13	628 ± 0	605.95 ± 0	490 ± 0	150.72 ± 0	20.2 ± 0	4.18 ± 0
Final	3-8	7.5 ± 0.14	0.93 ± 0.92	146 ± 42	122.45 ± 35.09	340 ± 36	72.82 ± 11.84	18.5 ± 0.2	3.79 ± 0.81
Zero	3-8	6.02 ± 0.07	1.89 ± 0.92	627 ± 0	605.5 ± 0	498 ± 0	150.86 ± 0	19.3 ± 0	4.3 ± 0
Final	3-9	7.55 ± 0.04	7.06 ± 0.15	20 ± 9	12.43 ± 6.69	27 ± 12	9.04 ± 1.36	5.2 ± 2.4	5.06 ± 0.64
Zero	3-9	5.99 ± 0.01	6.5 ± 0.13	35 ± 0	24.22 ± 0	35 ± 0	9.21 ± 0	10.8 ± 0	3.66 ± 0
Final	3-10	7.65 ± 0	7.81 ± 0.1	33 ± 18	18.59 ± 13.45	59 ± 28	46.54 ± 18.21	6 ± 0.1	11.37 ± 0.81
Zero	3-10	7.95 ± 0.03	7.63 ± 0.02	74 ± 0	52.89 ± 0	70 ± 0	18.43 ± 0	21.5 ± 0	7.31 ± 0
Final	3-11	6.84 ± 1.29	3.11 ± 0.22	5 ± 0	2.78 ± 0.08	5 ± 2	1.27 ± 0.08	0.71 ± 0	1.04 ± 0.02
Zero	3-11	5.92 ± 0	1.93 ± 0.67	7 ± 0	4.84 ± 0	3 ± 0	1.88 ± 0	1.2 ± 0	0.89 ± 0
Final	3-12	7.65 ± 0	2.78 ± 1.21	4 ± 1	2.49 ± 0.45	3 ± 1	1.48 ± 0.78	0.89 ± 0.42	1.35 ± 0.19
Zero	3-12	7.21 ± 0.01	2.45 ± 0.19	7 ± 0	5.29 ± 0	7 ± 0	1.84 ± 0	2.2 ± 0	0.73 ± 0
Final	4-13	7.16 ± NA	7.96 ± NA	108 ± NA	82.49 ± NA	199 ± NA	62.03 ± NA	26.2 ± NA	8.3 ± NA
Zero	4-13	6.95 ± NA	8.67 ± NA	137 ± NA	114.91 ± NA	227 ± NA	58.86 ± NA	16.4 ± NA	6.06 ± NA
Final	4-14	8.16 ± 0.07	7.84 ± 0.2	37 ± 3	19.58 ± 2.76	29 ± 5	13.5 ± 2.41	5 ± 0.2	12.9 ± 5.1
Zero	4-14	7.34 ± 0.13	8.53 ± 0.03	83 ± 0	58.29 ± 0	99 ± 0	17.85 ± 0	6.2 ± 0	8.85 ± 0
Final	4-15	7.83 ± 0.09	6.87 ± 0.06	23 ± 9	14.39 ± 7.46	10 ± 3	6.4 ± 0.64	3.6 ± 0.9	4.34 ± 0.7
Zero	4-15	6.85 ± 0.05	7.51 ± 0.14	45 ± 0	33.82 ± 0	68 ± 0	9.46 ± 0	3 ± 0	5.54 ± 0
Final	4-16	8.15 ± 0.05	6.89 ± 0.04	26 ± 14	15.9 ± 10.28	16 ± 8	8.63 ± 1.73	2.8 ± 1.3	13.8 ± 2.37
Zero	4-16	6.98 ± 0.06	7.63 ± 0.2	48 ± 0	35.41 ± 0	41 ± 0	9.24 ± 0	4.1 ± 0	5.52 ± 0

Table B-1 continued.

Day	No.	pH	Conductivity	TS	VS	TCOD	SCOD	TVFA	TALK
Final	4-17	8.01 ± 0.13	4.49 ± 0.27	6 ± 0	3.18 ± 0.63	5 ± 2	4.44 ± 0.04	4.4 ± 4.9	2.35 ± 0.53
Zero	4-17	7.11 ± 0.01	4.26 ± 0.89	28 ± 0	26.59 ± 0	32 ± 0	3.4 ± 0	1.2 ± 0	1.88 ± 0
Final	5-18	6.43 ± 0.04	6.63 ± 0.31	86 ± 11	69.39 ± 9.07	147 ± 12	81.2 ± 16.18	35.8 ± 10.2	5.91 ± 1.37
Zero	5-18	7.12 ± 0.59	7.36 ± 0.56	138 ± 0	119.73 ± 0	180 ± 0	59.84 ± 0	12 ± 0	2.78 ± 0
Final	5-19	7.95 ± 0.24	8.2 ± 0.07	43 ± 6	27.61 ± 4.7	39 ± 11	14.15 ± 2.62	8 ± 3.3	15.04 ± 1.79
Zero	5-19	7.88 ± 0.05	7.92 ± 0.1	61 ± 0	43.3 ± 0	52 ± 0	8.84 ± 0	3.9 ± 0	7.14 ± 0
Final	5-20	7.73 ± 0.12	6.85 ± 0.54	27 ± 2	18.22 ± 1.75	27 ± 5	6.84 ± 0.65	3.3 ± 0.6	6.12 ± 1.88
Zero	5-20	7.54 ± 0.18	7.29 ± 0.08	35 ± 0	25.27 ± 0	36 ± 0	4.61 ± 0	2.1 ± 0	4.67 ± 0
Final	5-21	7.73 ± 0.07	7.19 ± 0.07	17 ± 6	10.77 ± 4.48	31 ± 2	9 ± 1.82	5.3 ± 0.2	8.95 ± 0.98
Zero	5-21	7.62 ± 0.22	7.08 ± 0.24	34 ± 0	25.56 ± 0	35 ± 0	7.64 ± 0	2.6 ± 0	4.07 ± 0
Final	5-22	7.09 ± 0.11	4.23 ± 0.17	5 ± 2	3.17 ± 1.55	4 ± 1	3.26 ± 0.34	0.7 ± 0.01	2.35 ± 0.1
Zero	5-22	7.86 ± 0.12	4.61 ± 0.29	12 ± 0	11.27 ± 0	12 ± 0	2.07 ± 0	0.87 ± 0	1.78 ± 0

Units are in g L^{-1} except for conductivity (mS cm^{-1}) and pH (unitless). n = 3.

Table B-2. The mean ± standard deviation of digester influent (day zero) and effluent (final day) characteristics for each lab-digester group (2).

Day	No.	TKN	TAN	Sulfate	Tannin	TP	OP	Fe	Ni
Final	2-1	3.65 ± 0.09	2.63 ± 0.18	5.65 ± 0.26	2.12 ± 1.36	6.48 ± 0.93	3.87 ± 0.61	0.005 ± 0.001	0.006 ± 0
Zero	2-1	1.53 ± 0	1.81 ± 0	6.97 ± 0	2.43 ± 0	2.12 ± 0	2.12 ± 0	0.014 ± 0	0.004 ± 0
Final	2-2	4.53 ± 1.03	2.65 ± 0.17	5.03 ± 1.18	2.58 ± 0.53	6.67 ± 0.38	3.6 ± 0	0.013 ± 0.011	0.004 ± 0
Zero	2-2	1.45 ± 0	1.75 ± 0	6.99 ± 0	2.34 ± 0	2.06 ± 0	2.06 ± 0	0.012 ± 0	0.004 ± 0
Final	2-4	2.8 ± 0.63	4.03 ± 0.27	5.09 ± 1.04	4.11 ± 0.73	6.1 ± 1.03	1.6 ± 0	0.011 ± 0.015	0.003 ± 0.001
Zero	2-4	2.42 ± 0	3.37 ± 0	5.67 ± 0	3.71 ± 0	4.38 ± 0	1.7 ± 0	0.062 ± 0	0.003 ± 0
Final	2-5	0.3 ± 0	0.2 ± 0.02	0.09 ± 0.01	0.06 ± 0.01	0.93 ± 0.07	0.4 ± 0	0.001 ± 0	0 ± 0
Zero	2-5	0.16 ± 0	0.28 ± 0	0.58 ± 0	0.28 ± 0	1.25 ± 0	0.11 ± 0	0.005 ± 0	0 ± 0
Final	2-6	0.22 ± 0.02	0.13 ± 0.01	0.12 ± 0	0.22 ± 0.2	1.24 ± 1.12	0.02 ± 0.01	0 ± 0	0 ± 0
Zero	2-6	0.24 ± 0	0.34 ± 0	0.57 ± 0	0.37 ± 0	0.44 ± 0	0.17 ± 0	0.006 ± 0	0 ± 0
Final	3-7	1.23 ± 0.11	2.56 ± 0.24	2.51 ± 0.2	1.97 ± 0.18	6.92 ± 0.68	1.67 ± 0.31	0.025 ± 0.011	0.005 ± 0.002
Zero	3-7	0.92 ± 0	1.34 ± 0	6.39 ± 0	2.49 ± 0	4.96 ± 0	1.76 ± 0	0.039 ± 0	0.007 ± 0
Final	3-8	1.05 ± 0.37	1.84 ± 0.08	3.75 ± 0.94	2.34 ± 0.01	5.99 ± 0.17	2.6 ± 0	0.065 ± 0.015	0.006 ± 0
Zero	3-8	0.92 ± 0	1.35 ± 0	6.37 ± 0	2.43 ± 0	5.01 ± 0	1.75 ± 0	0.039 ± 0	0.008 ± 0
Final	3-9	1.46 ± 0.37	1.28 ± 0.13	2.08 ± 1.31	1.62 ± 0.68	3.01 ± 0.77	1.27 ± 0.23	0.014 ± 0.011	0.003 ± 0.001
Zero	3-9	1.12 ± 0	1.16 ± 0	3.74 ± 0	2.18 ± 0	3.12 ± 0	0.7 ± 0	0.021 ± 0	0.001 ± 0
Final	3-10	2.75 ± 0.23	3.02 ± 0.42	4.11 ± 0.52	2.82 ± 0.93	3.18 ± 1.27	2.5 ± 0.14	0.019 ± 0.02	0.007 ± 0.003
Zero	3-10	2.23 ± 0	2.32 ± 0	7.48 ± 0	4.35 ± 0	6.24 ± 0	1.4 ± 0	0.043 ± 0	0.003 ± 0
Final	3-11	0.24 ± 0.04	0.34 ± 0.05	0.42 ± 0.3	0.24 ± 0.04	0.96 ± 0.17	1.4 ± 1.41	0.005 ± NA	0 ± NA
Zero	3-11	0.23 ± 0	0.25 ± 0	0.72 ± 0	0.43 ± 0	0.67 ± 0	0.14 ± 0	0.004 ± 0	0.001 ± 0
Final	3-12	0.18 ± 0.05	0.26 ± 0.12	0.15 ± 0	0.26 ± 0.22	1.21 ± 0.48	0.6 ± 0.28	0.006 ± NA	0.001 ± NA
Zero	3-12	0.22 ± 0	0.23 ± 0	0.75 ± 0	0.44 ± 0	0.62 ± 0	0.14 ± 0	0.004 ± 0	0 ± 0
Final	4-13	2.38 ± NA	2.93 ± NA	6.85 ± NA	3.78 ± NA	6.61 ± NA	3.6 ± NA	0.025 ± NA	0.007 ± NA
Zero	4-13	1.83 ± NA	1.88 ± NA	6.94 ± NA	3.03 ± NA	5.98 ± NA	2.56 ± NA	0.035 ± NA	0.007 ± NA
Final	4-14	1.88 ± 0.39	2.3 ± 0.71	3.63 ± 0.58	2.24 ± 0.25	2.97 ± 0.13	1.87 ± 0.61	0.031 ± 0.016	0.009 ± 0.004
Zero	4-14	2.12 ± 0	3.02 ± 0	7.04 ± 0	5.23 ± 0	7.55 ± 0	1.47 ± 0	0.029 ± 0	0.003 ± 0
Final	4-15	1.09 ± 0.12	1.2 ± 0.04	0.84 ± 0.45	0.92 ± 0.03	1.56 ± 0.23	1.93 ± 1.14	0.01 ± 0.001	0.003 ± 0
Zero	4-15	1 ± 0	1.37 ± 0	3.14 ± 0	2.65 ± 0	3.02 ± 0	0.7 ± 0	0.011 ± 0	0.002 ± 0
Final	4-16	1.11 ± 0.3	1.37 ± 0.15	1.62 ± 1.15	1.13 ± 0.28	1.7 ± 0.12	2 ± 0.53	0.013 ± 0.005	0.004 ± 0.002
Zero	4-16	1.32 ± 0	1.26 ± 0	4.09 ± 0	1.99 ± 0	2.72 ± 0	1 ± 0	0.019 ± 0	0.001 ± 0
Final	4-17	0.69 ± 0.29	0.33 ± 0.01	0.6 ± 0.37	0.36 ± 0	0.74 ± 0.03	1 ± 0	0.013 ± 0.003	0.002 ± 0.001
Zero	4-17	0.4 ± 0	0.58 ± 0	1.38 ± 0	1.05 ± 0	1.22 ± 0	0.32 ± 0	0.006 ± 0	0.001 ± 0
Final	5-18	3.72 ± 0.37	2.24 ± 0.45	4.93 ± 0.72	2.37 ± 0.47	6.71 ± 1.2	6.27 ± 1.22	0.069 ± 0.07	0.009 ± 0.001
Zero	5-18	2.49 ± 0	2.16 ± 0	10.48 ± 0	3.12 ± 0	7.32 ± 0	3.09 ± 0	0.118 ± 0	0.011 ± 0
Final	5-19	3.36 ± 0.95	3.22 ± 0.37	4.37 ± 0.56	3.21 ± 1.34	4.03 ± 1.8	2.07 ± 0.23	0.024 ± 0.005	0.005 ± 0.001

Table B-2 continued.

Day	No.	TKN	TAN	Sulfate	Tannin	TP	OP	Fe	Ni
Zero	5-19	2.02 ± 0	2.79 ± 0	9.23 ± 0	3.07 ± 0	4.29 ± 0	1.4 ± 0	0.033 ± 0	0.009 ± 0
Final	5-20	1.29 ± 0.35	1.37 ± 0.5	3.14 ± 0.81	1.65 ± 0.64	3.13 ± 1.45	1.13 ± 0.12	0.015 ± 0.006	0.011 ± 0.012
Zero	5-20	1.33 ± 0	1.46 ± 0	4.71 ± 0	1.47 ± 0	2.64 ± 0	0.77 ± 0	0.016 ± 0	0.005 ± 0
Final	5-21	2.12 ± 1.25	1.32 ± 0.2	2.38 ± 0.25	1.17 ± 0.26	1.51 ± 0.28	1.27 ± 0.12	0.015 ± 0.002	0.005 ± 0.002
Zero	5-21	1.11 ± 0	1.45 ± 0	4.19 ± 0	1.52 ± 0	2.4 ± 0	0.8 ± 0	0.017 ± 0	0.005 ± 0
Final	5-22	0.53 ± 0.02	0.52 ± 0.06	0.22 ± 0.03	0.36 ± 0.11	0.7 ± 0.1	0.44 ± 0.06	0.009 ± 0.001	0.001 ± 0
Zero	5-22	0.46 ± 0	1.6 ± 0	1.6 ± 0	0.61 ± 0	0.86 ± 0	0.32 ± 0	0.008 ± 0	0.002 ± 0

Units are in g L^{-1}. n = 3.

Table B-3. The mean ± standard deviation of digester influent (day zero) and effluent (final day) characteristics for each lab-digester group (3).

Day	No.	Cu	TN	InorgN	SCOD : TCOD	OP : TP	Fe(II) : TP	TCOD : TN : TP	TVFA : TALK
Final	2-1	0.005 ± 0.001	3.708 ± 0.104	0.056 ± 0.025	0.24 ± 0.09	0.61 ± 0.16	0.001 ± 0.001	8.08 ± 3	2.53 ± 0.92
Zero	2-1	0.004 ± 0	1.55 ± 0	0.053 ± 0	0.25 ± 0	1 ± 0	0.011 ± 0	45.52 ± 0	1.41 ± 0
Final	2-2	0.003 ± 0.001	4.6 ± 1.106	0.066 ± 0.076	0.26 ± 0.01	0.54 ± 0.03	0.003 ± 0.003	5.16 ± 0.75	1.89 ± 0.3
Zero	2-2	0.004 ± 0	1.474 ± 0	0.055 ± 0	0.24 ± 0	1 ± 0	0.01 ± 0	50.21 ± 0	1.53 ± 0
Final	2-4	0.003 ± 0.001	2.916 ± 0.641	0.12 ± 0.007	0.19 ± 0.1	0.27 ± 0.05	0.003 ± 0.004	5.25 ± 1.72	0.49 ± 0.14
Zero	2-4	0.002 ± 0	2.434 ± 0	0.04 ± 0	0.24 ± 0	0.39 ± 0	0.024 ± 0	6.35 ± 0	0.51 ± 0
Final	2-5	0 ± 0	0.342 ± 0.005	0.025 ± 0.016	2.23 ± 0.2	0.43 ± 0.03	0.002 ± 0	3.79 ± 0.91	0.28 ± 0.04
Zero	2-5	0 ± 0	0.168 ± 0	0.004 ± 0	0.13 ± 0	0.09 ± 0	0.007 ± 0	46.01 ± 0	0.81 ± 0
Final	2-6	0 ± 0	0.246 ± 0.001	0.043 ± 0.004	2.23 ± 0.48	0.02 ± 0.01	0 ± 0	6.78 ± 5.14	0.84 ± 0.21
Zero	2-6	0 ± 0	0.243 ± 0	0.006 ± 0	0.24 ± 0	0.39 ± 0	0.024 ± 0	63.54 ± 0	0.51 ± 0
Final	3-7	0.003 ± 0.001	1.268 ± 0.082	0.042 ± 0.029	0.22 ± 0.05	0.24 ± 0.07	0.006 ± 0.002	40.39 ± 7.93	3.47 ± 1.36
Zero	3-7	0.007 ± 0	0.953 ± 0	0.119 ± 0	0.31 ± 0	0.35 ± 0	0.013 ± 0	103.55 ± 0	4.84 ± 0
Final	3-8	0.005 ± 0	1.093 ± 0.383	0.044 ± 0.016	0.21 ± 0.01	0.43 ± 0.01	0.018 ± 0.004	54.59 ± 15.17	5 ± 1.11
Zero	3-8	0.007 ± 0	0.952 ± 0	0.099 ± 0	0.3 ± 0	0.35 ± 0	0.013 ± 0	104.46 ± 0	4.5 ± 0
Final	3-9	0.004 ± 0.001	1.527 ± 0.395	0.095 ± 0.013	0.42 ± 0.29	0.43 ± 0.04	0.009 ± 0.009	6.64 ± 4.37	1.04 ± 0.55
Zero	3-9	0.001 ± 0	1.13 ± 0	0.6 ± 0	0.26 ± 0	0.22 ± 0	0.012 ± 0	9.97 ± 0	2.94 ± 0
Final	3-10	0.007 ± 0.002	2.845 ± 0.238	0.063 ± 0.032	0.81 ± 0.08	0.86 ± 0.39	0.013 ± 0.016	6.42 ± 1.11	0.53 ± 0.03
Zero	3-10	0.002 ± 0	2.26 ± 0	0.3 ± 0	0.26 ± 0	0.22 ± 0	0.012 ± 0	4.99 ± 0	2.94 ± 0
Final	3-11	0.001 ± NA	0.276 ± 0.017	0.034 ± 0.01	0.26 ± 0.12	1.35 ± 1.23	0.358 ± 0.494	19.76 ± 5.43	0.68 ± 0.01
Zero	3-11	0.001 ± 0	0.228 ± 0	0.06 ± 0	0.6 ± 0	0.21 ± 0	0.617 ± 0.858	20.59 ± 0	1.37 ± 0
Final	3-12	0.001 ± NA	0.218 ± 0.061	0.036 ± 0.027	0.47 ± 0.16	0.49 ± 0.04	0.299 ± 0.414	12.74 ± 5.83	0.64 ± 0.22
Zero	3-12	0 ± 0	0.226 ± 0	0.002 ± 0	0.26 ± 0	0.22 ± 0	1.082 ± 1.514	49.85 ± 0	2.94 ± 0
Final	4-13	0.003 ± NA	2.452 ± NA	0.073 ± NA	0.31 ± NA	0.54 ± NA	0.007 ± NA	12.27 ± NA	3.16 ± NA
Zero	4-13	0.006 ± NA	1.932 ± NA	0.154 ± NA	0.26 ± NA	0.43 ± NA	0.01 ± NA	19.65 ± NA	2.71 ± NA
Final	4-14	0.011 ± 0.006	2.024 ± 0.44	0.028 ± 0.02	0.47 ± 0.05	0.63 ± 0.21	0.018 ± 0.01	4.92 ± 1.03	0.45 ± 0.23
Zero	4-14	0.005 ± 0	2.21 ± 0	0.051 ± 0	0.18 ± 0	0.19 ± 0	0.006 ± 0	5.94 ± 0	0.7 ± 0
Final	4-15	0.003 ± 0.001	1.147 ± 0.109	0.103 ± 0.053	0.66 ± 0.17	1.19 ± 0.54	0.011 ± 0.003	5.54 ± 0.14	0.86 ± 0.32
Zero	4-15	0.001 ± 0	1.032 ± 0	0.062 ± 0	0.14 ± 0	0.23 ± 0	0.006 ± 0	21.77 ± 0	0.55 ± 0
Final	4-16	0.003 ± 0.003	1.187 ± 0.306	0.148 ± 0.048	0.6 ± 0.21	1.19 ± 0.36	0.012 ± 0.004	7.59 ± 1.2	0.21 ± 0.1
Zero	4-16	0.001 ± 0	1.342 ± 0	0.102 ± 0	0.23 ± 0	0.37 ± 0	0.012 ± 0	11.17 ± 0	0.74 ± 0
Final	4-17	0.003 ± 0.001	0.725 ± 0.276	0.031 ± 0.01	0.89 ± 0.32	1.36 ± 0.06	0.03 ± 0.009	11.64 ± 8.42	1.68 ± 1.71
Zero	4-17	0.002 ± 0	0.425 ± 0	0.022 ± 0	0.11 ± 0	0.26 ± 0	0.008 ± 0	61.47 ± 0	0.62 ± 0
Final	5-18	0.008 ± 0.001	3.701 ± 0.347	0.02 ± 0.024	0.56 ± 0.15	0.97 ± 0.35	0.02 ± 0.022	6.03 ± 0.99	6.5 ± 2.84

Table B-3 continued.

Day	No.	Cu	TN	InorgN	SCOD : TCOD	OP : TP	Fe(II) : TP	TCOD : TN : TP	TVFA : TALK
Zero	5-18	0.006 ± 0	2.64 ± 0	0.067 ± 0	0.33 ± 0	0.42 ± 0	0.027 ± 0	9.32 ± 0	4.3 ± 0
Final	5-19	0.005 ± 0	3.264 ± 0.917	0.044 ± 0.04	0.38 ± 0.06	0.62 ± 0.37	0.012 ± 0.006	3.9 ± 3.03	0.52 ± 0.16
Zero	5-19	0.01 ± 0	2.084 ± 0	0.031 ± 0	0.17 ± 0	0.33 ± 0	0.013 ± 0	5.86 ± 0	0.55 ± 0
Final	5-20	0.015 ± 0.009	1.272 ± 0.359	0.021 ± 0.019	0.26 ± 0.05	0.42 ± 0.19	0.009 ± 0.005	9.13 ± 7.32	0.56 ± 0.1
Zero	5-20	0.005 ± 0	1.308 ± 0	0.032 ± 0	0.13 ± 0	0.29 ± 0	0.01 ± 0	10.37 ± 0	0.44 ± 0
Final	5-21	0.005 ± 0.002	2.073 ± 1.218	0.098 ± 0.031	0.29 ± 0.08	0.86 ± 0.16	0.018 ± 0.003	12.46 ± 6.51	0.6 ± 0.07
Zero	5-21	0.005 ± 0	1.279 ± 0	0.065 ± 0	0.22 ± 0	0.33 ± 0	0.012 ± 0	11.44 ± 0	0.63 ± 0
Final	5-22	0.001 ± 0	0.512 ± 0.001	0.018 ± 0.024	0.75 ± 0.09	0.63 ± 0	0.022 ± 0.001	12.29 ± 1.04	0.3 ± 0.02
Zero	5-22	0.002 ± 0	0.476 ± 0	0.017 ± 0	0.17 ± 0	0.37 ± 0	0.015 ± 0	29.69 ± 0	0.49 ± 0

Units for Cu, TN, and InorgN are in g L^{-1}, the rest are unitless. n = 3.

Table B-4. The mean ± standard deviation of digester influent (day zero) and effluent (final day) characteristics for each lab-digester group (4).

Day	No.	TAN : TKN	TCOD : Sulfate	TCOD : TKN	FS : TS	VS : TS	Fe(II) : S
Final	2-1	0.72 ± 0.04	34.3 ± 12.04	52.41 ± 16.64	0.21 ± 0.01	0.79 ± 0.01	0.001 ± 0
Zero	2-1	1.18 ± 0	21.45 ± 0	97.77 ± 0	0.18 ± 0	0.82 ± 0	0.003 ± 0
Final	2-2	0.6 ± 0.18	31.84 ± 8.7	34.96 ± 6.55	0.2 ± 0	0.8 ± 0	0.005 ± 0.005
Zero	2-2	1.21 ± 0	21.81 ± 0	105.13 ± 0	0.19 ± 0	0.81 ± 0	0.003 ± 0
Final	2-4	1.5 ± 0.41	18.43 ± 6.56	33.7 ± 13.76	0.32 ± 0.01	0.68 ± 0.01	0.004 ± 0.005
Zero	2-4	1.39 ± 0	11.95 ± 0	28.04 ± 0	0.29 ± 0	0.71 ± 0	0.019 ± 0
Final	2-5	0.68 ± 0.07	13.21 ± 0.54	4.02 ± 0.73	0.48 ± 0	0.52 ± 0	0.023 ± 0.002
Zero	2-5	1.71 ± 0	16.6 ± 0	59.71 ± 0	0.37 ± 0	0.63 ± 0	0.014 ± 0
Final	2-6	0.6 ± 0.01	11.92 ± 2.83	6.17 ± 0.87	0.41 ± 0.05	0.59 ± 0.05	0 ± 0
Zero	2-6	1.39 ± 0	11.95 ± 0	28.04 ± 0	0.29 ± 0	0.71 ± 0	0.019 ± 0
Final	3-7	2.09 ± 0.09	140.85 ± 29.02	292.4 ± 78.33	0.13 ± 0.08	0.87 ± 0.08	0.017 ± 0.006
Zero	3-7	1.47 ± 0	76.6 ± 0	535.08 ± 0	0.03 ± 0	0.97 ± 0	0.01 ± 0
Final	3-8	1.88 ± 0.73	92.65 ± 13.83	339.24 ± 84.63	0.16 ± 0	0.84 ± 0	0.03 ± 0.001
Zero	3-8	1.47 ± 0	78.25 ± 0	542.84 ± 0	0.03 ± 0	0.97 ± 0	0.011 ± 0
Final	3-9	0.92 ± 0.28	15.29 ± 5.05	18.47 ± 6.99	0.41 ± 0.09	0.59 ± 0.09	0.01 ± 0.006
Zero	3-9	1.04 ± 0	9.39 ± 0	31.48 ± 0	0.3 ± 0	0.7 ± 0	0.01 ± 0
Final	3-10	1.11 ± 0.24	13.95 ± 5.08	21.84 ± 12.02	0.48 ± 0.13	0.52 ± 0.13	0.009 ± 0.01
Zero	3-10	1.04 ± 0	9.39 ± 0	31.48 ± 0	0.29 ± 0	0.71 ± 0	0.01 ± 0
Final	3-11	1.43 ± 0.03	14.32 ± 5.26	23.18 ± 12.75	0.41 ± 0.03	0.59 ± 0.03	0.015 ± NA
Zero	3-11	1.12 ± 0	4.37 ± 0	13.96 ± 0	0.3 ± 0	0.7 ± 0	0.01 ± 0
Final	3-12	1.36 ± 0.25	19.55 ± 3.66	16.56 ± 1.07	0.4 ± 0.01	0.6 ± 0.01	0.061 ± NA
Zero	3-12	1.04 ± 0	9.39 ± 0	31.48 ± 0	0.29 ± 0	0.71 ± 0	0.01 ± 0
Final	4-13	1.23 ± NA	29.03 ± NA	83.54 ± NA	0.23 ± NA	0.77 ± NA	0.006 ± NA
Zero	4-13	1.03 ± NA	32.69 ± NA	124.26 ± NA	0.16 ± NA	0.84 ± NA	0.009 ± NA
Final	4-14	1.29 ± 0.54	8.24 ± 2.72	15.79 ± 3.76	0.48 ± 0.03	0.52 ± 0.03	0.015 ± 0.006
Zero	4-14	1.42 ± 0	14.1 ± 0	46.68 ± 0	0.3 ± 0	0.7 ± 0	0.007 ± 0
Final	4-15	1.11 ± 0.12	13.11 ± 3.38	9.19 ± 1.72	0.41 ± 0.1	0.59 ± 0.1	0.025 ± 0.014
Zero	4-15	1.37 ± 0	21.59 ± 0	68.09 ± 0	0.26 ± 0	0.74 ± 0	0.006 ± 0
Final	4-16	1.26 ± 0.17	12.18 ± 6.2	13.88 ± 2.83	0.43 ± 0.09	0.57 ± 0.09	0.018 ± 0.013
Zero	4-16	0.96 ± 0	9.95 ± 0	30.96 ± 0	0.26 ± 0	0.74 ± 0	0.008 ± 0
Final	4-17	0.51 ± 0.2	9.82 ± 2.9	9 ± 6.44	0.49 ± 0.07	0.51 ± 0.07	0.042 ± 0.017

Table B-4 continued.

Day	No.	TAN : TKN	TCOD : Sulfate	TCOD : TKN	FS : TS	VS : TS	Fe(II) : S
Zero	4-17	1.43 ± 0	23.02 ± 0	78.72 ± 0	0.06 ± 0	0.94 ± 0	0.007 ± 0
Final	5-18	0.61 ± 0.16	30.42 ± 6.76	39.95 ± 7.02	0.19 ± 0.01	0.81 ± 0.01	0.02 ± 0.024
Zero	5-18	0.87 ± 0	17.19 ± 0	72.37 ± 0	0.13 ± 0	0.87 ± 0	0.019 ± 0
Final	5-19	1 ± 0.25	9.03 ± 3.09	12.54 ± 5.8	0.36 ± 0.02	0.64 ± 0.02	0.098 ± 0.031
Zero	5-19	1.38 ± 0	5.67 ± 0	25.95 ± 0	0.28 ± 0	0.72 ± 0	0.006 ± 0
Final	5-20	1.04 ± 0.14	8.69 ± 0.7	22.86 ± 11.29	0.32 ± 0.01	0.68 ± 0.01	0.021 ± 0.019
Zero	5-20	1.1 ± 0	7.61 ± 0	27 ± 0	0.27 ± 0	0.73 ± 0	0.006 ± 0
Final	5-21	0.73 ± 0.26	13.3 ± 1.99	17.87 ± 7.91	0.37 ± 0.04	0.63 ± 0.04	0.044 ± 0.04
Zero	5-21	1.31 ± 0	8.37 ± 0	31.73 ± 0	0.24 ± 0	0.76 ± 0	0.007 ± 0
Final	5-22	0.97 ± 0.06	20.75 ± 7.46	8.32 ± 1.45	0.44 ± 0.09	0.56 ± 0.09	0.018 ± 0.024
Zero	5-22	3.49 ± 0	7.62 ± 0	26.58 ± 0	0.09 ± 0	0.91 ± 0	0.008 ± 0

Unitless. n = 3.

Table B-5. The mean ± standard deviation of the chemical characteristics of substrate and inoculum collected from field digesters (1).

Digester	Batch	Sub/Ino	pH	Conductivity	TS	VS	TCOD	SCOD	TVFA	TALK
B	1	EF-L	8.31 ± 0.79	9.06 ± 0.06	41 ± 0	29.35 ± 4.81	54 ± 2	43.02 ± 18.34	4.3 ± 2.6	9.05 ± 2.19
B	1	INFL	5.5 ± NA	8.24 ± NA	125 ± 2	109.3 ± 1.85	236 ± 22	105.12 ± NA	15.4 ± 1.6	3.14 ± 1.78
B	1	DL-W	8.1 ± NA	9.28 ± NA	72 ± 1	51.87 ± 1.06	56 ± 12	57.11 ± NA	5.2 ± 1.9	10.49 ± 1.49
B	2	INFL	6.67 ± NA	9.82 ± NA	103 ± 1	84.63 ± 0.78	159 ± 7	40.09 ± 7.15	9.6 ± 0.3	5.93 ± 0.11
B	2	EF-W	7.64 ± 0.02	10.77 ± NA	66 ± 3	46.7 ± 2.73	68 ± 11	16.12 ± 1.65	6.2 ± 1.1	12.19 ± 2.16
B	2	DL-W	7.47 ± 0.13	10.24 ± NA	77 ± 2	48.5 ± 2.44	97 ± 3	12.12 ± NA	7.5 ± 2	6.6 ± NA
B	3	INFL	6.75 ± NA	6.34 ± NA	689 ± 68	667.4 ± 69.24	536 ± NA	165.42 ± NA	20.1 ± 1.2	3.84 ± 0.35
B	3	EF-W	7.96 ± 0.03	7.52 ± 0.18	74 ± 2	52.89 ± 2.14	93 ± 40	18.43 ± 0.67	21.5 ± NA	7.31 ± 3.34
B	3	DL-W	7.67 ± NA	8.8 ± NA	69 ± 5	48.45 ± 4.4	154 ± 12	19.83 ± 0.94	12.2 ± NA	8.43 ± 0.92
B	4	EF-E	6.98 ± 0.08	8.53 ± 0.03	83 ± 1	58.29 ± 1.16	99 ± NA	17.85 ± 0.69	6.2 ± 0.6	8.85 ± 1.41
B	4	DL-E	6.82 ± NA	8.18 ± NA	96 ± 12	70.83 ± 11.27	82 ± 14	18.48 ± 0.2	8.2 ± 1	11.04 ± 0.98
B	4	INFL	7.02 ± NA	9.09 ± NA	136 ± 1	110.41 ± 1.05	244 ± 17	69.32 ± 0.95	19.1 ± 1.2	5.22 ± NA
B	4	EF-W	7.21 ± NA	8.69 ± NA	141 ± 8	132.93 ± 18.74	159 ± NA	17.01 ± 0.44	5.8 ± 0.6	9.41 ± 0.96
B	4	DL-W	7.21 ± NA	8.68 ± NA	91 ± 2	67.64 ± 2.86	136 ± NA	18.91 ± 0.12	6 ± 0.2	11.09 ± NA
B	5	EF-E	7.88 ± 0.05	7.92 ± 0.1	61 ± 2	43.3 ± 1.49	52 ± 0	8.84 ± 0.38	3.9 ± 0.3	7.14 ± 0.87
B	5	DL-E	7.77 ± NA	8.19 ± NA	69 ± 5	50.54 ± 5.23	72 ± 1	9.22 ± 1.73	4.1 ± 0.3	9.33 ± 0.2
B	5	INFL	6.99 ± NA	7.99 ± NA	157 ± 1	51.11 ± 7.12	210 ± 43	72.22 ± 21.93	13.9 ± 0.8	1.26 ± 0.17
B	5	EF-W	7.58 ± NA	10.15 ± NA	62 ± 4	46.41 ± 3.89	61 ± 4	10.34 ± 0.5	4.4 ± 0.2	8.88 ± 1.05
B	5	DL-W	7.67 ± NA	8.09 ± NA	67 ± 7	51.11 ± 7.12	70 ± 14	15.28 ± 0.08	5.1 ± 0.6	8.15 ± 0.83

Note: Sub/Ino = substrate / inoculum.

Units are in g L^{-1} except for conductivity (mS cm^{-1}) and pH (unitless). n = 3.

Table B-6. The mean ± standard deviation of chemical characteristics of substrate and inoculum collected from field digesters (2).

Digester	Batch	Sub/Ino	TKN	TAN	Sulfate	Tannin	TP	OP	Fe	Ni
B	1	EF-L	2.24 ± 0.92	2.19 ± 0.28	3.59 ± 0.4	2.57 ± 0.95	3.68 ± 0.22	2.36 ± 0.62	0.056 ± NA	0.005 ± NA
B	1	INFL	1.32 ± 0.21	1.71 ± 0.14	5.07 ± 1.23	1.71 ± 0.14	5.1 ± 0.77	3.13 ± 0.12	0.204 ± 0.085	0.011 ± 0.003
B	1	DL-W	2.03 ± 0.04	2.45 ± 0.16	3.89 ± 1.61	2.04 ± 0.99	4.6 ± 1.02	1.42 ± 1.28	0.042 ± 0.009	0.007 ± 0.001
B	2	INFL	1.43 ± 0.23	1.64 ± 0.04	7.12 ± 0.28	2.29 ± 0.13	5.07 ± 0.58	2.17 ± 0.4	0.008 ± 0	0.004 ± 0
B	2	EF-W	2.42 ± 0.08	3.37 ± NA	5.67 ± NA	3.71 ± NA	4.38 ± 0.25	1.7 ± NA	0.062 ± 0	0.003 ± 0
B	2	DL-W	1.62 ± NA	2.78 ± 0.13	5.83 ± 0.43	2.79 ± 0.39	12.54 ± NA	1.1 ± NA	0.048 ± 0	0.003 ± 0
B	3	INFL	0.77 ± 0.02	1.24 ± 0.06	6.27 ± 0.28	2.28 ± 0.37	4.82 ± 0.45	1.8 ± 0.35	0.038 ± 0.005	0.008 ± 0.001
B	3	EF-W	2.25 ± 0.03	2.32 ± 0.22	7.48 ± NA	4.35 ± NA	6.24 ± NA	1.4 ± 0	0.043 ± 0.003	0.003 ± 0
B	3	DL-W	2.25 ± NA	2.34 ± 0.15	7.2 ± 0.25	3.74 ± 0.52	6.71 ± NA	1.33 ± 0.12	0.047 ± 0.005	0.006 ± 0.004
B	4	EF-E	2.12 ± 0.03	3.02 ± 0.04	7.04 ± 3.1	5.23 ± 0.11	7.55 ± 0.05	1.47 ± 0.12	0.029 ± 0.002	0.003 ± 0.001
B	4	DL-E	2.63 ± 0.12	2.51 ± 0.27	8.19 ± 1.31	3.97 ± 0.64	5.44 ± NA	2 ± 0	0.039 ± 0.003	0.003 ± 0
B	4	INFL	1.78 ± 0.12	1.62 ± 0.07	6.95 ± 0.95	2.48 ± 0.35	5.95 ± 0.25	2.8 ± NA	0.037 ± 0.005	0.007 ± 0
B	4	EF-W	2.02 ± 0.1	2.89 ± NA	6.91 ± 3.55	5.24 ± NA	6.09 ± NA	1.6 ± 0	0.028 ± 0	0.007 ± 0.004
B	4	DL-W	1.99 ± 0.03	2.74 ± 0.22	6.28 ± 1.04	5.3 ± 0.14	6.03 ± 1.19	1.4 ± 0.2	0.023 ± 0.003	0.003 ± 0
B	5	EF-E	2.02 ± 0	2.79 ± 0.13	9.23 ± 0.45	3.07 ± 0.11	4.29 ± 0.1	1.4 ± 0	0.033 ± 0	8.948 ± 1.513
B	5	DL-E	2.65 ± 0.19	2.91 ± 0.12	9.42 ± 0.1	2.95 ± 0.05	5.29 ± 0.54	1.53 ± 0.12	0.032 ± 0	0.009 ± 0.001
B	5	INFL	2.54 ± 0.15	1.98 ± 0.14	11.1 ± 0.97	3.2 ± 0.28	8.07 ± 0.13	3.47 ± 0.23	0.138 ± 0	0.012 ± 0
B	5	EF-W	2.29 ± 0.16	2.87 ± 0.21	8 ± 0.26	2.8 ± 0.14	4.31 ± 0.26	1.6 ± 0.2	0.038 ± 0	0.009 ± 0.001
B	5	DL-W	2.21 ± 0.01	2.91 ± 0.2	8.38 ± 0.09	3.04 ± 0.23	4.8 ± 0.13	1.6 ± 0	0.033 ± 0.001	0.01 ± 0.001

Note: Sub/Ino = substrate / inoculum.
Units are in g L^{-1}. n = 3.

Table B-7. The mean ± standard deviation of chemical characteristics of substrate and inoculum collected from field digesters (3).

Digester	Batch	Sub/Ino	Cu	TN	InorgN	SCOD : TCOD	OP : TP	TCOD : TN : TP	TVFA : TALK
B	1	EF-L	0.006 ± NA	2.28 ± 1.035	0.111 ± 0.073	0.812 ± 0.378	0.64 ± 0.13	7.36 ± 3.12	0.45 ± 0.16
B	1	INFL	0.008 ± 0.005	0.114 ± 0.011	1.438 ± 0.201	0.446 ± NA	0.63 ± 0.11	419.64 ± 105.94	5.7 ± 2.12
B	1	DL-W	0.007 ± 0	2.13 ± 0.055	0.104 ± 0.02	1.136 ± NA	0.31 ± 0.24	5.81 ± 1.35	0.51 ± 0.21
B	2	INFL	0.005 ± 0	1.451 ± 0.243	0.054 ± NA	0.252 ± 0.038	0.42 ± 0.04	22.37 ± 6.14	1.59 ± 0
B	2	EF-W	0.002 ± 0	2.434 ± 0.099	0.04 ± NA	0.24 ± 0.017	0.4 ± NA	6.4 ± 1.37	0.52 ± 0.09
B	2	DL-W	0.004 ± 0	1.677 ± NA	0.057 ± NA	0.129 ± NA	0.09 ± NA	4.47 ± NA	0.81 ± NA
B	3	INFL	0.008 ± 0.002	0.808 ± 0.047	0.054 ± 0.017	0.308 ± NA	0.37 ± 0.04	117.75 ± NA	5.29 ± 0.82
B	3	EF-W	0.002 ± 0	2.26 ± 0.029	0.319 ± 0.397	0.221 ± 0.081	0.22 ± NA	4.73 ± NA	6.23 ± NA
B	3	DL-W	0.002 ± 0	1.84 ± 0.384	0.211 ± 0.265	0.129 ± 0.007	0.21 ± NA	9.39 ± NA	1.37 ± NA
B	4	EF-E	0.005 ± 0	2.21 ± 0.014	0.102 ± NA	0.185 ± NA	0.19 ± 0	5.96 ± NA	0.72 ± 0.17
B	4	DL-E	0.003 ± 0.001	2.684 ± 0.186	0.123 ± NA	0.212 ± 0.026	0.37 ± NA	6.11 ± NA	0.75 ± 0.16
B	4	INFL	0.004 ± 0	1.885 ± 0.065	0.164 ± NA	0.292 ± 0.029	0.46 ± NA	21.84 ± 2.51	3.42 ± NA
B	4	EF-W	0.012 ± 0	2.123 ± 0.113	0.104 ± 0.015	0.105 ± NA	0.26 ± NA	13.1 ± NA	0.62 ± 0.08
B	4	DL-W	0.003 ± 0	2.065 ± 0.021	0.073 ± 0.048	0.139 ± NA	0.23 ± 0	12.79 ± NA	0.57 ± NA
B	5	EF-E	0.01 ± 0.002	2.084 ± 0.002	0.065 ± 0.005	0.169 ± 0.006	0.33 ± 0.01	5.86 ± 0.16	0.56 ± 0.09
B	5	DL-E	0.01 ± 0	2.615 ± 0.356	0.064 ± 0.015	0.127 ± 0.023	0.29 ± 0.03	5.24 ± 0.18	0.44 ± 0.04
B	5	INFL	0.005 ± 0	2.705 ± 0.001	0.062 ± 0.001	0.394 ± 0.147	0.43 ± 0.03	8.54 ± 0.82	11.18 ± 1.95
B	5	EF-W	0.01 ± 0	2.381 ± 0.146	0.087 ± 0.011	0.172 ± 0.002	0.37 ± 0.05	5.98 ± 0.83	0.52 ± 0.09
B	5	DL-W	0.01 ± 0	2.559 ± 0.482	0.062 ± 0.004	0.235 ± 0.063	0.33 ± 0.01	5.54 ± 1.68	0.64 ± 0.12

Note: Sub/Ino = substrate / inoculum.
Units for Cu, TN, and InorgN are in g L^{-1}, the rest are unitless. n = 3.

Table B-8. The mean ± standard deviation of chemical characteristics of substrate and inoculum collected from field digesters (4).

Digester	Batch	Sub/Ino	TAN : TKN	TCOD : Sulfate	TCOD : TKN	FS : TS	VS : TS	Fe(II) : S	Fe(II) : TP
B	1	EF-L	1.04 ± 0.25	15.04 ± 1.62	26.48 ± 26.48	0.29 ± 0.12	0.71 ± 0.12	0.026 ± NA	0.024 ± NA
B	1	INFL	1.31 ± 0.25	47.98 ± 9.61	179.93 ± 179.93	0.13 ± 0	0.87 ± 0	0.076 ± 0.042	0.07 ± 0.035
B	1	DL-W	1.21 ± 0.06	15.05 ± 2.84	27.38 ± 27.38	0.28 ± 0.01	0.72 ± 0.01	0.02 ± 0.004	0.016 ± 0.003
B	2	INFL	1.17 ± 0.23	22.34 ± 1.83	112.58 ± 112.58	0.18 ± 0	0.82 ± 0	0.002 ± 0	0.003 ± 0
B	2	EF-W	1.34 ± NA	10.17 ± NA	28.14 ± 28.14	0.29 ± 0.01	0.71 ± 0.01	NA ± NA	0.024 ± 0.002
B	2	DL-W	1.81 ± NA	16.68 ± 1.57	57.96 ± 57.96	0.37 ± 0.01	0.63 ± 0.01	0.015 ± 0	NA ± NA
B	3	INFL	1.61 ± 0.12	81.35 ± NA	676.38 ± 676.38	0.03 ± 0.01	0.97 ± 0.01	0.011 ± 0.001	0.014 ± 0.001
B	3	EF-W	1.03 ± 0.1	8.96 ± NA	41.26 ± 41.26	0.29 ± 0.01	0.71 ± 0.01	0.009 ± NA	0.011 ± NA
B	3	DL-W	1.12 ± NA	21.41 ± 2.43	63.7 ± 63.7	0.3 ± 0.01	0.7 ± 0.01	0.011 ± 0.001	0.01 ± NA
B	4	EF-E	1.42 ± 0.04	9.36 ± NA	47.43 ± 47.43	0.3 ± 0	0.7 ± 0	0.008 ± 0.003	0.006 ± 0.001
B	4	DL-E	0.99 ± 0.09	9.94 ± 0.29	30.86 ± 30.86	0.26 ± 0.03	0.74 ± 0.03	0.008 ± 0.001	0.013 ± NA
B	4	INFL	0.92 ± 0.1	35.45 ± 4.66	137.68 ± 137.68	0.19 ± 0.01	0.81 ± 0.01	0.009 ± 0.002	0.011 ± 0.002
B	4	EF-W	1.52 ± NA	14.45 ± NA	83.41 ± 83.41	0.05 ± 0.17	0.95 ± 0.17	0.008 ± 0.003	0.008 ± NA
B	4	DL-W	1.38 ± 0.13	19.33 ± NA	67.02 ± 67.02	0.26 ± 0.02	0.74 ± 0.02	0.006 ± 0	0.007 ± 0.002
B	5	EF-E	1.38 ± 0.06	5.68 ± 0.28	25.95 ± 25.95	0.28 ± 0.01	0.72 ± 0.01	0.006 ± 0	0.013 ± 0
B	5	DL-E	1.1 ± 0.13	7.61 ± 0.17	27.08 ± 27.08	0.27 ± 0.02	0.73 ± 0.02	0.006 ± 0	0.011 ± 0
B	5	INFL	0.73 ± 0.03	18.8 ± 2.28	73.49 ± 73.49	0.67 ± 0.05	0.33 ± 0.05	0.023 ± 0	0.029 ± 0.001
B	5	EF-W	1.25 ± 0.06	7.62 ± 0.5	26.67 ± 26.67	0.25 ± 0.02	0.75 ± 0.02	0.008 ± 0	0.016 ± 0
B	5	DL-W	1.31 ± 0.09	8.08 ± 2.3	29.88 ± 29.88	0.24 ± 0.02	0.76 ± 0.02	0.007 ± 0	0.012 ± 0

Note: Sub/Ino = substrate / inoculum.
Unitless. n = 3.

Table B-9. The specific methane yield (SMY) and calculated foam potential for the lab-scale digester tests.

Lab-digester Group No.	**SMY** mL CH_4 g VS^{-1}	**Foam Potential** mL g TS
2-1	8.81 ± 2.13	29.15 ± 4.79
2-2	4.27 ± 3.49	33.78 ± 0
2-4	46.96 ± 26.43	104.46 ± 25.22
2-5	44.63 ± 5.81	90.17 ± 39.99
2-6	14.78 ± NA	80.23 ± NA
3-7	0.17 ± 0.1	2.71 ± 0.87
3-8	0.21 ± 0.15	3.68 ± 1.3
3-9	74.66 ± 33.45	82.38 ± 26.69
3-10	60.73 ± 8.56	75.39 ± 11.57
3-11	50.49 ± 14.75	121.95 ± 73.24
3-12	52.79 ± 23.47	106.14 ± 16.44
4-13	4.09 ± NA	17.73 ± NA
4-14	53.34 ± 64.02	48.8 ± 69.53
4-15	80.13 ± 49.2	83.12 ± 47.87
4-16	92.96 ± 34.49	93.18 ± 31.81
4-17	22.98 ± 8.11	42.67 ± 13.37
5-18	1.2 ± 0.72	18.6 ± 2.8
5-19	105.91 ± 20.56	101.21 ± 26.59
5-21	115.75 ± 52.46	118.08 ± 42.27
5-21	184.21 ± 10.92	191.63 ± 15
5-22	48.93 ± 22.35	68.40 ± 33.53

Table B-10. The *P* values and significance levels of the measured Day 0 chemical concentrations for the non-foaming and foaming DL field digester samples.

Characteristic	D0 g L^{-1}, non-foaming	D0 g L^{-1}, foaming	*P* value	Significance
Cu	0.009 ± 0.002	0.003 ± 0.001	0	***
Fe	0.037 ± 0.007	0.038 ± 0.011	.743	
Ni	0.009 ± 0.001	0.004 ± 0.002	.002	**
TP	4.89 ± 0.66	7.35 ± 3	.007	**
OP	1.52 ± 0.65	1.53 ± 0.35	.959	
TKN	2.30 ± 0.3	2.22 ± 0.39	.643	
TAN	2.76 ± 0.27	2.59 ± 0.25	.152	
Sulfate	7.09 ± 2.82	6.93 ± 1.2	.869	
TS	69 ± 5	83 ± 12	.007	**
VS	51 ± 5	59 ± 12.	.105	
pH	7.85 ± 0.23	7.35 ± 0.31	.045	*
TCOD	66 ± 12	113 ± 33	.001	**
SCOD	21 ± 20	18 ± 3	.171	
TALK	9.32 ± 1.33	9.51 ± 1.9	.81	
TVFA	4.8 ± 1.1	7.7 ± 2.1	.002	**
Conductivity	8.52 ± 0.66	8.98 ± 0.89	.494	
Tannic acid	2.67 ± 0.7	3.95 ± 0.99	.003	**
TN	2.435 ± 0.379	2.144 ± 0.441	.144	
Inorganic N	0.08 ± 0.02	0.12 ± 0.13	.918	
SCOD : TCOD	0.37 ± 0.43	0.15 ± 0.04	.343	
OP : TP	0.31 ± 0.12	0.23 ± 0.1	.207	
TCOD : TN : TP	5.53 ± 1.11	8.19 ± 3.69	.063	
TVFA : TALK	0.53 ± 0.15	0.83 ± 0.29	.02	*
TAN : TKN	1.21 ± 0.12	1.25 ± 0.3	.676	
TCOD : Sulfate	10.51 ± 4.15	16.34 ± 5.01	.018	*
FS : TS	0.26 ± 0.02	0.30 ± 0.05	.069	
VS : TS	0.74 ± 0.02	0.70 ± 0.05	.069	
Fe(II) : S	0.012 ± 0.007	0.01 ± 0.003	.462	
Fe(II) : TP	0.013 ± 0.003	0.009 ± 0.003	.062	
TCOD : TKN	28.11 ± 4.31	46.88 ± 17.96	.009	**

** P < 0.05, ** P < .01, *** P < .001*.

Table B-11. The *P* values and significance levels of the measured Day 0 chemical concentrations for the non-foaming and foaming EFFL field digester samples.

Characteristic	D0 g L^{-1}, no-foaming	D0 g L^{-1}, foaming	*P* value	Significance
Cu	0.01 ± 0.001	0.006 ± 0.004	.304	
Fe	0.036 ± 0.003	0.038 ± 0.013	.844	
Ni	4.479 ± 5.234	0.004 ± 0.003	.008	**
TP	4.3 ± 0.17	5.8 ± 1.45	.03	*
OP	1.5 ± 0.17	1.51 ± 0.12	.761	
TKN	2.16 ± 0.18	2.2 ± 0.16	.594	
TAN	2.83 ± 0.16	2.78 ± 0.43	.801	
Sulfate	8.62 ± 0.75	6.87 ± 2.57	.142	
TS	61 ± 3	91 ± 31	< .001	***
VS	45 ± 3	73 ± 37	.003	
pH	7.81 ± 0.16	7.50 ± 0.42	.185	
TCOD	57 ± 5	93 ± 37	.005	**
SCOD	10 ± 1	17 ± 1	< .001.	***
TALK	8.01 ± 1.28	9.44 ± 2.61	.151	
TVFA	4.1 ± 0.4	7.6 ± 4.9	.001	**
Conductivity	8.47 ± 1.12	8.45 ± 1.08	1	
Tannic acid	2.93 ± 0.19	4.83 ± 0.65	< .001.	***
TN	2.23 ± 0.19	2.26 ± 0.14	.754	
Inorganic N	0.08 ± 0.01	0.16 ± 0.20	.352	
SCOD : TCOD	0.17 ± 0	0.21 ± 0.06	.218	
OP : TP	0.35 ± 0.04	0.25 ± 0.09	.082	
TCOD : TN : TP	5.92 ± 0.54	7.17 ± 3.1	.937	
TVFA : TALK	0.54 ± 0.08	1.18 ± 1.78	.165	
TAN : TKN	1.32 ± 0.09	1.28 ± 0.22	.678	
TCOD : Sulfate	6.65 ± 1.12	10.73 ± 2.53	.008	**
FS : TS	0.27 ± 0.02	0.23 ± 0.13	.291	
VS : TS	0.73 ± 0.02	0.77 ± 0.13	.291	
Fe(II) : S	0.008 ± 0.003	0.008 ± 0.003	.315	
Fe(II) : TP	0.014 ± 0.002	0.013 ± 0.008	.793	
TCOD : TKN	26.31 ± 1.69	42.38 ± 20.54	.029	*

** P < .05, ** P < .01, *** P < .001.*

Table B-12. The *P* values and significance levels of the foam potential (mL g TS^{-1}) values for non-foaming and foaming samples.

Sample	*P* value	Significance
EF	.666	
INF	.864	
DL	.012	*

** P < .05.*

Table B-13. The *P* values and significance levels of the SMY (mL g VS^{-1}) values for non-foaming and foaming samples.

Sample	*P* value	Significance
EF	.031	*
INF	.331	
DL	.003	**

** P < .05, ** P < .01, *** P < .001.*

Table B-14. Models used for supervised machine learning of foam potential and their RMSE and R^2 values.

Model	RMSE	R^2
RF	0.63	0.76
SVM	0.85	0.66
NN	1.05	0.63
KNN	0.74	0.69
Linear	0.81	0.64

Foam potential was predicted using regression models in the caret package in RStudio as described in the Materials and Methods Section 5.3.4. The RMSE and R^2 values were used in place of accuracy and the kappa values as the data was continuous. The RMSE and R^2 values determined how well the predicted data points compared to the test data points.

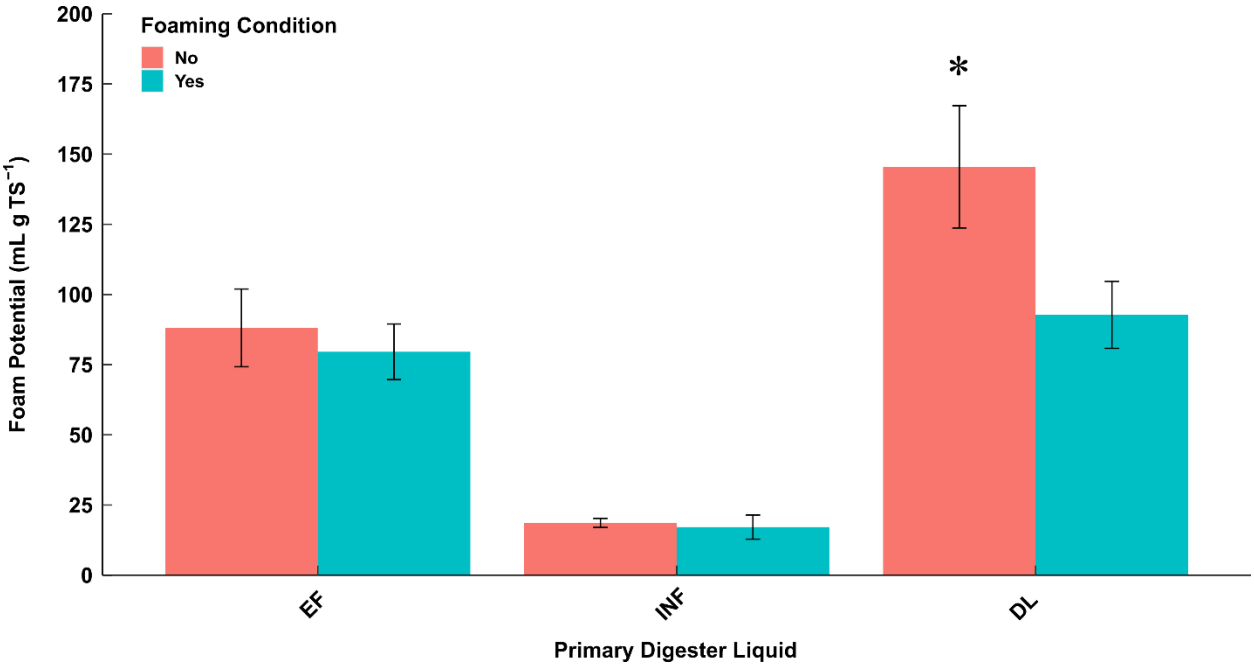

Figure B-1. The foam potential (mL g TS^{-1}) for non-foaming and foaming lab-digester samples grouped by primary digester liquid. * $P < .05$

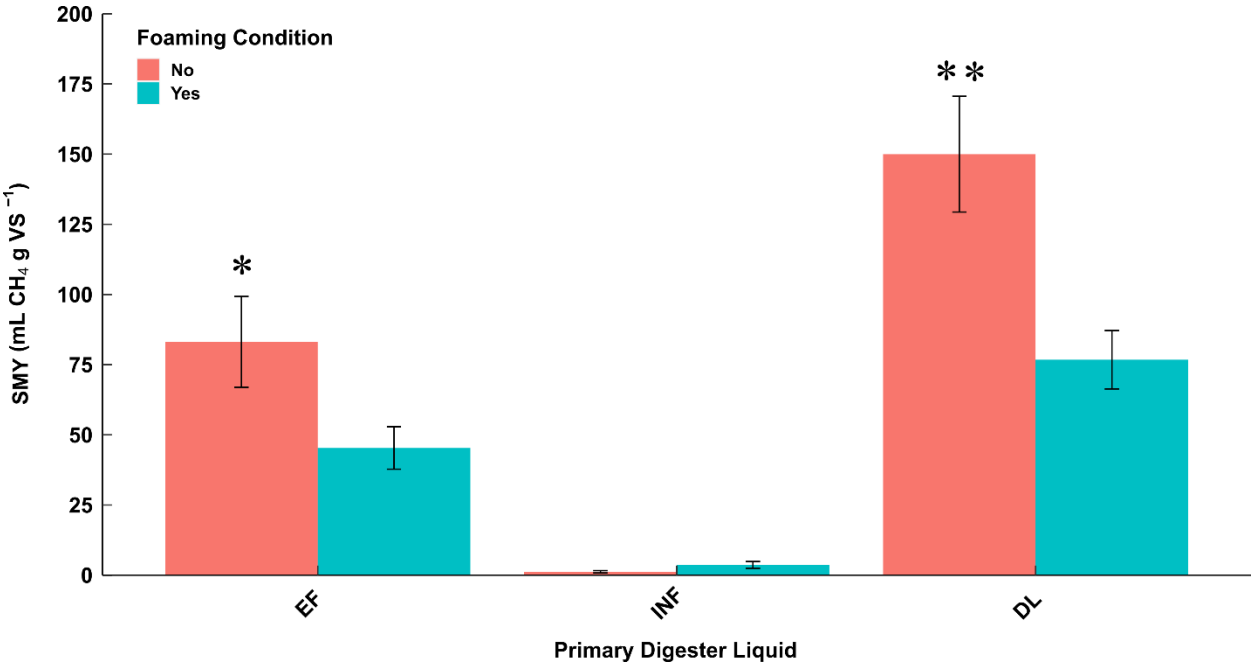

Figure B-2. The SMY (mL g VS^{-1}) for non-foaming and foaming lab-digester samples grouped by primary digester liquid. * $P < .05$, ** $P < .01$.

APPENDIX C. CHAPTER 6 SUPPLEMENTARY

Table C-1. The effect percentages of how well each BMP model from the literature fitted the measured SMY (mL CH_4 g VS^{-1}).

Lab-digester Group No.	1st Order	1st Order Combined	Chen & Hashimoto	Gompertz	2nd Order
1-1	1%	1%	-4%	1%	1%
1-2	2%	2%	-10%	3%	2%
1-3	2%	0%	-7%	3%	2%
1-4	4%	4%	-14%	4%	4%
1-5	10%	10%	-39%	10%	10%
2-7	-1%	-1%	1%	1%	-1%
2-8	0%	0%	-2%	1%	0%
2-10	1%	-2%	0%	1%	1%
2-11	38%	32%	37%	-109%	38%
2-12	17%	15%	-8%	-29%	17%
3-13	-176%	-181%	253%	2%	135%
3-14	-236%	-43%	106%	91%	80%
3-15	-1%	-1%	0%	1%	0%
3-16	0%	-1%	0%	0%	0%
3-17	1%	-2%	-1%	1%	1%
3-18	-5%	0%	2%	2%	1%
4-19	-7%	-13%	27%	-5%	-2%
4-20	6%	4%	2%	-12%	4%
4-21	4%	2%	2%	-8%	3%
4-22	5%	3%	1%	-10%	5%
4-23	-3%	4%	-16%	4%	12%
5-24	18%	-123%	89%	3%	17%
5-25	1%	1%	-5%	1%	1%
5-26	5%	5%	-20%	5%	5%
5-27	1%	0%	-4%	1%	1%
5-28	0%	4%	-18%	7%	7%
6-29	4%	5%	-7%	-4%	4%
6-30	39%	40%	-123%	13%	39%
6-31	0%	0%	-1%	1%	0%
6-32	10%	10%	-21%	-6%	10%
6-34	163%	164%	-647%	158%	163%
6-35	1%	1%	-7%	2%	1%
6-36	115%	115%	-434%	94%	115%
6-37	1%	-1%	-2%	1%	1%
6-38	60%	60%	-197%	25%	60%
6-39	28%	27%	-85%	7%	27%
6-40	95%	95%	-343%	66%	95%
6-41	13%	16%	-46%	7%	12%
6-42	10%	6%	-13%	-6%	6%
6-43	-2%	-1%	2%	2%	-2%
6-44	31%	32%	-86%	0%	31%
6-45	5%	5%	-22%	6%	5%

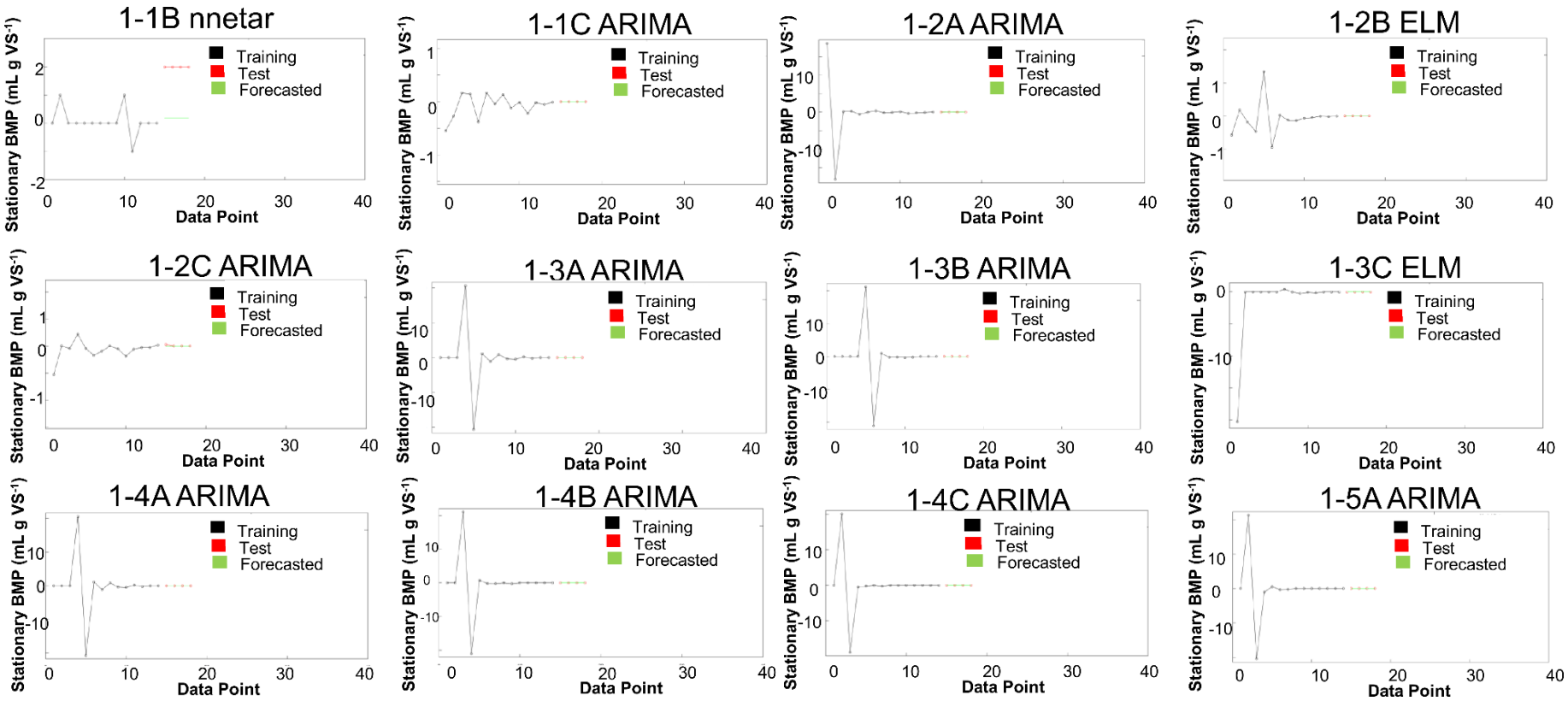

Figure C-1. The training data (black), test data (red), and forecasted data (green) from time series forecasting from the transformed BMP yields (mL g VS^{-1}) for the best forecasting number for each digester group in Batch 1.

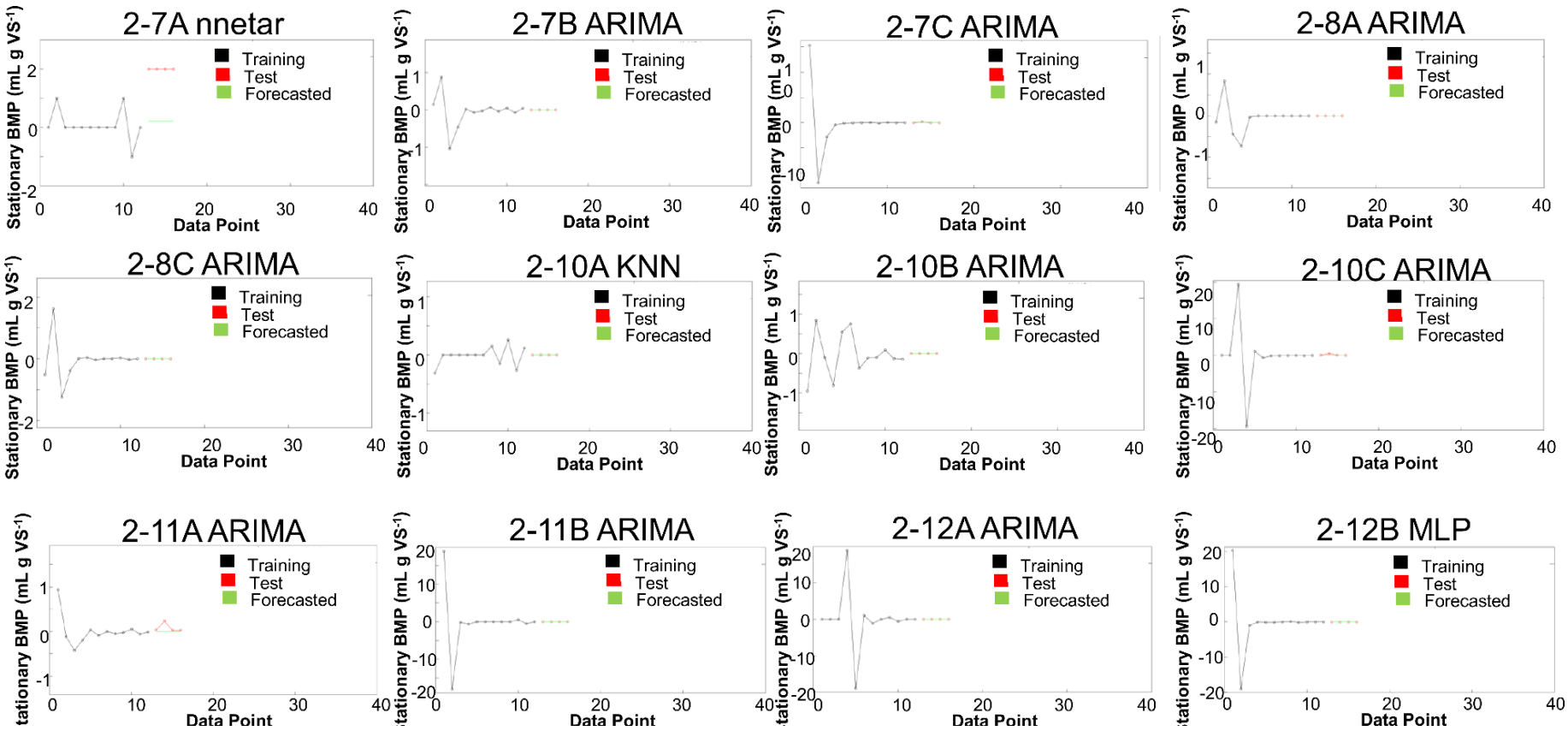

Figure C-2. The training data (black), test data (red), and forecasted data (green) from time series forecasting from the transformed BMP yields (mL g VS^{-1}) for the best forecasting number for each digester group in Batch 2.

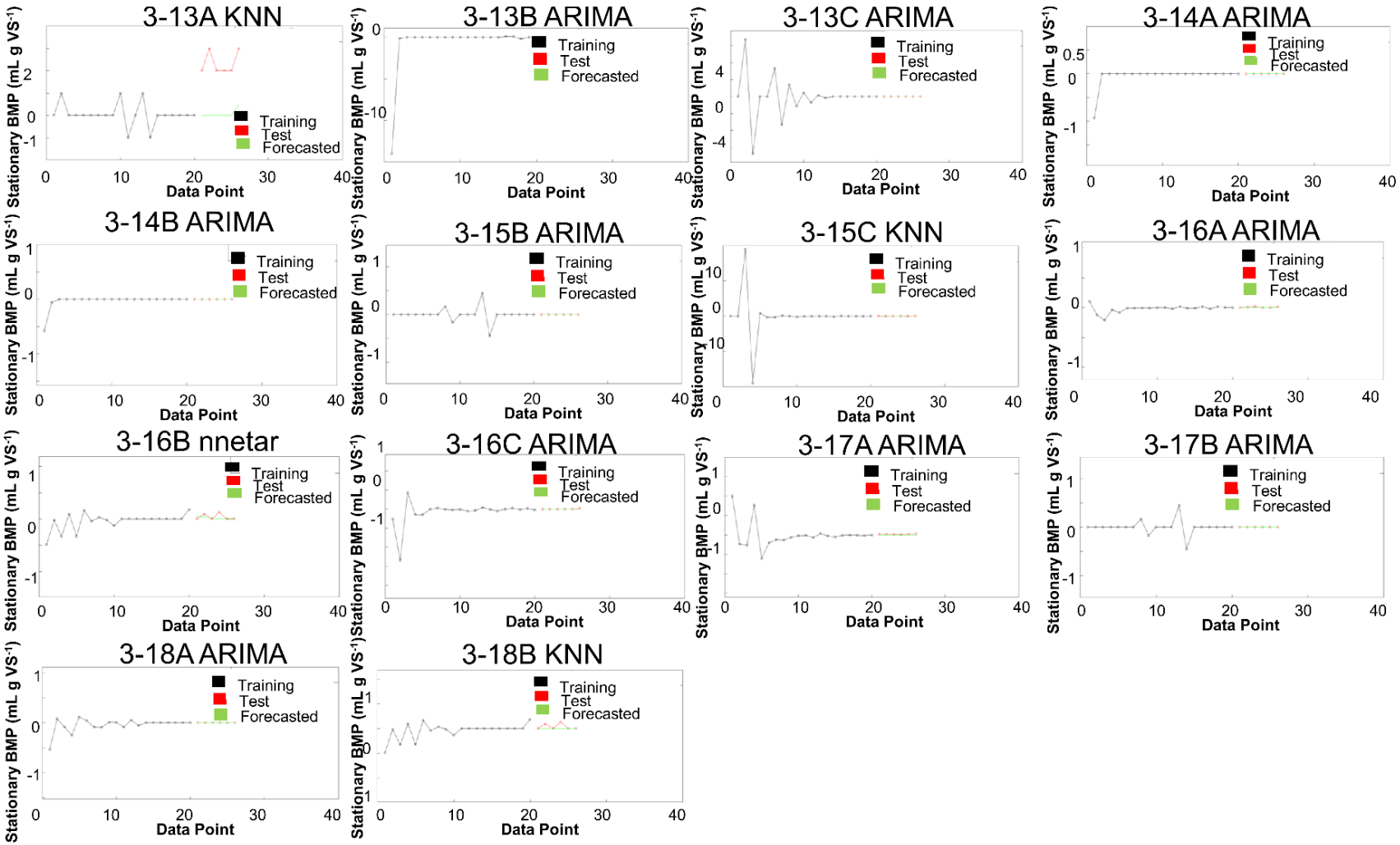

Figure C-3. The training data (black), test data (red), and forecasted data (green) from time series forecasting from the transformed BMP yields (mL g VS^{-1}) for the best forecasting number for each digester group in Batch 3.

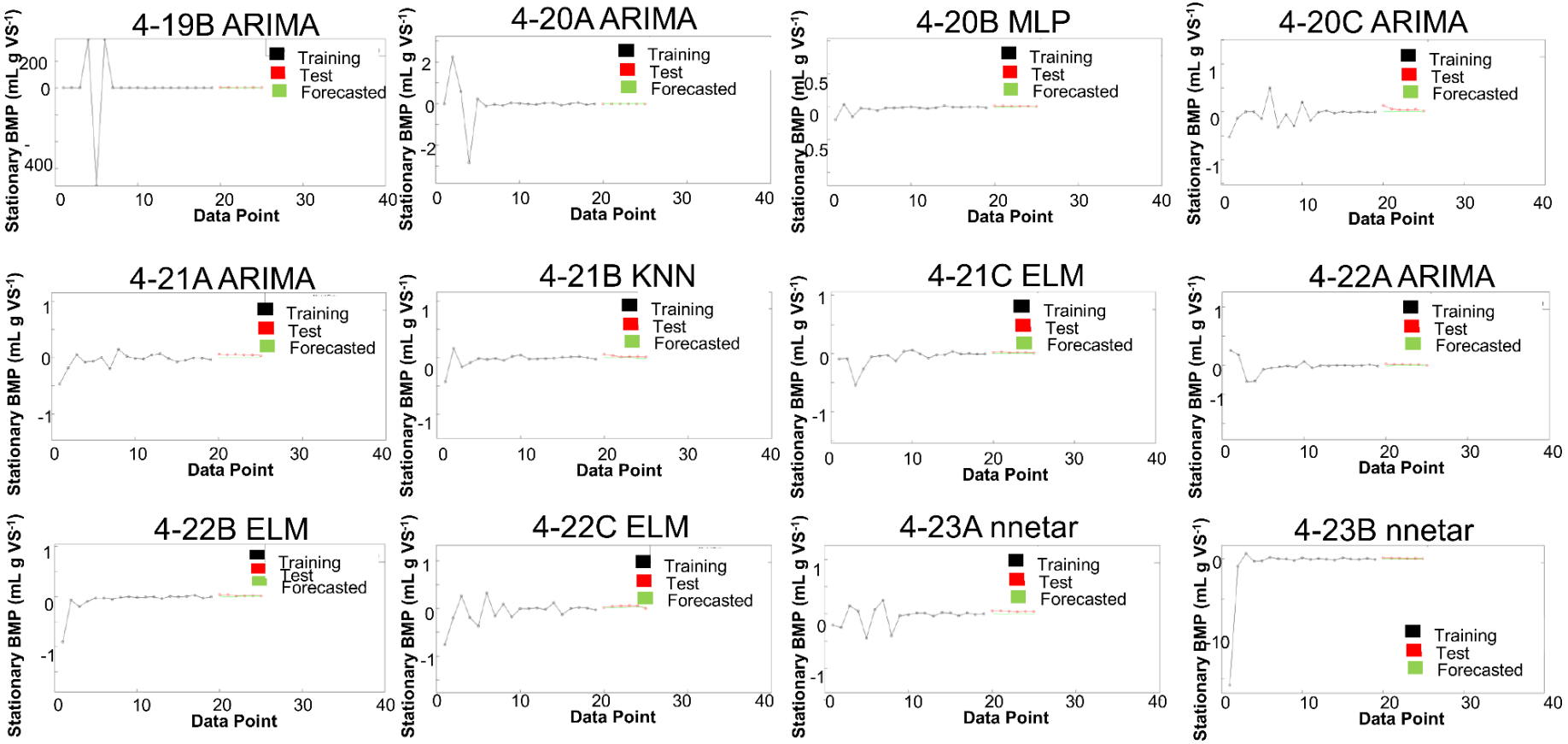

Figure C-4. The training data (black), test data (red), and forecasted data (green) from time series forecasting from the transformed BMP yields (mL g VS^{-1}) for the best forecasting number for each digester group in Batch 4.

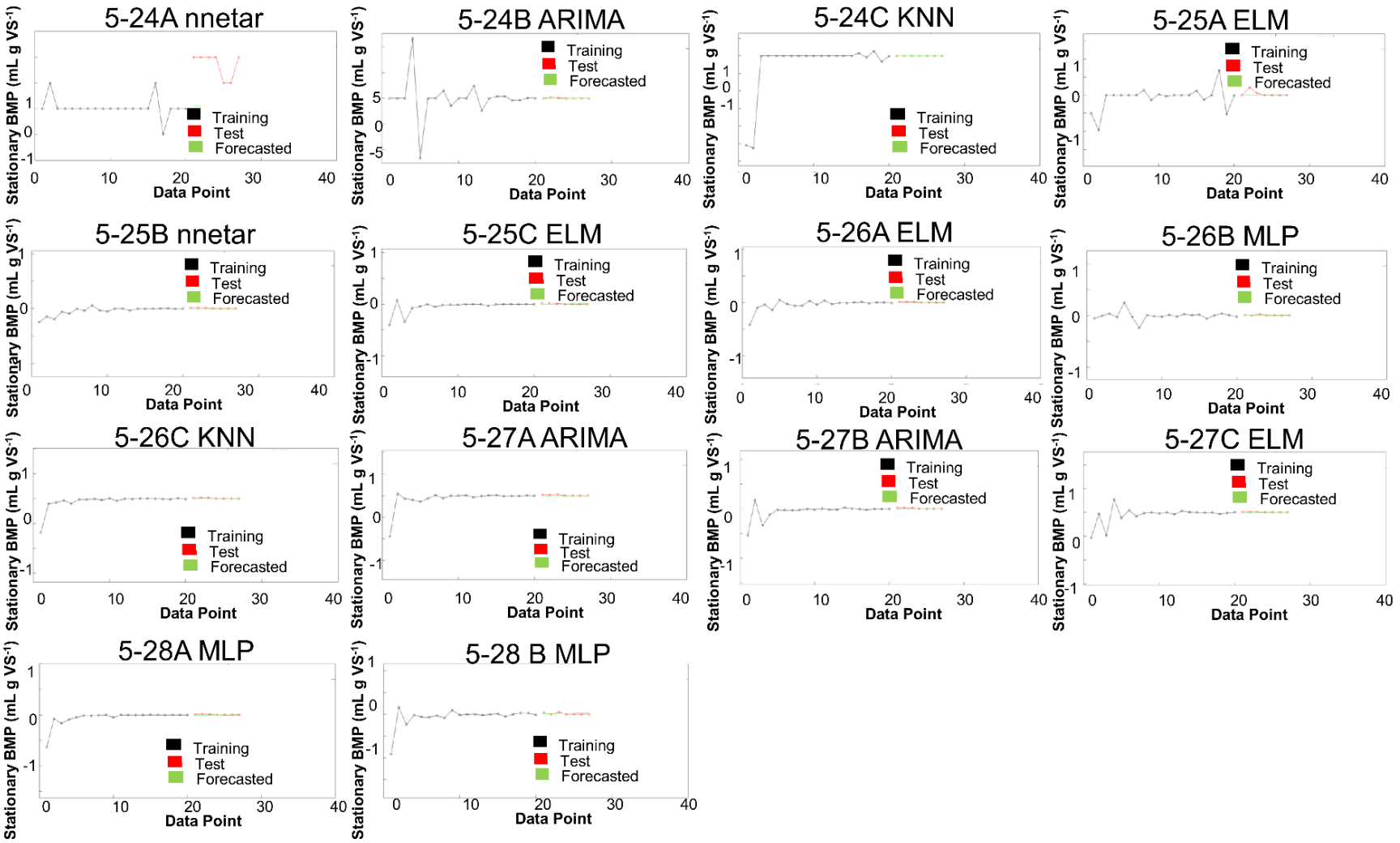

Figure C-5. The training data (black), test data (red), and forecasted data (green) from time series forecasting from the transformed BMP yields (mL g VS^{-1}) for the best forecasting number for each digester group in Batch 5.

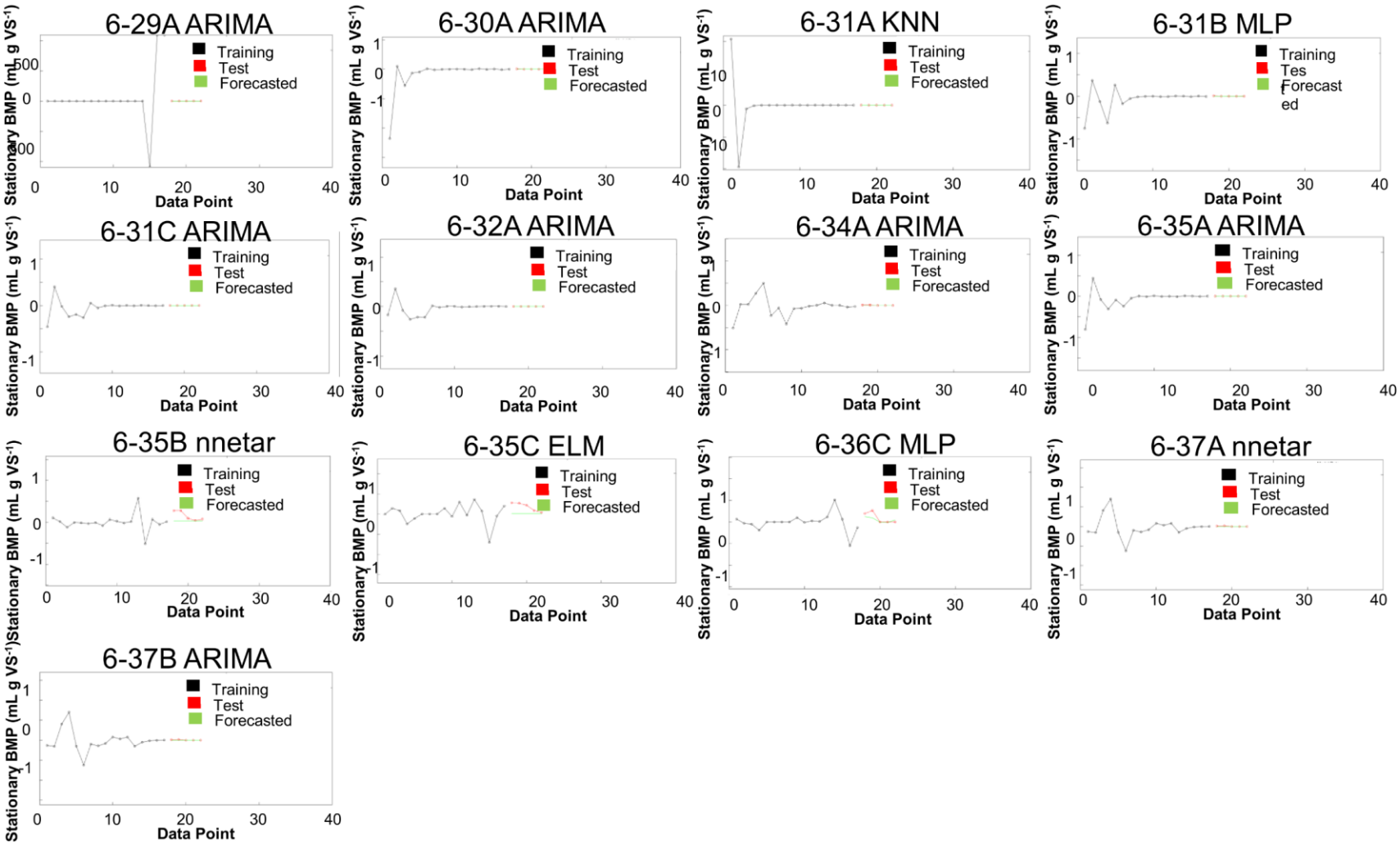

Figure C-6. The training data (black), test data (red), and forecasted data (green) from time series forecasting from the transformed BMP yields (mL g VS^{-1}) for the best forecasting number for each digester group in Batch 6.

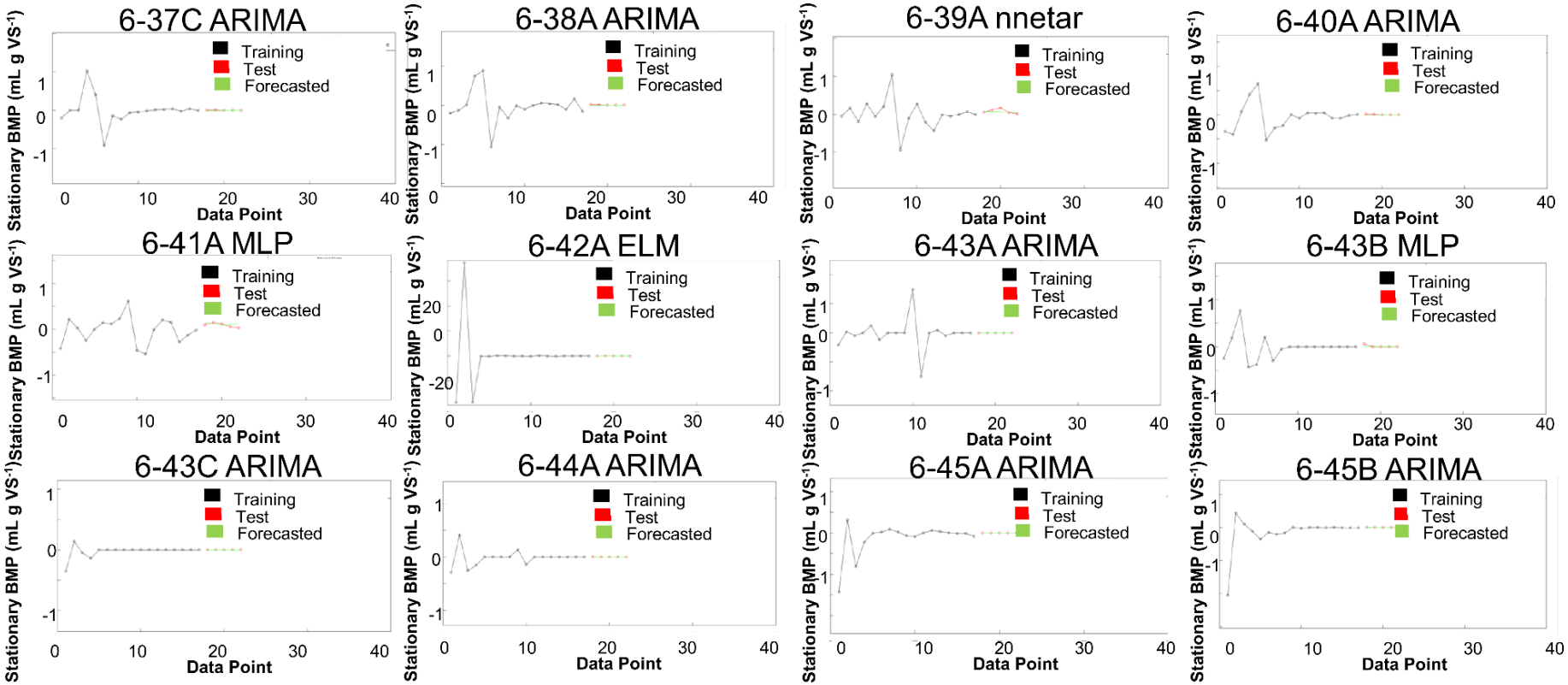

Figure C-7. The training data (black), test data (red), and forecasted data (green) from time series forecasting from the transformed BMP yields (mL g VS^{-1}) for the best forecasting number for each digester group in Batch 6.

VITA

Sarah Daly is originally from Ohio. After graduating from Normandy High School in 2010, she attended Cornell University where she earned Bachelor and Master degrees in Biological Engineering. Her Master's thesis was on the fermentation of food waste. She joined Dr. Ni's research group at Purdue University in August 2016 and is pursuing a Ph.D. in Agricultural and Biological Engineering. Her research examines anaerobic digestion. During her time at Purdue, she served as President and Professional Development Chair of the Agricultural and Biological Engineering Graduate Student Association. In 2020, she was named as one of the new faces of ASABE-Professionals. She is expected to graduate in August 2020.

PUBLICATIONS

Journal Articles

1. Spirito C. M., Daly S. E., Werner J. J. and Angenent L. T. (2018). Redundancy of anaerobic digestion microbiomes during disturbances by the antibiotic monensin. *Applied and Environmental Microbiology*, Vol. 84, No. 9, e02692-17. DOI:10.1128/AEM.02692-17.
2. Thompson L. R., Sanders J. G., ..., Gilbert J. A., Rob Knight R. and The Earth Microbiome Project Consortium (Sarah E. Daly as a Consortium Member). (2017). A communal catalogue reveals Earth's multiscale microbial diversity. *Nature*, Vol. 551, pp. 457-463. DOI:10.1038/nature24621.

Research Posters

1. Daly, S.E. and Ni, J.-Q. (2020). Characteristics of Substrates Producing Hydrogen Sulfide in Anaerobic Digestion. ASABE Annual International Meeting Virtual & On Demand, Jul. 13-15, 2020.
2. Daly, S.E. and Ni, J.-Q. (2019). Bio-methane potential testing and modelling in anaerobic digestion. North American Manure Expo, Jul. 31-Aug. 1, 2019, Fair Oaks, IN.
3. Daly, S.E. and Ni, J.-Q. (2019). Bio-methane potential testing and modelling in anaerobic digestion. ASABE Annual International Meeting, Jul. 7-10, 2019, Boston, MA.
4. Daly, S.E. and Ni, J.-Q. (2018). Improving modelling in the bio-methane potential test. Big Ten + Graduate School Exposition, Sept. 30-Oct. 1, 2018 West Lafayette, IN.
5. Daly, S.E. and Ni, J.-Q. (2017). Improving modelling in the bio-methane potential test. Big Ten + Graduate School Exposition, Sept. 24-25, West Lafayette, IN.
6. Daly S.E., Usack J. G. and Angenent L. T. (2016). Acidification of food waste during storage after grinding with InSinkerator® technology. Food Waste-to-Low Carbon Energy Conference, Apr. 27-28, 2016, New Brunswick, NJ.
7. Spirito, C.M., Daly, S.E., Werner, J.J. and Angenent, L.T. (2015). Time course analysis of the effects of antibiotic disturbances on anaerobic reactor microbiomes. 14th World Congress on Anaerobic Digestion, Nov. 15-18, 2015, Viña del Mar, Chile.

8. Spirito, C.M., Daly, S.E. and Angenent, L.T. (2013). Effect of a dairy antibiotic on the microbiomes of the cow hindgut and anaerobic digesters. 2nd Conference on the Microbiology of the Built Environment, May 23-25, 2013, Boulder, CO.

Oral Presentations

1. Daly, S.E. and Ni, J.-Q. (2020). Characteristics of Substrates Related to Anaerobic Digester Foaming. ASABE Annual International Meeting Virtual & On Demand, Jul. 13-15, 2020.
2. Daly, S.E. and Ni, J.-Q. (2019). Bio-methane Potential Testing Methodologies — A Review. ASABE Annual International Meeting, Jul. 7-10, 2019, Boston, MA.
3. Daly, S.E. and Ni, J.-Q. (2019). Development of a model for early prediction of anaerobic digester performance. 6th Annual ABE Graduate Industrial Research Symposium, Mar. 25, 2019, West Lafayette, IN.